

**ANALYSIS OF PROTEIN-PROTEIN INTERACTIONS
IN THE SHELL OF HERPES SIMPLEX VIRUS TYPE 1
(HSV-1) CAPSIDS**

By

SHARON JOANNE MACNAB BAIN

**A THESIS FOR THE DEGREE OF DOCTOR OF PHILOSOPHY
IN THE FACULTY OF SCIENCE AT
THE UNIVERSITY OF GLASGOW**

**MRC VIROLOGY UNIT
INSTITUTE OF VIROLOGY
CHURCH STREET
GLASGOW
G11 5JR**

AUGUST, 1999

ProQuest Number: 13834095

All rights reserved

INFORMATION TO ALL USERS

The quality of this reproduction is dependent upon the quality of the copy submitted.

In the unlikely event that the author did not send a complete manuscript and there are missing pages, these will be noted. Also, if material had to be removed, a note will indicate the deletion.



ProQuest 13834095

Published by ProQuest LLC (2019). Copyright of the Dissertation is held by the Author.

All rights reserved.

This work is protected against unauthorized copying under Title 17, United States Code
Microform Edition © ProQuest LLC.

ProQuest LLC.
789 East Eisenhower Parkway
P.O. Box 1346
Ann Arbor, MI 48106 – 1346

CONTENTS

ACKNOWLEDGEMENTS

ABSTRACT

ABBREVIATIONS

CHAPTER 1: INTRODUCTION

1. HISTORICAL PERSPECTIVE	1
2. CLASSIFICATION OF HERPESVIRUSES	1
2.1 ALPHAHERPESVIRINAE	2
2.2 BETAHERPESVIRINAE	2
2.3 GAMMAHERPESVIRINAE	2
2.4 FUTURE TRENDS IN CLASSIFICATION	2
3. HERPESVIRUSES WHICH INFECT HUMANS	3
3.1 HSV-1 (HHV-1)	4
3.2 HSV-2 (HHV-2)	5
3.3 VZV (HHV-3)	5
3.4 EBV (HHV-4)	5
3.5 HCMV (HHV-5)	6
3.6 HHV-6	6
3.7 HHV-7	7
3.8 HHV-8	7
4. HSV-1 VIRAL ARCHITECTURE	8
4.1 THE GENOME	8
4.1.1 ORGANISATION OF THE GENOME	8
4.1.2 PACKAGED STATE OF THE GENOME	9
4.2 THE TEGUMENT	10
4.2.1 ASSEMBLY OF THE TEGUMENT	10
4.2.2 FUNCTION OF THE TEGUMENT	10
4.3 THE ENVELOPE	12
4.4 THE CAPSID	12
4.4.1 MOLECULAR COMPOSITION	13
4.4.2 MOLECULAR ARRANGEMENT OF THE CAPSID PROTEINS	19
4.4.3 CAPSID MODELS	23
5. HSV-1 LIFE CYCLE	27
5.1 ENTRY INTO HOST CELLS	27

5.1.1	ATTACHMENT	27
5.1.2	PENETRATION	28
5.2	DISRUPTION OF HOST CELL FUNCTIONS	29
5.3	THE GENE EXPRESSION CASCADE	30
5.3.1	CLASSES OF VIRAL GENES	30
5.3.2	MECHANISM OF REPLICATION	31
5.4	CLEAVAGE AND PACKAGING OF DNA	33
5.5	TEGUMENTATION AND ENVELOPEMENT	35
5.6	LATENCY	36

CHAPTER 2: MATERIALS AND METHODS

1 MATERIALS 39

1.1	CHEMICALS	39
1.2	ENZYMES	40
1.3	OLIGOMERS	40
1.4	TISSUE CULTURE MEDIUM	40
1.5	CELL LINES	41
1.6	VIRUSES	41
1.7	BACTERIAL CULTURE MEDIUM	41
1.8	BACTERIAL STRAINS	42
1.9	EXPRESSION PLASMIDS	42
1.10	ANTIBODIES	42
1.11	BUFFERS AND SOLUTIONS	43
1.12	COMMERCIAL KITS	47
1.13	MISCELLANEOUS MATERIALS AND SUPPLIERS	47

2 METHODS 48

2.1	GEL ELECTROPHORESIS AND WESTERN BLOTTING	48
2.1.1	ANALYTICAL AGAROSE GELS OF DNA	48
2.1.2	ISOLATION OF DNA FROM AGAROSE GELS	48
2.1.3	PURIFICATION OF SYNTHETIC OLIGONUCLEOTIDE FROM POLYACRYLAMIDE GELS	49
2.1.4	SDS-PAGE OF PROTEIN SAMPLES	49
2.1.5	TCA PRECIPITATION	50
2.1.6	SILVER STAINING	50
2.1.7	ANALYSIS OF ³⁵ S LABELLED PROTEINS	50
2.1.8	SEMI-DRY WESTERN BLOTTING	50
2.2	HSV-1 VIRUS PREPARATION AND MANIPULATION	51
2.2.1	BHK CELL CULTURE	51
2.2.2	PREPARATION OF HIGH TITRE VIRUS STOCKS	52
2.2.3	TITRATION OF VIRUS STOCK	53
2.2.4	STERILITY CHECKS OF VIRUS STOCK	53
2.2.5	PREPARATION AND PURIFICATION OF WILD-TYPE HSV-1 CAPSIDS	53
2.3	BACULOVIRUS PREPARATION AND MANIPULATION	55
2.3.1	SF 21 CELL CULTURE	55
2.3.2	PREPARATION OF LOW TITRE VIRUS STOCK	56
2.3.3	PREPARATION OF HIGH TITRE VIRUS STOCK	56

2.3.4	TITRATION OF VIRUS STOCK	56
2.3.5	STERILITY CHECKS OF VIRUS STOCK	57
2.3.6	CONFIRMATION OF EXPRESSION OF BACULOVIRUS PROTEINS	57
2.3.7	CONSTRUCTION OF RECOMBINANT BACULOVIRUSES	58
2.3.8	PREPARATION AND PURIFICATION OF RECOMBINANT HSV-1 CAPSIDS	59
2.4	OLIGOMERS	60
2.4.1	CLEAVAGE AND STORAGE OF OLIGONUCLEOTIDES	60
2.4.2	CLEAVAGE, ANALYSIS AND STORAGE OF OLIGOPEPTIDES	60
2.5	GENE CLONING	61
2.5.1	PREPARATION OF <i>E COLI</i> COMPETENT CELLS	61
2.5.2	TRANSFORMATION OF PLASMID DNA	62
2.5.3	PREPARATION OF A STARTER CULTURE	62
2.5.4	PREPARATION OF GLYCEROL STOCKS	63
2.5.5	SMALL SCALE PLASMID PREPARATION	63
2.5.6	PHENOL:CHLOROFORM (1:1) EXTRACTION OF DNA	63
2.5.7	ETHANOL / ISOPROPANOL PRECIPITATION OF DNA	64
2.5.8	RESTRICTION ENDONUCLEASE DIGESTS OF DNA	64
2.5.9	PURIFICATION OF DNA FROM AN AGAROSE GEL SLICE	65
2.5.10	LIGATION OF DNA	65
2.5.11	LARGE SCALE PLASMID PREPARATION	65
2.5.12	QUANTIFICATION OF DNA	66
2.5.13	SITE DIRECTED MUTAGENESIS	66
2.5.14	PCR	67
2.5.15	SEQUENCING ANALYSIS OF DNA	68
2.6	IMMUNOFLUORESCENCE STAINING	68
2.6.1	TRANSFECTION OF PLASMID DNA	68
2.6.2	STAINING	69
2.7	MICROSCOPIC ANALYSIS OF CAPSIDS	69
2.7.1	ELECTRON MICROSCOPIC EXAMINATION OF CAPSIDS	69
2.7.2	CRYO-ELECTRON MICROSCOPY EXAMINATION OF CAPSIDS	70
2.8	QUANTIFICATION OF PROTEINS	70
2.9	SIZING OF PROTEINS	70
2.10	ENZYME LINKED IMMUNOSORBENT ASSAY (ELISA)	71
2.11	EPITOPE MAPPING BY SPOTSCAN	71
2.12	PURIFICATION OF ANTIBODY SUPERNATANT BY AMMONIUM SULPHATE PRECIPITATION	73

CHAPTER 3 (RESULTS): A STUDY OF THE MULTIPLE INTERACTIONS CONTROLLING THE INTRACELLULAR LOCALISATION OF HSV-1 CAPSID PROTEINS BY IMMUNOFLUORESCENCE LABELLING

1.	INTRODUCTION	74
2.	CONSTRUCTION OF EXPRESSION PLASMIDS	74
2.1	VP23, VP5 AND PREVP22A	74

2.2	VP19C AND VP26	74
2.3	EPITOPE TAGGED VERSIONS OF VP19C, VP5 AND VP26	75
2.3.1	VP19C	75
2.3.2	VP5	76
2.3.3	VP26	77
3. INTRACELLULAR DISTRIBUTION OF CAPSID PROTEINS		78
3.1	DISTRIBUTION OF VP19C	79
3.2	INFLUENCE OF VP19C ON THE DISTRIBUTION OF VP5 AND VP23	79
3.2.1	VP19C + VP5	79
3.2.2	VP19C + VP23	79
3.3	INFLUENCE OF PREVP22A ON THE DISTRIBUTION OF VP5	79
3.4	DISTRIBUTION OF VP26	80
3.4.1	INFLUENCE OF OTHER CAPSID PROTEIN ON THE DISTRIBUTION OF VP26	80
3.4.2	LOCALISATION OF VP26 TO THE NUCLEUS	80
3.5	DISTRIBUTION OF N- AND C- TERMINAL DELETIONS OF VP5	81
4. DISCUSSION OF IMMUNOFLUORESCENCE		81
5. PRODUCTION AND ANALYSIS OF A NEW EPITOPE TAG, CHLORAMPHENICOL ACETYL TRANSFERASE (CAT)		84
5.1	INTRODUCTION	84
5.2	OPTIMISATION OF CAT PROTEIN AND 5/24 ANTIBODY	85
5.2.1	OPTIMISATION OF CAT PROTEIN	85
5.2.2	OPTIMISATION OF 5/24 ANTIBODY TO 50NG OF CAT PROTEIN	86
5.3	GENERATION OF OLIGOPEPTIDES BY SPOTSCAN METHODOLOGY	87
5.4	ANTIBODY ASSAY OF SPOTs OLIGOPEPTIDES	87
5.5	OLIGOPEPTIDE SYNTHESIS OF CAT208	88
5.6	REACTIVITY OF CAT208 OLIGOPEPTIDES (1013A, 1013C, 1013D) WITH 5/24 ANTIBODY SUPERNATANT	89
5.6.1	CONFIRMATORY ANALYSIS OF OLIGOPEPTIDE 1013C	89
5.7	PRODUCTION OF RABBIT POLYCLONAL ANTIBODIES TO CAT208 OLIGOPEPTIDE 1013C.2	90
5.8	CONSTRUCTION OF PLASMIDS EXPRESSING CAT208	91
5.9	ANALYSIS OF CAT208 CONSTRUCTS	92
5.9.1	RESTRICTION ENZYME DIGESTS	92
5.9.2	WESTERN BLOT ANALYSIS	92
5.9.3	IMMUNOFLUORESCENCE LABELLING	92
6. DISCUSSION OF MAPPING CAT208		92

CHAPTER 4 (RESULTS): PURIFICATION OF VP26 AND VP5

1. INTRODUCTION	94
<hr/>	
2. VP26	95
<hr/>	
2.1 CONSTRUCTION OF EXPRESSION PLASMID	95
2.1.1 PET28MOD	95
2.1.2 PET35PP65	95
2.2 EXPRESSION OF VP26PP65	96
2.3 SOLUBILITY OF VP26PP65	97
2.3.1 TEMPERATURE AND TIME OF INDUCTION	97
2.3.2 BACTERIAL DENSITY	98
2.3.3 CONCENTRATION OF IPTG AT INDUCTION	98
2.3.4 TIME, TEMPERATURE AND CONCENTRATION OF IPTG AT INDUCTION	98
2.3.5 TREATMENT WITH VARIOUS BUFFERS AND PH CONDITIONS	98
2.3.6 TREATMENT WITH DENATURANT	99
2.4 PURIFICATION OF VP26PP65	100
2.4.1 BINDING OF VP26PP65 TO NI-NTA AGAROSE	100
2.4.2 DENATURING ELUTION CONDITIONS	100
2.4.3 NON-DENATURING ELUTION CONDITIONS	102
2.5 RE-NATURATION OF VP26PP65	104
<hr/>	
3. VP5	106
<hr/>	
3.1 CONSTRUCTION OF EXPRESSING BACULOVIRUS	106
3.2 PRODUCTION OF A RECOMBINANT BACULOVIRUS EXPRESSING VP5HIS (IE 191A)	106
3.3 EXPRESSION OF 191A	106
3.4 PURIFICATION OF 191A	107
3.4.1 BINDING AND ELUTION OF 191A FROM NI-NTA AGAROSE	107
<hr/>	
4. DISCUSSION	107

CHAPTER 5 (RESULTS): CHARACTERISATION OF VP26pp65 AND MAPPING THE POINTS OF INTERACTION BETWEEN VP26 AND VP5

1. INTRODUCTION	109
<hr/>	
2. FUNCTIONAL VALIDITY OF VP26PP65	109
<hr/>	
2.1 REATTACHMENT OF VP26PP65 TO VP26 MINUS (VP26-) CAPSIDS	109

2.1.1	PREPARATION OF CAPSIDS	110
2.1.2	ATTACHMENT OF VP26PP65 TO VP26- CAPSIDS	113
2.1.3	CRYO-EM ANALYSIS OF VP26PP65+ CAPSIDS	114
3. IDENTIFICATION OF THE N-TERMINUS OF VP26PP65		115
4. CHARACTERISATION OF VP26PP65		116
4.1.1	OLIGOMERIC STATUS OF VP26PP65	117
4.1.2	SECONDARY STRUCTURE OF VP26PP65	118
5. MAPPING OF THE POINTS OF INTERACTION BETWEEN VP26 AND VP5		119
5.1 DEVELOPMENT OF AN ELISA ASSAY USING VP26 INHIBITORY OLIGOPEPTIDES		119
5.1.1	OPTIMISING ELISA CONDITIONS; VP26- STRIPPED CAPSIDS + VP26PP65	120
5.1.2	OPTIMISING ELISA CONDITIONS; PURIFIED VP5 (191A) + VP26PP65	121
5.1.3	BLOCKING THE INTERACTION OF VP5 -VP26 WITH UL35 OLIGOPEPTIDES	122
5.2 ATTACHMENT OF VP26 MUTANTS TO VP26- CAPSIDS		124
5.2.1	CONSTRUCTION OF DELETION MUTANTS	124
5.2.2	EXPRESSION AND PURIFICATION	125
5.3 CONSTRUCTION OF INSERTION MUTANTS		126
5.3.1	EXPRESSION AND PURIFICATION	127
5.4 DEVELOPMENT OF AN INTERACTION ASSAY SYSTEM FOR 3xG MUTANTS AND VP26- CAPSIDS		128
5.4.1	PRODUCTION OF VP26- CAPSIDS BY TREATMENT WITH 4M UREA	128
5.4.2	ATTACHMENT OF 3xG PROTEINS (VP26PP65.1 – VP26PP65.10) TO VP26- CAPSIDS	128
5.4.3	ATTACHMENT OF VP26PP65.1 TO VP26PP65.10 TO VP26- CAPSIDS	129
6. DISCUSSION		131
6.1	FUNCTION VALIDITY OF VP26PP65	131
6.2	POSSIBLE LOCATION OF THE N-TERMINUS OF VP26	131
6.3	OLIGOMERIC STATUS AND SECONDARY STRUCTURE OF VP26	132
6.4	MUTATIONS OF VP26PP65	135
6.5	AMINO ACID RESIDUES IMPORTANT FOR BINDING VP26 TO VP5	136

CHAPTER 6 (RESULTS): IDENTIFICATION OF THE SITES OF INTERACTION BETWEEN THE SCAFFOLD AND OUTER SHELL IN HSV-1 CAPSIDS

1. INTRODUCTION	139
2. PREPARATION OF CAPSIDS	140
2.1 SMALL CORED B CAPSIDS	140
2.2 LARGE CORED B-CAPSIDS	141
2.3 SDS-PAGE ANALYSIS OF SMALL AND LARGE CORED CAPSIDS	141
3. ANALYSIS OF WILD TYPE AND PROTEASE MINUS CAPSIDS	141
3.1 SYMMETRY OF WILD TYPE AND PROTEASE MINUS CAPSIDS	141
3.1.1 COMPARISON OF CAPSID SHELLS	141
3.1.2 COMPARISON OF CAPSID MASS DISTRIBUTIONS	142
3.1.3 STRUCTURAL DISAGREEMENT FACTOR	142
3.2 IDENTIFICATION OF THE POINTS OF CONTACT BETWEEN SCAFFOLD AND SHELL	143
3.2.1 VISUAL INSPECTION	143
3.2.2 ANALYSIS OF ASYMMETRIC UNITS	144
4. DISCUSSION	145

CHAPTER 7: CONCLUSION

1 THE PATTERN OF THE CAPSID PROTEIN-PROTEIN INTERACTIONS	148
2 A STUDY OF THE INTERACTION OF VP26 WITH VP5	148
3 A STUDY OF THE INTERACTION OF SCAFFOLD WITH VP5	150
4 INHERENT PROPERTIES OF VP5, VP19C, VP23 AND SCAFFOLD	150

4.1	VP5 AND VP19C	151
4.2	VP23	151
4.3	SCAFFOLD	152
5	<u>HSV-1 PROCAPSID ASSEMBLY MODEL AND ANALOGIES WITH BACTERIOPHAGE</u>	153
6	<u>PROPOSED MODEL FOR CAPSID ASSEMBLY</u>	156

REFERENCES

LIST OF FIGURES AND TABLES

Figure / Table Number	Title	After page number
Figure 1.1	Electron micrograph of an HSV-1 virion	(before page) 1
Table 1.1	Classification of <i>Herpesviridae</i>	(before page) 1
Figure 1.2	Phylogenetic tree	2
Figure 1.3	Structure of the HSV-1 genome	7
Table 1.2	Tegument proteins	9
Table 1.3	Envelope Glycoproteins	11
Table 1.4	Capsid proteins	12
Figure 1.4	Organisation of the UL26 and UL26.5 ORFs	15
Figure 1.5	Processing products of UL26 and UL26.5	15
Figure 1.6	3D image reconstruction of a wild type HSV-1 capsid	18
Figure 1.7	Capsid hexon arrangement	19
Table 1.5	Herpesvirus capsid protein homologues	22
Table 1.6	Genes involved in cleavage and packaging DNA	32
Figure 1.8	Possible routes of HSV-1 egress	34
Figure 3.1	Construction of pET38T1	74
Figure 3.2	Consensus predictions for VP5	75
Figure 3.3	Construction of pSJM 19N65 and pSJM19C65	76
Figure 3.4	Sequence of oligonucleotides 19C-T (1) and 19C-T (2)	76
Figure 3.5	Sequence of oligonucleotides 19N-T (1) and 19N-T (2)	76
Figure 3.6	Construction of pET35T1	76
Figure 3.7	Intracellular distribution of VP19c	78
Figure 3.8	Intracellular distribution of VP23 and VP5 alone	78
Figure 3.9	Redistribution of VP5 and VP23 to the nucleus	78
Figure 3.10	Redistribution of VP5pp65 to the nucleus by preVP22a	78
Figure 3.11	Intracellular distribution of VP26	79
Figure 3.12	Redistribution of VP26 to the nucleus	79
Figure 3.13	Intracellular distribution of VP5N65 and VP5C65	80
Figure 3.14	Schematic representation of the stepwise synthesis of oligopeptides	84

Figure 3.15	Optimisation of CAT proteins to the 5/24 monoclonal antibodies	85
Figure 3.16	Optimisation of 5/24 monoclonal antibodies to 50ng of CAT	85
Figure 3.17	For the SPOTscan procedure: PC generated oligopeptide list and pipetting schedule for the CAT sequence	86
Figure 3.18	SPOTs membranes	86
Figure 3.19	Position of CAT208 within the amino acid sequence	87
Table 3.1	Summary of 1013 oligopeptide sequences	87
Table 3.2	Summary of 1013 oligopeptide analysis	87
Figure 3.20	Reactivity of oligopeptides 1013 with 5/24 antibody supernatant	88
Figure 3.21	Reactivity of oligopeptides 1013c.2 with 5/24 antibody supernatant (1:32) compared to controls	88
Table 3.3	Inoculation schedule for the production of rabbit polyclonals to oligopeptide 1013c.2	89
Figure 3.22	Construction of CAT208 epitope tagged UL19 (VP5) and UL35 (VP26) in pCMV10BglΔEco	90
Figure 3.23	Construction of pET35CAT	90
Figure 3.24	Western blot analysis of VP26CAT	91
Figure 3.25	Intracellular distribution of VP5CAT and VP26CAT	91
Figure 4.1	Example of a 6xhis tag sequence	93
Figure 4.2	Construction of pET35pp65	94
Figure 4.3	Oligonucleotides required for cloning the VP26 coding sequence into a bacterial expression vector	94
Figure 4.4	Comparison of the amino acid sequences of VP26 and VP26pp65	95
Figure 4.5	Expression of pET35pp65	95
Figure 4.6	Attempts to solubilise VP26pp65	96
Table 4.1	'Good buffers' to solubilise VP26pp65	98
Figure 4.7	Treatment of VP26pp65 with 6M GuHCl	99
Figure 4.8	Schematic representation of the interaction of 6xhis tagged proteins with Ni-NTA resin	99
Figure 4.9	Comparison of the structures of imidazole and histidine	99
Figure 4.10	Elution of VP26pp65 with imidazole	100
Figure 4.11	Rapid dilution and dialysis of VP26pp65	104
Figure 4.12	Construction of pAcCl19his (191A)	105
Figure 4.13	Purification of 191A through Ni-NTA	106
Table 4.2	Summary of the conditions tested to solubilise VP26pp65	107

Table 4.3	Summary of the purification protocol for VP26pp65 (pET35pp65)	107
Figure 5.1	PAcAB3 Baculovirus transfer vector	110
Figure 5.2	Cloning strategy to generate pAcAB3.1	110
Figure 5.3	Cloning strategy to generate pAcAB3.4	111
Figure 5.4	Cloning strategy to generate pAcAB3.6	111
Figure 5.5	Attachment of VP26pp65 to VP26- capsids	112
Figure 5.6	Location of VP26 and VP26pp65 on the capsid	114
Figure 5.7	Comparison of the 3D image reconstructions of VP26- and VP26+ capsids	115
Figure 5.8	Location of an extra mass in averaged hexons of VP26pp65+ capsids	115
Figure 5.9	Elution profile of VP26pp65 from the superdex 75 column	116
Figure 5.10	Sequence relatedness of VP26 proteins	117
Figure 5.11	Consensus protein predictions of alpha and beta herpesviruses	118
Figure 5.12	Microtitre plate plan for ELISA of VP26- capsids and VP26pp65	119
Figure 5.13	Optimisation of ELISA conditions for the interaction of VP26pp65 with VP26- capsids	119
Figure 5.14	Optimisation of ELISA conditions for the interaction of VP26pp65 with VP5 (191A)	120
Figure 5.15	UL35 oligopeptide sequences	121
Table 5.1	Summary of 35/1-35/10 oligopeptide analysis	121
Figure 5.16	Oligopeptides (35/1-35/10) interaction with pp65 antibody	122
Figure 5.17	Oligopeptides (35/1-35/10) inhibition of the VP26-VP5 interaction	122
Figure 5.18	Location of the inhibitory oligopeptides, 35/4, 35/5, 35/6, in the UL35 ORF	123
Figure 5.19	Location of restriction enzyme sites in UL35	123
Figure 5.20	Construction of pET35pp65 N-terminal deletion mutants	123
Figure 5.21	Construction of pET35pp65 C-terminal deletion mutants	124
Figure 5.22	Sequence and location of 3 x Glycine (3xG) insertion primers	126
Figure 5.23	Sequence data for pET35pp65.1	126
Figure 5.24	Elution of VP26pp65 3xG mutants in 200mM imidazole	127
Figure 5.25	Generation of VP26- capsids by treatment with 4M urea	127
Figure 5.26	Mini gradients and western blots of VP26pp65+ capsids and VP26- capsids mixed with 3xG VP26pp65 constructs	128

Figure 5.27	Confirmation of attachment of VP26pp65.5 (3xG mutant) to VP26- capsids	130
Figure 5.28	Electron micrographs of VP26pp65+ capsids and VP26pp65.5+ capsids	130
Figure 6.1	Comparison of wild type and protease minus B capsids' protein profiles	140
Figure 6.2	Comparison of the outer shells and internal cores of wild type and protease minus capsid reconstructions	141
Figure 6.3	Identification of additional attached mass in protease- capsids	142
Figure 6.4	Visualisation of additional densities attached to the floor of protease minus capsids	143
Figure 6.5	Contact points of scaffolding proteins on the capsid floor	143
Figure 6.6	Interaction sites between scaffolding and outer shell	143
Figure 7.1	Pattern of protein-protein interactions	147
Figure 7.2	Transition from large cored to small cored capsids	149
Figure 7.3	Procapsid assembly model	152
Figure 7.4	Possible mechanism of preVP22a in the procapsid to capsid transition	157

ACKNOWLEDGEMENTS

I would like to sincerely thank all members of lab 209 (past and present) who have helped me to complete this thesis. In particular, I would like to thank Dr Frazer J Rixon for advice and help throughout the course of my project and for proof-reading my thesis so thoroughly.

I must also thank Mrs Joyce Mitchell and Mr David McNab, not only allowing me to utilise their technical expertise but, for providing support and friendship when I needed it most. In this respect, I would also like to acknowledge Dr David McClelland and thank both him and Dr Marina Kirkitadze for providing me with their CD data.

I would also like to acknowledge Dr Wah Chiu and Dr Hong Zhou, and their respective groups (Texas, USA), for performing all the cryo-EM analysis and producing the 3D image reconstructions.

Thanks also goes to lab 106a, especially Dr Howard Marsden, for advice on ELISA and oligopeptide work and Mrs Karen McCauley, Miss Gillian McVey and Dr Susan Graham for help in the initial stages of my work.

All the results described in this thesis were obtained by the author's own efforts, unless stated otherwise.

Last, but by no means least, I would like to thank all of my family for support, love and encouragement throughout my studies. Without them I do not know how I would have made it through the more difficult experiments and traumatic times.

I would like to dedicate this thesis to my mum and dad, my husband, Clark and my sister, Suzanne.

ABSTRACT

Much is known about the structural appearance of the HSV-1 capsid however, the aim of this project was to build on existing knowledge by studying the interactions and properties of individual capsid proteins, principally VP26, but also VP5 and preVP22a.

As good antibodies to many capsid proteins were not available, a short amino acid sequence tag, derived from the HCMV pp65 protein was inserted. This approach provided a tool for monitoring VP26, VP5 and VP19c in a series of interaction studies using an anti-pp65 monoclonal antibody. Extensive immunofluorescence studies of plasmid transfection experiments, showed that VP19c had an intrinsic ability to localise to the nucleus. Furthermore, nuclear localisation of VP26 was only observed when VP5 was present together with either VP19c or preVP22a (see Chapter 3). In an attempt to produce an unrelated tag, a short amino acid sequence derived from the CAT enzyme and recognised by an anti-CAT monoclonal antibody, was mapped and characterised. An oligopeptide of this sequence was synthesised and used in an unsuccessful attempt to raise monospecific antisera in rabbits for use in double labelling experiments.

The VP26 ORF was sub-cloned into a bacterial expression vector to allow more detailed studies of the protein to be performed. The pET expression plasmid offered a system where high quantities of protein could be produced, readily purified (using a 6xhis tag and nickel affinity chromatography) and easily manipulated to produce mutant proteins. Although the VP26 tagged protein was induced to high levels, it was extremely insoluble. A successful procedure was developed by which VP26 was purified in a denatured form and renatured by dialysis against buffer. This process consistently produced concentrations of purified VP26 protein at 0.5-1.0mg/ml (see Chapter 4).

The functionality of the purified renatured VP26 was demonstrated by its ability to assemble correctly on capsids. An experimental protocol was developed for attaching the tagged VP26 to capsids lacking VP26. Cryo-EM analysis of these capsids confirmed that the VP26 protein had attached at the correct location and in the expected orientation,

forming a star shaped ring on the tips of the VP5 hexons. This provided proof that the bacterially expressed protein mimicked the properties of the natural VP26 protein and that the extra sequences, contributed by the epitope and 6xhis tags, did not interfere with the binding of VP26 to VP5. An area of extra mass that was detected in the hexons with the tagged VP26 protein attached, was considered to be indicative of the tag sequence. As the tag had been inserted into the N-terminus of the UL35 ORF, this identified the probable location of the N-terminus of VP26 (see Chapter 5).

To analyse sequences important for the interaction of VP26 with VP5 an ELISA assay was developed. Initially, binding of purified VP26 to capsids which lacked the endogenous VP26 were examined. Subsequently, the assay was refined by replacing the VP26 minus capsids with purified and soluble VP5, expressed from a baculovirus vector. Using this assay, it was possible to map the points of contact between the two proteins. Ten overlapping oligopeptides, spanning the entire UL35 ORF, were made and tested for their ability to block binding of VP26 to VP5 in an inhibition type ELISA assay. Several of the oligopeptides had an inhibitory effect, most notably those containing sequences between amino acid residues 31 and 70 in the UL35 ORF (see Chapter 5).

The solubility of the VP26 tagged protein was not high enough to allow X-ray crystallography or NMR studies. Therefore a protein predict computer package was used to try and gain an insight into the secondary structure of the protein. The protein predict model was used to guide the construction of a series of mutant VP26 proteins. Although the prediction has since proved inaccurate, through CD analysis, the mutant proteins produced have been extremely useful. Experiments using VP26 proteins, with three glycine insertions at different locations, showed that insertion in the region between amino acid residues 40 and 60 on the UL35 ORF (a region incorrectly predicted to consist largely of alpha helix) affected the binding of VP26 to capsids. These insertions mapped within the region of VP26 previously shown to be important for binding in the oligopeptide inhibition studies, suggesting that this region contains sequences involved in the interaction with VP5.

ABSTRACT

TO ACCOUNT FOR THE PRESENCE OF VP26 ON HEXONS BUT NOT PENTONS (WHICH ARE ALSO FORMED BY VP5) IT HAD BEEN SUGGESTED THAT VP26 FORMED 6-MERS PRIOR ITS BINDING TO CAPSIDS. ANALYSIS OF THE OLIGOMERIC STATUS OF PURIFIED VP26 SUGGESTED THAT THE PROTEIN WAS PRESENT AS MONOMERS AND DIMERS (IN A RATIO OF 3:1) BUT NOT 6-MERS. THE IMPLICATIONS OF THIS RESULT, WITH REGARD TO CAPSID ASSEMBLY MODELS, IS DISCUSSED IN CHAPTER 5.

THIS PROJECT ALSO SOUGHT TO STUDY THE INTERACTION BETWEEN THE UNCLEAVED SCAFFOLDING PROTEIN, preVP22a, AND THE MAJOR CAPSID PROTEIN VP5. IT WAS KNOWN THAT THE UNCLEAVED SCAFFOLDING PROTEIN FORMED CONTACTS WITH VP5 THROUGH 25 OF ITS C-TERMINAL AMINO ACIDS. CLEAVAGE, BY THE PROTEASE, BREAKS THE LINK BETWEEN SCAFFOLD AND LARGE CORED B CAPSIDS ARE CONVERTED TO SMALL CORED B CAPSIDS. LARGE AND SMALL CORED B CAPSIDS WERE PRODUCED AND ANALYSED BY CRYO-EM. THIS REVEALED AREAS OF ICOSAHEDRALLY ORDERED MASS, PRESENT IN ONLY THE PROTEASE MINUS CAPSIDS AND ATTACHED TO THE INNER SHELL. FURTHER ANALYSIS SHOWED ROD LIKE DENSITIES, PRESENT UNDERNEATH THE TRIPLEXES SURROUNDING THE C HEXON. THESE RESULTS HAVE ALLOWED THE PROBABLE POINTS OF CONTACT BETWEEN preVP22a AND VP5 TO BE IDENTIFIED (SEE CHAPTER 6).

THE RESULTS ATTAINED IN THIS THESIS HAVE INCREASED OUR KNOWLEDGE OF CAPSID STRUCTURE AND THE PROCESS INVOLVED IN CAPSID ASSEMBLY. IN PARTICULAR, THE STUDIES ON VP26 HAVE REFINED THE UNDERSTANDING OF THE NATURE OF THE INTERACTION BETWEEN THE TWO SHELL PROTEINS VP26 AND VP5.

ABBREVIATIONS

A

A _n	absorbance
Ac	<i>Autographa californica</i>
AcNPV	<i>Autographa californica</i> nuclear polyhedrosis virus
ADP	adenosine diphosphate
ATP	adenosine triphosphate
Amp	ampicillin
APS	ammonium persulfate
ATP	adenosine triphosphate
ATPase	adenosine triphosphatase

B

BHIB	brain heart infusion broth
BHK	baby hamster kidney
bp	base pairs
BFA	brefeldin A
BSA	bovine serum albumin
BTV	blue tongue virus

C

C-	carboxy
°C	degrees centigrade
CAT	chloramphenicol acetyl transferase
CAV	cell associated virus
CCV	channel catfish virus
Ci	Curie
CIP	calf intestinal phosphatase
cm	centimetre(s)
CPE	cytopathic effect
CRV	cell released virus

D

3D	three-dimensional
Da	dalton
dATP	2'-deoxyadenosine-5'-triphosphate
dCTP	2'-deoxycytidine-5'-triphosphate
dGTP	2'-deoxyguanosine-5'-triphosphate
dTTP	2'-deoxythymidine-5'-triphosphate
dH ₂ O	distilled water
DCM	dichloromethane
DMF	dimethylfluoride
DMSO	dimethyl sulphoxide
DNA	deoxyribonucleic acid
DR	direct repeat
ds	double stranded
DTT	dithiothreitol

dNTPs
— 2'-deoxynucleoside
— 5'-triphosphates

E
 E early genes
E coli *Escherichia coli*
 EBV Epstein-Barr virus
 EDR envelopment, deenvelopment, reenvelopment pathway
 EDTA ethylenediaminetetra-acetic acid
 EHV-1 equine herpes virus 1
 ELISA(s) enzyme linked immunoabsorbent assay(s)
 EM electron microscope / microscopy
 ES *Exanthem subitum*
 EtBr ethidium bromide

F
 FCS foetal calf serum
 FITC fluorescein thiocynate
 F-moc 9-fluorenylmethloxycarbonyl
 fPH final plate harvest

G
 3xG 3 glycines
 G guanidine
 GFP green fluorescent protein
 GMEM Glasgow modified Eagle's medium
 GuHCl guanidine hydrochloride

H
 h hour(s)
 HCl hydrochloric acid
 HCMV human cytomegalovirus
 HHV human herpesvirus
 6xhis 6 histidines
 HSV herpes simplex virus
 Hve herpesvirus mediator

I
 ICP infected cell polypeptide
 IE immediate early genes
 Ig immunoglobulin
 iPI initial plate isolate
 IRL internal long repeat
 ISL internal short repeat
 IPTG isopropylthio- β -D-galactoside

K
 k kilo (10^3)
 kan kanamycin
 kb/kbp kilobase pairs
 KS Kaposi's sarcoma

L	
L	long segment / late genes
l	litre
LAT	latency associated transcript
M	
m	milli (10^{-3})
M	molar
mA	milliamps
mAb	monoclonal antibody
MAP	multiple antigenic peptide(s)
MCP	major capsid protein
min	minute(s)
mg	milligram(s)
ml	millilitre
mM	millimolar
moi	multiplicity of infection
Mw	molecular weight
mRNA	messenger RNA
N	
n	nano (10^{-9})
N-	amino
NaCl	sodium chloride
NCS	newborn calf serum
Ni ²⁺	nickel ion
NMR	nuclear magnetic resonance imaging
NP40	nonidet P40
NPT	non-permissive temperature
NTA	nitriilo-tri-acetic acid
O	
OBP	origin binding protein
OD	optical density
o/n	overnight
ORF	open reading frame
ori	origin of replication
oriL	origin of replication in U _L
oriS	origin of replication in U _S
P	
PAGE	polyacrylamide gel electrophoresis
PBS	phosphate buffered saline
PC	personal computer
PCR	polymerase chain reation
pfu	plaque forming units
PH	plate harvest
pi	post infection
pol	polymerase
PRV	pseudorabies virus

PS / Pen/Strep penicillin/streptomycin
PG proteoglycan(s)
PT permissive temperature
Pvr2 poliovirus receptor related protein 2

R

RGB resolving gel buffer
RNA ribonucleic acid
RNaseA ribonuclease A
rpm revolutions per minute
rt room temperature

S

S short segment
³⁵[S] sulphur-35 radioisotope
SCMV simian cytomegalovirus
SDS sodium dodecyl sulphate
sec second(s)
Sf21 *Spodoptera frugiperda* 21 insect cells
SPOTs SPOTscan technique
ss single stranded
SV-40 simian virus 40

T

T thymidine
TCA trichloroacetic acid
TEMED N,N,N',N'-tetramethylethylene diamine
TFA trifluoroacetic acid
TNF tumour necrosis factor
Tris tris (hydroxymethyl) aminoethane

U

μ micro (10⁻⁶)
μg microgram
μl microlitre
UL unique long
US unique short
UV ultra violet

V

V Volts
vhs virion host shut-off protein
v/v volume to volume ratio
VZV varicella-zoster virus

W

W watts
wt wild type
w/v weight to volume ratio

w/w weight to weight ratio

X
X-gal 5-bromo-4-chloro-3-indolyl- β -D-galactosidase

One and Three Letter Abbreviations For Amino Acids

Amino acid	Three letter code	One letter code
Alanine	Ala	A
Arginine	Arg	R
Asparagine	Asn	N
Aspartic acid	Asp	D
Cysteine	Cys	C
Glutamine	Gln	Q
Glutamic acid	Glu	E
Glycine	Gly	G
Histidine	His	H
Isoleucine	Ile	I
Leucine	Leu	L
Lysine	Lys	K
Methionine	Met	M
Phenylalanine	Phe	F
Proline	Pro	P
Serine	Ser	S
Threonine	Thr	T
Tryptophan	Trp	W
Tyrosin	Tyr	Y
Valine	Val	V

One Letter Abbreviations for DNA/RNA Bases

Base	One letter code
Adenine	A
Cytosine	C
Guanine	G
Thymidine	T
Uracil	U

CHAPTER 1

INTRODUCTION

**Figure 1.1: Electron Micrograph of
an HSV-1 Virion**

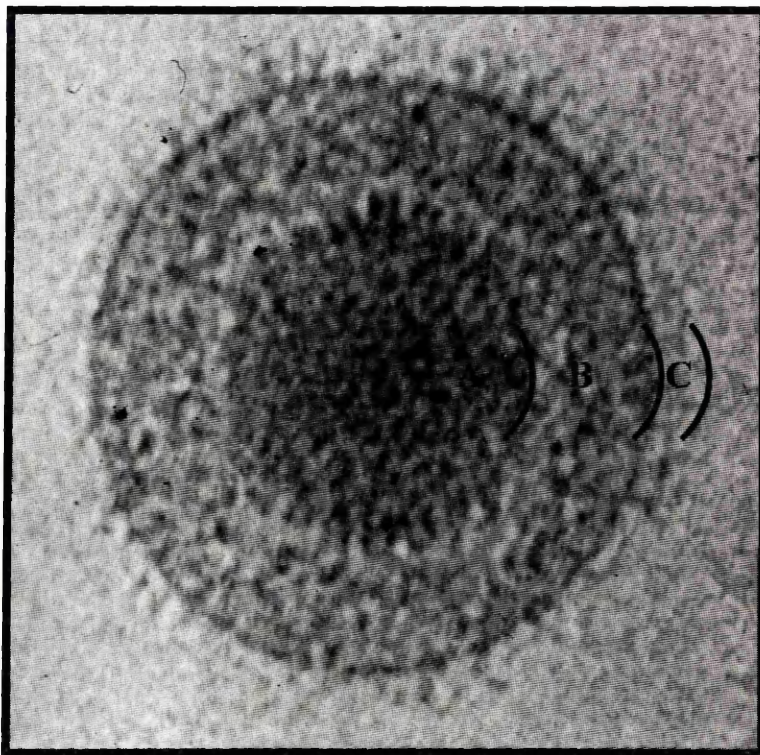


Figure 1.1: Electron micrograph of a frozen hydrated HSV-1 virion. The major structural features are indicated by A- the capsid, B- the tegument and C- the envelope, with associated glycoproteins.

This figure was reproduced with permission from W Chiu, Baylor College of Medicine, USA.

Table 1.1: Classification of Herpesviridae

Family : <i>Herpesviridae</i>							
Sub-family	<i>Alphaherpesvirinae</i>			<i>Betaherpesvirinae</i>		<i>Gammaherpesvirinae</i>	
Genera	<i>Simplicivirus</i>	<i>Varicellovirus</i>	<i>Cytomegalovirus</i>	<i>Murinegalovirus</i>	<i>Roseolovirus</i>	<i>Lymphocryptovirus</i>	
Virus	HSV-1 / (HHV-1)* HSV-2 / (HHV-2)* BOVINE MAMMILLITIS BHV-2	VZV / (HHV-3)* EQUID HERPESVIRUS / EHV-1 PSEUDORABIES VIRUS / PRV	HCMV / (HHV-5)*	MURINE CMV / (MHV-1)	HHV-6* HHV-7*	EBV / (HHV-4)*	Rhadinovirus HERPESVIRUS ATELES-2 HERPESVIRUS SAIMIRI-2 HHV-8*

* Herpesviruses which infect humans

1. HISTORICAL PERSPECTIVE

Herpesviruses were named after the clinical manifestation of the diseases which some of them cause. The word 'herpes' has been used in medicine for the last 25 centuries and derives from the Greek meaning to creep or to crawl (Beswick, 1962). The word 'herpes' was used in writings dating back to Hippocrates, but probably denoted a type of lesion as opposed to a specific disease and would describe eczemas, cancers of the skin and, up until 1938, ringworm (reviewed by Wildy, 1973). Probably few of the conditions designated as being a Herpesvirus infection today, would have been called so by the original definition of the word.

It was not until the late nineteenth century and early twentieth century that specific diseases were attributed to specific herpesviruses. After the introduction of negative staining, which was first performed on HSV-1 in 1959 (Brenner & Horne, 1959), viruses began to be classified on their structural appearance under the microscope.

2. CLASSIFICATION OF HERPESVIRUSES

Herpesviruses belong to the family of *Herpesviridae* and have been isolated from almost every vertebrate species investigated indeed, at least 112 distinct species have thus far been recognised (Roizman *et al*, 1992), eight of which are known to infect humans. The virions within the family vary in their antigenic properties, size and composition, however, membership to the *Herpesviridae* family is based on rigid criteria governing the architecture of the virion. The virion is composed of 3 distinct layers (see figure 1.1):

- the capsid - this contains the double stranded DNA genome
- the tegument - this amorphous protein layer surrounds the capsid
- the envelope - this is the outermost layer which is composed of a lipid bilayer and has glycoprotein spikes protruding from it.

During the course of evolution, members of the family have evolved to form three distinct subfamilies: *Alphaherpesvirinae*, *Betaherpesvirinae* and *Gammaherpesvirinae*, which each contain 2 or 3 genera (see table 1.1). These 3 sub-families were initially classified on the basis of their biological properties such as host range, reproductive cycle patterns, cytopathology and latency characteristics (Roizman *et al*, 1981).

Recently a more consistent re-classification has been drawn on the basis of lineages of gene content and sequence homology (Roizman *et al*, 1992).

2.1 Alphaherpesvirinae

Historically this sub-type includes viruses which can infect a wide range of cell types in tissue culture, have a short (less than 24 hours) reproductive cycle, a rapid spread in cell culture and establishment of latency primarily, but not exclusively, in ganglia. The virus genome has a Mw range of 85-110 x 10⁶.

2.2 Betaherpesvirinae

The biological properties of this set of viruses include a long incubation period with slow spread. This often results in the development of a cytomeglia where infected cells become grossly enlarged. Latency is generally established in the secretory glands, lymphoreticular cells, kidneys and other tissues. The virus genome ranges from Mw 110-150 x 10⁶.

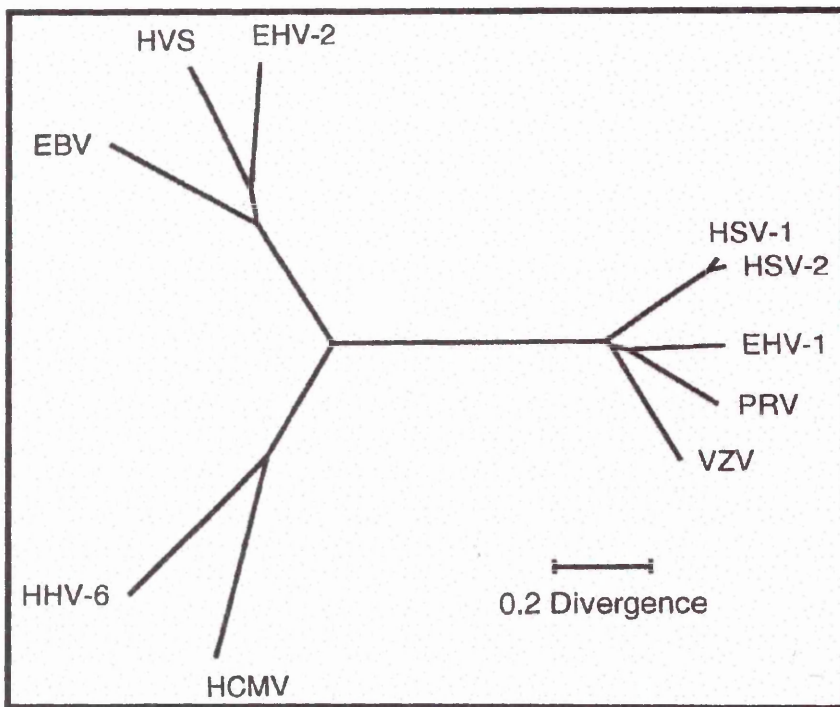
2.3 Gammaherpesvirinae

Herpesviruses are classified to this category when they replicate *in vitro* in lymphoblastoid (T or B) cells and have variable cytopathology and reproductive cycles. Establishment of latency is in the lymphoid tissue and the genome has a Mw of less than 110 x 10⁶.

2.4 Future Trends in Classification

On the whole the classification based on biological properties has proved accurate and few viruses have needed to be re-classified. Generally a high degree of sequence homology and genome relatedness is observed between current genera. There are of course notable exceptions: Marek's disease virus (a contagious virus in chickens characterised by lymphoid tumours) and herpesvirus of turkeys, were regarded as belonging to the Gammaherpesvirinae sub-family. Sequence analysis has re-assigned them to the Alphaherpesvirinae (Buckmaster *et al*, 1988). Similarly, the newly described viruses HHV-6 and HHV-7 were initially classified as Gammaherpesviruses as they exhibited lymphotropism, but sequence analysis re-assigned them to the Betaherpesvirinae.

Figure 1.2: Phylogenetic Tree



Introduction

Herpesviruses are a large family of DNA viruses that infect a wide range of animals.

The family is divided into three subfamilies: Alpha-, Beta- and Gamma-herpesvirinae.

Figure 1.2 shows a phylogenetic tree of a selection of herpesvirus genes.

Herpesviruses

VZV (varicella-zoster virus) is a member of the Alpha-herpesvirinae subfamily.

EBV (Epstein-Barr virus) is a member of the Gamma-herpesvirinae subfamily.

CMV (Cytomegalovirus) is a member of the Beta-herpesvirinae subfamily.

HSV-1 (Herpes simplex virus 1) is a member of the Alpha-herpesvirinae subfamily.

HSV-2 (Herpes simplex virus 2) is a member of the Alpha-herpesvirinae subfamily.

Figure 1.2 shows a phylogenetic tree of a selection of herpesvirus genes.

The tree highlights three major sublineages which correspond to the three subfamilies (ie Alpha-, Beta- and Gamma-herpesvirinae) and indicates their relative sequence relatedness.

The Alpha-herpesvirinae subfamily is the most diverse and includes VZV, HSV-1 and HSV-2.

The Beta-herpesvirinae subfamily includes CMV and HHV-8.

The Gamma-herpesvirinae subfamily includes EBV and KSHV.

Figure 1.2: This figure is reproduced from McGeoch *et al* 1995) and shows a phylogenetic tree of a selection of herpesvirus genes (see reference). This figure highlights three major sublineages which correspond to the three subfamilies (ie Alpha-, Beta- and Gamma-herpesvirinae) and indicates their relative sequence relatedness.

Herpesviruses

Herpesviruses are a large family of DNA viruses that infect a wide range of animals.

The family is divided into three subfamilies: Alpha-, Beta- and Gamma-herpesvirinae.

Figure 1.2 shows a phylogenetic tree of a selection of herpesvirus genes.

The tree highlights three major sublineages which correspond to the three subfamilies (ie Alpha-, Beta- and Gamma-herpesvirinae) and indicates their relative sequence relatedness.

The Alpha-herpesvirinae subfamily is the most diverse and includes VZV, HSV-1 and HSV-2.

The Beta-herpesvirinae subfamily includes CMV and HHV-8.

The Gamma-herpesvirinae subfamily includes EBV and KSHV.

Herpesviruses

3. Herpesviruses Which Infect Humans

Over 80 herpesviruses are known to infect humans. The most common are:

Herpes simplex virus 1 (HSV-1) and 2 (HSV-2) - both of which cause oral and genital herpes.

Varicella-zoster virus (VZV) - which causes chickenpox and shingles.

Cytomegalovirus (CMV) - which is a common cause of congenital infection.

It is clear from sequence comparisons and detailed phylogenetic analysis that the *Alpha-*, *Beta-* and *Gamma-herpesvirinae* evolved from a common ancestor (McGeoch et al, 1995). Figure 1.2 shows an example of the sequence relatedness between some herpesviruses.

VZV (an Alphaherpesvirus) and EBV (a Gammaherpesvirus) share a sizeable subset of conserved genes. These were probably part of the progenitor virus's genetic components (Davison & Taylor, 1987). However, when the herpesvirus channel catfish virus (CCV) was sequenced, no homology was seen with any of the other herpesviruses (Davison, 1992). This data can be interpreted in 2 different ways:

- the lack of homology is indicative of a separate origin for CCV from other herpesviruses and therefore it should no longer be included in the family
- the presence of a common virion and capsid morphology in CCV and other herpesviruses (Wolf & Darlington, 1971) indicates a very distant, but still related origin.

More detailed analysis has since established that CCV does belong to the herpesvirus family (Booy *et al*, 1996). Recently, other fish viruses have been isolated which have homology to CCV but are unrelated to mammalian herpesviruses (Davison, 1998; Davison *et al*, 1999).

It has also been proposed that the herpesviruses should be re-named (Roizman *et al*, 1992) taking into account their taxonomic unit and host. Although this can be applied to newly discovered viruses, it is unlikely that traditional nomenclature will be dropped readily. Also, in future herpesvirus classification may be required to take account of complete nucleotide sequences of the virus. Such factors as: (i) the arrangement of terminal sequences involved in packaging, (ii) conservation and positioning of genes and gene clusters, (iii) the presence of nucleotides subject to methylation, should all be considered.

3. Herpesviruses Which Infect Humans

Currently 8 herpesviruses are known to infect humans (see table 1.1). Most of these herpesviruses are widespread in both the developed and the underdeveloped world (reviewed by Whitley & Schlitt, 1991).

Natural animal vectors have not been described and humans remain the sole reservoir for transmission. Virus is transmitted by person to person contact and it is estimated that, at any given time, over one third of the World's population has a productive herpesvirus infection. Symptoms of the viruses cover a broad spectrum of clinical manifestations. For example HSV-1 can range from minor lesions (indiscernible to many patients) to severe and life-threatening encephalopathies, generally observed in the immunocompromised host. In fact, HSV has been recognised as the most common cause of sporadic and fatal encephalitis in the USA (Whitley & Schlitt, 1991)

All herpesviruses are capable of existing within their host in a dormant or latent state. Thus, after infection with a herpesvirus, DNA remains in the individual for their entire lifetime. Reactivation of the virus may occur after months or even years and the trigger is poorly understood. Both internal and external factors, such as mental and physical stress, hormone changes, age and exposure to UV radiation, appear to be important for reactivation.

3.1 HSV-1 (HHV-1)

HSV-1 (reviewed by Subak-Sharpe & Dargan, 1998) is closely related to HSV-2 and it was not until the mid-1960's that 2 distinct antigenic sub-types of HSV were recognised (Nahmias & Dowdle, 1968). HSV-1 has a predilection for oral and facial regions although this is not exclusive and it can also be detected in genital areas. Viral infection is dependant on close personal contact and it is generally transmitted through oral secretions or respiratory droplets.

HSV-1 must come in to contact with abraded skin or mucosal surfaces for infection to be initiated. The most common manifestation is the appearance of lesions on the face or lip, known as 'cold sores'. The lesion is induced by a combination of viral replication in the mucous membranes and epithelial cells and the inflammatory immune response. The virion also travels through the neurons to the trigeminal ganglia where it remains in a latent state until subsequent reactivation, when a new round of lesions may occur.

3.2 HSV-2 (HHV-2)

HSV-2 (reviewed by Levine, 1992) is usually acquired through sexual contact and so individuals with multiple sexual partners are most at risk. As with HSV-1 the virus causes lesions by first infecting epithelial cells and mucous membranes, generally but not exclusively, of the genitalia. It then travels along axons of the sensory neurons to the sacral ganglia, where it becomes latent. Reactivation may result in the recurrence of painful and uncomfortable lesions, however it may also produce an asymptomatic infection, which obviously will aid viral spread.

One of the most damaging aspects of HSV-2 is that it can be passed from infected mothers to their babies either in the uterus, during childbirth (75-80% of neonatal infections occur this way), or after childbirth due to poor hygiene practice. The consequences of newborn infection can be extremely serious with encephalitis and extensive skin lesions not uncommon. For this reason HSV-2 positive mothers, with active infections, will usually deliver by caesarean section to avoid passage of the baby through the birth canal.

3.3 VZV (HHV-3)

VZV (reviewed by Gelb, 1990) causes two distinct diseases, chickenpox and shingles. Chickenpox is the primary infection and generally occurs during childhood. The virus enters through the oral cavity and replicates in the upper respiratory tract. After a few days it spreads and begins to infect organs, seeding the skin to form the distinctive pockmarks. The immune system clears productive virus within a few weeks however, the viral DNA enters the sensory neurons where it becomes latent. The virus can remain here for several decades causing no apparent effects. In some elderly or immunocompromised individuals the virus reactivates, travels down the sensory neurons to the skin where it causes the painful and distinctive rash, characteristic of shingles.

3.4 EBV (HHV-4)

EBV (reviewed by Miller, 1990) can cause mononucleosis if contracted in early adulthood. The disease is more commonly known as glandular fever or the kissing disease, as it is passed through oral secretions. The virus replicates actively in the mouth tongue and salivary glands causing a sore throat and lymphadenopathy. It then spreads to T and B cells of the immune system where it can become latent. Infiltration of B cells

in the nervous system can create a severe malaise which can last anything from a week to a few months.

EBV has also been associated with certain cancers such as nasopharyngeal carcinoma and Burkitt's lymphoma (Levine, 1992). In immunodeficient individuals such as AIDS patients, fatal B-cell lymphomas may develop after infection with EBV.

3.5 HCMV (HHV-5)

HCMV (reviewed by Britt, 1996b) has nearly universal occurrence in the human population where the virus establishes life-long infection. However, it rarely shows definable symptoms in healthy individuals. Immunosuppression, which results in T lymphocyte depression, correlates highly with susceptibility to HCMV disease suggesting that the cellular immune response is involved in suppressing HCMV associated disease. It is not surprising therefore that AIDS patients often exhibit HCMV associated clinical manifestations, such as retinitis and gastrointestinal dysfunction. Occasionally HCMV causes clinical symptoms in adults indistinguishable from EBV mononucleosis however, the major damaging effects of the virus are seen in neonates.

Congenital HCMV is a major cause of brain damage in infants (Britt, 1996a). For example in the USA it is estimated that 1-2% annually of all live births have congenital defects due to this virus. A variable percent of these children will show defects in their CNS or permanent brain damage and/or reduced perception functions during the first 2 years of their life. This may develop into continuing and severe learning difficulties. Acquisition of HCMV during pregnancy seems to pose the greatest risk, but this is difficult to monitor as the mother often does not show clinical symptoms of disease. There has been limited success in preventing *in utero* spread using gancyclovir.

3.6 HHV-6

HHV-6 (reviewed by Levy, 1997) was first recognised in 1987 from the blood of an AIDS patient who exhibited lymphoma (Salahuddin *et al*, 1986). Two major variants A and B have been identified on the basis of monoclonal antibody reactions and cell culture properties (Ablashi *et al*, 1991). It would appear that the B variant can be isolated more frequently from the population, except in AIDS patients where the A variant is more common.

The virus replicates mainly in CD 8+ T cells but also has tropism for other cells of the immune system and it appears to form a latent state in peripheral mononuclear cells. Infection is spread through saliva and is estimated to occur naturally in >85% of the population. Symptoms are rare and appear to be associated with a benign childhood illness, *Exanthum subitum*. In most cases infants will exhibit a sudden fever which resolves in a few days. A rash appears as the fever subsides. In previously healthy adults a mononucleosis-like illness can occur but, in HIV and AIDS individuals, the virus has been associated with retinal disorders, lymphomas and leukaemias.

3.7 HHV-7

HHV-7 (reviewed by Levy, 1997) can be found in the peripheral blood of the general population with transmission occurring early in childhood. The virus was first isolated from CD4+ T cells of a healthy individual (Frenkel *et al*, 1990) and shows a high homology with HHV-6 (see figure 1.2).

The virus is capable of down-modulating CD4 cells however, a direct association with human disease has not been recognised although increased virus levels have been isolated from individuals with chronic fatigue syndrome. It has also been suggested that HHV-7 is able to reactivate HHV-6 from latency and boost viral replication but further study of this is required.

3.8 HHV-8

Recently a new candidate human tumour virus HHV-8, previously termed KSHV, has been identified associated with Kaposi's sarcoma (KS) (reviewed by Levy, 1997; Brooks *et al*, 1997). The virus was first discovered by a PCR based technique where DNA in a KS lesion was compared with DNA from normal skin (Chang *et al*, 1994). This novel approach revealed KS specific sequences which had homology with γ -herpesviruses.

KS was first described in 1872 by Moritz Kaposi as a rare and benign skin tumour associated with elderly Mediterranean men. Over the last 20 years there has been an increasing incidence which, it is now clear, is associated with the AIDS pandemic. These individuals show atypical and aggressive KS which is frequently fatal.

Figure 1.3: The HSV viral genome consists of 2 covalently linked components, L and S (double headed arrows) which contain unique sequences UL and US (solid lines). These are flanked by terminal and internal repeat elements (open and shaded boxes). The α sequence is represented by the unshaded box and is present at each end of the genome and in an inverted orientation at the L-S junction. The L and S regions can invert relative to each other to produce 4 isomers (single headed arrows). These are P (prototype), IL (inversion of L), LS (inversion of S) and ISL (inversion of L and S).

The figure is not drawn to scale.

HHV-8 resembles EBV in its tropism for B cells and its existence in a latent state. Indeed, the viral DNA is usually found associated with EBV in tumours however, some lymphomas contain HHV-8 alone, suggesting that the virus has a direct role in the transformation process.

Transmission of HHV-8 has been difficult to demonstrate and unlike HHV-6 and HHV-7, seropositivity is not common before puberty (<5%). This together with the high incidence in HIV positive homosexual males is indicative of the role of anal intercourse as the major transmission route.

4. HSV-1 Viral Architecture

The macromolecular structure of the virion is conserved throughout the Herpesviridae, however, this study was concerned with HSV-1 and so the description of the virion architecture will centre around this virus, with particular emphasis on the capsid structure. It is nevertheless important to understand the nature of the whole virion. The DNA, tegument, envelope and capsid will each be discussed in turn.

4.1 The Genome

The complete sequence of the dsDNA genome (strain 17⁺) was published in 1988 and was shown to contain 152260 residues, which was predicted to contain 72 genes encoding 70 proteins (McGeoch *et al*, 1988). 56 ORFs were identified within the unique long region and 12 within the unique short region. UL15 was spliced and the intron contained both the UL16 and UL17 ORFs. Since this publication several other genes have been identified and currently 84 protein encoding genes have been identified (Roizman, 1996).

4.1.1 Organisation of the Genome

The genome is composed of 2 unique regions, the unique long region (UL) and the unique short region (US) (see figure 1.3). Each unique segment is flanked and linked by a set of internal repeats (IR) and terminal repeats (TR) (Sheldrick & Berthelot, 1974; Delius & Clements, 1976); TRL/IRL and IRS/TRS. There is also a variable short sequence (250-500bp), termed the 'a' sequence, present as a direct repeat at each

terminus and in an inverted orientation at the L-S junction (Sheldrick & Berthelot, 1974; Wadsworth *et al*, 1976; Delius & Clements, 1976; Hayward *et al*, 1975; Davison & Wilkie, 1981). This sequence is composed of unique (U) and direct repeat (DR) regions. For example, the HSV-1 strain F *a* sequence can be represented as DR₁ – U_b – DR_{2_n} – DR_{4_m} – U_c – DR₁, where U_b and U_c equal 65 and 58 bp respectively (Mocarski & Roizman, 1982). The DR₂ (12bp) varies from 19-22 copies and DR₄ (37bp) from 2-3 copies. It is this variation which accounts for the difference in size of the *a* sequence between virus strains.

The *a* sequence appears to be important for a number of functions including circularisation of DNA and site specific recombination events (Davison, 1983; Poffenberger & Roizman, 1985; Mocarski & Roizman, 1981; 1982). It also has functions in the cleavage and packaging processes (Varmuza & Smiley, 1985; Deiss *et al*, 1986; reviewed by Roizman & Sears, 1996).

During virus infection US and UL can invert, relative to one another, to form 4 isomeric arrangements (summarised in figure 1.3). These have been designated P (prototype), IL (inversion of long segment), IS (inversion of short segment) and ISL (inversion of long and short segments) (Clements *et al*, 1977; Wilkie, 1976; Roizman, 1979). The isomers occur with equal frequency in virions.

4.1.2 Packaged State of the Genome

Originally the DNA was considered to exist as a toroid arrangement (Furlong *et al*, 1972) around a central protein plug, thought to consist of VP21 (Gibson & Roizman, 1972). This hypothesis evolved from a series of electron micrographs produced in the late 1970's (reviewed by Dargan, 1986) which appeared to show convincing evidence of a toroid-like arrangement within the nucleocapsid. Despite the fact that the DNA was mainly seen as a uniform and densely staining area, the toroid model became firmly established. Indeed, when a toroid pattern was not observed, its absence was attributed the plane of section or preparation procedure.

Cryo-EM examinations have provided no evidence for a toroid structure. Instead it would appear that packaged DNA exists in a liquid crystalline state (Booy *et al*, 1991a),

Table 1.2: Tegument Proteins

Gene	Protein	Approx Mr (kDa)	Properties
UL4			function unknown
UL11		11	myristylated, role in envelopment & transport of nascent virions
UL13	VP18.5	57	protein kinase, phosphorylates UL49
UL21			function unknown
<u>UL25</u>		63	role in penetration, cleavage & packaging DNA
<u>UL36</u>	VP1/2	336	role in releasing DNA at the nuclear pore
<u>UL37</u>		121	phosphoprotein, function unknown
UL41	vhs	55	virion host shut off protein
UL46	VP11/12	79	modulates Vmw65 transactivation
UL47	VP13/14	74	modulates Vmw65 transactivation
<u>UL48</u>	Vmw65	54	transactivates IE genes
<u>UL49</u>	VP22	32	secreted & exported to surrounding cells via microtubules
UL54	Vmw63	55	IE2 transcription / post transcription regulator
UL56			function unknown
RL2	Vmw110	79	IE1 transcription regulator
<u>RS1</u>	Vmw175	133	IE3 transcription regulator
US3		53	protein kinase, phosphorylates UL34
US9		10	phosphoprotein, function unknown
US10		34	function unknown
US11		18	involved in translation at ribosomes

similar to that of bacteriophage λ and T4, and arranged as parallel bundles (Booy *et al*, 1991b). Recent cryo-electron microscopy images (Zhou *et al*, 1999) have produced characteristic patterns expected for a spool model. However, unlike the bacteriophage T7, HSV does not have a central protein plug around which the genome is arranged. Instead, the molecule is proposed to wrap itself around the inner surface of the capsid shell, accumulating one layer at a time and becoming less ordered. Up to 10 concentric DNA layers have been observed (Zhou *et al*, 1999). Therefore it would seem that this featureless appearance of the majority of DNA containing capsids, in thin section, is an accurate reflection of their structure and the toroid model is an artefact (Puvion-Dutilleul *et al*, 1987). However, the spooling model does account for the changing appearance of DNA under negative staining. As the molecule is formed along a definite axis certain sections may appear to resemble a toroidal core.

4.2 The Tegument

The tegument is an amorphous protein layer (Zhou *et al*, 1999) which lies between the nucleocapsid and envelope (Wildy *et al*, 1960). It is a poorly understood structure and it is not entirely clear how it interacts with adjacent structural components however, Zhou *et al* (1999) have produced some interesting cryo-EM images which shall be discussed later. The tegument is known to consist of at least 18 proteins (see table 1.2), many of whose functions have not been fully elucidated.

4.2.1 Assembly of the Tegument

Studies with Light (L) particles (Szilagi & Cunningham, 1991) have shown that tegument proteins have the ability to assemble into stable structures in the absence of capsids. L-particles consist solely of envelope and tegument (Rixon *et al*, 1992). They are able to attach and fuse to host cells but cannot initiate infection, as they contain no DNA (McLauchlan *et al*, 1992a). The tegument proteins in these particles appear to be very similar to virion tegument (McLauchlan & Rixon, 1992) indicating that capsids are not required for assembly of apparently normal tegument *in vitro*.

4.2.2 Function of the Tegument

The precise role of the tegument is unclear however functions related to morphogenesis, uncoating and regulation of gene expression, have been assigned to its component proteins. Currently VP16 (UL48) and the product of UL11 have been implicated in assembly, as deficient mutants fail to form an envelope (Weinheimer *et al*, 1992; Baines

& Roizman, 1992; MacLean *et al*, 1992). VP16 trans-induces HSV-1 IE gene transcription (Post *et al*, 1981; Batterson & Roizman, 1983; Campbell *et al*, 1984) and will be discussed in more detail later (Section 5.2). Other tegument proteins also appear to play an important role early in infection. For example UL41 (designated virion host shut-off protein, vhs) and UL13 disrupt host cell functions (see section 5.2).

The pathway of the HSV-1 life cycle (see section 5) is such that after envelope fusion with the host cell, the tegument and capsid are released into the cytoplasm. It appears that tegument proteins, VP1-3 (UL36), have a role in facilitating release of DNA from the capsid. Ts mutants of this gene (tsB7), fail to release the genome at the non-permissive temperature (Batterson *et al*, 1983). It has recently been suggested that this protein may be interacting directly with the pentonal sites of the capsid. Zhou *et al*, 1999, visualised the intact virion (by cryo-electron microscopy) and produced a 3D image which highlighted a small area of ordered tegument attached to this outer capsid surface. As VP1-3 has been detected as one of the few remaining tegument proteins in capsid/tegument fractions treated with detergents (Spear, 1972; Vernon, 1978) this protein is strongly tipped to be forming this interaction.

Two tegument proteins, VP18.5 (UL13) and the product of US3, are protein kinases. VP22 (UL49) is a substrate for VP18.5 (Coulter *et al*, 1993) and UL34 envelope protein is a substrate for US3 (Purves & Roizman, 1992). VP22 is one of the most abundant tegument components, however, it would seem that its abundance in the tegument is not fixed. Leslie *et al* (1996) showed that increasing the levels of VP22 expression allowed more of this protein to be incorporated into the tegument. However, this resulted in a decrease of VP13/14, demonstrating that the composition of the tegument can vary. Elliott & O'Hare (1997) have convincingly shown that VP22 has a mechanism which allows it to travel intercellularly. This process is so efficient that, following expression in a small population of cells, the protein spreads to the whole monolayer. The transport mechanism has been visualised using time lapse photography of VP22 fused to a green fluorescent protein (Elliott & O'Hare, 1999). This study revealed that when VP22 was initially expressed, it was present in diffuse cytoplasmic locations. However, particulate material formed which travelled through an exclusively

Table 1.3: Envelope Glycoproteins

Protein	Gene	Approx Mr (kDa)	Properties
gB	<u>UL27</u>	100	Role in entry, protein present as a dimer
gC	UL44	44	Role in attachment to host cells, binds to heparin sulphate
gD	<u>US6</u>	43	Role in entry
gE	US8	59	protects against immune neutralisation by binding to Fc portion of IgG
gG	US4	25	Function unknown
gH	<u>UL22</u>	90	complexes with gL to mediate viral entry
gI	US7	41	complexes with gE
gJ	US5	10	function unknown
gK	UL53	38	role in envelopment and egress
gL	<u>UL1</u>	25	complexes with gH to mediate viral entry
gM	UL20	24	role in egress

(The genes underlined are essential for virion infectivity).

cytoplasmic pathway to the cell periphery. VP22 may have a role in trafficking proteins between cells.

Recent mutational analysis has revealed that the UL17 gene products are associated with the virion tegument and are required for cleavage and packaging of DNA. This is the first tegument protein to be definitively shown to be required for these process (Salmon *et al*, 1998).

4.3 The Envelope

The virion is enclosed by a trilaminar envelope (Wildy *et al*, 1960) which is approximately spherical and has prominent protein spikes protruding from it, visible under negative staining (Wildy *et al*, 1960; Stannard *et al*, 1987). These spikes are known to consist of glycoproteins which have been shown, by immunogold labelling, to vary in size from approximately 80-240Å (Stannard *et al*, 1987). Currently 11 glycoproteins have been identified (reviewed by Spear, 1993 and Haar & Skulstad, 1994). These have each been given an alphabetical designation, in chronological order of discovery, preceded by a g. No glycoprotein A (Spear, 1976) exists, as it was found to be identical to gB (Eberle & Courtney, 1980) and gF (Balachandran *et al*, 1981) was renamed gC-2, as it was found to be a gC homologue in HSV-2 (Zezulak & Spear, 1984). The exact number of envelope proteins is unknown but, the 11 which have thus far been identified in the virion, are detailed in table 1.3.

It is interesting to note that none of the glycoproteins have been shown to be essential for assembly or envelopment. However, gB, gD, gH and gL are required for infectivity (Cai *et al*, 1988; Ligas & Johnson, 1988; Desai *et al*, 1988; Hutchinson *et al*, 1992).

4.4 The Capsid

The capsid is an icosahedral lattice which surrounds the viral DNA. It has T=16 icosahedral symmetry and is composed of 162 capsomeric sub-units. There are 3 main types of HSV-1 capsid, which have been distinguished in thin section:

- A (or empty capsids), which are seemingly empty shells
- B (or intermediate capsids), which contain scaffold
- C (or full capsids), which contain the viral DNA

Table 1.4: Capsid Proteins

(i) Major Capsid Proteins

Gene	Protein	Approx Mr (kDa)			Location in Capsid	Presence in A capsids	
<u>UL18</u>	VP23	33	32	33	34	icosahedral shell, triplexes	+
<u>UL19</u>	VP5	155	155	154	150	icosahedral shell, capsomeres	+
<u>UL26</u>	VP21	44		40	42	scaffold	-
<u>UL26</u>	VP24	25	25	25	25	unknown, probably scaffold	+
<u>UL26.5</u>	VP22a	39	40	38	40	scaffold	-
<u>UL35</u>	VP26		12	12	12	icosahedral shell, tips of hexons	+
<u>UL38</u>	VP19c	53	50	50	54	icosahedral shell, triplexes	+
Ref		a	b	c	d		

(ii) Minor Capsid Proteins

Gene	Approx Mr (kDa)	Location in Capsid
<u>UL6</u>	74	unknown
<u>UL12.5</u>	60	unknown
<u>UL15</u>	81	unknown
<u>UL25</u>	63	unknown
<u>UL28</u>	85.5	unknown

Table 1.4: HSV-1 capsid proteins and the genes which encode them. The seven major capsid proteins are detailed in panel (i). The approximate Mr of each varies slightly in the published literature. The references (Ref) quoted in this table are:

- a** Gibson & Roizman, 1972
- b** Zweig *et al*, 1979
- c** Cohen *et al*, 1980
- d** Rixon *et al*, 1990

The five minor capsid proteins, thus far identified, are detailed in panel (ii).

The genes underlined are essential for virion infectivity.

The 3 species have also been designated as lights, intermediates and heavies, respectively, based on their sedimentation position on a sucrose density gradient. All 3 capsid types have a common shell composition, however, A and C capsids lack the internal scaffold (Newcomb *et al*, 1993). A series of pulse-chase experiments have indicated that B capsids mature into C capsids, with A capsids representing failed DNA packaging products (Perdue *et al*, 1976). The situation may not be as straight forward as previously thought as a procapsid has recently been identified (Newcomb *et al*, 1994). This aspect is fully discussed in Chapter 7, Conclusion.

4.4.1 Molecular Composition

The capsid is composed of 7 major proteins and several minor proteins. The proteins which make up the capsid are detailed in table 1.4 and shall now be discussed individually.

4.4.1.1 VP5 (UL19)

VP5 is the major capsid protein (MCP) having both a highest Mr of all the capsid proteins and constituting 72%, by mass, of the capsid shell (Gibson & Roizman, 1972; Newcomb *et al*, 1989).

It is encoded by the UL19 gene (Costa *et al*, 1984; McGeoch *et al*, 1988) which initiates at position 40528 and terminates at position 36406 (McGeoch *et al*, 1988), being transcribed from right to left. This results in an ORF of 4122bp, which corresponds to a predicted protein Mr=149075 Da. This approximately matches the observed Mr of 155kDa, (Gibson & Roizman, 1972; Zweig *et al*, 1979b) 154kDa, (Cohen *et al*, 1980) and 150kDa (Rixon *et al*, 1990) indicating that the protein does not undergo extensive post-translational modifications.

VP5 is the major component of both the hexons and pentons (Newcomb *et al*, 1993; Zhou *et al*, 1994). Five copies interact to form each of the 12 pentons and six copies interact to form each of the 150 hexons, totalling 960 copies of VP5 per capsid. It is not therefore surprising that VP5 is essential for capsid formation. A VP5 null mutant virus (Desai *et al*, 1993) and a ts mutant, tsG8, which had a lesion in the UL19 gene (Weller *et al*, 1987), were both unable to form capsids. Similarly, work using the baculovirus

system has confirmed that VP5 is essential for capsid formation, as when the protein is absent, no capsids are formed (Tatman *et al*, 1994; Thomsen *et al*, 1994).

4.4.1.2 VP19c

VP19c was originally designated VP19, after a 53kDa virion protein (Gibson & Roizman, 1972) which co-migrated with the capsid protein. The 2 proteins were later resolved and the capsid protein was designated VP19c (Heine *et al*, 1974).

A series of lengthy and confused investigations were undertaken to try and locate the gene encoding VP19c (Costa *et al*, 1983; Braun *et al*, 1984; Pertuiset *et al*, 1989). Finally, Rixon *et al* (1990) sequenced the amino terminus of the protein, from purified capsids, and aligned it with the amino terminus of the UL38 ORF, confirming that UL38 encoded VP19c.

UL38 initiates at position 84531 and terminates at position 85926 (McGeoch *et al*, 1988), being transcribed from left to right. This results in an ORF of 1395bp, which corresponds to a predicted protein Mr=50260 Da. This approximately matches the observed Mr of 53kDa, (Gibson & Roizman, 1972) 50kDa, (Zweig *et al*, 1979a; Cohen *et al*, 1980) and 54kDa (Rixon *et al*, 1990) indicating that the protein does not undergo extensive post-translational modifications.

In HSV-2 VP19c is linked by disulphide bonds to VP5 (Zweig *et al*, 1979a) and it is known that this protein forms part of the triplex complex, linking adjacent capsomeres, in HSV-1 and HSV-2 (Newcomb *et al*, 1993). One copy of VP19c and two copies of VP23 interact to form the triplex structure.

Baculovirus studies have shown that this protein is essential for capsid formation (Tatman *et al*, 1994; Thomsen *et al*, 1994). Similarly, mutant studies have confirmed the finding that VP19c is essential for capsid formation as null mutants do not produce detectable virions (Desai *et al*, 1998).

4.4.1.3 VP23

VP23 was identified as a 33kDa protein in 1972 (Gibson & Roizman, 1972). The protein was originally designated as being a component, or substrate, of the protein

kinase, as it was thought to be phosphorylated (Lemaster & Roizman, 1980). However, it was later discovered that VP23 had been confused with a tegument protein with similar electrophoretic mobility (Braun *et al*, 1984).

VP23 is encoded by the UL18 gene (Rixon *et al*, 1990), which is co-terminal with UL19. UL18 initiates at position 36051 and terminates at position 35097 (McGeoch *et al*, 1988), being transcribed from right to left. This results in an ORF of 954bp, which corresponds to a predicted protein $M_r=34268$ Da. This approximately matches the observed M_r of 33kDa, (Gibson & Roizman 1972; Cohen *et al*, 1980) 32kDa, (Zweig *et al*, 1979b) and 34kDa (Rixon *et al*, 1990) indicating that the protein does not undergo extensive post-translational modifications.

Two copies of this protein interact with one copy of VP19c (Newcomb *et al* 1993) to form the triplex. Therefore, like VP19c, this protein is essential for capsid assembly. A null mutant lacking VP23 failed to produce capsids (Desai *et al*, 1993) and baculovirus work has shown that when this is the only absent capsid protein, only densely staining, smaller particles are produced (Tatman *et al*, 1994; Thomsen *et al*, 1994; Rixon *et al*, 1996).

4.4.1.4 VP26

The smallest capsid protein, VP26, was not discovered as a capsid component until 1979 (Heilman *et al*, 1979) when it was designated p12, by virtue of its M_r . The ORF of VP26 was mapped by sequencing fragments of VP26, from purified capsids, and aligning them to the UL35 ORF (Davison *et al*, 1992).

UL35 initiates at position 70566 and terminates at position 70902 (McGeoch *et al*, 1988), being transcribed from left to right. This results in an ORF of 336bp which corresponds to a predicted protein $M_r=12095$ Da. This closely matches the observed M_r of 12kDa (Heilman *et al*, 1979; Cohen *et al*, 1980; Rixon *et al*, 1990) indicating that the protein does not undergo extensive post-translational modifications.

VP26 is located at the tips of the VP5 hexons but not the pentons (Booy *et al*, 1994; Zhou *et al*, 1994; 1995). Six copies of VP26 are arranged in a star shaped pattern at these positions (Zhou *et al*, 1995) amounting to 900 copies of VP26 per capsid.

Figure 1.4: Organisation of UL26 and UL26.5 ORFs

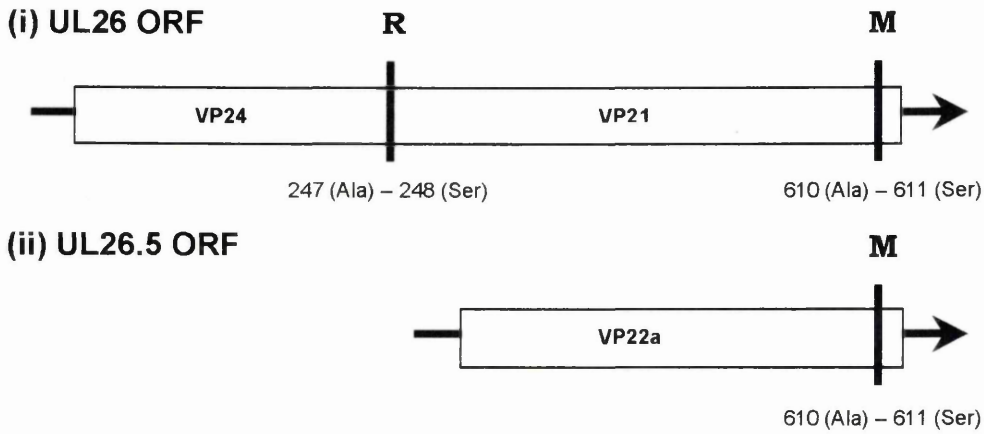


Figure 1.5: Processing Products of UL26 and UL26.5

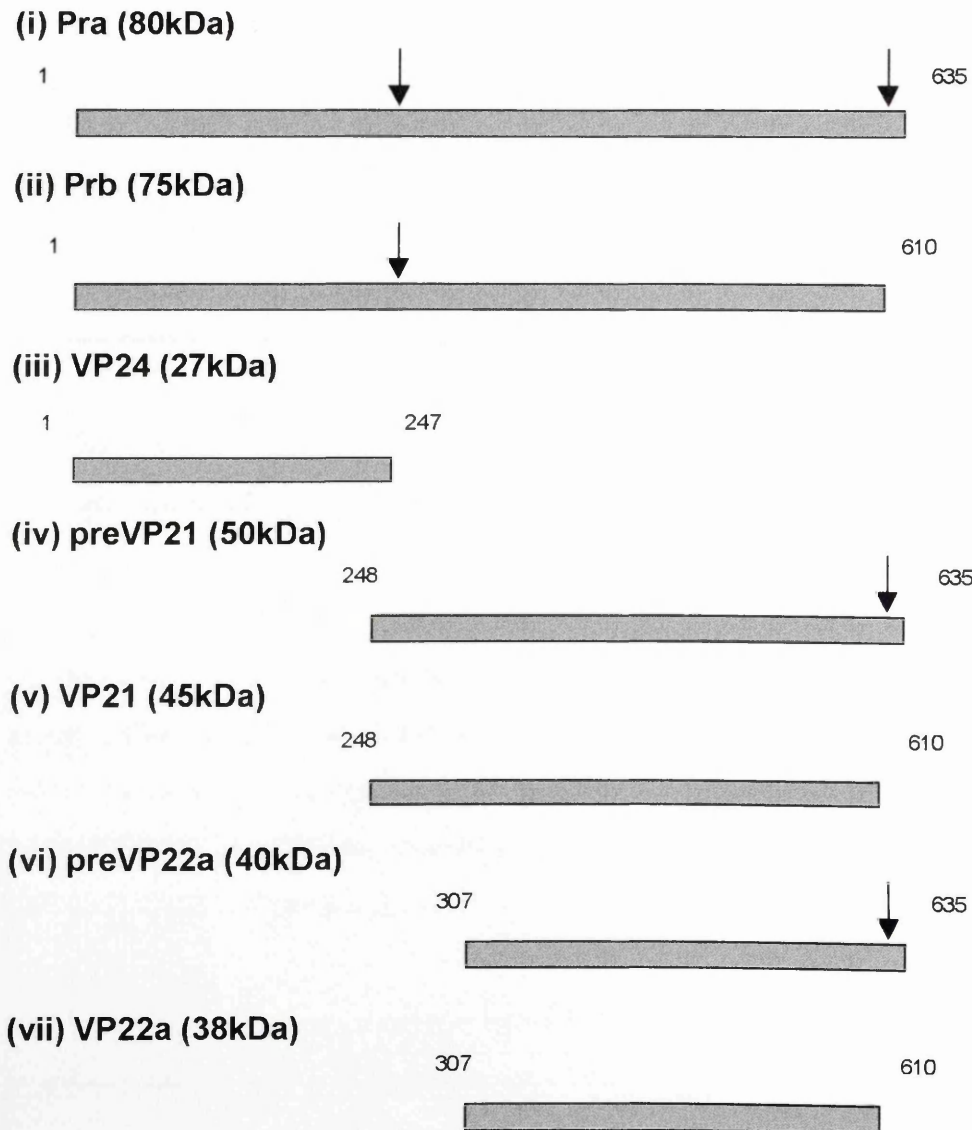


Figure 1.4: The 3' co-terminal transcripts are shown by arrows which are overlaid by open boxes, indicating the position of the ORF, specifying UL26 [panel (i)] and UL26.5 [panel (ii)] gene products. Proteolytic cleavage takes place between the alanine and serine residues, indicated by R and M

Figure 1.5: The proteolytic cleavage products are described in the text. The arrowheads indicate HSV 1 cleavage sites.

Baculovirus studies have shown that it is not essential for capsid formation as recognisable capsids are formed when only this protein is absent (Tatman *et al*, 1994; Thomsen *et al*, 1994). VP26 can also be removed from capsids by treatment with 2M GuHCl, leaving the capsid shell largely intact (Newcomb & Brown, 1991; Booy *et al*, 1994) and illustrating that this protein is not vital for capsid stability.

Recent studies with VP26 null mutants has shown that VP26 is not required for viral growth in cell culture however, the protein does appear to be important for production of infectious virus in the nervous system (Person & Desai, 1998). Studies with mice have shown that virus yield and reactivation is greatly reduced in the VP26 null mutants, compared to wild type virus.

4.4.1.5 VP21, VP22a and VP24

VP21, VP24 and VP22a have been grouped together as they are 3 capsid proteins, which are derived from 2 overlapping genes (figure 1.4) and form a central scaffold structure. There was initially much confusion as to the nature and relationship of these proteins to each other and the capsid. Firstly, VP21 and VP22a are only present in B capsids and absent from mature C capsids (Gibson & Roizman, 1972) whereas, VP24 is also a component of A and C capsids. Secondly, there are a number of variants of these proteins due to the nature of the proteolytic processing of the genes which encode them (see figure 1.5) (Liu & Roizman, 1991b; Preston *et al*, 1992) and this aspect shall now be discussed.

VP24 and VP21 are the products of the UL26 gene (Davison *et al*, 1992) which initiates at position 50809 and terminates at position 52714 (McGeoch *et al*, 1988), being transcribed from left to right. This results in an ORF of 1905bp, which corresponds to a predicated protein $M_r=62466$. This is considerably larger than any single capsid protein whose sequence has been aligned to this area. In fact, UL26 encodes both VP24 and VP21. VP24 is encoded by the 5' portion and VP21 is encoded by the 3' portion of the gene (Davison *et al*, 1992). UL26 encodes a maturational protease, which is essential for the formation of C capsids, containing DNA (Preston *et al*, 1983; Gao *et al*, 1994). The full-length product of UL26 is designated pra [figure 1.5, panel (i)]. Self cleavage at site R, can occur between alanine 247 and serine 248, to generate two cleavage products, VP24 [figure 1.5, panel (iii)] and preVP21 [figure 1.5, panel (iv)] (DiIanni *et*

al, 1993). The N-terminal product, VP24, contains the active catalytic viral protease (Weinheimer *et al*, 1993). VP24 has an observed Mr of 25kDa, (Gibson & Roizman, 1972; Zweig *et al*, 1979b) 26kDa, (Cohen *et al*, 1980) 24kDa (Rixon *et al*, 1990).

Cleavage at site M, occurs between alanine 610 and serine 611, to generate either prb [figure 1.5, panel (ii)], where this single cleavage has occurred and removed the C-terminal 25 amino acids or, VP21, [figure 1.5, panel (v)] where the double cleavage (R+M) has occurred. The C-terminal product encoding VP21 has an observed Mr of 44kDa, (Gibson & Roizman, 1972) 40kDa (Cohen *et al*, 1980) and 42kDa (Rixon *et al*, 1990).

In addition, a third protein, VP22a, was initially identified as the product of the UL26 gene (Preston *et al*, 1983). However, as previously discussed, the predicted Mr of 62466 was much greater than the observed Mr of 38.8kDa, (Gibson & Roizman, 1972) 40kDa (Zweig *et al*, 1979b; Rixon *et al*, 1990) and 38kDa (Cohen *et al*, 1980). This puzzle was resolved when Liu & Roizman (1991a) mapped a transcriptional unit which overlapped the C-terminal 329 amino acids of UL26. This gene initiated at position 51727 (within the UL26 ORF) and terminated at the same site as UL26, position 52714 (McGeoch *et al*, 1988), being transcribed from left to right. This ORF encoded 987bp and was designated UL26.5 [figure 1.4, panel (ii)].

The full-length product of the UL26.5 ORF is termed preVP22a [see figure 1.5, panel (vi)]. However, as UL26.5 and UL26 carry identical 3' residues, the M site present in UL26 is therefore also found in UL26.5 and proteolytically cleaved between alanine 610 and serine 611. This removes the C-terminal 25 amino acids of preVP22a (Liu & Roizman, 1992; Preston *et al*, 1992) and generates VP22a [figure 1.5, panel (vii)]. It is known that preVP22a interacts with VP5, in the capsid shell, through these C-terminal 25 amino acids (Hong *et al*, 1996). Proteolytic cleavage therefore breaks the connection between the scaffold and shell.

Interestingly, VP22a is in much higher abundance (approximately 1000 to 1500 copies per capsid) than VP21 and VP24 combined (approximately 100 copies per capsid) (Liu & Roizman 1991b; Newcomb *et al*, 1993). This situation appears to relate to differential

expression of the promoters controlling UL26 and UL26.5. The transcriptional initiation site of UL26 mRNA is approximately 180 nucleotides upstream of the ATG (Liu & Roizman, 1991a). However, the promoter controlling the UL26.5 transcript is found in the 5' terminal domain of UL26, approximately 99 nucleotides upstream of the ATG (Liu & Roizman, 1991a; 1991b). The 2 promoters are therefore more than 1000 nucleotides apart and expression of the 2 genes UL26 and UL26.5 is separately controlled.

4.4.1.6 Minor Capsid Proteins

Relatively recently five proteins, UL6, UL12.5, UL15, UL25 and UL28 have been identified as minor components of the capsid shell [table 1.4, panel (ii)].

The product of the UL6 gene, has been identified as a minor component of A, B and C capsids (Patel & Maclean, 1995). The exact location of the UL6 protein within the capsid remains to be determined however, it is obviously tightly associated as treatment with 2M GuHCl does not remove it. Baculovirus studies have shown that this protein is not essential for capsid formation (Patel & Maclean, 1995). However, studies with HSV-1 mutants defective in the UL6 gene showed that only B type capsids accumulated (Patel *et al*, 1996). This indicates that these capsids were unable to package DNA and implies that the UL6 protein has a role in packaging DNA.

UL12.5 was identified as a capsid associated deoxyribonuclease by Western blot analysis (Bronstein *et al*, 1997). It appears to be tightly associated with the capsid and is not removed by treatment with 2M GuHCl. It has been suggested that the protein has a role in processing genomic DNA.

UL15 is a spliced gene encoding 2 distinct proteins with a molecular weight of 81kDa and 87kDa respectively (Yu *et al*, 1997). The products of the UL15 gene are essential for cleavage and packaging of DNA (Poon & Roizman, 1993; Baines *et al*, 1994) and appear to form a close association with UL28. UL15 carries a NLS (Yu & Weller, 1998) which relocates UL28 to the nucleus of infected cells (Koslowski *et al*, 1997). UL15 has recently been identified in highly purified B capsids (Salmon & Baines, 1998). It is tightly associated and not removed by treatment with 2M GuHCl. Mutant studies have revealed that UL28, UL17 and UL6 require to be present in order for UL15 to

Figure 1.6: 3D Image Reconstruction of a Wild Type HSV-1 B Capsid

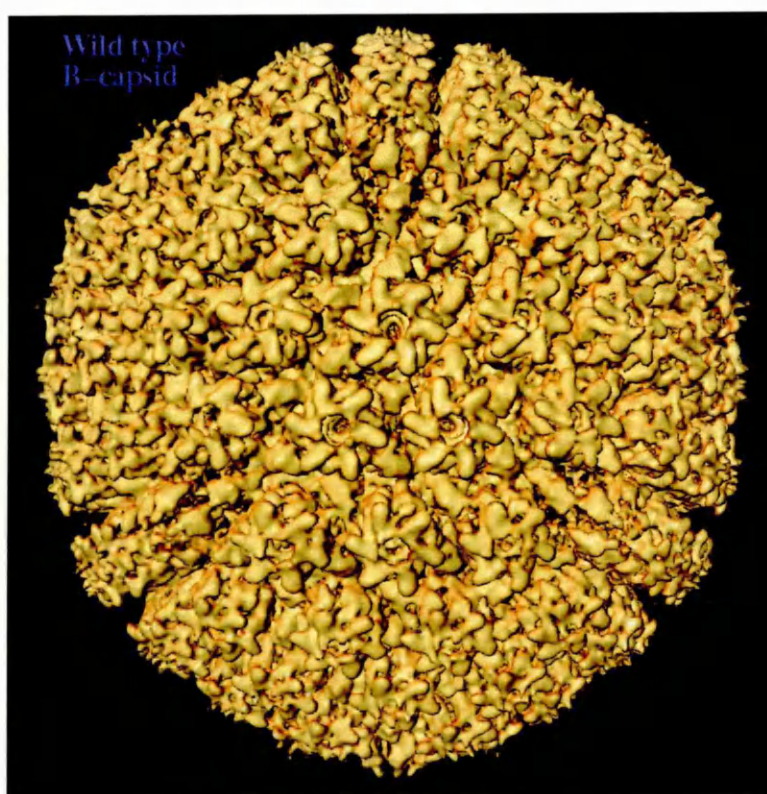


Figure 1.6: 3D image reconstruction of the HSV-1 B capsid, from cryo-EM analysis (reproduced with permission from Dr Wah Chui, Baylor College of Medicine, Texas).

complex to capsids (Salmon & Baines, 1998). UL17 has recently been shown to be a tegument protein, required for cleavage and packaging DNA (Salmon *et al*, 1998). As UL28 has been shown to complex with UL15, it is possible that this protein is also associated with the capsid.

UL25 has been confirmed as a virion component (Ali *et al*, 1996) and implicated as having a role in virus penetration of the host cell (Addison *et al*, 1984). Recently, UL25 has been detected associated with A, B and C capsids (McNab *et al*, 1998). This group found that UL25 was essential for packaging but not cleavage of DNA.

4.4.2 Molecular Arrangement of the Capsid Proteins

Cryo-electron microscopy has allowed the 3D structure of the capsid to be accurately visualised (see figure 1.6) (Schrag *et al*, 1989; Baker *et al*, 1990; Booy *et al*, 1991a; Trus *et al*, 1992; Newcomb *et al*, 1993; Zhou *et al* 1994) to a resolution of 13Å (Zhou *et al*, 1998b). This data together with baculovirus generated (Tatman *et al*, 1994; Thomsen *et al*, 1994) and GuHCl treated capsids (Newcomb & Brown 1991; Trus *et al*, 1992) has allowed the location of individual capsid proteins to be elucidated and thus the structural components defined.

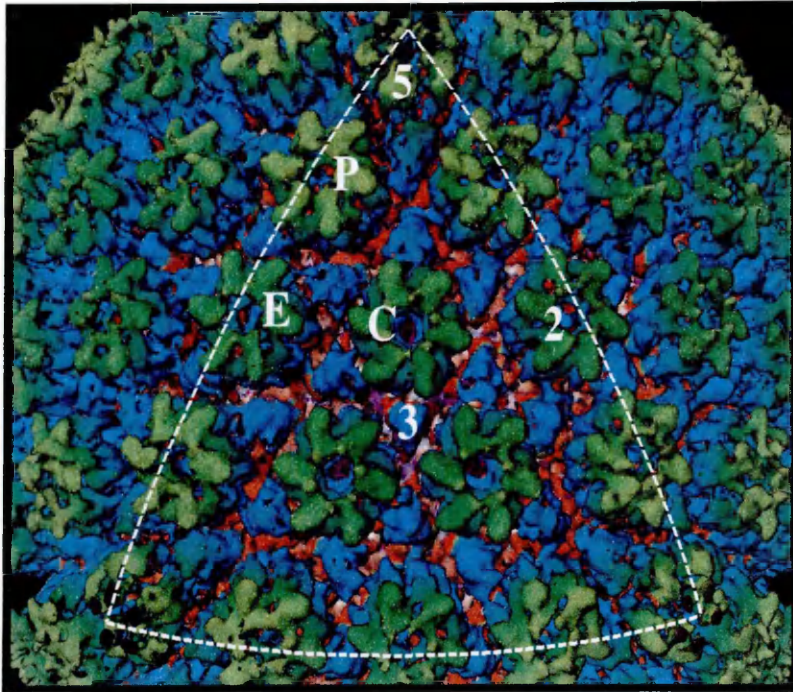
The capsid is 125nm in diameter and varies in its composition, depending on capsid type. A, B and C capsids are all composed of a shell (with an outer, middle and inner, or floor, area) which is approximately 150Å thick. The shell is composed of capsomeres and triplexes. In addition, B capsids contain an inner scaffold layer and C capsids contain the viral DNA.

4.4.2.1 Asymmetric Unit

An asymmetric unit is a single building block, which contains all the information necessary to build the entire capsid shell by repeating these units. An HSV-1 capsid asymmetric unit consists of one fifth of a penton, one c hexon, one p hexon, one half of an e hexon, one of each of Ta-Te triplexes and one third of Tf (see section 4.4.2.3 for further clarification on triplex types).

Figure 1.7: Capsid Hexon Arrangement

(i)



(ii)

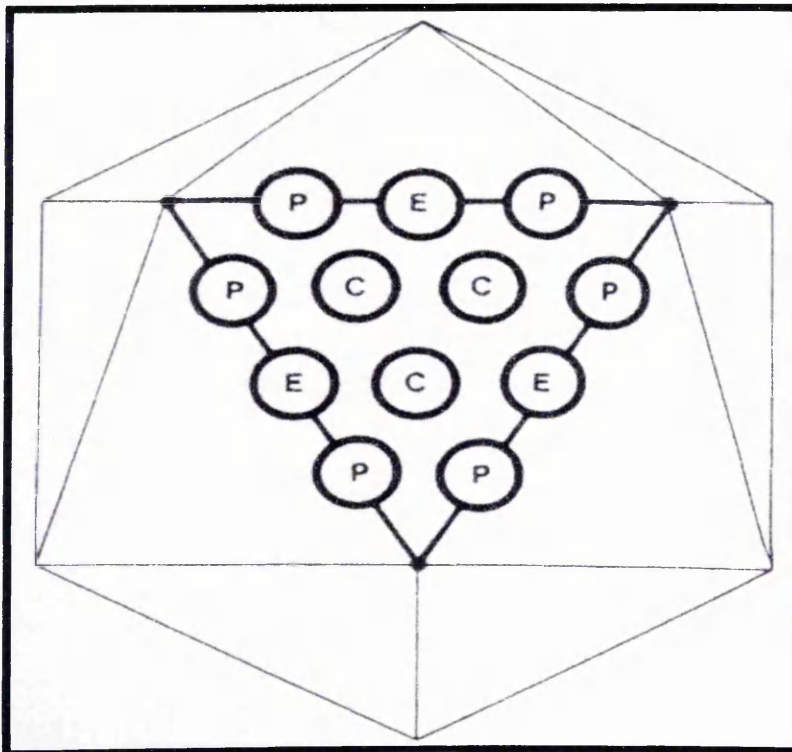


Figure 1.7: Panel (i) shows a section of a 3D image reconstruction of a wild type B capsid. The dashed white outlines represent an icosahedral facet. An example of a p, e and c hexon are marked in white and the numbers 2, 3 and 5 indicate the symmetry at these points. Panel (ii) shows a schematic representation of the distribution of the 3 classes of hexon (p, e and c) on an icosahedral facet.

4.4.2.2 Capsomeres

(i) VP5

As early as 1975, VP5 was considered to be present on the capsid surface (Powell & Watson, 1975). Surface erosion of capsids by Ar ions resulted in the rapid loss of VP5 (Newcomb *et al*, 1989) and confirmed that this protein was indeed a surface component.

There are 162 capsomeres, of which 12 are pentons (pentamers of VP5) and 150 are hexons (hexamers of VP5 and VP26). In order for VP5 to adopt both a pentameric and hexameric arrangement, it must have the ability to alter its conformational state. Indeed the two types of capsomeres have distinct properties.

Monoclonal antibody studies (Trus *et al*, 1992) have shown that 2 separate antibodies bind to hexons and pentons and do not cross react with each other. Similarly VP26 [see next subsection (ii)] is found only on the tips of the VP5 hexons, as a horn shaped mass, and not on pentons (Zhou *et al*, 1994). Finally, treatment of capsids with 2M GuHCl or 4M urea (Newcomb & Brown, 1991; Newcomb *et al*, 1993) readily removes pentons. However, the structural integrity of the hexons and indeed the capsid, remains intact. These points illustrate that while the hexons and pentons are both composed of VP5, their symmetry and positioning in the capsid affects their properties.

The capsomeres are arranged on a T=16 icosahedral lattice. Due to the nature of the symmetry, the pentons are found at the vertices and the hexons are found at the faces and edges. Three classes of hexon exist, P, E and C, which vary slightly due to their quasiequivalent environments in an icosahedral facet (figure 1.7). P hexons are found adjacent to pentons. C hexons lie at the centre of the facet and E hexons form an edge, which is not adjacent to the vertex (Steven *et al*, 1986; Schrag *et al*, 1989).

VP5 capsomeres traverse the capsid shell, extending from the outermost radius to the capsid floor (Baker *et al*, 1990). PreVP22a, representing uncleaved scaffold, has been shown attached to VP5 in the capsid floor (Zhou *et al*, 1998a and Chapter 6).

The capsomeres all have axial channels running through them. These vary slightly between hexons and pentons. Pentons are approximately cylindrical, being 14.5nm in

diameter and 14nm in height with a 5nm channel running through them (Zhou *et al*, 1994). Hexons are also approximately cylindrical, being 17nm in diameter and 14nm in height (Steven *et al*, 1986; Schrag *et al*, 1989; Zhou *et al*, 1994) with a 5nm channel, tapering to 2nm, present from outside to inside of the capsid (Zhou *et al*, 1994).

(ii) VP26

Initially there was much confusion as to the exact location of VP26, but cryo-electron microscopy comparisons of capsids with and without VP26 have localised the protein to the outer tips of the VP5 hexons (Booy *et al*, 1994; Zhou *et al*, 1994) (see Results, Chapter 5). The VP26 minus capsids were either prepared in the baculovirus system, omitting AcUL26 (Tatman *et al*, 1994; Zhou *et al*, 1995), or, wild type capsids were stripped of VP26 by treatment with 2M GuHCl (Newcomb & Brown, 1991; Booy *et al*, 1994). Both these approaches have defined the location and shown that VP26 is not essential for capsid formation and stability.

VP26 forms a star-shaped ring on the tips of each hexon. Six copies of the protein form a continuous ring which overlays the VP5 subunits. The conformation of each 6-mer varies slightly, in concordance with the variation of each hexon type (Zhou *et al*, 1995). VP26 does not attach to the penton subunits, even although they are composed of the VP5 protein.

4.4.2.3 Triplexes

In the 1970's 2.5nm long fibrillic densities were observed under negative staining, connecting adjacent capsomeres (Vernon *et al*, 1974; Palmer *et al*, 1975; Almeida *et al*, 1978). Early computer reconstructions wrongly detected this area, now designated the triplex, as a Y-shaped mass (Schrag *et al*, 1989; Baker *et al*, 1990; Booy *et al*, 1991). Partial removal of VP19c and VP23 with 2M GuHCl correlated with the loss of 120 of the 320 triplexes (Newcomb *et al*, 1993) and implicated these proteins as forming the triplex. It is now accepted that the triplex is a heterotrimer consisting of one copy of VP19c (totalling 320 copies per capsid) and two copies of VP23 (totalling 640 copies per capsid) (Newcomb *et al*, 1993).

Higher resolution images have revealed that the triplexes are located in the midlayer of the capsid and do not form a Y-shaped arrangement (Zhou *et al*, 1994). Some triplexes connect only two adjacent capsomere subunits, whereas others connect 3. In fact 6 different types of triplex have been identified and designated Ta to Tf (figure 6.5) (Zhou *et al*, 1994). These vary due to their position in the capsid and thus their respective interactions with capsomeres. Ta to Te are asymmetric, whereas Tf, appears to have 3-fold symmetry. However, as it is found at the 3-fold axis, this may be an artefact of the reconstruction.

The triplex may interact with VP5 only through VP19c, VP23 does not appear to participate in the interaction (Nicholson *et al*, 1994; Rixon *et al*, 1996; Chapter 3). Four types of interaction have been described between VP19c and VP5, these are strong, weak, tail and arm (Zhou *et al*, 1998b). It would seem that the triplexes play a role in helping to define the curvature of the capsid (this aspect is fully discussed in Chapter 7, Conclusion).

4.4.2.4 Scaffold

The scaffold of B capsids is composed of one major (VP22a, or scaffold) and two minor (VP21 and VP24) proteins. It exists, encased by the capsid shell, in two forms, large and small cored. Large cored B capsids result when preVP22a is not cleaved by the protease. These capsid types can be made in the baculovirus system by omitting the UL26 gene (Tatman *et al*, 1994; Thomsen *et al*, 1994). They are also found in ts1201 mutants at the NPT. Ts1201 has a lesion within the UL26 gene (Preston *et al*, 1983), which results in a defective protease. This is unable to cleave itself at positions M and R (see figure 1.4 and figure 1.5) to release VP21 and VP24 and convert preVP22a to VP22a. However, this situation is reversible. When the mutant is downshifted to the PT, small cored capsids and C capsids containing DNA are produced (Preston *et al*, 1983).

VP22a, the processed scaffolding protein, was first identified as an internal component of the B capsids by antibody studies when Rixon *et al* (1988) observed VP22a along the inner margin of B capsids by immunoelectron microscopy.

As previously described (Section 4.4.1.5), the scaffold protein is initially transcribed as preVP22a. It appears that this molecule is associated with capsids during assembly but,

Table 1.5: Herpesvirus Capsid Protein Homologues

HSV-1 protein name	Approx Mr of Capsid Proteins (kDa)						
	HSV-1	HSV-2	EHV-1	HCMV	EBV	PRV	VZV
VP5	155	155	148	153	160	150	155
VP19c	53	53	59	30	52	63	57
VP21	42	44	*	37	46	41	36
VP22a	38	38	46	36	40	35	32
VP23	33	33	36	34	37	27	34.5
VP24	25	25	30	28	28	22.5	31.5
VP26	12	12	12	11	18	*	17.5
Ref	a	b	c	d/e/f	g	h	i

Table 1.5: The capsid proteins of HSV-1 are compared to equivalent proteins of other herpesviruses. A * represents a protein which has not been identified. The references (ref) for each set of data are:

- a Gibson & Roizman, 1972; Rixon *et al*, 1990
- b Gibson & Roizman, 1972; Heilman *et al*, 1979
- c Perdue *et al*, 1975; 1976; Newcomb *et al*, 1989
- d Irmiere & Gibson, 1985
- e Gibson *et al*, 1996
- f Gibson *et al*, 1998
- g Dolyniuk *et al*, 1976; Van Grunsven *et al*, 1993
- h Stevenly, 1975; Ladin *et al*, 1982
- i Zweerink & Neff, 1981; Friedrichs & Grose, 1986

is lost when DNA is packaged (Rixon *et al*, 1998). Cleavage of preVP22a by the viral protease removes the C-terminal 25 amino acids of the protein (Lui & Roizman, 1992; Preston *et al*, 1992), generating VP22a and breaking the connection between scaffold and shell. These connection points have recently been visualised (Chapter 6 and Zhou *et al*, 1998a).

The minor scaffold components, VP21 and VP24, constitute less than 5% of the B capsid mass (Newcomb *et al*, 1993). Baculovirus studies have revealed that when both of these proteins are absent (ie UL26 is omitted), large cored capsids are produced. When VP22a is absent (ie UL26.5 is omitted), a very small number of apparently intact small cored capsids are visible (Tatman *et al*, 1994; Thomsen *et al*, 1994). However, the majority of structures resemble aberrant shells. It would therefore appear that the products of the UL26 gene can substitute for preVP22a, with a much lower efficiency. This is perhaps surprising in view of the fact that VP22a is the major component of the scaffold. However, most of the sequence of VP21 overlaps that of VP22a and it is possible that preVP21 substitutes for preVP22a.

When the products of UL26 and UL26.5 are expressed alone in baculovirus infected cells, large numbers of core-like structures are evident (Preston *et al*, 1994) indicating that these proteins are able to self-assemble into a scaffolding type structure.

The role of scaffold in capsid assembly and the *in vitro* assembly model are discussed further in Chapters 6 and 7.

4.4.3 Capsid Models

The main topic of this thesis centres around HSV-1 capsids, however a knowledge of assembly patterns of other viruses can help interpretation of new HSV-1 results and allow models to be derived.

Although the viral capsids of 6 of the eight human herpesviruses have been examined, the capsid of HSV-1 remains the best studied of all the herpesviruses. Proteins analogous to most of the HSV-1 capsid proteins have been identified and are summarised in table 1.5. However, as in most cases, less is known about the assembly patterns of these capsids, they shall not be discussed further. Instead, the well

characterised assembly pathways of P22 bacteriophage and adenovirus shall be discussed. These viruses were chosen as firstly, the pathway of P22 has many similarities to HSV-1 and secondly, adenovirus is a large animal virus which has been well studied and characterised.

4.4.3.1 P22 Bacteriophage

P22 is a dsDNA bacteriophage of *Salmonella typhimurium*. The assembly pathway of its capsid and DNA packaging mechanism has been extensively studied and is reviewed by King and Chiu, 1997. The P22 capsid forms a spherical procapsid intermediate during assembly, which subsequently angularises into the mature icosahedron. A similar model has recently been suggested for HSV-1 capsids (Newcomb *et al*, 1993) and is fully discussed in Chapter 7, Conclusion.

P22 structural intermediates have been readily isolated by extensive mutational analysis and this has revealed that a spherical procapsid shell is the initial capsid product. The procapsid is formed by a portal protein (gp1), the coat protein (gp5), the scaffold protein (gp8) and other minor proteins (Prevelige & King, 1993). The scaffold protein is extremely important for procapsid assembly but, is removed upon DNA packaging (King & Casjens, 1974). This is analogous to preVP22a in HSV-1. However, unlike preVP22a, gp8 is recycled by the phage and used in the assembly of subsequent procapsids. In the absence of gp8, a very small number of capsids are formed but, aberrant spirals and small capsid forms predominate (Thuman-Commike *et al*, 1996).

DNA enters through the portal protein (gp1) (Earnshaw & Casjens, 1980). Entry of DNA is associated with shell expansion from 580Å to 610Å diameter in parallel with maturation to the polyhedral capsid. The portal protein is also the exit point for DNA when it is injected into the host cell.

Cryo-EM analysis of P22 has revealed that the particle is composed of 60 hexamers and 12 pentamers, composed of the coat protein (gp5). These are linked by connecting arms (Prasad *et al*, 1993). Due to their quasi-equivalent environments, the structural conformations of the hexons and pentons vary. Indeed, 7 types of capsomeric subunits occur, all composed of the same protein (Prasad *et al*, 1993). An equivalent situation is found with HSV-1 VP5 (Section 4.4.2.1).

Although the procapsid of P22 is 30Å smaller than the mature form, it still has T=7 symmetry. However, protein arrangements of the 2 forms vary. For example, the procapsid has a more open structure, with holes visible at the centres of the hexons and pentons (Prasad *et al*, 1993; Thuman-Commike *et al*, 1996) where it is thought that the scaffold protein may be lost (Greene and King, 1994).

The scaffold can be extracted from procapsids under denaturing conditions (Fuller & King, 1981) or by heating to 49°C (Galisteo & King, 1993). This situation is reversible and when denaturant is removed, scaffold can reenter the procapsid (Greene & King, 1994). However, the scaffold cannot enter the angularised mature capsid, indicating that expansion eliminates the scaffold entry point and/or binding site.

The trigger for shell expansion and angularisation is not clear. Several studies have shown that small fragments of DNA can be packaged without expansion occurring (Earnshaw & Casjens, 1980; Hohn, 1983). It would appear that longer lengths of DNA are necessary to stimulate capsid maturation. Certainly, the expansion and angularisation of the capsid requires energy (Galisteo & King, 1993). One estimate has suggested that 3 ATP molecules per monomer of shell protein would be required to expand the shell (Steven, 1993).

3D reconstructions of procapsids containing scaffold protein has revealed that the scaffold is not icosahedral. It appears to be attached, by finger-like densities extending in towards the capsid core, around the internal hexon channel (Thuman-Commike *et al*, 1996). Similarly rod-like densities, attributable to scaffold, have recently been identified in HSV-1 attached to VP5 (see Chapter 6 and Zhou *et al*, 1998a). In this case, the scaffold was also found not to have icosahedral symmetry.

4.4.3.2 Adenovirus

Adenoviruses of humans cause a variety of diseases, from mild respiratory infections, to life threatening dysentery (Monoto, 1992) and oncogenesis is also associated with these viruses (Shenk, 1996). *In vitro*, some adenoviruses are relatively easy to propagate and so have been widely studied.

The adenovirus virion consists of a non-enveloped icosahedral capsid, composed of 252 capsomeres, 240 hexons and 12 pentons, with fibres protruding from each vertex (Horne *et al.*, 1959). The capsomeres were initially designated as hexons and pentons however, this name is misleading as straightforward 5-mers and 6-mers of proteins are not involved. The hexons are composed of trimers and not hexamers and so there is not exact symmetry. The molecule is therefore designated as having pseudo T=25.

The capsid is composed of 11 proteins, designated II to XI, by order of decreasing molecular mass on SDS PAGE (Maizel *et al.*, 1968), and μ protein, whose function is unknown (Hosokawa & Sung, 1976).

Hexons are composed of homotrimers of polypeptide II (Grutter & Franklin, 1974). The trimer arrangement is extremely stable and resistant to 8M urea treatment (Shenk, 1996). This is the MCP, constituting 63% of the capsid mass.

Pentons are composed of 2 distinct proteins. The penton base is a 5-mer of polypeptide III (Van Oostrum & Burnett, 1985) and the fibres are composed of polypeptide IV. The fibre is a trimer (Ruigrok *et al.*, 1990) and is believed to be involved in attachment to host cells (Greber *et al.*, 1993). Polypeptide IX is a major stabilising or cementing protein in the capsid. It forms hexon to hexon contacts, linking well defined groups of nine hexons (GONs). Mutants lacking this protein are extremely unstable and thermolabile (Colby & Shenk, 1981).

Apart from polypeptide VIII, whose location is unknown, all the other proteins are found within the capsid shell, forming part of the core. Polypeptides V and VII are found tightly associated with the DNA (Black & Centre, 1979). However, it is polypeptide VI which appears to have a major role in helping to define the correct curvature of and assembly of the capsid, before it is proteolytically cleaved.

Polypeptide VI may play a similar role to preVP22a, in HSV-1, and gp8, in P22. The protein is assembled as a full length precursor in the immature virion. Here it weakly interacts at the inner capsid surface and anchors the peripentonal hexons to the core (Stewart *et al.*, 1993). Unlike preVP22a and gp8, cleavage of the protein by the viral

protease does not lead to its loss, instead it enhances its binding to the hexon (Matthews & Russell, 1995). This suggests a model where there is weak binding to help guide assembly and correct errors but, the interaction is locked or cemented upon proteolytic cleavage. Proteolysis is essential for correct assembly of virions (Weber, 1976).

5. HSV-1 Life Cycle

The stages of the life cycle, from initial infection, to release of free virions, will now be discussed in turn

5.1 Entry into Host cells

5.1.1 Attachment

The initial stages of virion infection involve the binding of viral components to the cell surface, followed by fusion with the plasma membrane. HSV-1 attaches to cells through the glycoprotein spikes, protruding from the envelope (see table 1.3). The virus appears to have a selection of mechanisms, with varying efficiencies, for binding to the host cell (reviewed by Spear, 1993).

Through studies with deletion and temperature sensitive mutants, only 4 glycoproteins, gB (Sarmiento *et al*, 1979; Haffey & Spear, 1980; Little *et al*, 1981; Cai *et al*, 1987) gD (Ligas & Johnson, 1988; Johnson & Ligas, 1988) gH and gL (Hutchinson *et al*, 1992) have been shown to be essential for virion infectivity. Infection appears to be initiated by viral binding to heparin sulphate proteoglycan (PG), which explains the ability of glycosaminoglycan heparin to inhibit infection *in vitro* (WuDunn & Spear, 1989). PG are ubiquitous molecules, present as integral membrane proteins of cells and extracellular matrixes.

Although gC is dispensable for viral entry and gC negative mutants have been isolated from humans (Hidaka *et al*, 1990), this protein, when present, plays a principal role in the absorption of virus to cells (Herold *et al*, 1991). It has been shown to be capable of tightly binding to heparin sulphate PG. However, as gC mutants can still infect cells, the virus obviously has more than one attachment mechanism.

Many investigators have found that gD also appears to interact with cell surface receptors other than PG (Campadelli-Fiume *et al*, 1988; Chase *et al*, 1993; Johnson *et*

al, 1990; Karger & Mettenleiter, 1993; Lee & Fuller, 1993). Recently the gD receptor was identified as, a previously undescribed, human TNF receptor (Montgomery *et al*, 1996) and has since been designated herpesvirus entry mediator A (HveA) (Warner *et al*, 1998). HveA is expressed in many human tissues including lung, liver and kidneys however, it is most abundant in lymphoid organs and cells (Hsu *et al*, 1997; Kwon *et al*, 1997; Marsters *et al*, 1997). Studies with anti-HveA antibodies have shown that HveA is a principle receptor for HSV-1 (Montgomery *et al*, 1996) but, viruses can still infect cells which do not carry it. Further studies have revealed a second mediator of HSV-1 entry. This was shown to be poliovirus receptor related protein 2 (Pvr2) and was designated HveB (Warner *et al*, 1998). Although this receptor facilitated entry of some mutant viruses, it failed to allow entry of wild type HSV-1 (Warner *et al*, 1998). However, this line of investigation has lead to the discovery that Pvr1, designated HveC, can interact with wild type virus (Geraghty *et al*, 1998). As this protein is found on epithelial and neuronal cells, it may be a prime target for HSV-1 infection of mucousal surfaces and subsequent spread to the nervous system.

5.1.2 Penetration

Once initial attachment has been achieved, the viral envelope fuses with the cell plasma membrane (Morgan *et al*, 1968). gB and gD and the products of the UL25 gene appear to have a function in viral fusion and successful penetration (Cai *et al*, 1988; Campadelli-Fiume *et al*, 1988; Addison *et al*, 1984). Recent evidence has suggested that the gD receptor, HveA, also plays an important role in virus induced cell fusion (Terry-Allison *et al*, 1998).

The nucleocapsid is rapidly transported through the cytoplasm to the nuclear pores. The high viscosity inside the cytoplasm means that the capsid cannot travel by free diffusion. In neurons, it is transported along the axons to the nucleus (Roizman & Sears, 1990) but in other cell types the mechanism is less well understood. Limited evidence has suggested that capsids bind to microtubules and use this network to traverse the cell to the nuclear pores (Penfold *et al*, 1994). A study with fibroblast cells has found that the capsid sheds most of its associated tegument proteins and binds to dynein (Sodeik *et al*, 1997).

Dynein is a cytoplasmic component responsible for direction of chromosomes and membrane organelles along microtubules (Mitchison, 1988). The viral protein which binds to this molecule has not yet been identified. However, it would appear that HSV-1 is utilising the cellular machinery responsible for retrograde transport in host cells.

Once present at the nucleus, the capsid releases its viral DNA through the nuclear pores, and itself becomes associated with the pores (Batterson *et al*, 1983; Lycke *et al*, 1988) and remains intact for a while (Miyamoto & Morgan, 1971). The exact mechanism of DNA extrusion from capsids is not known. DNA can be removed from capsids *in vitro* by treatment with 0.5M GuHCl (Newcomb & Brown, 1994). In this instance, DNA appears to exit at the capsid vertices as thick strands. Studies with mutants indicated that the tegument protein VP1 (UL36) has a role in DNA release (Batterson & Roizman, 1983).

5.2 Disruption of Host Cell Functions

Viral infection not only results in the replication of viral DNA and assembly of new virions, but host cell functions are also affected. Virion components are involved in shut-off of host macromolecular synthesis. Early in infection ribosomes are affected and mRNA is degraded (reviewed by Roizman & Sears, 1996). Viral DNA replication and expression of viral proteins disrupt cell protein synthesis further (delayed shut-off) (Nishioka & Silverstein, 1978; Fenwick & Clark, 1982).

The UL41 ORF, which encodes a 53 kDa tegument protein (McLauchlan *et al*, 1992b), appears to be the viral protein which has host shut-off activity. In fact the 53kDa protein (UL41) has been designated virion host shut-off protein (vhs) (Kwong *et al*, 1988). The vhs appears to form a complex with VP16, which blocks the ability of this tegument protein to interact with cellular factors or switch on IE genes (Smibert *et al*, 1994). Similarly, the UL13 ORF, which encodes a 57 kDa protein kinase, also appears to have shut-off activity.

The host cell microtubule network is also disrupted by viral infection. The virus causes the cells to lose their integrity as the microtubules and Golgi apparatus are redistributed. The infected cells appear to round up and have a more spherical appearance as their supporting network becomes disorganised (Avitabile *et al*, 1995). The nucleolus appears

to disintegrate and host chromatin is dispersed to the edge of the nucleus and degraded. The nuclear envelope and other cell membranes become distorted too (reviewed by Roizman & Sears, 1996).

5.3 The Gene Expression Cascade

5.3.1 Classes of Viral Genes

Herpesvirus genes are all transcribed in the nucleus (Wagner & Roizman, 1969) by the cells' DNA dependent RNA transcriptase (Costanzo *et al*, 1977) in an ordered cascading fashion. They are classified into 3 groups according to their time of expression during the replication cycle. The first genes to be transcribed are the immediate early (IE) (also known as alpha genes), these are followed by the early (E) (also known as beta genes) and finally the late (L) (also known as gamma genes) (Swanstrom & Wagner, 1974; Honess & Roizman, 1974). This whole process initiates approximately 1h pi and continues for at least 15h (Wilkie, 1973).

The IE genes are transcribed by the pre-existing cellular apparatus, stimulated by the tegument component VP16 (UL48) (Batterson & Roizman, 1983; Campbell *et al*, 1984). Five IE proteins have been identified; IE1 (Vmw110), IE2 (Vmw63), IE3 (Vmw175), IE4 (Vmw68) and IE5 (Vmw12) (reviewed by Hayward, 1993; Subak-Sharpe & Dargan, 1998).

Transcription of other herpesvirus genes requires IE polypeptides for maximum activity. In particular, Vmw110 (Everett, 1984) and Vmw175 (Preston, 1979) appear to have a regulatory role in initiating early gene expression. Vmw 175 alone can activate E gene expression however, the process is much more efficient when Vmw110 is also present (Everett, 1984). Recent studies on Vmw110 has revealed that this protein binds to a 135kDa cellular ubiquitin specific protease (Everett *et al*, 1997) through its C-terminus (Meredith *et al*, 1995) and migrates to discrete nuclear structures. The binding of Vmw110 to the cellular protein enhances its ability to stimulate E gene expression (Everett *et al*, 1995; 1997).

A third IE protein, Vmw63 is also involved in the activation of transcription from HSV-1 promoters, but only in the presence of both Vmw110 and Vmw175. This protein

appears to enhance expression of some late genes, including the MCP, VP5 (Everett, 1984).

The second class of genes to be transcribed are the E genes. These peak approximately 5-7h pi and decline at later times (see later). The level of expression is largely independent of DNA replication. They are never stimulated in the absence of IE proteins (Preston, 1979; Dixon & Schaffer, 1980; O'Hare & Hayward, 1985; Quinlan & Knipe, 1985) illustrating that the IE products are essential for productive viral infection. Expression of the E genes signals the onset of viral DNA synthesis.

The third class of genes to be transcribed are the L genes. Although designated as the L genes, some of these proteins are expressed quite early during infection. However, their transcription levels are enhanced during DNA replication and peak 8-10h pi and persist for the remainder of the lytic cycle (Hones & Roizman, 1974; Harris-Hamilton & Bachenheimer, 1985). They consist mainly of structural proteins, eg VP5.

5.3.2 Mechanism of Replication

DNA replication appears to initiate at distinct virus specific structures in the nucleus. These appear to be induced by infection and have been designated replication compartments (Quinlan *et al*, 1984). However, as infection proceeds, the entire nucleus becomes involved (see Roizman & Sears, 1996).

The majority of the progeny viral DNA exists as large concatemeric molecules, which suggests that a rolling circle type mechanism exists for replication (Jacob *et al*, 1979; Poffenberger & Roizman, 1985). Replication initiates when an initiator protein recognises and binds to an origin of replication. In HSV-1 there are 3 cis-acting origins of replication (ori) (Frenkel *et al*, 1976; Schroder *et al*, 1975). In the inverted repeat sequence, flanking the short component of the genome, two copies of oriS exist (oriS1 and oriS2) (Stow, 1982; Stow & McConagle, 1983). OriL is located in the unique long component, between UL29 and UL30 (Weller *et al*, 1985). Not all origins are required for successful viral growth and oriL and 1 copy of oriS have been shown to be dispensable (Polvino-Bodnar *et al*, 1987; Longnecker & Roizman, 1986; Smith *et al*, 1989).

Seven HSV-1 genes (UL5, UL8, UL9, UL29, UL30, UL42, and UL52) appear to fulfil the minimal requirements for ori dependent DNA synthesis (Challberg, 1986; Wu *et al*, 1988; Stow *et al*, 1993). All these genes are essential for virus replication and DNA synthesis *in vitro* (Weller, 1991).

UL9: The UL9 gene is the initial protein to bind an ori and has been shown to interact with both oriS and oriL (Olivo *et al*, 1988). It has therefore been designated as an origin binding protein (OBP). The exact events which follow UL9 binding are not entirely clear, but it is known that the parental DNA must be unwound before replication can be initiated and it is thought that this may be mediated by the helicase activity of this protein (Bruckner *et al*, 1991).

UL29: UL29 encodes the major ssDNA binding protein ICP8 (Conley *et al*, 1981). This protein has been shown to interact specifically with several replication proteins (Vaughn *et al*, 1984; Bush *et al*, 1991; McLean *et al*, 1994) suggesting that it may have a role in organising a multi-protein complex at the replication fork by providing specific contacts with other proteins.

UL30: The DNA polymerase (pol) is encoded by the UL30 ORF (Powell & Purifoy, 1977; Knopf, 1979; Quinn & McGeoch, 1985) and has intrinsic 3'-5' exonuclease activity which acts as a proof reading function (O'Donnell *et al*, 1987). It also has a 5'-3' exonuclease/ribonuclease, which specifically degrades RNA primers present on the 5' Okazaki fragments on the lagging strand during semi-discontinuous synthesis (Crute & Lehman, 1989).

UL42: UL42 exists as a heterodimer with pol in a 1:1 ratio (Crute & Lehman, 1989). This accessory protein appears to stimulate activity of pol by up to 10-fold (Gallo *et al*, 1989) and can increase its ability to synthesise longer DNA fragments (Hernandez & Lehman, 1990; Gottlieb *et al*, 1990). This function may be enhanced by the ability of the UL42 protein to strongly bind DNA (Marsden *et al*, 1987) and so stop the polymerase from dissociating from the template after each cycle of catalysis.

Table 1.6: Genes Involved in Cleavage and Packaging DNA

Gene	Approx Mr (kDa)	Capsid Protein	Cleavage	Packaging
UL6	74	yes	yes	yes
UL12	67.5	no	no	no
UL12.5	60	yes	no	yes
UL15	81	yes	yes	yes
UL17	77	?	yes	yes
UL25	63	yes	no	yes
UL28	85.5	yes	yes	yes
UL32	64	?	yes	yes
UL33	14	?	yes	yes

(? – not yet known if protein is associated with the capsid)

UL5, UL8 and UL52: These 3 proteins co-purify from infected cells and constitute 3 subunits of the helicase-primase complex (Crute *et al*, 1988; 1989; Wu *et al*, 1988; McGeoch *et al*, 1988; Dodson *et al*, 1989; Crute & Lehman, 1991). The enzymatic activities of the complex are associated with UL5 and UL52 (Calder & Stow, 1990; Dodson & Lehman, 1991) while UL8 appears to be required for efficient nuclear localisation of the complex (Calder *et al*, 1992). The helicase activity of this complex unwinds duplex DNA, in a 5'→3' direction, while the primase component synthesises oligoribonucleotide primers. Therefore, the overall function of this complex is to prime lagging-strand DNA synthesis as it unwinds DNA at the viral replication fork (Crute *et al*, 1988; Crute & Lehman, 1991).

Although the 7 genes discussed are necessary and sufficient for DNA replication in expression systems, there are of course other enzymes and proteins which participate in and control the process *in vivo*. The expression and functions of these genes shall not be discussed further in the context of this study but are reviewed by Challberg, 1991 and Roizman & Sears, 1996.

5.4 Cleavage and Packaging of DNA

DNA is cleaved and packaged into preformed B capsids. Capsid assembly takes place in the nucleus of infected cells (Morgan *et al*, 1954; 1959). The mechanism by which the proteins are transported to the nucleus is fully explored in Chapter 3 (see also Rixon *et al*, 1996). Baculovirus studies have shown that 6 genes (UL18, UL19, UL26, UL26.5, UL35 and UL38) are essential to form apparently normal capsids (Tatman *et al*, 1994; Thomsen *et al*, 1994).

Aspects of capsid assembly are more fully discussed elsewhere in the thesis, with a proposed model shown in Chapter 7, Conclusion.

Cleavage of DNA is closely associated with packaging into capsids and involves 6 genes (see table 1.6), some of which have been shown to be minor constituents of the capsid. After DNA is replicated as large, probably branched (Sevanni *et al*, 1994; Zhang *et al*, 1994) concatemers, it is cleaved into unit length monomers at a novel a-a joint (Mocarski & Roizman, 1981; 1982) and a single copy is packaged into capsids. The a

sequences are present at both genomic termini and at internal repeats (see Section 4.1.1). The *a* sequence therefore acts as marker points for unit lengths of DNA.

Cleavage and packaging is also closely linked to capsid formation. For example, deletion mutants of the capsid protein genes UL18 or UL19 replicate DNA but, do not cleave the concatemer (Desai *et al*, 1993).

In the absence of any 5 of the 6 packaging genes (ts packaging mutants) DNA is not cleaved and only B capsids are found (reviewed by Homa & Brown, 1997). In addition, the product of the UL12 gene is important, though not essential, for the cleavage and packaging process. This gene encodes an alkaline nuclease which, when absent, reduces virus yield 100 to 1000 fold (Martinez *et al*, 1996). This protein appears to play a direct role in packaging by resolving branched structures formed during replication. An alternate reading frame, designated UL12.5, has been identified within the UL12 gene and its protein readily detected in intact virions and capsid preparations (Bronstein *et al*, 1997). The protein has been shown to possess nucleolytic activity and is thought to play a role in processing DNA during encapsidation (Bronstein *et al*, 1997).

UL25, which has recently been shown to be a minor capsid component (see Section 4.4.1.6) appears to have a role in the packaging process. McNab *et al* (1998) isolated a UL25 null mutant which was able to synthesise viral DNA but could not form plaques or produce infectious virus in non-complementing cell lines. Analysis of the nucleus of cells used to propagate the mutant virus revealed large numbers of both A and B capsids but, no C capsids. Restriction enzyme digestion and pulse-field gel electrophoresis confirmed the presence of genome sized viral DNA in the infected cells. These results have generated the assumption that the UL25 gene is required for packaging but not cleavage of replicated viral DNA. This is an example of how the cleavage and packaging genes are often coupled with capsid function.

The mechanism by which DNA enters capsids is unknown. In bacteriophage P22 DNA enters through a unique vertex formed by the portal protein (see section 4.4.3). No such site has been identified for HSV-1. Booy *et al* (1991b) visualised DNA in C capsids and reported it to have a liquid crystalline appearance which was tightly packaged. Recently,

Figure 1.8: Possible Routes of HSV-1 Egress

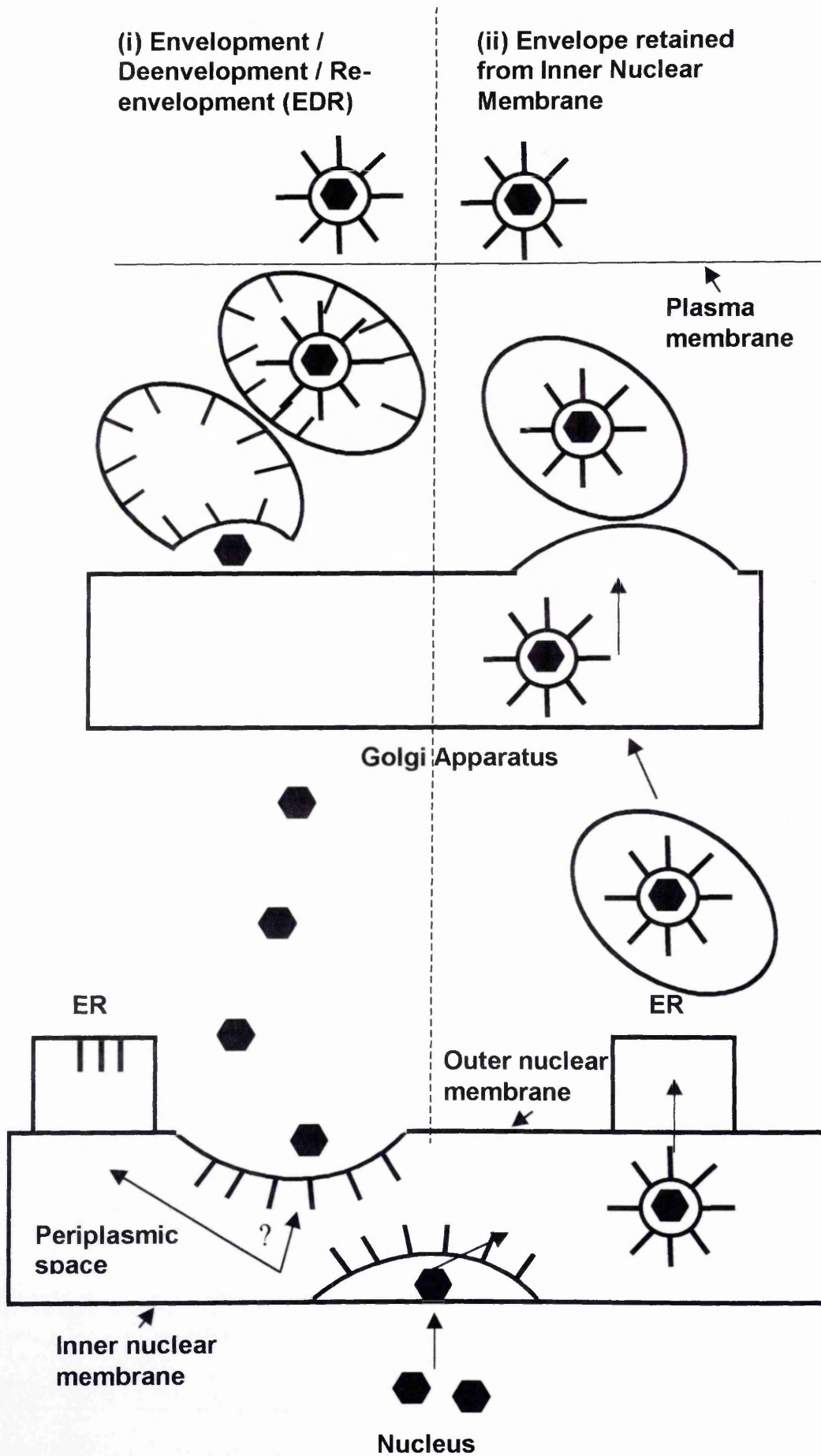
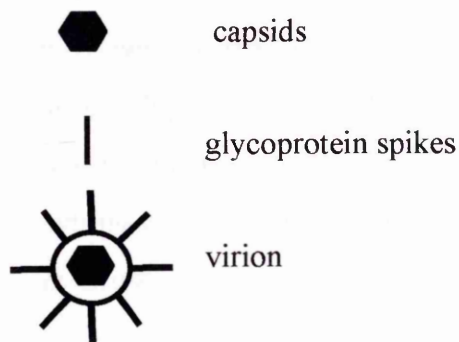


Figure 1.8: The 2 suggested routes of viral egress are shown schematically in this figure. Panel (i) represents the possible envelopment, deenvelopment, reenvelopment (EDR) pathway. Virus particles lose their initial membrane by fusion at the outer membrane/ER (endoplasmic reticulum) and acquire their final membrane at the Golgi/post-Golgi compartment. Panel (ii) represents the possible envelope retention from the inner nuclear membrane pathway. Virus particles acquire their envelope at the inner nuclear membrane and retain this until they leave the cells.



Zhou *et al* (1999) have suggested that the DNA is packaged as a spool (see section 4.1.2) Obviously the whole packaging process is very complex and involves multiple steps.

5.5 Tegumentation and Envelopment

Once DNA has been packaged in to the capsids, they leave the nucleus and acquire a tegument and envelope (reviewed by Rixon, 1993). The pathway of envelopment and tegumentation is poorly understood. The initial stage appears to involve the capsid budding through the inner lamella of the nuclear membrane (Nii *et al*, 1968a; Darlington & Moss, 1968; Roizman & Furlong, 1974). It first attaches to distorted sites on the membranes (Asher *et al*, 1969; Ben-Porat & Kaplan, 1971; Spear & Roizman, 1972), which are readily observed in HSV-1 infected cells (Nii *et al*, 1968b) and thought to be present where cellular proteins have been disrupted. It is not clear whether tegumentation takes place in the nucleus before, or as a consequence of, binding to the inner membrane, or, whether it occurs in the cytoplasm. Studies with HCMV (Haguenau & Michelson-Fiske, 1975; Severi *et al*, 1988) and HHV-6 (Roffman *et al*, 1990) have shown that tegumentation and envelopment occur in the cytoplasm. If a similar model is envisaged for HSV-1, capsids would bud through the inner nuclear membrane acquiring an envelope. The envelope would fuse with the outer nuclear membrane and release non-enveloped capsids into the cytoplasm. The virus then acquires a new envelope at the cytoplasmic membranes, probably those of the Golgi apparatus (Stackpole, 1969; Jones & Grose, 1988) and exits via an endocytotic pathway (see figure 1.8).

Support for an envelopment, deenvelopment and reenvelopment pathway (EDR) comes from observations that capsids, lacking tegument, have been observed in the cytoplasm of infected cells (Campadelli-Fiume *et al*, 1991). However, these static images under the electron microscope do not allow an accurate mechanism of the pathway to be derived.

In further support of the EDR pathway, Van Genderen *et al* (1994) have shown that the phospholipid content of the extracellular virions varies significantly from the nuclear membrane of cells. However, this work is obviously not conclusive since the host membrane is known to be altered by virion proteins and the virion membrane may be altered during transport through the cytoplasm. The best support for this pathway has come from a genetic approach whereby gH is retained at the inner nuclear membrane by

means of an ER targeting signal (Browne *et al*, 1996). If the inner nuclear membrane was retained, then there would have been no effect on the virion's infectivity however, the investigators found that the progeny virus were non-infectious and contained no gH, supporting the EDR pathway (see figure 1.6). Further support for this pathway has been generated through work by Elliott & O'Hare (see below).

The mechanism of transport of the virion through the cytoplasm appears to be through Golgi-derived vesicles. Treatment with brefeldin A (BFA), which inhibits transport between the endoplasmic reticulum and the Golgi, results in accumulation of non-enveloped capsids in the cytoplasm (Cheng *et al*, 1991; Whealy *et al*, 1991; Eggers *et al*, 1992). Vesicles which reach the cellular plasma membrane, fuse with it releasing the virion into the extracellular space.

As mentioned previously, the major tegument protein, VP22, has been shown to demonstrate a non-classical Golgi-independent transport mechanism (Elliott & O'Hare, 1997). Recent visualisation of the GFP labelled VP22 protein has shown that the protein evolves from a diffuse to particulate material which travels through a cytoplasmic pathway to the cell periphery (Elliott & O'Hare, 1999). This pathway is sensitive to cytochalasin D, which inhibits actin cytoskeleton transport. It is not clear how this relates to virus exit or entry but there is obviously a complex network of reactions transporting different proteins and virion assembly products through the cell.

Transport of the virus from the nucleus to the plasma membrane has been shown to involve several gene products. A null mutation of the UL11 gene both reduces the efficiency of envelopment and of viral export (Baines & Roizman, 1992). Similarly, deletion of gE or gI appears to inhibit cell-to-cell spread of the virus (Dingwell *et al*, 1994). Obviously the pathway is extremely complex and warrants further study.

5.6 Latency

The lytic cycle of HSV-1 is obviously important and has been discussed however, herpesviruses are unusual in that they also have the ability to exist in a dormant or latent state. Herpes simplex virus becomes latent within the human peripheral nervous system. It can remain there for the entire lifetime of the host and may reactivate to cause recurrent disease. The mechanism of latent infection is widely studied but shall only be

very briefly summarised here as it is such an important part of the virion life cycle (for review see Steiner & Kennedy, 1995).

A latent viral genome exists in cells without producing any infective virions and is undetected by the immune system. However, it has the ability to reactivate and resume replication to cause recurrent disease. It appears that, following peripheral infection and viral replication, HSV-1 can be transported to the trigeminal ganglia by retrograde transport through the axons (Cook & Stevens, 1973; Kristensson *et al*, 1986). Here it establishes latency.

The genome is not integrated into the host genome (Mellerick & Fraser, 1987) and the viral DNA content is difficult to estimate. Early experimentation suggested 1.00 genomes per neuron were present (Efstathiou *et al*, 1989) but PCR data indicated that the viral DNA content was much higher (Mehta *et al*, 1995). More recent work has found that the number of viral genome copies within individual latently infected neurons is extremely variable and may be viral strain specific (Sawtell *et al*, 1998).

The IE gene Vmw65 appears to play an important role in the latency pathway. Lack of Vmw65 function is associated with a higher proportion of latently infected cells (Steiner *et al*, 1990; Steiner & Kennedy, 1995). Similarly, cellular factors also appear to aid the establishment of latency. Oct-2, a transcriptional factor in nerve cells, appears to inhibit viral replication by binding to a protein complex containing Vmw65 (Lillycrop *et al*, 1993). This action appears to down regulate the replication cascade.

The only expression known to occur during HSV latency is from the latency associated genes, which are contained within a 10.4kb fragment within the repeat regions (Stevens *et al*, 1987; Deatly *et al*, 1987; Stevens *et al*, 1988). From this area, latency associated transcripts, LATs, are transcribed which accumulate during latent infection (Spivack & Fraser, 1988). LAT negative mutants have been produced which appear to retain their ability to become latent however, their ability to reactivate is hindered (Javier *et al*, 1988; Ho & Mocarski, 1989; Hill *et al*, 1990; Trousdale, 1991).

Host factors associated with latency are stress, fever, immunosuppression and UV radiation (Hill, 1985). Therefore, both viral and cellular factors must be involved in the establishment and control of latent viral infection.

CHAPTER 2

MATERIALS AND METHODS

1 Materials

1.1 Chemicals

All chemicals used were of an analytical grade and supplied by either BDH Chemicals, Gibco/BRL or Sigma Chemical Company, except those shown below:

SUPPLIER	CHEMICAL
Agar Scientific Ltd	gluteraldehyde
Aldrich	TFA (trifluoroacetic acid)
Bio-Rad Laboratories Ltd	APS (ammonium persulphate) TEMED (N,N,N',N',-tetramethylethylene diamine) Coomassie Brilliant Blue R250
Boehringer Mannheim	Tris [2-amino-2(hydroxymethyl)-1,3- propandiol]
Citifluor Ltd	Citifluor
Difco Laboratories	Bactopeptone BHIB (brain heart infusion broth) SAB (sabouraud medium) Trypsin TPB (tryptose phosphate broth)
Koch-Light Laboratories Ltd	DMSO (dimethyl sulphoxide)
May and Baker Ltd	chloroform

	glycerol
Novabiochem (UK) Ltd	F-moc amino acids
Rhone-poulenc Ltd	acetic acid hydrochloric acid
Rathburn	DMF (dimethylfluoride)
Walkerburn	piperidine diethyl ether

1.2 Enzymes

All enzymes and their buffers were obtained from either: Boehringer Mannheim, Gibco/BRL, Life Technologies, New England Biolabs, Pharmacia or Sigma.

1.3 Oligomers

(i) Oligonucleotides were synthesised in-house (MRC Institute of Virology, Glasgow) on a Biosearch 8600 DNA Synthesiser by Mr David McNab or Mr Alex Orr.

(ii) Oligopeptides were synthesised in-house by myself on the PSSM-8 Synthesiser on a 4-branched resin, with no glycine spacers, using HBTU chemistry as per the manufacturers instructions. The SPOTscan kit was also used to produce oligopeptides to map the epitope sequence of the CAT antibody.

1.4 Tissue Culture Medium

(i) Sf 21 cells: grown in TC100/5 medium which consisted of TC100 (Gibco/BRL) supplemented with 5% foetal calf serum (FCS) and 1% P/S (1000 units/ml penicillin, 10mg/ml streptomycin) (Gibco/BRL).

1.8 Bacterial Strains

E coli BL21 (DE3) pLysS: commercially competent bacterial cells (supplied by Promega). These can be used with protein expression vectors under the control of the T7 promoter eg pET vectors.

E coli JM109: commercially competent bacteria supplied by Promega

E coli CJ236 *dut ung*⁻: commercially competent bacteria supplied by New England Biolabs (NEB). These can be used for the Kunkel method of site directed mutagenesis (Kunkel, 1985).

1.9 Expression Plasmids

pAcYM1: baculovirus transfer vector which contains a section of AcNPV EcoRI restriction fragment I with a BamHI cloning site situated 3' of the polyhedrin gene promoter (Mastuura *et al*, 1987).

pAcCl29.1: baculovirus transfer vector derived from pAcYM1 which contains a polylinker downstream of the polyhedrin promoter (Livingston & Jones, 1989).

pCMV10: transient expression plasmid containing the immediate early promoter of HCMV and the RNA processing signals of SV40 (Stow *et al*, 1993).

pET28a-c(+): expression plasmid containing T7 RNA polymerase promoter. Supplied by Novagen.

1.10 Antibodies

LP12: mouse monoclonal used against VP5 protein in HSV-1, the product of UL19 (from Dr A Minson).

1060: mouse monoclonal used against VP23 protein in HSV-1, the product of UL18 (Nicholson *et al*, 1994).

- 186: rabbit polyclonal used against VP23 protein in HSV-1, the product of UL18 (from David McClelland)
- 5010: mouse monoclonal used against HSV-1 preVP22a, the un-processed product of UL26.5 (Rixon *et al*, 1988)
- 20999: rabbit antisera raised against a synthetic peptide (14 amino acids) whose sequence is contained within the UL26 ORF, immediate upstream of the C-terminal residues. Recognises preVP22a (Preston *et al*, 1992)
- pp65 (9220): mouse monoclonal antibody which recognises a 10 amino acid epitope from HCMV pp65 protein (McLauchlan *et al*, 1994). Supplied by Capricorn Products Incorporated as 9220 but referred to as pp65.
- 5/24: mouse monoclonal antibody against CAT (from Dr S Graham) and used in SPOTscan mapping procedures.
- GAM-HRP: goat anti-mouse antibody conjugated to horse radish peroxidase was supplied by Sigma and used in Western blots, ELISA's and SPOTscan.
- TRITC-GAM: goat anti-mouse antibody with texas red isothiocyanite conjugate. Used in immunofluorescence experiments (supplied by Sigma)
- FITC-GAM: goat anti-rabbit antibody conjugated to fluoroscein isothiocyanite (supplied by Sigma) and used in immunofluorescence studies

1.11 Buffers and Solutions

Some commonly used buffers and solutions are detailed below:

BUFFER / SOLUTION	RECIPE
FPLC equilibration buffer	20mM Tris-HCl pH 8.0, 500mM NaCl, 5% glycerol, 1mM DTT
HBS	20mM HEPES, 150mM NaCl pH 7.4
loading buffer (5x)	5x TBE, 50% glycerol, bromophenol blue, xylene cyanol
NTE	500mM NaCl, 20mM Tris-HCl pH 7.5, 1mM EDTA
phenol / chloroform (1:1)	mix phenol & chloroform 1:1 & saturate with 10mM Tris-HCl pH 8.0
PBS A	170mM NaCl, 3.4mM KCl, 10mM Na ₂ HPO ₄ , 1.8mM KH ₂ PO ₄ , pH 7.2
PBS complete	PBS A + 6.8mM CaCl ₂ , 4.9mM MgCl ₂
TAE	40mM Tris-HCl pH 7.8, 20mM acetic acid, 100mM EDTA
TBE	89mM Tris-HCl pH 8.0, 2mM EDTA, 89mM boric acid
TBS	20mM Tris-HCl pH 7.5, 500mM NaCl
Trypsin	0.25% (w/v) trypsin dissolved in TBS

Sodium phosphate buffer
A: Na_2HPO_4 2.84g/l
B: NaH_2PO_4 3.13g/l
Add B to A until pH 7.0

Versene
600mM EDTA dissolved in PBS A
containing 0.0002% phenol red

Bacterial purification:

Sonication buffer
20mM Tris-HCl pH 8.0, 10% glycerol,
0.1% NP40

Buffer A
6M GuHCl, 100mM NaH_2PO_4 , 10mM
Tris-HCl pH 8.0

Buffer B
8M urea, 100mM NaH_2PO_4 , 10mM Tris-
HCl pH 8.0

Buffer C
20mM imidazole + buffer B

Buffer D
60mM imidazole + buffer B

Buffer E
200mM imidazole + buffer B

ELISA:

blocking buffer
PBS A + 2% BSA

wash solution
PBS complete + 2% Tween 20

signal developer
ABTS peroxidase substrate : peroxidase
solution B (1:1) (supplied by Kindergaard
& Perry Laboratories)

Plasmid preparation:

solution 1
25mM Tris-HCl pH 8.0, 10mM EDTA,
50mM glucose

solution 2 200mM NaOH, 1% (w/v) SDS
 solution 3 3M KAc, 2M acetic acid

Peptide cleavage:

81.5% TFA, 5% thioanis, 5% phenol, 5%
 Reagent K dH₂O, 2.5% EDT (1,2 ethanedithiol), 1%
 TIPS (triisopropylsilanes)
 Trp cleavage mixture 93% TFA, 3% thioanis OR phenol, 1%
 TIPS, 3% 2-methylindole

SDS-PAGE:

Dissociation mix 40% SGB, 10% glycerol, 4.75% 2-
 mercaptoethanol, 2% SDS, 0.01%
 bromophenol blue
 RGB 0.47M Tris-HCl pH 8.9, 1% SDS
 SGB 0.122M Tris-HCl pH 6.7, 0.1% SDS
 tank buffer 52mM Tris, 53mM glycine, 0.1% SDS
 Coomassie blue stain methanol : H₂O : acetic acid (50 : 880 :
 70) 0.2% Coomassie brilliant blue R250
 fix methanol : H₂O : acetic acid (50:50:7)
 destain methanol : H₂O : acetic acid (50:880:70)

Silver staining:

solution 1 30% ethanol, 10% acetic acid
 solution 2 30 % ethanol, 500mM sodium acetate,
 500mM gluteraldehyde, 0.2% Na₂S₂O₃
 solution 3 dH₂O
 solution 4 0.1% silver nitrate, 0.02% formaldehyde
 solution 5 2.5% sodium carbonate, 0.01%
 formaldehyde

SPOTscan:

regeneration Buffer A	8M urea, 1%SDS, 0.01% 2-mercaptoethanol
regeneration Buffer B	50% ethanol, 10% acetic acid

Western Blotting:

transfer buffer	40mM Tris, 48mM glycine, 20% methanol, 0.4% SDS
blocking buffer	TBS + 1% gelatin
TTBS	TBS + 0.1% Tween 20
antibody buffer	TTBS + 1% gelatin
stripping buffer	100mM β -mearptoethanol, 62.5mM Tris-HCl, pH 7.0, 2% SDS

1.12 Commercial Kits**SUPPLIER**

Anachem
Hybaid
National Diagnostics
Pharmacia
Bio-101
Qiagen

KIT

Gene clean II
Recovery Plasmid midi prep kit
SequagelTM
SephaglassTM bandprep
Mermaid DNA prep kit
Plasmid midi kit (50)

1.13 Miscellaneous materials and Suppliers**SUPPLIER**

Amersham International Plc

MATERIAL

rainbowTM protein molecular weight

	marker
Beecham Research Laboratories Ltd	ampicillin
Bio-Rad	protein assay solution
	gene pulser cuvette (0.1 cm)
	poly-prep columns (0.8 x 4.0 cm)
Dynatech Laboratories	Immunlon-2 flat bottomed UV irradiated microtitre plate
Gibco/BRL Ltd	100 bp DNA marker
Kodak Ltd	X-Omat-S-film
Life Technologies	SOC medium IPTG
New England Biolabs	λ BstE II (1kb) DNA marker
Qiagen	Ni-NTA agarose (slurry)

2 Methods

2.1 Gel Electrophoresis and Western Blotting

2.1.1 Analytical Agarose Gels of DNA

A 1% (w/v) agarose gel dissolved in 1x TBE and containing 0.5 μ g EtBr per ml was submerged in 1x TBE and run at 50V for 30-40 minutes. Restriction enzyme digests or DNA preparations were checked by mixing DNA 5:1 with loading buffer. DNA was examined and photographed under UV transillumination. Size markers were run in adjacent wells to the DNA to determine the size of the fragments.

2.1.2 Isolation of DNA from Agarose Gels

5-20 μ g of DNA was mixed with loading gel buffer and was loaded onto a 1% (w/v) TAE agarose gel and electrophoresed at 40V. The DNA profile was visualised under

long wave UV light and the appropriate fragments excised with a sterile scalpel. The gel slice was stored in a 1.5ml reaction vial at 4°C until required for purification (Section 2.5.9).

2.1.3 Purification of Synthetic Oligonucleotide from Polyacrylamide Gels

Dried oligonucleotide pellets were resuspended in a 50:50 mix of dH₂O:formamide by boiling for 5 min. The product of a preparation was run between 4 adjacent wells using a 10% Sequagel in 0.5x TBE. 1x loading gel buffer was run in adjacent wells, to monitor progression of fragments. The gel was electrophoresed at 50mA until the loading dye had reached the bottom of the gel. The gel was carefully removed, wrapped in cling film and viewed on a silica gel thin layer chromatography plate under short wave UV radiation. The band was excised with a sterile scalpel and placed into a glass universal containing 500µl of dH₂O. The sample was agitated o/n at 37°C to allow the oligonucleotide to diffuse. The oligonucleotide solution was transferred into a 1.5ml reaction vial, phenol/chloroform extracted, isopropanol precipitated and resuspended in 100µl of dH₂O. The oligonucleotide was then quantified (Section 2.8) and stored at -20°C until required.

2.1.4 SDS-PAGE of Protein Samples

Analysis of protein samples was typically carried out on 'mini-gels' run on a Bio-Rad Mini Protean II™ apparatus. Single concentration gels were prepared with commercial polyacrylamide (30% acrylamide / Bis-acrylamide 37.5:1, Bio-Rad) at concentrations of either 10% or 15%. A 5% stacking gel was polymerised on the top. The protein samples were boiled in dissociation mix for 2 min before being loaded in parallel with molecular weight rainbow markers. Electrophoresis occurred in tank buffer (52mM Tris, 53mM glycine, 0.1% SDS) at 50V until the bromophenol blue dye had reached the bottom of the gel. The gel was then stained with Coomassie gel stain for at least 1h. Protein bands were visualised by shaking the gel o/n in a solution of destain. Alternatively a silver staining procedure was used (see Section 2.1.5).

For permanent storage, the gels were dried onto Whatman 3mm paper under vacuum on a Bio-Rad gel drier.

2.1.5 TCA Precipitation

GuHCl causes SDS to precipitate out of solution and so samples containing GuHCl cannot be mixed directly with dissociation mix, for analysis by SDS-PAGE. The GuHCl was therefore removed by addition of 5% TCA (trichloroacetic acid), followed by incubation on ice for 20 min. The solution was spun at 13000rpm for 15 min and the pellet washed with 100% ethanol, air dried and resuspended in dissociation mix. The sample could then be loaded onto a gel immediately, or stored at -20°C, until required.

2.1.6 Silver Staining

To detect protein bands by silver staining a series of solutions, detailed in Section 1.11, were used. The electrophoresed gel was first fixed in solution 1 for 25-30 min before being incubated, with gentle agitation, in solution 2 for 20-30 min. After washing for 3x 10 min in solution 3, solution 4 was added for 15-20 min. The reaction was developed by addition of solution 5 which was stopped by the addition of 50mM EDTA when the bands had become evident.

2.1.7 Analysis of ³⁵S Labelled Proteins

To visualise radioactive protein samples the polyacrylamide gel was dried down and placed in a cassette in contact with Kodak XS-1 film and incubated in the dark o/n and developed through a Kodak X-Omat Processor (model: ME3). Alternatively the gel was placed against an Image Screen (supplied by Molecular Dynamics) which had been wiped of all previous samples by exposure to an Image Screen Eraser (Molecular Dynamics) for 10 min. The polyacrylamide gel was placed against a blank screen for 4h-o/n. The gel profile was scanned into the PhosphoImager (Molecular Dynamics) and the bands viewed on the PC using the ImageQuant programme.

2.1.8 Semi-dry Western Blotting

(i) Transfer

Proteins were transferred from a mini-protein polyacrylamide gel onto a nitro-cellulose membrane using 2117-Multiphor II Electrophoresis Unit (Pharmacia), with the surfaces coated in transfer buffer. The proteins were transferred for 1h at 40mA. Confirmation that transfer had occurred was monitored visually using Rainbow markers.

The blot was stored at rt in transfer buffer until required.

(ii) Detection

Proteins were detected by a series of washing and antibody reaction steps. The membrane was first placed in blocking buffer at 37°C for 30 min to reduce non-specific binding to the membrane. This was followed by 2x 5 minute washes in TTBS and the addition of the primary antibody, diluted in antibody buffer, for 4h at 37°C. The membrane was washed (2x 10 min) in TTBS before addition of the secondary antibody (usually GAM-HRP), diluted in antibody buffer, for at least 4h at 37°C. The blot was again washed in 5 min cycles at 37°C, twice in TTBS and twice in TBS. Visualisation occurred by enhanced chemiluminescence (ECL). The ECL developing reagents were applied to the membrane for 2 min. The developing reagents were supplied by Amersham international plc. Reagent 1 was mixed 1:1 with reagent 2 to give a volume equivalent to 0.125ml/cm² of membrane. The membrane was then exposed for approximately 5 sec to 1 min on Kodak XS-1 film.

(iii) Stripping

The nitro-cellulose membrane could be stripped and re-probed with the antibodies by bathing the blot in stripping buffer (Section 1.11) for 30-40 min at 55°C. It was then washed in TBS briefly ready for re-probing.

2.2 HSV-1 Virus Preparation and Manipulation

2.2.1 BHK Cell Culture

2.2.1.1 Estimation of Cell Densities

All cell densities were estimated using a Neubauer counting chamber. Cells were counted under the light microscope and cells/ml values calculated.

2.2.1.2 BHK C13 Cells

(i) Passage

BHK cells were passaged routinely every 3-4 days in 850cm² roller bottles. The cells were seeded at 2×10^7 in 100ml of ETC₁₀ with 5% CO₂ atmospheric conditions. Roller bottles were rotated slowly at 37°C. Confluent monolayers were harvested after 2 versene washes followed by trypsinisation with trypsin/versene (1:4). A confluent monolayer typically yielded 1×10^8 cells.

Confluent BHK cells could be maintained in roller bottles in a viable state at 31°C for at least one week

(ii) Freezing and Storage

A healthy flask of 150cm² BHK C13 cells, was harvested and spun at 3000 rpm for 10 min. The cells were resuspended in 3ml 40% ET_{-serum}, 40% NBCS, 20% glycerol, aliquoted into 3 screw cap vials, placed in a polystyrene container and stored at -70°C o/n before transfer to liquid nitrogen.

(iii) Recovery

One vial of cells was defrosted and recovered into a large flask containing growth medium and incubated at 37°C in 5% CO₂. The medium was changed the following day and when confluent, the monolayer of cells was passaged as normal.

2.2.2 Preparation of High Titre Virus Stocks

Confluent monolayers of BHK C13 cells in roller bottles were used to grow high titre HSV-1 virus. Virus was infected at 0.001 pfu/cell in 50ml of ETC₁₀ and incubated at 31°C for 4-5 days. The cells were removed by gentle shaking and harvested in 225ml falcon tubes at 2000 rpm for 10 min using a Sorvall RT7 centrifuge. The supernatant and cell pellet were separated to produce two individual stocks.

- Cell associated virus (CAV): the pellet was sonicated in 2ml of ETC₁₀ per 850cm² roller bottle, and spun at 3000 rpm for 5 min in a Sorvall RT7 centrifuge, to pellet the cell debris. The supernatant was removed to 1.5ml reaction vials and stored as CAV stock.
- Cell released virus (CRV): the supernatant was spun in Sorvall GSA bottles at 12000 rpm for 2h (Sorvall GSA rotor) and the pellet resuspended in 2ml of ETC₁₀ per 850cm² roller bottle, by sonication. The CRV stock was aliquoted and stored in 1.5ml screw cap reaction vials.

Both the CAV and CRV stocks were stored at -70°C.

2.2.3 Titration of Virus Stock

Stocks were titrated on 50mm dishes on approximately 80% confluent monolayers of BHK C13 cells. The cell medium was removed and replaced with 100µl of virus serially diluted 10-fold in PBS complete, containing 5% NBCS. After 1h at 37°C, the inoculum was removed, replaced with 4ml EMC₁₀ and incubated at 37°C for 3-4 days. Staining with 4ml of Giemsa for 15 min revealed clear plaques which could be counted using a dissection microscope and expressed as pfu/ml.

2.2.4 Sterility Checks of Virus Stock

Viral stocks were regularly monitored for their sterility by routine checks. A small amount (typically 5µl) of the stock was inoculated into bacterial medium eg TPB or fungal medium eg SAB and incubated at 28°C or 37°C for up to one week or until visible signs of contamination appeared. In addition, samples were also streak plated onto blood agar plates (supplied by E&O Laboratories Ltd) and generally incubated at 28°C.

2.2.5 Preparation and Purification of Wild-type HSV-1 Capsids

2.2.5.1 Infection of BHK C13 Cells

Confluent cell monolayers of BHK C13 cells in roller bottles, were infected with 5pfu/cell of HSV-1 virus in 40ml of ETC₁₀ and incubated at 37°C for 18-24h.

2.2.5.2 Purification of Capsids

Capsids were purified using a modification of the method of Booy *et al*, 1991. The infected cells were removed from the roller bottle by two washes with 30ml of PBS complete containing 1% NP40. The suspension was transferred to a 225ml falcon tube and centrifuged in a Sorvall RT7 at 2000 rpm for 10 min. 30ml of ice cold NTE, with 1% NP40, was added to the pellet and incubated on ice for 10 min. Probe sonication using a Branson soniprobe, lysed the nuclei and released the capsids into the medium. The debris was pelleted at 2000 rpm for 10 min (in a Sorvall RT7 centrifuge) and the supernatant concentrated through a 5ml, 40% (w/v), sucrose cushion at 20000 rpm for 1h at 4°C in an AH629 rotor. The pellet was rinsed carefully with NTE, to remove residual sucrose, before resuspension in NTE. The capsids were then banded on a sucrose gradient:

- Small scale capsid preparations (2 roller bottles/gradient) were loaded onto 12ml gradients of 10-40% (w/v) sucrose in NTE and spun at 40000 rpm for 20 min in TsT41 rotor.
- large scale capsid preparations (5 roller bottles/gradient) were loaded onto 30ml gradients of 20-50% (w/v) sucrose in NTE. These were spun at 25000 rpm for 1h in AH629 rotor.

Gradient bands were viewed in a darkened room under a fibre optic light and removed by side puncture with an 18-gauge needle. A (top band), B (middle band), and C (bottom band) capsid preparations were pooled, diluted 10-fold in NTE and spun at 24000 rpm at 4°C in a Sorvall TsT41 rotor for 1h. Capsid pellets were resuspended in 100-200µl of NTE or PBS by bath sonication and stored at -70°C until required. Correct capsid protein profiles were confirmed on a mini-gel as described in Section 2.1.4.

2.3 Baculovirus Preparation and Manipulation

2.3.1 Sf 21 Cell Culture

Cell densities were estimated as in Section 2.2.1.1.

(i) Passage

Sf 21 cell monolayers were passaged every 3-4 days in 150cm² tissue culture flasks containing 50-75ml of TC100/5 medium. The cells were dislodged in 10ml of TC100/5 medium by sharply tapping the flask against the hand and pipetting up and down to disperse clumps. Yield from a confluent flask was typically 4-6 x 10⁷ cells and new flasks were seeded by a 1:4 split.

Sf cell suspensions were set up from a confluent flask harvest in 850cm² roller bottles containing 300ml of TC100/5. The roller bottles were turned continuously (4 rpm) at 28°C to prevent the cells adhering to the sides of the bottle. The cells reached a density of 2-3 x 10⁶ cells/ml after 4-5 days, when they were split 1:10 to seed a new roller bottle.

(ii) Freezing and Storage

A confluent flask of Sf cells was harvested in 10ml of TC100/5 medium (as described above) and pelleted at 1500 rpm in a Sorvall RT7 centrifuge. The cell pellet was resuspended in 3ml of 90% FCS, 10% DMSO and split between 3 screw cap vials. The cells were stored at -70°C for 3-4h before being transferred to liquid nitrogen.

(iii) Recovery

Sf cells were thawed rapidly at 37°C and spun at 3000 rpm to pellet the cells and remove the DMSO. The cells were resuspended in TC100/5 and transferred to a 25cm² tissue culture flask, containing 10ml of TC100/5 and incubated at 28°C o/n. The medium was then removed and replaced with fresh growth medium to remove any dead cells. Once the cells had formed a confluent monolayer, generally 4-5 days they were dislodged and transferred into 150cm² flasks and passaged as normal.

2.3.2 Preparation of Low Titre Virus Stock

A 25cm² tissue culture flask was seeded with 1×10^6 cells in 10ml of TC100/5 and incubated at 28°C until a 50% confluent monolayer was formed (2-3 days). The medium was then discarded and replaced with 100µl of the plaque purified plate harvest (Section 2.3.7.4) for 1h at rt. 10ml of fresh growth medium was added and the flask was incubated at 28°C for 4-5 days when extensive CPE was observed. The medium was harvested in a 15ml falcon tube at 2000 rpm (Sorvall RT7 centrifuge) for 5 min and the supernatant aliquoted into bijoux (5ml in each). This low titre stock was stored at 4°C and used to grow high titre stocks.

2.3.3 Preparation of High Titre Virus Stock

High titre baculovirus stocks were prepared in 300ml suspensions of Sf21 cells in TC100/5 medium, which had reached a density of 5×10^5 cells/ml. Cells were infected at a moi of 0.1 pfu/cell with titred virus stock. The cells were incubated at 28°C for 4-5 days. The medium was harvested by spinning in 225ml falcon tubes at 2000 rpm (Sorvall RT7 centrifuge) for 10 min to remove cells and debris. The virus was then pelleted from the supernatant at 12000 rpm for 2h in a Sorvall GSA rotor. The viral pellet was allowed to resuspend o/n at 4°C in 4ml of TC100/5 and dispersed in a Kerry ultrasonic bath. The stocks were aliquoted into 1.5ml screw cap reaction vials. High titre 'working' stocks were stored at 4°C whereas the 'elite' stocks were stored at -70°C.

2.3.4 Titration of Virus Stock

Stocks were titrated on 35mm dishes on a uniform Sf cell monolayer (approximately 60-70%) (Brown & Faulkner, 1977). The cell medium was removed and replaced with 100µl of virus diluted in TC100/5. The virus was diluted 10-fold, 10^{-2} - 10^{-6} for low titre stock and 10^{-5} - 10^{-8} for high titre virus stock. After 1h at rt, with periodic gentle agitation, the inoculum was removed and replaced with 1.5ml of overlay which consisted of 50% TC100/5 and 50% of 3% Seaplaque agarose, maintained at 45°C until required to prevent setting. Once the overlay had set on the plates, 1.5ml of TC100/5 medium was added. After 4-5 days at 28°C, the cells were stained with 1.5ml of neutral

red stain (0.4% neutral red mixed 1:50 with TC100/5) for 4-8h. The stain was poured off, the plates inverted and left to clarify o/n in the dark.

Distinct clear plaques could be visualised and counted either by eye or under 10x magnification on a dissecting microscope (Wild, Heerburgg). The titre was calculated at pfu/ml.

If recombinant virus plaques were to be identified through the loss of the *lacZ* marker gene, then 250µg of X-gal was added to each ml of neutral red stain. The mixture of parental (*lacZ*-positive) and recombinant (*lacZ*-negative) viruses were separated as the recombinant produced clear plaques and the parental produced blue plaques on the pink background of non-infected cells.

2.3.5 Sterility Checks of Virus Stock

Both high and low titre virus stocks were regularly monitored for their sterility by routine checks as described in Section 2.2.4.

2.3.6 Confirmation of Expression of Baculovirus Proteins

The expression of baculovirus proteins was confirmed by an analytical protein gel. For radio-active labelling 35mm dishes were seeded with 6×10^5 Sf cells in 1.5ml of TC100/5. The plates were incubated o/n at 28°C to form a 50% confluent monolayer (1×10^6). The medium was removed and 100µl of virus added at 5 pfu/cell for 1 hour before the addition of 1.5ml of TC100/5. The plates were again placed at 28°C for 24-30h. The medium was then removed and replaced with 1ml of TC100_{-met} for 1h prior to incubation in TC100/5:TC100_{-met} (1:4) containing 30µCi/ml of [³⁵S]-methionine for 18h at 28°C. The cells were gently pipetted off and transferred to a 1.5ml reaction vial, pelleted by a microfuge at 6500 rpm for 3 min, washed twice in PBS complete and resuspended in 100µl of dissociation mix. The cell lysates were stored at -20°C before analysis by SDS-PAGE (see Section 2.1.6).

2.3.7 Construction of Recombinant Baculoviruses

2.3.7.1 Preparation of AcPAK6 DNA

AcPAK6 was used to infect 2 roller bottles containing 300ml of 2×10^5 Sf21 cells/ml at 1pfu/cell and harvested in the usual manner (Section 2.2.3). The pellet was resuspended in 2ml of TC100/5 medium by sonication with a Branson ultra soniprobe and reconcentrated in a SS34 rotor by centrifugation at 18000 rpm for 90 min at 4°C in a Sorvall RC-5B centrifuge. After resuspension in TE buffer (SDS 0.25%, proteinase K 500µg/ml) o/n at 31°C, the DNA was phenol/chloroform extracted, chloroform extracted and precipitated in ethanol. The DNA pellet was resuspended at 37°C in 200µl of dH₂O.

2.3.7.2 Digestion of AcPAK6 DNA

25µg of AcPAK6 DNA was digested with 60 units of restriction enzyme Bsu36I in a 100µl reaction mix containing 1x NEB 3 buffer and 100µg/ml acetylated BSA. The reaction mix was incubated at 37°C for 4-5h, treated for 30 min with 1 unit of calf intestinal phosphatase, phenol:chloroform extracted, ethanol precipitated and the PAK6(Bsu361) DNA resuspended in 100µl of dH₂O at 37°C.

Successful digestion was confirmed by digesting PAK6(Bsu361) DNA and PAK6 DNA with EcoRI and comparing the profiles on an analytical agarose gel. Correct digestion of the DNA was confirmed by a noticeable shift in a large fragment and the appearance of a smaller band.

2.3.7.3 Transfection of Viral DNA

Viral DNA was transfected on 60-70% confluent monolayers of Sf21 cells in 35mm dishes using CELLFECTIN™ reagent (Life Technologies) and the protocol suggested by the manufacturer. Basically two reaction mixes were prepared, A and B, in 15ml falcon tubes:

- A 0.5µg PAK6(Bsu361) DNA, 1-2µg plasmid DNA, 100µl TC100.
- B 4µl CELLFECTIN™, 100µl TC100.

A and B were then mixed gently, and incubated at rt for 30-45 min. The medium was decanted from the monolayers and the cells were washed once in TC100 before the addition of the transfection mix. After incubation at 28°C for 5h, the mix was removed and replaced with 2ml of TC100/10 and incubated for a further 72h at 28°C. Cells were harvested at 13000 rpm (microfuge) for 2 min and the supernatant medium transferred to a 1.5ml screw cap reaction vial for storage at -70°C until plaque purification.

2.3.7.4 Plaque Picking and Purification

(i) Initial Plaque Isolate (iPI)

The transfection supernatant was titrated as a low titre stock as described in Section 2.3.2 and stained to reveal lacZ minus recombinants. Well isolated clear plaques were picked by removing a plug of agarose with a pipette tip and washing it out in 250 µl of TC100/5. The virus was released into the medium by 3x freeze-thawing and this initial plaque isolate stored at -70°C.

(ii) Final Plaque Harvest (fPH)

The iPI medium was plated and stained as described above, through at least another 2 cycles, to produce the final plaque harvest (fPH).

(iii) Plate Harvest 1 (PH1)

100µl of the fPH was plated onto 50% confluent Sf21 cells on 35mm dishes and allowed to absorb at rt for 1h with periodic agitation. 1.5ml of TC100/5 was then added and the cells incubated at 28°C for 4-5 days. The PH1 cells were harvested and 100µl used as the inoculum to produce low titre and high titre virus stocks described in Section 2.3.2.

2.3.8 Preparation and Purification of Recombinant HSV-1 Capsids

2.3.8.1 Infection of Sf21 Cells

Roller bottles containing Sf21 cells at 1×10^6 cells/ml were infected with the appropriate recombinant baculovirus at 5pfu/cell and incubated at 28°C for 48-65h. Infected cells were harvested in 225ml Falcon tubes at 2000 rpm for 10 min using a Sorvall RT7 centrifuge.

2.3.8.2 Purification of Capsids

Capsids were purified as described in Section 2.2.5.2.

2.4 Oligomers

2.4.1 Cleavage and Storage of Oligonucleotides

(i) Cleavage

Oligonucleotides were removed from the synthesis column with ammonia [specific gravity = 0.88, (Fisons)] and deprotected at 55°C for 5h. The deprotected oligonucleotide was aliquoted equally between 3x 1.5ml reaction vials and the ammonia removed by evaporation o/n in a rotary drier.

(ii) Storage

The dried pellets were stored at -20°C until required for gel purification (Section 2.1.3).

2.4.2 Cleavage, Analysis and Storage of Oligopeptides

(i) Cleavage

The resin [see Section 1.3, (ii)] was first washed with a series of chemicals (tertiary amyl alcohol, acetic acid, tertiary amyl alcohol and 2x diethyl ether) to remove uncoupled oligopeptides. The resin was then thoroughly dried by passing N₂ through it before the peptide was removed from the resin by cleavage with either Reagent K for 5h or Trp cleavage mixture for 7h, depending on the amino acid sequence of the peptide (see results). The cleavage mixture was collected from the column and mixed with 20ml of ether, to precipitate the oligopeptide, and spun at 10000 rpm (SS34 rotor) for 10 min. The oligopeptide pellet was washed twice in 20ml diethyl ether and solubilised in 25ml of dH₂O [see (iii)]. The solution was freeze dried in a 100ml round-bottomed flask.

(ii) Storage

Oligopeptides were stored in their powdered form in sealed glass universals at -20°C. Upon removal from storage, they were pre-warmed to rt before opening to prevent condensation forming on the dried oligopeptide.

(iii) Solubilisation

Oligopeptides, where possible, were dissolved in dH₂O for analysis. Those which were not easily solubilised were treated with a small amount of either formic acid (if the peptide was basic) or ammonia vapour (if the peptide was acidic) to alter the pH and aid solubilisation.

(iv) Mass spectrometry

The Mr of each peptide was determined by mass spectrometry analysis. The oligopeptides were analysed by laser desorption mass spectrometric analysis. The peptide was dissolved at 1mg/ml in dH₂O and diluted in analysis buffer (70% acetonitril, 0.1% TFA). 5mg of the matrix, alpha-cyano-4 hydroxycinnamic acid (ALDRICH), was dissolved in 500µl of the analysis buffer. The test peptide was mixed 1:1 with a control peptide and this solution was mixed 1:1 with the matrix. 1µl of this mixture was spotted onto a Lasermat sample slide and left to dry for 10 min. The oligopeptides were analysed on a Finnigan MAT Lasermat. The peptide Mr were identified using the software on the PC and calibrated using the known peptide Mr.

2.5 Gene Cloning

2.5.1 Preparation of *E coli* Competent Cells

(i) BL21

1.6ml of a starter culture was added to 100ml of L-broth and incubated until the $A_{600}=0.2-0.3$. The bacteria were spun down at 3000 rpm (in a Sorvall RT7 centrifuge) for 10 min in 225ml Falcon tubes, resuspended in 40ml of sterile 100mM CaCl₂ and incubated on ice for 2h. A 13000 rpm spin followed in the SS34 rotor. The pellet was resuspended in 1ml of 100mM sterile CaCl₂ and incubated on ice for a further 2h. 80µl of the competent bacteria were aliquoted into 1.5ml reaction vials, and stored at -70°C until required for transformation procedures.

(ii) JM109

These were supplied in a form ready to use for transformations and required no further preparation. They were stored at -70°C.

2.5.2 Transformation of Plasmid DNA

A single vial of *E coli* competent cells was used for each transformation reaction. The cells were thawed on ice and 1-50ng of plasmid DNA added (generally 1µl of the ligation mix) and incubated on ice for 10 min.

(i) Electroporation

Competent cells were induced to take up DNA by subjecting the cells to a short electrical pulse. The cells containing the plasmid DNA were placed in a cold gene pulser cuvette (Bio-Rad) and electroporated at 1800V using the Hybaid 'Cell Shock' apparatus. 1ml of SOC medium was added and the culture incubated at 37°C for 1h with agitation.

(ii) Heat shock

Competent cells were induced to take up DNA by heat shock at 42°C for 45-50 sec. The cells were then returned to the ice bath for 2 min before addition of 1ml of SOC medium followed by incubation at 37°C for 1h with agitation.

100µl of transformed cells in (i) or (ii) was plated onto L-broth agar + antibiotics plates, inverted and incubated at 37°C o/n.

2.5.3 Preparation of a Starter Culture

A starter culture was prepared by inoculating 20ml of L-broth + antibiotic with transformed bacteria from either:

- a single well isolated colony from an agar plate
- 20µl from a small scale preparation (Section 2.5.5)
- 5µl from a glycerol stock (Section 2.2.4)

The culture was shaken at 37°C for 4h-o/n.

2.5.4 Preparation of Glycerol Stocks

(i) Standard preparation

Normally a 1ml starter culture was spun at 6500 rpm (microfuge) for 4 min in a 1.5ml reaction vial. The supernatant was discarded and the pellet resuspended in 500µl of sterile bactopectone (20%) : glycerol (80%) (1:1).

(ii) pET clones

As pET constructs were sensitive to high glycerol concentrations (ie >10%), the method was slightly varied. Bacterial cultures were grown to an $A_{600}=0.6-0.8$ when 900µl of suspension was removed and mixed thoroughly with 100µl of 80% glycerol.

All the stocks were stored at -70°C until required.

2.5.5 Small Scale Plasmid Preparation

A small scale plasmid preparation of DNA or a 'mini-prep' was prepared essentially as described by Maniatis *et al*, 1982. Typically 12 well isolated transformed bacterial colonies were picked from a plate and inoculated into 2ml of L-broth + antibiotic. They were incubated at 37°C , with shaking for at least 5h. 1.5ml of each suspension was transferred to a 1.5ml reaction vial and spun at 13000 rpm (microfuge) for 40 sec. The supernatant was discarded and the cell pellet resuspended in 100µl of solution 1 (Section 1.11) by vigorous vortexing. Once the pellet had completely resuspended, 200µl of freshly prepared solution 2 (Section 1.11) was added for 5 min to lyse the cells. 150µl of ice cold solution 3 (Section 1.11) was added next and the mixture incubated on ice for 5 min. The cell debris was pelleted at 13000 rpm (microfuge) for 5 min and the resulting supernatant removed to a fresh 1.5ml reaction vial for phenol extraction and precipitation (Section 2.5.6 and 2.5.7). The DNA pellet was resuspended at 37°C in 50µl of dH_2O and typically 5µl would be used in a restriction enzyme confirmatory digest reaction.

2.5.6 Phenol:Chloroform (1:1) Extraction of DNA

DNA samples were always extracted in volumes not less than 200µl. If the sample volume was less than this, the appropriate amount of dH_2O was added.

Phenol chloroform (1:1) was saturated with TE and a volume equal to that of the DNA solution was added. The mixture was then vortexed and centrifuged at either 13000 rpm or 3000 rpm in a microfuge for 5 min, depending on the volume. The top layer, containing the DNA was removed to a fresh tube ready for precipitation.

2.5.7 Ethanol / Isopropanol Precipitation of DNA

Sodium acetate (pH 5.4) was added as 1/10 of the volume and one of two alcohols was used:

- isopropanol: an equal volume of isopropanol was added to that already in the tube to aid precipitation of larger fragments of large fragments of DNA.
- ethanol: 2.5x the volume of ethanol was added to aid precipitation of smaller fragments of DNA.

The mixtures were incubated at -20°C for at least 30 min and the DNA pelleted at 13000 rpm (microfuge) for 5 min or 3000 rpm (Sorvall RT7 centrifuge) for 10 min, depending on the size of the sample. The pellet was gently washed in 70% ethanol and dried on a rotary evaporator, ready for resuspension in dH_2O at 37°C . Presence of DNA was confirmed on an analytical agarose gel and samples were stored at -20°C until required.

2.5.8 Restriction Endonuclease Digests of DNA

DNA was digested using the appropriate restriction enzyme(s) and corresponding reaction buffer under the conditions recommended by the manufacturer. Routinely, 10 units of enzyme was added per μg of DNA and incubation occurred at 37°C for 1 hour, unless another temperature was recommended. RNaseA was often included in the reaction mix, especially miniprep samples, at $10\mu\text{g/ml}$ to digest any residual RNA and prevent smearing on the analytical gel.

If the DNA required to be digested by 2 enzymes which reacted in incompatible buffers then 2 approaches were taken:

- a single digest would be carried out and after 1 hour the buffer would be appropriately modified, eg by the addition of salt, and the second enzyme would be allowed to act.
- digests would be performed sequentially. The first enzyme was used on the DNA. A portion was checked on a gel and the remainder was phenol extracted and precipitated before being digested with the second enzyme.

All digests were confirmed by analytical agarose gel electrophoresis (Section 2.1.1).

2.5.9 Purification of DNA from an Agarose Gel Slice

DNA was extracted and purified from an agarose gel slice using the protocols from one of several commercially available kits: Gene clean II (for fragments >1000 bp), Sephaglass bandprep kit (for fragments >200 bp), Mermaid kit (for fragments >50 bp).

2.5.10 Ligation of DNA

(i) Standard ligation

Appropriately digested DNA and vector strands were mixed 3:1 respectively in the presence of 1x BRL ligation buffer and 1 unit of T4 DNA ligase in a total volume of 20 μ l. The ligation mix was incubated for at least 4h, often o/n, at 15°C.

(ii) Oligonucleotide ligation

Purified complementary oligonucleotides (0.5-1.0 μ g) were boiled in 1x BRL ligation buffer without ATP for 1 min. The mixture was then incubated at 37°C for 20 min before the addition of the vector DNA (1 μ g), 1 unit of T4 DNA ligase and 1mM ATP. The mixture was then incubated at 15°C as above.

Following any ligation reaction, the DNA would be stored at -20°C until required for a transformation reaction (Section 2.4.5).

2.5.11 Large Scale Plasmid Preparation

A starter culture (Section 2.5.3) was inoculated into 100ml of L-broth + antibiotic and agitated at 37°C o/n. The bacterial cells were harvested at 6000 rpm for 15 min in a

GSA rotor. DNA was purified using the standard 'midi' protocol for the Qiagen resin kit. DNA was isopropanol precipitated and resuspended in 200 μ l of dH₂O. The presence of DNA was confirmed by running 2-5 μ l on an agarose gel (Section 2.1.1).

2.5.12 Quantification of DNA

DNA was serially diluted 1:10, 1:50, 1:100 in dH₂O. The optical density was then measured on a mass spectrophotometer at A₂₆₀ and A₂₈₀. The resultant stable A₂₆₀ value was multiplied to convert to μ g/ml based on the dilution factor and the conversion factors:

- oligonucleotide: 1OD = 20 μ g/ml
- ds DNA: 1OD = 50 μ g/ml

2.5.13 Site Directed Mutagenesis

A modified Kunkel method of site directed mutagenesis (Kunkel, 1985) was used to generate mutants with amino acid inserts. A series of steps were performed to produce suitable DNA for the insertion of extra amino acids:

(i) Preparation of Uracil-enriched DNA

CJ236 *dut⁻ ung⁻* (supplied by NEB) cells were transformed by electroporation with, for the purpose of this study, the pET plasmid. A single colony was picked into an L-broth + Kan starter culture. This was incubated at 37°C, shaking o/n and sub-cultured into 200ml of fresh medium containing 100 μ g/ml of uridine. After 30 min shaking at 37°C, 1 x 10¹¹ pfu/flask of M13 R408 phage (supplied by Promega) was added followed by a further 9h incubation. The culture was spun at 9000 rpm for 10 min (GSA rotor) and the supernatant decanted and spun for a further 10 min. 0.25 volumes of 20% PEG-6000 in 2.5M NaCl was added to the supernatant. The solution was incubated on ice for 30 min and pelleted at 12000 rpm for 15 min. The phage pellet was resuspended in 5ml of supernatant mix and pelleted at 7000 rpm for 15 min (SS34 rotor). After the supernatant had been thoroughly removed, the pellet was resuspended in 2 ml of TE and phenol chloroform extracted. After centrifugation, the aqueous layer (top) was further extracted, twice with phenol:chloroform:isoamylalcohol (24:24:1) and once with

chloroform:isoamylalcohol (24:1). The aqueous layer was precipitated with 4M NaCl, 50mM EDTA and 2.5 volumes of ethanol, for at least 2h at -20°C . The ss uracil-enriched DNA was concentrated at 13000 rpm (microfuge) for 10 min, dissolved in dH_2O and stored at -20°C until required.

(ii) Annealing and Second Strand Synthesis

A series of oligonucleotides (see Results, Chapter 5) were annealed to the ss uracil-enriched DNA. The oligonucleotides were first phosphorylated in 1x kinase buffer, 20mM ATP and T4 kinase, for 40 min at 37°C . The mixture was heat inactivated at 70°C for 10 min and the oligonucleotides stored at -20°C , until required.

0.5 μg of the ss uracil-enriched DNA was required to separately anneal 1.0 μg of each phosphorylated oligonucleotide at 70°C , cooling to rt for 1h. 30 μl of a mix containing 1x ligation buffer, 0.5 units NEB ligase and 0.5 units T7 DNA polymerase, was added to the annealed DNA. The samples were incubated at rt for 1h and 37°C for a further 1h. The sample volumes were then increased to 200 μl by the addition of 16 μl of 50mM EDTA:4M NaCl. The DNA was phenol:chloroform extracted, ethanol precipitated and resuspended in 20 μl of dH_2O and stored at -20°C until required.

The DNA was transformed into BL21 competent cells and selected on L-broth + Amp plates.

Expression of the modified proteins, incorporating the oligonucleotide sequences is described in Results, Chapter 5.

2.5.14 PCR

All PCR reactions were carried out using a Biometra Trio-Thermoblock machine. 50 μl mixes were prepared in dH_2O and consisted of:

- 5 μl each of two purified oligonucleotide primers at 10 $\eta\text{M}/\mu\text{l}$
- dNTPs to a final concentration of 200 μM

- 0.1µg of template DNA
- 5µl of 10x reaction buffer (500mM KCl, 100mM tris-HCl pH 8.3, 50mM MgCl₂)
- MgSO₄ to a final concentration of 2mM
- 2 units of *Taq* polymerase

The mixture was gently agitated and sealed with 200µl of mineral oil to prevent evaporation. It is important to note that a control mixture was always set up in parallel with the reaction mixture and contained all the ingredients above except the DNA template.

The initial cycling temperatures were carried out as follows:

- 97°C for 2 min - to denature the DNA
- 50°C for 2 min - to anneal the primers
- 72°C for 2 min - to allow the primers to extend.

All 30 subsequent cycles were performed at the respective temperatures. Upon completion, the block was held at 10°C until the samples were removed.

The PCR samples were usually set up in triplicate to increase yield of DNA. The products were confirmed on a agarose gel, containing the appropriate size markers, before gel purification.

2.5.15 Sequencing Analysis of DNA

Sequencing analysis was performed in house on an ABI PRISM™ 377 DNA Sequencer. DNA was used at 200ng per reaction.

2.6 Immunofluorescence Staining

2.6.1 Transfection of Plasmid DNA

All fluorescence experiments were performed with BHK C13 cells cultured as previously described. The cells were grown in 1ml of ETC₁₀ on 13mm glass cover slips

in 24 well tissue culture dishes. The wells were seeded with 5×10^4 cells/ml or 1×10^5 cells/ml and incubated o/n at 37°C. The wells which exhibited a 50% confluent monolayer were chosen for transfection by cationic liposome method (described by Rose *et al*, 1991). The transfection mix was prepared in 15ml falcon tubes: 1µg of plasmid DNA mixed in 20µl of Hbs (20mM HEPES, 150mM NaCl, pH7.4) with 6µl of synthetic liposomes was allowed to interact for 10 min at rt. 500µl of Optimem 1 (Gibco-BRL) was added and the mixture was added to the BHK cells. After 4-5h incubation at 37°C, 500µl of ETC₁₀ was added and the cells were incubated o/n. Fixing of the cells involved removing the medium and replacing it with 1ml of chilled (-20°C) methanol for a minimum of 30 min or until required for staining.

2.6.2 Staining

All subsequent steps were carried out in a humidified chamber at rt. Firstly all antibodies were diluted in solution A, (PBS complete containing 0.05% Tween 20 and 5% NBCS) and incubated on ice. (NB: for all double labelling experiments the 2 antibodies were mixed at this stage, prior to addition to the coverslips). Meantime, each coverslip was incubated in solution A for 10 min. It was then drained and 50µl of the primary antibody added for a 45 min. The coverslips were carefully washed by 3x 10 sec washes in solution A. The secondary antibody (50µl), containing the dye conjugate, was reacted for a further 45 min. Again a series of washing steps ensued consisting of 5x 10 sec washes in solution A and 2x rinses in deionised water. The coverslips were then drained and mounted on glass microscope slides in Citifluor and sealed using clear nail varnish.

The slides were stored at 4°C wrapped in tin foil until required for viewing using a Zeiss Axioplan fluorescence microscope and photographed on Kodak Ektachrome Elite 400 film.

2.7 Microscopic Analysis of Capsids

2.7.1 Electron Microscopic Examination of Capsids

To confirm the integrity of capsids, they were examined under the electron microscope by negative staining. Approximately 2µl of a capsid preparation was allowed to absorb

onto parlodion-coated microscope grids. They were then negatively stained with 1% phosphotungstic acid and drained, before being air-dried and examined with a JEOL 100S electron microscope.

2.7.2 Cryo-Electron Microscopy Examination of Capsids

All Cryo-EM analysis and 3D image reconstructions were performed by collaborators: Dr Wah Chiu and Dr Z Hong Zhou at The Baylor College of Medicine, Houston, Texas, USA.

Details of the method of data processing can be found in Zhou *et al* (1998b).

2.8 Quantification of Proteins

Protein concentrations were quantified in 2 ways:

(i) using a standard Bradford Assay as described in 'Bio-Rad Protein Assay Instruction Manual'. Protein concentrations were calculated against protein standards prepared with BSA.

(ii) by measuring OD values at A_{280} and calculating the amount of protein in mg/ml using the following calculation:

$$\frac{\text{Extinction Coefficient}}{Mr} = \frac{A_{280}}{X \text{ (protein concentration, mg/ml)}}$$

2.9 Sizing of Proteins

Proteins were sized using fast phase liquid chromatography (FPLC) on a Akta Purifier (Pharmacia) using a Superdex 75 column. Basically, the column was equilibrated with equilibration buffer o/n. The protein was injected at 0.2mg/ml in a volume of 200 μ l. The samples were passed through the column at a flow rate of 1ml/min and protein detected at 280nm. The resulting peaks were calibrated against known protein standards.

2.10 Enzyme Linked Immunosorbent Assay (ELISA)

Wells of a flat bottomed microtitre plate (Dynatech), were coated at 37°C o/n with the primary antigen (see Results, Chapter 5 for concentrations). All the recipes for buffers and solutions are detailed in Section 1.11. The plates were washed 5x with wash solution and blocked with 200µl of blocking buffer for 1h at 37°C. Again the plates were washed 5x in wash buffer and the secondary antigen added in the presence or absence of an inhibitory peptide. After incubation at rt for at least 1h, the plates were washed 5x in wash solution and 50µl of the primary antibody, in PBS, allowed to react at 37°C for 1h. After washing 5x with wash solution, 50µl of the secondary antibody (usually GAM-HRP, in PBS) was added for 1h at 37°C. Extensive washing followed (10x in wash solution) and 100µl of the signal developer (supplied by Kindergaard & Perry Laboratories) was added. After 15-30 min of colour development, the A_{405} was read on a Multiskan plate reader (Titrtrek; ICN Biomedicals). In most cases the results are duplicate determinations and the background A_{405} was determined by adding developer alone to the plate. This value was subtracted from final the readings.

2.11 Epitope Mapping by SPOTscan

The SPOTs procedure was performed using the SPOTscan kit (supplied by Pharmacia). The protocol in the kit was followed and is summarised in steps (i) -(vi).

(i) Generation of Pipetting Schedule

The desired sequence was entered into the SPOTscan programme on the PC together with the required peptide length and overlay for each SPOT. A pipetting and amino acid weighing schedule was automatically generated.

(ii) Peptide Synthesis

Each F-moc amino acid solution was weighed and dissolved in NMP (1-methyl-2-pyrrolidinone). 1µl of the appropriate amino acid was added to each SPOT on the membrane, in a duplicate cycle, to double couple the reaction. Incubation at rt for 15 min followed each cycle.

(iii) Washing Steps

Upon the completion of each amino acid cycle, the membrane was bathed in a series of chemicals at rt:

- DMF - 2 min, to remove unbound amino acids and couple the reaction
- acetic anhydride - 5-10 min, to block any free amino acid groups that had not yet coupled
- DMF - 2 min, wash
- 20% piperidine in DMF - 5 min, deprotects ie exposes site ready for the addition of the next amino acid in the chain
- DMF - 2x 2 min, wash
- 1% bromophenol blue in DMF - added until SPOTs are restained for the next cycle (approximately 10 min)
- methanol - 2 min, final wash

The membrane was air dried and either, the next cycle begun immediately, or the membrane was stored at -20°C.

(iv) Side Chain Deprotection

If all the cycles had been completed, side chain deprotection was performed by a series of washing steps at rt:

- DCM:TFA:TBS (1:1:0.002) - 1h.
- DCM - 4x 2 min
- DMF - 3x 2 min
- methanol - 4x 2 min

The membrane was allowed to air dry.

Deprotection was carried out immediately preceding the antibody assay.

(v) Antibody Assay

The antibody assay was performed by first washing the membrane in TBS (2x 10 min). The membrane was then blocked with SPOTs Blocking Buffer (BB) (10% BB in T-TBS) o/n at rt. The membrane was washed (2x 5 min) in T-TBS and the test antibody added at the optimal concentration (see Results, Chapter 3), for 3-4h. Washing (2x 5 min in T-TBS) preceded addition of the secondary GAM antibody (1:100), conjugated to HRP, for 2h. After 2x 10 min washes in T-TBS, the kit signal developer was added until a colour reaction developed.

(vi) Regeneration of SPOTs membrane

The SPOTs membrane could be stripped and re-probed with antibody. First the membrane was washed in 2x dH₂O, 2x DMF and 2x dH₂O, for 5 min intervals. Regeneration Buffer A (Section 1.11) was added for 3x 30 min. Regeneration Buffer B (Section 1.11) was then added for 3x 10 min. The membrane was rinsed in methanol, air dried and either re-probed immediately, or, stored at -20°C until required.

2.12 Purification of Antibody Supernatant by Ammonium Sulphate Precipitation

Antibody supernatant was mixed at 4°C with ammonium sulphate at 1.56g/ml, for 20 min. The solution was spun at 10000 rpm (GSA rotor) for 10 min and the pellet resuspended in sodium phosphate buffer at 25% of the starting volume. The solution was dialysed o/n against the sodium phosphate buffer at 4°C and the purified antibody was stored at -20°C until required.

1. Introduction

Capsid assembly is known to occur in the nucleus of infected cells however, understanding the mechanism of assembly requires analysis of how the individual capsid proteins interact with each other. Immunofluorescence labelling is a very powerful technique to study the capsid protein-protein interactions. Nicholson *et al* (1994) had previously shown by fluorescence microscopy that VP5 and VP23 failed to localise efficiently to the nucleus either alone or in combination. This suggested that neither of these proteins have an intrinsic nuclear localisation signal. When VP5 was co-expressed with preVP22a it was efficiently transported to the nucleus, but the distribution of VP23 was unaffected.

To form a more complete picture of capsid protein-protein interactions this study undertook to utilise a plasmid based system to monitor the interactions of VP19c and VP26 with VP5, preVP22a and VP23.

The results of extensive immunofluorescence studies (Rixon *et al*, 1996) are detailed in this chapter and pulled together with other published literature to draw conclusions about the way in which the capsid proteins interact with each other.

2. Construction of Expression Plasmids

2.1 VP23, VP5 and preVP22a

Plasmids expressing VP23 (pE18) or VP5 (pE19) were made by P Nicholson and a plasmid expressing preVP22a (pJK2) was made by J Kennard. Cloning of these capsid genes is fully described in Nicholson *et al* (1994).

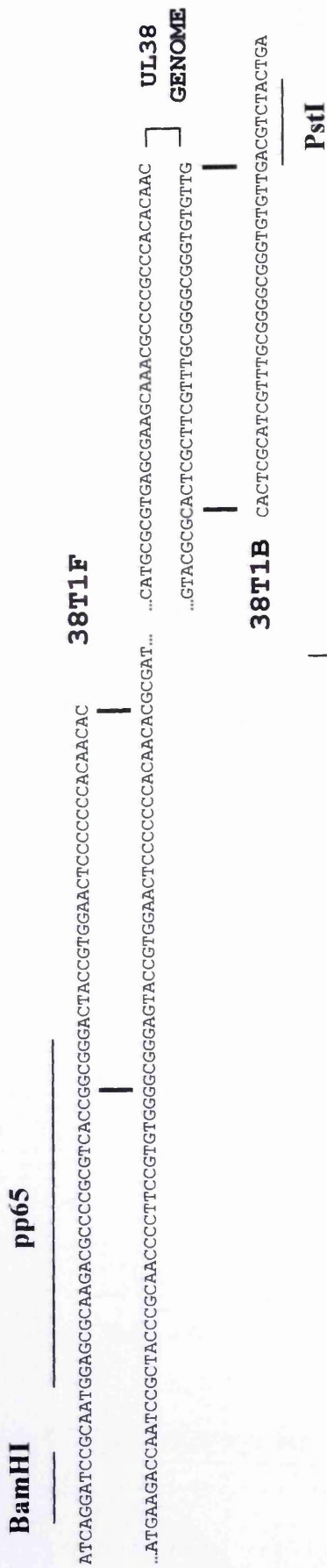
2.2 VP19c and VP26

The UL38 ORF expressing VP19c was cloned from pBJ182 (Nicholson *et al*, 1994) into pCMV10 (Stow *et al*, 1993) as a BamHI/HindIII fragment to generate pE38.

The UL35 ORF expressing VP26 was made as a PCR product, KpnI/BamHI digested and ligated into the similarly digested pUC19 to generate pUCUL35. This was

Figure 3.1: Construction of pE38T1

(i) Oligonucleotides 38T1F and 38T1B



(BamHI/PstI)

(ii) pCMV10 (BamHI/PstI)

ligate

(iii) pE38T1

Figure 3.1: Two primers, 38T1F and 38T1B, were used to generate a PCR fragment encoding the UL38 ORF with the pp65 epitope tag at the N-terminus [panel (i)]. The complementary residues to the UL38 ORF are indicated by the vertical lines. The PCR product was BamHI/PstI digested and ligated with BamHI/PstI digested pCMV10 (ii). This resulted in the formation of pE38T1 (iii), where the N-terminal 15 amino acids of VP19c were replaced by 11 amino acids including the pp65 epitope tag.

EcoRI/BamHI digested to release the UL35 ORF and cloned into EcoRI/BamHI digested pCMV10 to generate pE35.

Both pE38 and pE35 were made by J Tatman and are fully described in Tatman *et al* (1994).

2.3 Epitope Tagged Versions of VP19c, VP5 and VP26

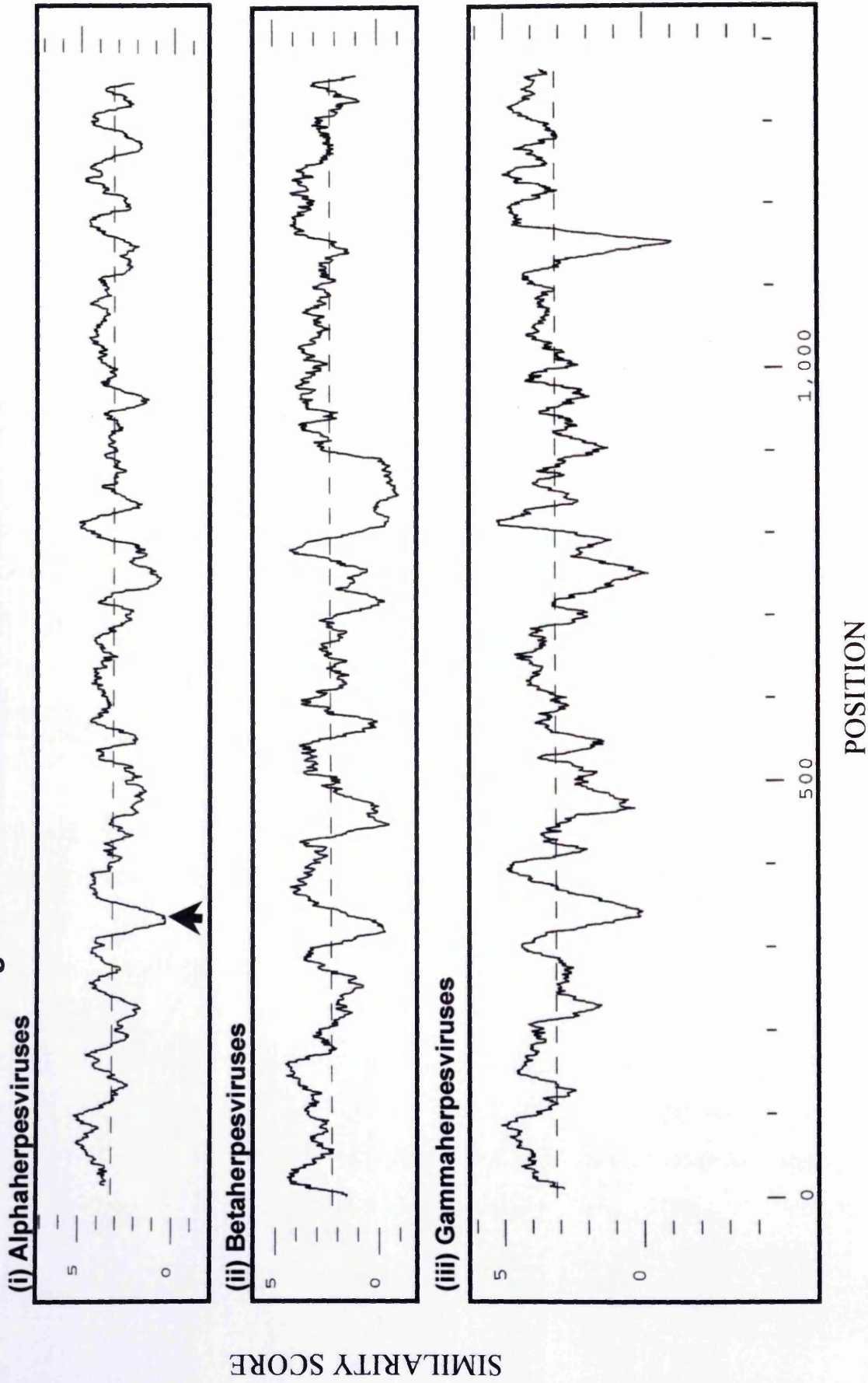
Good antibodies against some of the capsid proteins, in particular VP26 and VP19c, were lacking. Also the epitope sites of the available capsid protein antibodies had not been mapped and so it was not possible to gauge if the antibody would interact with any deletion mutants, where only portions of the protein were expressed. In view of these points, an epitope tag was cloned into VP5, VP19c and VP26. A number of tag-antibody combinations were available. In the following experiments the HCMV pp65 epitope tag (McLauchlan *et al*, 1994) was used and shall be referred to as pp65. Studies with this tag and several HSV proteins had shown that the antibody did not cross react with any HSV proteins and that this epitope on its own did not confer nuclear localisation on the host protein (McLauchlan *et al*, 1994). In addition, an attempt was made to produce my own tag, using an anti-CAT antibody. This is detailed in Section 5.

2.3.1 VP19c

To insert an epitope tag into VP19c, two primers, 38T1F and 38T1B, were made. 38T1F corresponded to bases 40-73 of UL38 ORF (84570-84603 on the sequence of McGeoch *et al*, 1988). 38T1B was complementary to 31 bases of UL38 ORF (85925-85955) and contained a PstI site at its 5' end [figure 3.1, panel (i)].

The two primers were used to generate a PCR product where VP19c had 15 amino acids removed and replaced with 11 amino acids containing the sequence for the pp65 epitope. The product was cloned as a BamHI/PstI fragment into BamHI/PstI digested pCMV10 to generate pE38T1 [figure 3.1, panels (ii) and (iii)]. This was made by A McGregor (Rixon *et al*, 1996).

Figure 3.2: Consensus Predictions for VP5



VP5 (100 amino acids) of HSV-1, PRV, VZV, HCMV, HHV-6, EBV, EHV-2 and HVS.

Sequence alignment was performed using the GCG plot similarity programme.

This indicated the location of a poorly conserved area between positions 300 and 400.

VP5 (100 amino acids) of HSV-1, PRV, VZV, HCMV, HHV-6, EBV, EHV-2 and HVS.

3.2. VP5

VP5 (100 amino acids) of HSV-1, PRV, VZV, HCMV, HHV-6, EBV, EHV-2 and HVS.

Sequence alignment was performed using the GCG plot similarity programme.

This indicated the location of a poorly conserved area between positions 300 and 400.

VP5 (100 amino acids) of HSV-1, PRV, VZV, HCMV, HHV-6, EBV, EHV-2 and HVS.

Sequence alignment was performed using the GCG plot similarity programme.

This indicated the location of a poorly conserved area between positions 300 and 400.

VP5 (100 amino acids) of HSV-1, PRV, VZV, HCMV, HHV-6, EBV, EHV-2 and HVS.

Sequence alignment was performed using the GCG plot similarity programme.

This indicated the location of a poorly conserved area between positions 300 and 400.

VP5 (100 amino acids) of HSV-1, PRV, VZV, HCMV, HHV-6, EBV, EHV-2 and HVS.

Sequence alignment was performed using the GCG plot similarity programme.

This indicated the location of a poorly conserved area between positions 300 and 400.

VP5 (100 amino acids) of HSV-1, PRV, VZV, HCMV, HHV-6, EBV, EHV-2 and HVS.

Sequence alignment was performed using the GCG plot similarity programme.

This indicated the location of a poorly conserved area between positions 300 and 400.

VP5 (100 amino acids) of HSV-1, PRV, VZV, HCMV, HHV-6, EBV, EHV-2 and HVS.

Sequence alignment was performed using the GCG plot similarity programme.

This indicated the location of a poorly conserved area between positions 300 and 400.

VP5 (100 amino acids) of HSV-1, PRV, VZV, HCMV, HHV-6, EBV, EHV-2 and HVS.

Sequence alignment was performed using the GCG plot similarity programme.

This indicated the location of a poorly conserved area between positions 300 and 400.

VP5 (100 amino acids) of HSV-1, PRV, VZV, HCMV, HHV-6, EBV, EHV-2 and HVS.

Sequence alignment was performed using the GCG plot similarity programme.

This indicated the location of a poorly conserved area between positions 300 and 400.

VP5 (100 amino acids) of HSV-1, PRV, VZV, HCMV, HHV-6, EBV, EHV-2 and HVS.

Sequence alignment was performed using the GCG plot similarity programme.

This indicated the location of a poorly conserved area between positions 300 and 400.

VP5 (100 amino acids) of HSV-1, PRV, VZV, HCMV, HHV-6, EBV, EHV-2 and HVS.

Sequence alignment was performed using the GCG plot similarity programme.

This indicated the location of a poorly conserved area between positions 300 and 400.

Figure 3.2: The GCG plot similarity programme was used to generate consensus predictions of VP5 between Alpha herpesviruses (HSV-1, EHV-1, PRV and VZV), panel (i), Beta herpesviruses (HCMV and HHV-6), panel (ii), and Gamma herpesviruses (EBV, EHV-2 and HVS), panel (iii). A poorly conserved area, in all 3 subfamilies of herpesvirus, was detected between position 300 and 400. An XhoI site fell within this region in HSV-1 and its approximate position is marked with an arrow [panel (i)].

F Rixon had shown that tagged VP19c (pE38T1) could be substituted for wt VP19c to form phenotypically normal capsids in the baculovirus system (personal communication). This indicated that the presence of the epitope tag not did affect the normal behaviour of VP19c and prevent it forming normal interactions with other capsid proteins.

2.3.2 VP5

To perform all subsequent cloning steps with both VP5 and VP26, it was necessary to remove the EcoRI site from an altered form of pCMV10, designated pCMV10Bgl and fully described in Nicholson *et al* (1994). Removal of the EcoRI site was done by restriction enzyme digest followed by filling in the overhanging ends with large fragment polymerase and ligating to produce pCMV10BglΔEco.

2.3.2.1 Cloning into pCMV10BglΔEco

The UL19 ORF was isolated from pJN6 (Nicholson *et al*, 1994) as a BglII fragment and ligated into BglII digested pCMV10BglΔEco to generate pE19Bgl, see figure 3.3, panel (i).

2.3.2.2 pp65 Epitope Tagged N- and C- Terminal Deletions of pE19Bgl

VP5 is reasonably well conserved between alpha herpesviruses. However, there is an area, approximately 300-400 amino acids from the N-terminus of the protein, which has very low homology, being variable in both sequence and length [figure 3.2, panel (i)]. This area of low homology is also found in the beta [figure 3.2, panel (ii)] and gamma [figure 3.2, panel (iii)] herpesvirus consensus. It was felt that this poorly conserved region would be the best place to insert an epitope tag into VP5, as it was probable that the precise sequence of this region was not important for the structural integrity of the protein. In order to insert the pp65 epitope tag this area, it was decided to first produce two terminal deletions, insert the appropriate enzyme sites and tag sequence using oligonucleotides and reconstruct the full-length VP5 protein.

(i) C-terminal deletion

To produce a C-terminal deletion, use was made of the XhoI site located in the poorly conserved area [see figure 3.2, panel (i)]. pE19Bgl was XhoI/XbaI digested to remove the C-terminal 3181 bp sequences. This was replaced by two partially complementary

Figure 3.3: Construction of pSJM19N65 and pSJM19C65

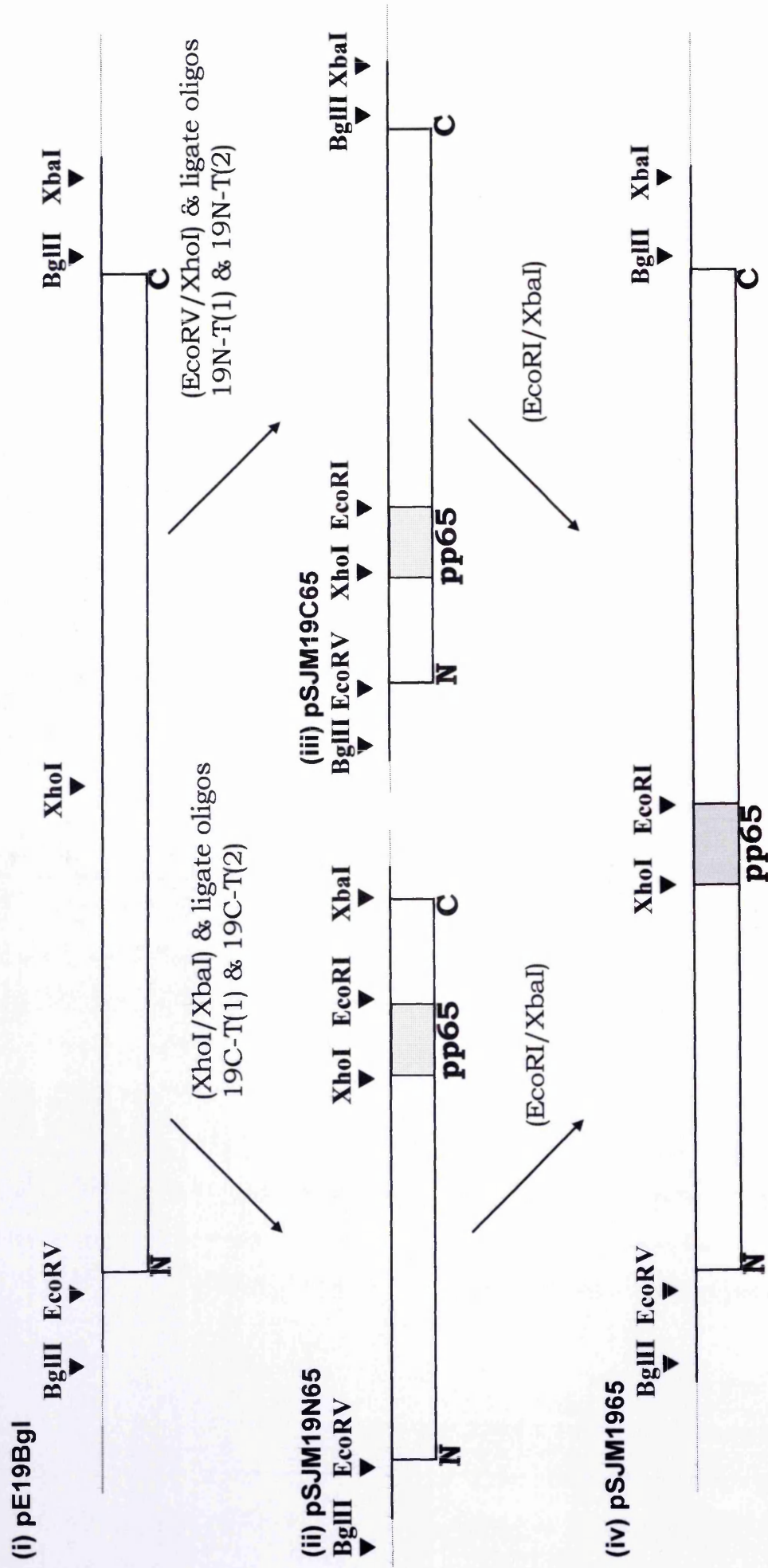


Figure 3.3: This figure details the cloning strategy employed to create pp65 epitope tagged versions of N- and C- terminal deletions of VP5 and a full-length pp65 tagged VP5. pE19Bgl [panel(i)] was first XhoI/XbaI digested, to remove the C-terminal sequences, and religated with two partially complementary oligonucleotides, 19C-T(1) and 19C-T(2) (figure 3.4). This generated the N terminal portion of UL19 with the pp65 epitope tag inserted at the C-terminus, designated pSJM19N65 [panel (ii)]. Similarly, pE19Bgl [panel(i)] was EcoRV/XhoI digested, to remove the N-terminal sequences, and religated with two partially complementary oligonucleotides, 19N-T(1) and 19N-T(2) (figure 3.5). This generated the C terminal portion of UL19 with the pp65 epitope tag inserted at the N-terminus, designated pSJM19C65 [panel (iii)].

To create full-length UL19, encoding the pp65 tag, pSJM19N65 [panels (ii) and pSJM19C65, panel (iii)] were EcoRI/XbaI digested. The fragment from pSJM19C65, containing the C-terminal portion of UL19, was purified and ligated with purified pSJM19N65, containing the N-terminal portion of the fragment plus the vector. This reconstructed full-length UL19 with pp65 at an internal site, designated pSJM1965 [panel(iv)].

Note, the diagrams are not drawn to scale

Figure 3.4: Sequence of Oligonucleotides 19C-T(1) and 19C-T(2)

<u>XhoI</u>	<u>EcoRI</u>											
TCGAGCGCAAGACGCCCCGCGTCACCGGCGGAATTCAGTAGT		19C-T(1)										
CGCGTTCTGCGGGGCGCAGTGGCCGCCTTAAGTCATCAGATC		19C-T(2)										
<table border="1" style="display: inline-table; border-collapse: collapse;"> <tr> <td>E</td><td>R</td><td>K</td><td>T</td><td>P</td><td>R</td><td>V</td><td>T</td><td>G</td><td>G</td> </tr> </table> I Q * <u>XbaI</u>		E	R	K	T	P	R	V	T	G	G	
E	R	K	T	P	R	V	T	G	G			

Figure 3.5: Sequence of Oligonucleotides 19N-T(1) and 19N-T(2)

<u>EcoRV</u>	<u>XhoI</u>	<u>EcoRI</u>													
ATCGCAATGCTCGAGCGCAAGACGCCCCGCGTCACCGGCGGAATTCAGG			19N-T(1)												
TAGCGTTACGAGCTCGCGTTCTGCGGGGCGCAGTGGCCGCCTTAAGTCCAGCT			19N-T(2)												
<table border="1" style="display: inline-table; border-collapse: collapse;"> <tr> <td>M</td><td>L</td><td>E</td><td>R</td><td>K</td><td>T</td><td>P</td><td>R</td><td>V</td><td>T</td><td>G</td><td>G</td> </tr> </table> I Q <u>ΔXho</u>		M	L	E	R	K	T	P	R	V	T	G	G		
M	L	E	R	K	T	P	R	V	T	G	G				

Figure 3.4: This figure details the base pair and amino acid sequences which make up oligonucleotides 19C-T(1) and 19C-T(2). These oligonucleotides are for inserting the pp65 epitope tag (shown in the rectangle) at the C-terminus of XhoI/XbaI digested pE19Bgl, to generate pSJM19N65.

Figure 3.5: This figure details the base pair and amino acid sequences which make up oligonucleotides 19N-T(1) and 19N-T(2). These oligonucleotides are for inserting the pp65 epitope tag (shown in the rectangle) at the N-terminus of EcoRI/XhoI digested pE19Bgl, to generate pSJM19C65. This insertion results in the destruction of the original XhoI site (ie Δ XhoI) and the generation of a new XhoI site.

Figure 3.6: Construction of pE35T1

(i) Oligonucleotides 35PCR (1) and 35PCR (2)

EcoRI

GACAGAAATTCAGGCCGTCCCGCAATTTCACCGC |

35PCR (1)

ATGGCCCGTCCCGCAATTTCACCGCCCGCAGCA.....

UL35
GENOME

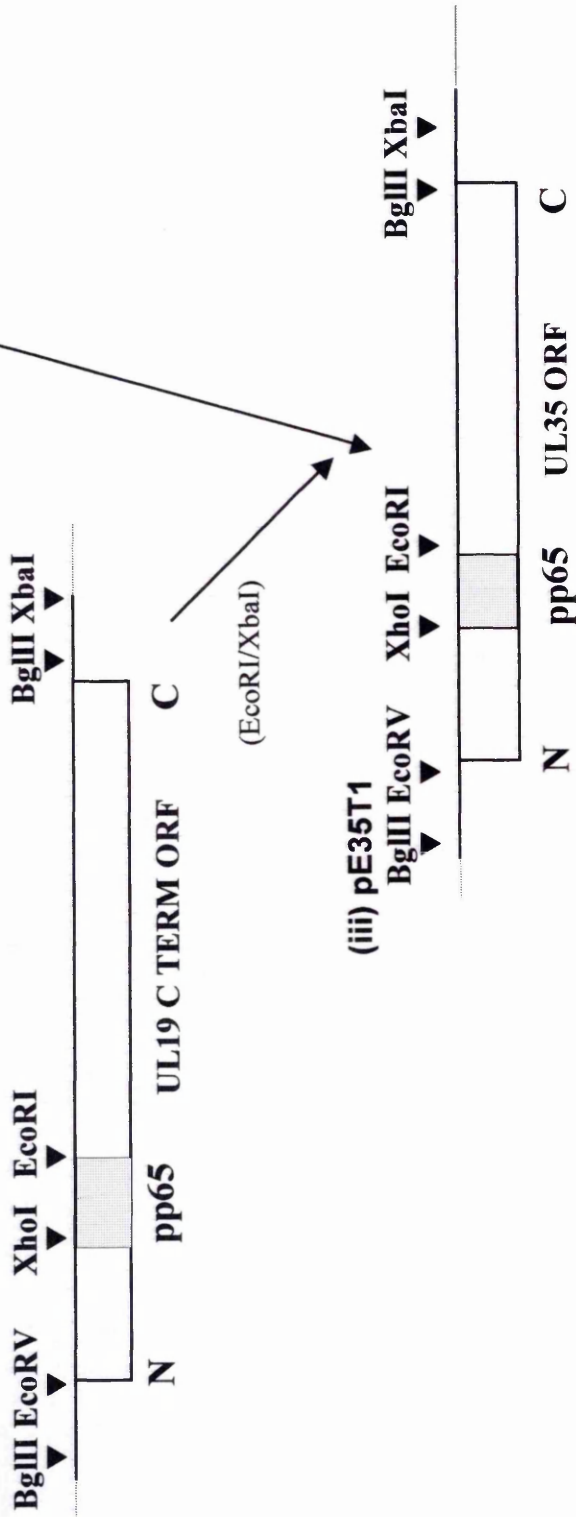
.....GGGGCACTCCGGCCCTCAAGGAAAGACCCCAAA

35PCR (2)

CCCTCAAGGAAGACCCCAAGATCTACAG

|
XbaI

(ii) pSJM19C65



(iii) pE35T1

BglIII EcoRV XhoI EcoRI

BglIII XbaI

N

pp65

UL35 ORF

C

oligonucleotides, 19C-T (1) and 19C-T (2) (figure 3.4), which also contained a stop codon and generated pSJM19N65 [figure 3.3, panel (ii)]. This construct contains the pp65 epitope tag sequences, linked to the 5' 350 amino acids of the UL19 ORF. This generated a protein with the pp65 epitope at the C-terminus of the N-terminal 1070 amino acids of VP5.

(ii) N-terminal deletion

To produce an N-terminal deletion, use was again made of the XhoI site discussed previously. pE19Bgl was XhoI/EcoRV digested to remove the N-terminal 1123 bp sequences. This was replaced by two partially complementary oligonucleotides which destroyed the existing XhoI site and inserted a new one. These oligonucleotides, 19N-T (1) and 19N-T (2) (figure 3.5), also contained a start codon and generated pSJM19C65 [figure 3.3, panel (iii)]. This construct contains the pp65 epitope tag sequences, linked to the 3' 2961 nucleotides of the UL19 ORF. This generated a protein with the pp65 epitope at the N-terminus of the C-terminal 987 amino acids of VP5.

2.3.2.3 *pp65 Tagged Full-length VP5*

The complete UL19 ORF containing the pp65 epitope tag was reconstructed by ligating the N- and C- terminal portions together [see figure 3.3, panel (iv)]. Firstly both pSJM19C65 and pSJM19N65 were EcoRI/XbaI digested and the appropriate fragments gel purified. The C-terminal portion released from pSJM19C65 (ie the smaller fragment consisting of 3100 bp) was ligated with the N-terminus plus the vector fragment from pSJM19N65 (ie the larger fragment consisting of 4300 bp). This generated pSJM1965 which contained the complete UL19 ORF with the pp65 epitope tag linked in frame at nucleotide 1070.

2.3.3 **VP26**

pSJM19C65 was used as a starting point for cloning VP26. The UL35 ORF was generated as a PCR product using oligonucleotides, 35PCR (1) and 35PCR (2), as primers [see figure 3.6, panel (i)].

- 35PCR (1) corresponds to bases 4-25 of the UL35 ORF (McGeoch *et al*, 1988) and incorporates an EcoRI site at the 5' end which is in the same frame as that in pSJM19C65.
- 35PCR (2) contains a XbaI site at its 5' end and is complementary to 20 bases downstream from the UL35 termination codon, between 70912-70932.

The UL35 PCR fragment was EcoRI/XbaI digested, gel purified and cloned into gel purified EcoRI/XbaI digested pSJM19C65 [figure 3.6, panel (ii)] to give pE35T1 [figure 3.6, panel (iii)]. This generated VP26 tagged with the pp65 tag at its N-terminus.

3. Intracellular Distribution of Capsid Proteins

Immunofluorescence was performed on BHK C13 cells as described in Methods, Section 2.6. To examine the intracellular distributions of proteins, a series of antibodies were used (see Materials, Section 1.10):

- LP12 for VP5 at 1:200 dilution
 - 1060 for VP23 at 1:200 dilution
 - 5010 for preVP22a at 1:100 dilution
 - pp65 for pp65 epitope tagged clones at 1:300 dilution
 - 5/24 supernatant for CAT208 epitope tagged clones at 1:32 dilution
- } mouse
-
- CAT208 for CAT208 epitope tagged constructs at 1:10, 1:100, 1:500 dilutions
 - 20999 for preVP22a at 1:50 dilution
- } rabbit
-
- FITC-GAM an anti-mouse antibody at 1:100 dilution
 - TRITC-GAR an anti-rabbit antibody at 1:100 dilution
 - GAM-HRP an anti-mouse antibody at 1:100 dilution
- } secondary antibody

Figure 3.7: Intracellular Distribution of VP19c



Figure 3.7: Cells were transfected with plasmid pE38T1 (VP19cpp65) and detected using the primary antibody, pp65 (1:300). Protein was visualised with FITC-GAM antiserum (1:100). VP19cpp65 was detected in the nuclei.

Magnification = x200

Figure 3.8: Intracellular Distribution of VP23 and VP5 Alone

(i)



(ii)



(iii)

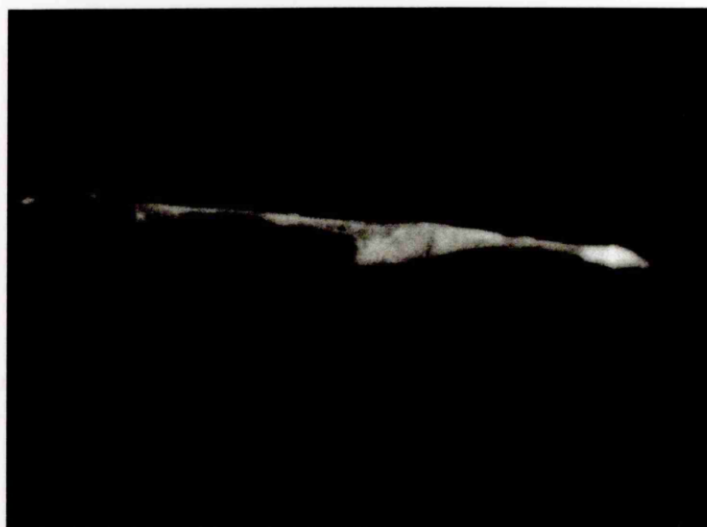


Figure 3.8: Cells were transfected with plasmids pE18 (VP23) [panel (i)], pE19 (VP5) [panel (ii)] or, pSJM1965 (VP5pp65) [panel (iii)]. The distribution of VP23 was detected using the primary antibody 1060 (1:200), with VP5 and VP5pp65 detected with LP12 (1:200) and pp65 (1:300) respectively. Proteins were visualised with FITC-GAM antiserum (1:100) and all were detected throughout the cell.

Magnification = panel (i) and panel (ii) x80
 panel (iii) x260

Figure 3.9: Redistribution of VP5 and VP23 by VP19c

(i)



(ii)

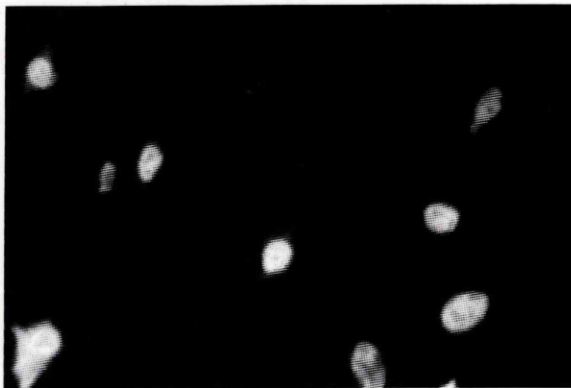
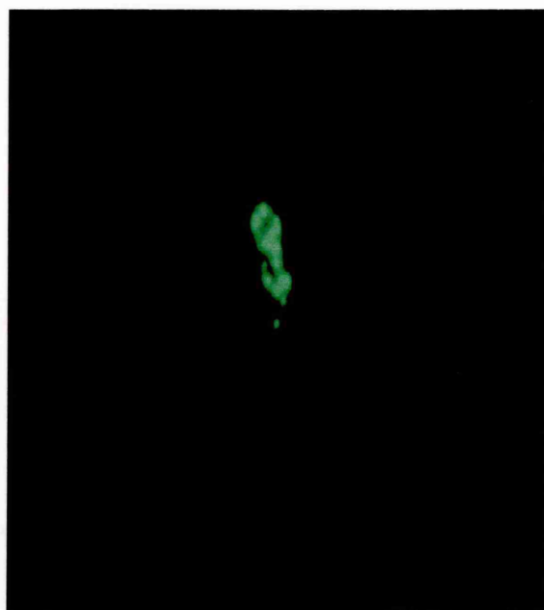


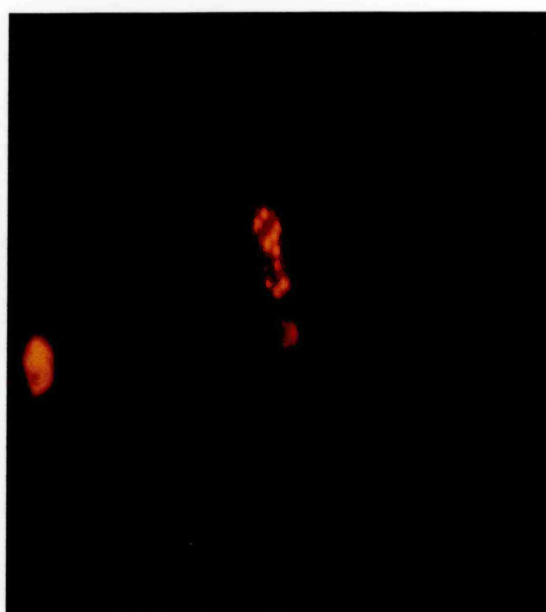
Figure 3.9: Cells were co-transfected with plasmid pE38T1 (VP19cpp65) and either pE19 (VP5) [panel (i)] or pE18 [panel (ii)]. The distribution of VP5 was detected using the primary antibody LP12 (1:200) with VP23 detected with 1060 (1:200). Proteins were visualised with FITC-GAM (1:100) and were detected in the nucleus in each case.

Figure 3.10: Redistribution of VP5pp65 to the Nucleus by preVP22a

(i)



(ii)



3.1 Distribution of VP2a:

As there was no evidence of VP2a in the cytoplasm of the cells, it is likely that the protein is localised to the nucleus.

3.2 Influence of VP2a on VP5pp65:

The data suggest that the presence of VP2a in the nucleus is essential for the localisation of VP5pp65 to the nucleus. In the absence of VP2a, VP5pp65 is localised to the cytoplasm.

Figure 3.10: Cells were co-transfected with pSJM1965 (VP5pp65) and pJK2 (preVP22a). Panels (i) and (ii) represent duplicate exposures of a single field. The distribution of VP5pp65 was detected using the primary antibody, pp65 (1:300) and preVP22a was detected with antibody 20999 (1:100). VP5pp65 was visualised with FITC-GAM (1:100) [panel (i)] and preVP22a was visualised with TRITC-GAR (1:100) [panel (ii)]. The proteins co-localised to the nucleus.

Magnification = x200

3.1 Distribution of VP19c

As there was no antibody against VP19c, the epitope tagged version pE38T1 was used in fluorescence studies. Following transfection and staining, VP19c was found to be localised predominantly in the nucleus of infected cells (figure 3.7).

3.2 Influence of VP19c on the Distribution of VP5 and VP23

Previous authors had shown that when VP5 and VP23 were expressed singly or co-transfected in combination, they were seen distributed throughout the cell (Nicholson *et al.*, 1994). The distribution patterns observed previously for the two proteins was confirmed in this study [figure 3.8, panels (i) and (ii)], which also showed that the pp65 tag did not alter the distribution of VP5 [figure 3.8, panel (iii) shows a representative example]. To monitor the effect of the influence of VP19c on the distribution of these two proteins, several co-localisation experiments were carried out.

3.2.1 VP19c + VP5

When pE38 (VP19c) or pE38T1 (VP19cpp65) was co-transfected with pE19(VP5), VP5 localised to the nucleus. VP5 was observed with a distinctive punctate pattern [figure 3.9, panel (i)], indicating that the proteins had aggregated in the nucleus of infected cells. Exactly the same pattern of interaction was observed when pSJM1965 was co-transfected with pE38 (not shown).

3.2.2 VP19c + VP23

When pE38 (VP19c) or pE38T1 (VP19cpp65) was co-transfected with pE18 (VP23), like VP5, the VP23 localised to the nucleus. However, in contrast to the pattern observed with VP5, VP23 was uniformly distributed throughout the nucleus, although absent from the nucleoli [figure 3.9, panel (ii)].

3.3 Influence of preVP22a on the Distribution of VP5

Nicholson *et al.* (1994) had shown that when VP5 was co-expressed with preVP22a, the VP5 co-localised to the nucleus with the preVP22a protein. A similar transfection was performed using pSJM1965 (VP5pp65). pSJM1965 was co-transfected with pJK2 (preVP22a) and both proteins were found to be localised to the nucleus [see figure 3.10, panels (iii) and (iv)] confirming the data obtained by Nicholson *et al.*

Figure 3.11: Intracellular Distribution of VP26

(i)



(ii)



(iii)



Figure 3.11: Cells were either infected singly with plasmid pE35T1 (VP26pp65) [panel (i)] or, co-transfected with pJK2 (preVP22a) [panels (ii) and (iii) represent duplicate exposures of a single field]. The distribution of VP26pp65 was detected using the primary antibody, pp65 (1:300), with preVP22a detected with 20999 (1:100). VP26pp65 was visualised with FITC-GAM (1:100) [panels (i) and (ii)] and was detected predominately in the cytoplasm in each case. preVP22a was visualised with TRITC-GAR (1:100) [panel (iii)] and was detected in the nucleus.

Magnification = x200

Figure 3.12: Redistribution of VP26 to the Nucleus

(i)



(ii)



(iii)



3.4 Distribution of VP26

3.4.1 Co-transfection of VP26pp65

3.4.1.1 Co-transfection of VP26pp65 with preVP22a

3.4.1.2 Co-transfection of VP26pp65 with VP19c

3.4.1.3 Co-transfection of VP26pp65 with VP5

3.4.1.4 Co-transfection of VP26pp65 with VP5 and preVP22a

3.4.1.5 Co-transfection of VP26pp65 with VP5 and VP19c

3.4.1.6 Co-transfection of VP26pp65 with VP5 and VP19c

3.4.1.7 Co-transfection of VP26pp65 with VP5 and VP19c

3.4.1.8 Co-transfection of VP26pp65 with VP5 and VP19c

3.4.1.9 Co-transfection of VP26pp65 with VP5 and VP19c

3.4.1.10 Co-transfection of VP26pp65 with VP5 and VP19c

3.4.1.11 Co-transfection of VP26pp65 with VP5 and VP19c

3.4.1.12 Co-transfection of VP26pp65 with VP5 and VP19c

3.4.1.13 Co-transfection of VP26pp65 with VP5 and VP19c

3.4.1.14 Co-transfection of VP26pp65 with VP5 and VP19c

3.4.1.15 Co-transfection of VP26pp65 with VP5 and VP19c

3.4.1.16 Co-transfection of VP26pp65 with VP5 and VP19c

3.4.1.17 Co-transfection of VP26pp65 with VP5 and VP19c

3.4.1.18 Co-transfection of VP26pp65 with VP5 and VP19c

3.4.1.19 Co-transfection of VP26pp65 with VP5 and VP19c

3.4.1.20 Co-transfection of VP26pp65 with VP5 and VP19c

3.4.1.21 Co-transfection of VP26pp65 with VP5 and VP19c

3.4.1.22 Co-transfection of VP26pp65 with VP5 and VP19c

3.4.1.23 Co-transfection of VP26pp65 with VP5 and VP19c

3.4.1.24 Co-transfection of VP26pp65 with VP5 and VP19c

3.4.1.25 Co-transfection of VP26pp65 with VP5 and VP19c

3.4.1.26 Co-transfection of VP26pp65 with VP5 and VP19c

3.4.1.27 Co-transfection of VP26pp65 with VP5 and VP19c

3.4.1.28 Co-transfection of VP26pp65 with VP5 and VP19c

3.4.1.29 Co-transfection of VP26pp65 with VP5 and VP19c

3.4.1.30 Co-transfection of VP26pp65 with VP5 and VP19c

3.4.1.31 Co-transfection of VP26pp65 with VP5 and VP19c

3.4.1.32 Co-transfection of VP26pp65 with VP5 and VP19c

3.4.1.33 Co-transfection of VP26pp65 with VP5 and VP19c

Figure 3.12: Cells were co-transfected with plasmid pE35T1 (VP26pp65) with either pE19 (VP5) and pJK2 (preVP22a) [panels (i) and (ii) represent duplicate exposures of a single field] or, pE19 (VP5) and pE38 (VP19c) [panel (iii)]. The distribution of VP26pp65 was detected using the primary antibody, pp65 (1:300), with preVP22a detected with 20999 (1:100). VP26pp65 was visualised with FITC-GAM (1:100) [panels (i) and (iii)] and was detected in the nucleus in each case. preVP22a was visualised with TRITC-GAR (1:100) [panel (ii)] and detected in the nucleus.

Magnification = x200

3.4 Distribution of VP26

J Tatman had previously shown that when VP26, expressed from pE35, was detected with an anti-VP26 rabbit antibody, trpE-UL35, the protein was present throughout the entire cell, predominantly in the cytoplasm (Tatman, 1996). This indicated that the protein had no nuclear targeting signal. This contrasts strongly with the exclusively nuclear localisation observed by McNabb and Courtney (1992) using the same antibody on HSV infected cells.

When VP26 (pE35T1) containing the pp65 epitope tag was transfected singly into cells and detected with the pp65 mouse monoclonal antibody, it was found to be distributed throughout the cell but, predominately in the cytoplasm, confirming the data of Tatman [figure 3.11, panel (i)]. This showed that the epitope tag did not interfere with normal protein expression and behaviour.

3.4.1 Influence of Other Capsid Protein on the Distribution of VP26

VP26pp65 (pE35T1) did not change its distribution when it was co-transfected with any one of the other capsid proteins; VP23, VP5, VP19c or preVP22a. Figure 3.11 shows a typical example of the pattern observed, with VP26 found predominately in the cytoplasm and preVP22a localised to the nucleus [panels (ii) and (iii) respectively].

Since VP5, VP23 and VP26 all had very similar distribution patterns, it was impossible to determine, from this experiment, if the VP26 protein was co-localising and therefore interacting with either of these proteins.

3.4.2 Localisation of VP26 to the Nucleus

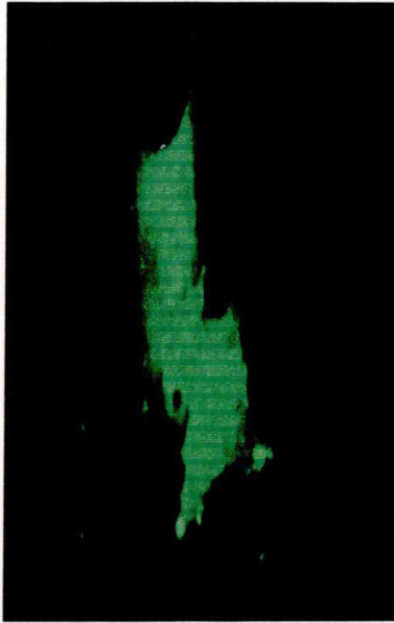
Multiple co-transfection assays were performed using all available combinations of capsid proteins to try and identify conditions under which VP26 would be localised to the nucleus. This revealed that the only conditions under which VP26 was translocated to the nucleus, was when VP5 (pE19) was also present in the nucleus.

When VP26 was co-transfected with VP5 and either preVP22a [figure 3.12, panels (i) and (ii)] or VP19c [figure 3.12, panel (iii)], it was transported to the nucleus. Also, the

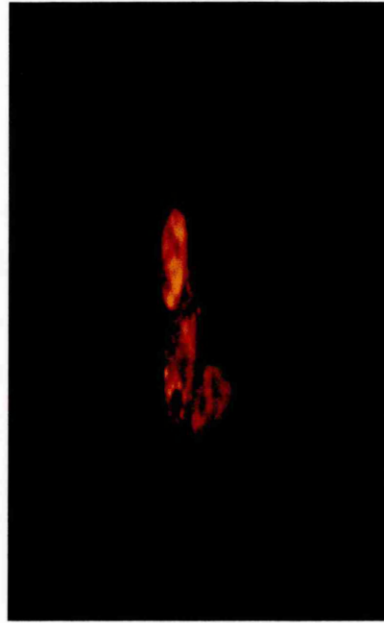
Figure 3.13: Intracellular Distribution of VP5N65 and VP5C65

(i) VP5N65

A

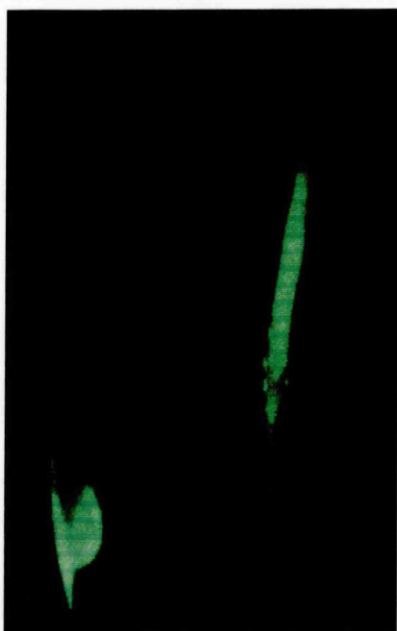


B



(ii) VP5C65

C



D

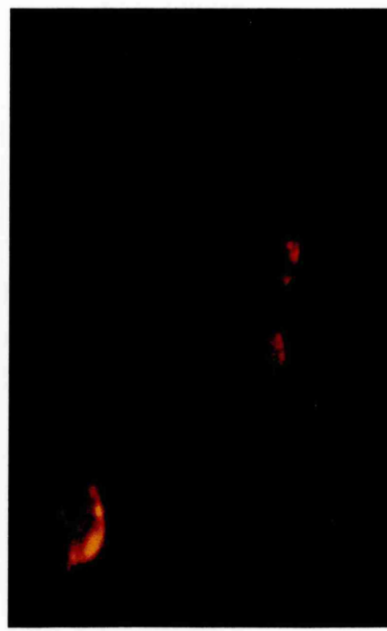


Figure 3.13: Cells were co-transfected with either pSJM19N65 (VP5Npp65) and pJK2 (preVP22a) (panel (i), A and B represent duplicate exposures of a single field), or, pSJM19C65 (VP5Cpp65) and pJK2 (preVP22a) (panel (ii), C and D represent duplicate exposures of a single field). The distribution of VP5Npp65 and VP5Cpp65 was detected using the primary antibody, pp65 (1:300) and preVP22a was detected with 20999 (1:100). VP5pp65 (panel A) and VP5Cpp65 (panel C) were visualised with FITC-GAM (1:100) and found to be present throughout the cell. preVP22a (panels B and D) was visualised with TRITC-GAR (1:100) and found to be present in the nucleus.

Magnification = x260

pattern of interaction closely mapped that exhibited by VP5 (compare with figure 3.9). Therefore, VP26 was uniformly present throughout the nucleus, except the nucleoli, when preVP22a was present however, defined spots were visible when VP19c was included instead of preVP22a.

3.5 Distribution of N- and C- Terminal Deletions of VP5

When either the C-terminal deletion (pSJM19C65) or N-terminal deletion (pSJM19N65) of VP5 were expressed singly, they were found distributed throughout the cell, sometimes absent from the nucleus (not shown). However, in contrast to the full length version of VP5, when either of the terminal deletions (VP5N65 or VP5C65) were expressed in combination with either preVP22a or VP19c, they failed to co-localise to the nucleus (see figure 3.13)

4. Discussion of Immunofluorescence Data

As HSV-1 capsid assembly occurs in the nucleus of cells it is not surprising that many researchers have found the capsid proteins predominantly in the nucleus of infected cells (Powell & Watson, 1975; Cohen *et al*, 1980; McNabb & Courtney, 1992). However, results presented in this chapter, together with data from Nicholson *et al* (1994) show that the concentration of capsid proteins in the nucleus is a result of multiple protein-protein interactions. It can also be concluded that, as the same pattern of interaction was observed when the pp65 epitope tag was present or absent, there was no interference with normal protein-protein interactions attributable to the tag.

preVP22a and VP19c each appear to carry an inherent nuclear localisation signal (NLS). The NLS of either has not been definitively mapped. NLS are often carried within hydrophilic regions of a protein. For example, the T antigen of SV40 has a NLS defined by 7 amino acids, ie Pro-Lys-Lys-Lys-Arg-Lys-Val. Within this sequence there are 5 consecutive positively charged residues. Within preVP22a, there is an area at approximately amino acid 120, which encodes Lys-Arg-Arg-Arg-Arg and could constitute a NLS. Similarly, within VP19c there is an area at approximately amino acid 415, which encodes Arg-Gln-Arg-Gln-Arg-Arg and this could also constitute a NLS.

Other capsid proteins do not appear to carry their own NLS. Neither VP5 or VP23 have a clear NLS and are concentrated in the nucleus when they are co-transfected with preVP22a or VP19c, indicating that their redistribution is the result of a complex formation. However, when each protein is co-transfected with VP19c, their nuclear distribution pattern significantly varies, with VP5 having a punctate appearance and VP23 appearing as uniform. This data strongly suggests that VP5 and VP23 are each exerting some influence on the distribution of VP19c within the nucleus.

EM examinations of insect cells infected with recombinant baculoviruses expressing combinations of VP19c, VP5 or VP23, go some way to explaining these different distribution patterns. F Rixon and J Tatman (Rixon *et al*, 1996) analysed complexes formed when Sf cells were infected with AcUL18 (VP23), AcUL19 (VP5) and AcUL38 (VP19c) combinations. They found no novel structures when AcUL18+AcUL19 or AcUL18+AcUL38 were co-infected. However, co-infections of AcUL19+AcUL38 resulted in the formation of a large number of densely staining particles, distinct from recombinant capsids. The particles were uniform, and formed a basic capsid-like shell. They were initially identified as having a diameter of 70nm. Subsequent cryo-EM analysis has shown them to be basically icosahedral with a diameter of 880Å and T=7 symmetry (Saad *et al*, 1999). (This aspect is discussed fully in Chapter 6 discussion.) These particles were present throughout the nucleus, frequently in large clusters. The clusters presumably account for the patchy and punctate distribution observed by VP5+VP19c immunofluorescence staining.

VP26 was only present in the nucleus when VP5 is also there and was not influenced by preVP22a or VP19c alone. This pattern of interaction provides evidence that a direct interaction between VP5 and VP26 is occurring and is consistent with the finding that VP26 is present on the tips of the VP5 hexons (Booy *et al*, 1994; Trus *et al*, 1995; Zhou *et al*, 1994; 1995).

As VP5 is the major capsid protein, constituting 60-70% of the capsid mass, it is not surprising to find that this protein forms multiple interactions. In summary, VP5 can form complexes with VP26, VP19c and preVP22a and effect their redistribution.

However, the lack of interaction between VP5 and VP23 (Section 3.2) was surprising in view of the fact that this protein constitutes part of the triplex complex which links adjacent capsomeres (Newcomb *et al*, 1993). The absence of a VP5-VP23 interaction is consistent with the findings of Nicholson *et al* (1994) and the lack of visible structures in electron micrographs of baculoviruses expressing VP5 and VP23 (Rixon *et al*, 1996). Furthermore, the presence of VP5-VP19c 880nm particles (Rixon *et al*, 1996) suggests that VP23 is not essential for the interaction of the triplex with the capsomere but, VP23 (together with VP5, VP19c and the scaffold proteins) is essential for intact capsid formation (Desai *et al* 1993). It would seem likely that the binding of VP23 to VP19c exerts a change in conformation of VP19c which modulates the structural integrity of the capsid. It may be that VP23 can interact with VP5 but only in the context of an intact capsid.

A second surprising finding was that neither the N- and C- terminal deletions of VP5 were able to localise to the nucleus with VP19c or preVP22a. This indicates that either:

- neither the N- nor C-terminal portions alone are sufficient to interact with preVP22a or VP19c.
- the vital binding site has been disrupted during the cloning of the deletion mutants. As the full length tagged version of VP5, made by ligating the two terminal portions together, behaved like wild type VP5, inaccurate flanking sequences or cloning errors were not responsible for the lack of redistribution of either the N- or C- terminal portions.
- the N- or C-terminal portions expressed alone do not have the same secondary structure as the N- and C-terminal portions expressed together in the complete VP5 molecule, ie the deletion mutants are misfolded .

Certainly it is known that only a small portion of preVP22a (25 amino acids) is necessary its for interaction with VP5 (Kennard *et al*, 1995; Mastusick-Kumar, 1995; Thomsen *et al*, 1995; Hong *et al*, 1996) and recent cryo-EM data (Chapter 6 and Zhou *et al*, 1998a) has confirmed this. As no protein-protein interactions were evident with

either of these large terminal portions of VP5, it seems probable the conformation adopted by the intact molecule is needed for the protein to bind to other capsid proteins.

Obviously protein-protein interactions which occur in the capsid are extensive and complex. From this analysis, it is clear that proteins can exert an influence upon one another's location and distribution patterns within an infected cell.

5. Production and Analysis of a New Epitope Tag, Chloramphenicol Acetyl Transferase (CAT)

5.1 Introduction

Since the pp65 tag was only available commercially and the supply was subject to some uncertainty, it was decided that it would be useful to map another epitope tag. There were several reasons for this line of thinking:

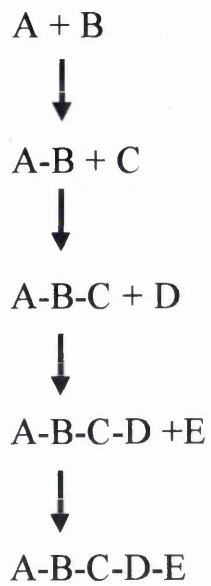
- The sequence could be incorporated into a cloning vector and used as an epitope tag.
- The new epitope could be synthesised as an oligopeptide and injected into rabbits to generate polyclonal antibodies for double labelling experiments.
- There would be a reliable source of antibody, over a long period of time with no concerns as to whether a company would continue to supply it.
- Production of an anti-tag antibody in-house was a more economical alternative.

The Chloramphenicol Acetyl Transferase (CAT) protein was chosen for this purpose. This protein was ideally suited as the source of a tag as the enzyme is totally foreign to HSV-1 and mammalian cells and so it was unlikely that the antibody would interact non-specifically with viral proteins. Also, there was a strong mouse monoclonal antibody available, 5/24, which could be used in the mapping procedure. This antibody was supplied by Dr Susan Graham who had shown it to work efficiently in Western blots.

The epitope was mapped using the SPOTscan technique which is fully described in Methods, Section 2.11. The SPOTscan technique is based on the Merrifield principles

Figure 3.14: Schematic Representation of Stepwise Synthesis of Oligopeptides

(i) Nature's Way



(ii) Laboratory Way

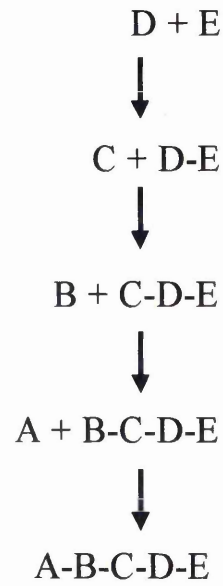


Figure 3.14: The figure shows a schematic representation of stepwise oligopeptide synthesis. A, B, C... etc represent individual amino acids. The N-terminus is written on the left and the C-terminus on the right. Panel (i) shows stepwise synthesis from the N- to C- terminus and represents the normal process of protein synthesis on an mRNA template. Panel (ii) shows stepwise synthesis from the C- to N-terminus and represents the most common route followed by chemical synthesis.

(Merrifield, 1964) of solid phase oligopeptide synthesis. Merrifield proposed that an oligopeptide could be synthesised by attaching one end to a solid and stable surface (in this instance a nitrocellulose membrane) and elongating the chain in a stepwise manner. In this instance 9-fluorenylmethyloxycarbonyl (F-moc) amino acid anhydrides were used to synthesise the oligopeptides. The initial amino acid was anchored to a nitrocellulose membrane through an ester bond. The oligopeptide chain was extended by cleaving the F-moc protecting group, to create an active site, and adding the next amino acid in the sequence. A series of deprotection, washing and coupling steps were repeated for each succeeding amino acid, until the desired sequence was assembled.

In nature, proteins are synthesised from the amino terminus [see figure 3.14, panel (i)]. This strategy is not used in the laboratory, where elongation occurs from the carboxyl terminus [see figure 3.14, panel (ii)]. This is because commercially available chemicals make it easier to assign a permanent protecting group to the carboxyl function and temporary protecting groups to the amino groups. The temporary protecting groups are removed at intermediate stages for the subsequent addition of residues.

A series of overlapping oligopeptides, spanning the entire sequence of CAT, were assembled on the membrane. They were assayed for their immunological activity and the positive SPOTs aligned to the sequence to identify the epitope site.

5.2 Optimisation of CAT Protein and 5/24 Antibody

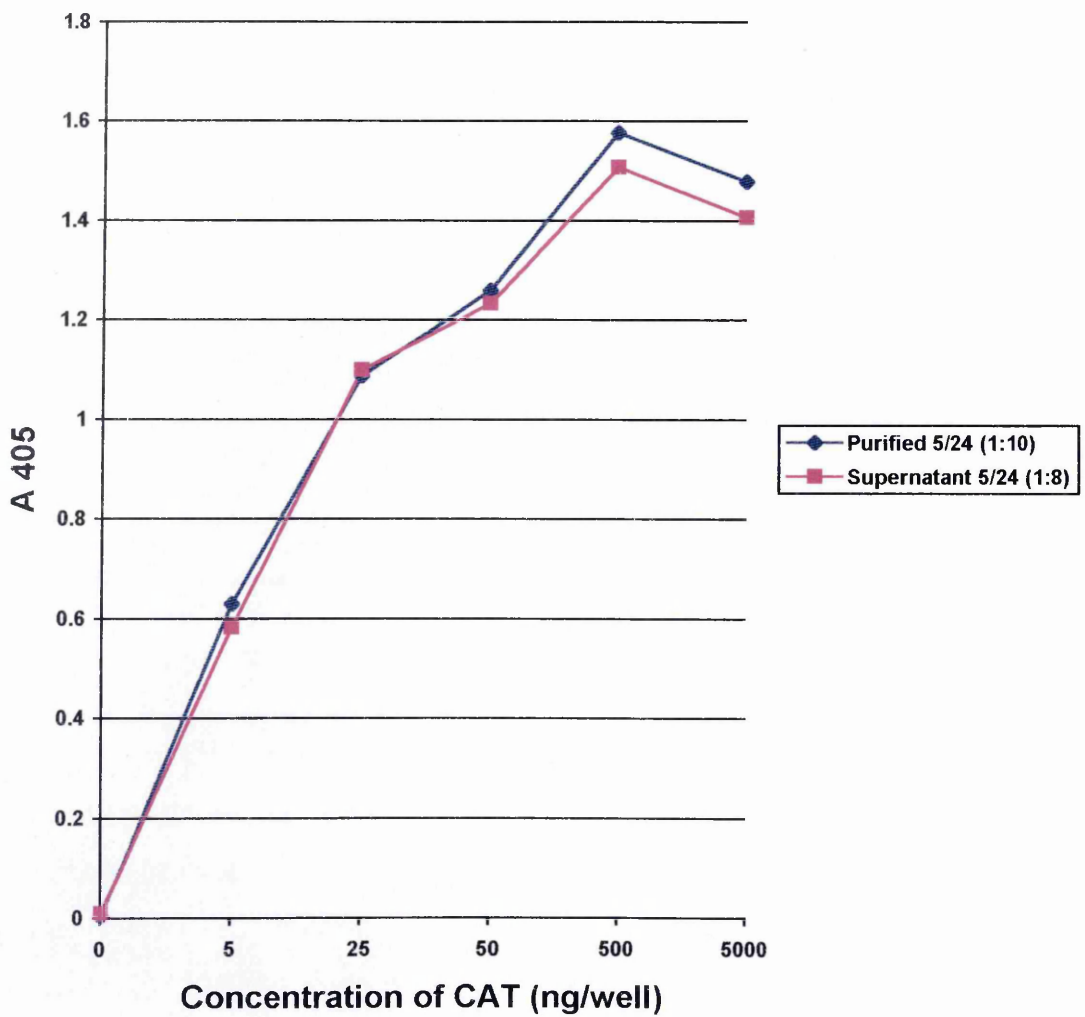
Before the SPOTs mapping procedure could be performed, it was first necessary to optimise the conditions under which the mouse monoclonal antibody (5/24) would be active against the CAT protein. This was determined by ELISA reactions which are detailed in the following sections.

5.2.1 Optimisation of CAT protein

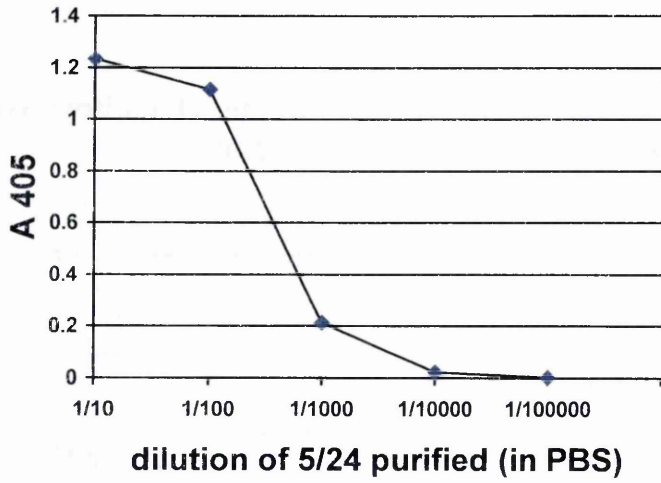
The CAT protein was used to coat microtitre wells and the system was optimised by testing a range of CAT protein concentrations against a range of antibody concentrations. The CAT protein was tested at various dilutions from 5000ng to 5ng per well. The 5/24 antibody was available in two forms, ammonium sulphate purified

Figure 3.15: Optimisation of CAT Protein to the 5/24 Monoclonal Antibodies

(i): Optimal Concentration of CAT Protein Against Purified (1:10) and Supernatant (1:8) 5/24 Antibody



(ii): Interaction of Purified 5/24 with 50ng of CAT



(iii): Interaction of Supernatant 5/24 with 50ng of CAT

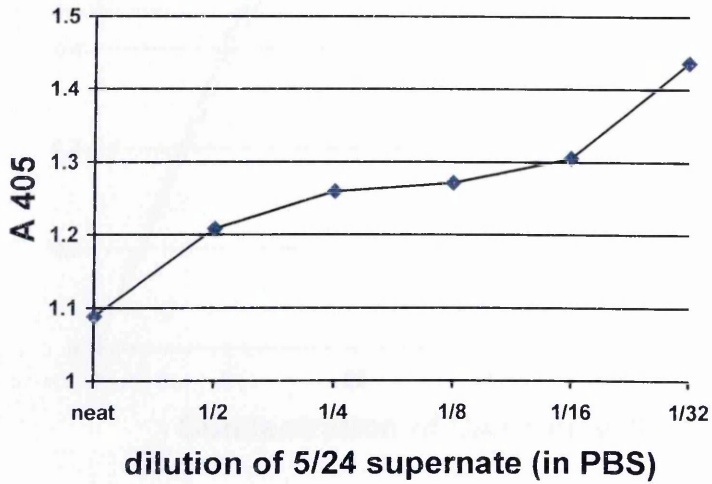
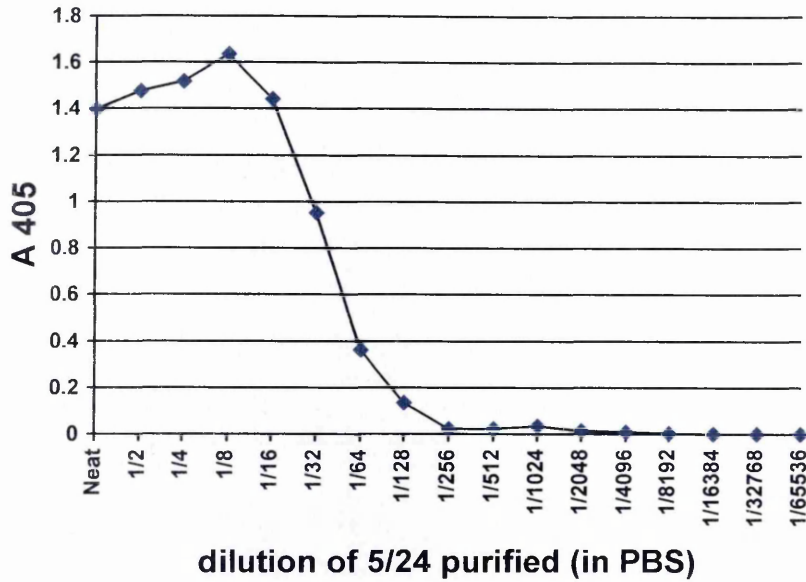


Figure 3.15: This figure shows a summary of the data obtained when optimising the concentration of CAT protein to be used in ELISA reactions. Panel (i) shows the signal obtained with the various concentrations of CAT protein (x-axis) and the two antibody preparations. This pattern was seen when the purified antibody was reacted at a 1:10 dilution (blue line) and the supernatant antibody was reacted at 1:8 dilution (pink line). The concentration of CAT protein chosen to be used in the assay system was 50ng/well. Therefore, the different antibody concentrations were assayed against 50ng of CAT protein, as shown the subsequent panels. Panel (ii) shows the absorbance obtained with of various dilutions of purified 5/24 antibody and panel (iii) shows the absorbance obtained with various dilutions of supernatant 5/24 antibody.

Figure 3.16: Optimisation of 5/24 Monoclonal Antibodies to 50ng of CAT

(i): Optimisation of Purified 5/24 to 50ng of CAT



(ii): Optimisation of Supernatant 5/24 to 50ng of CAT

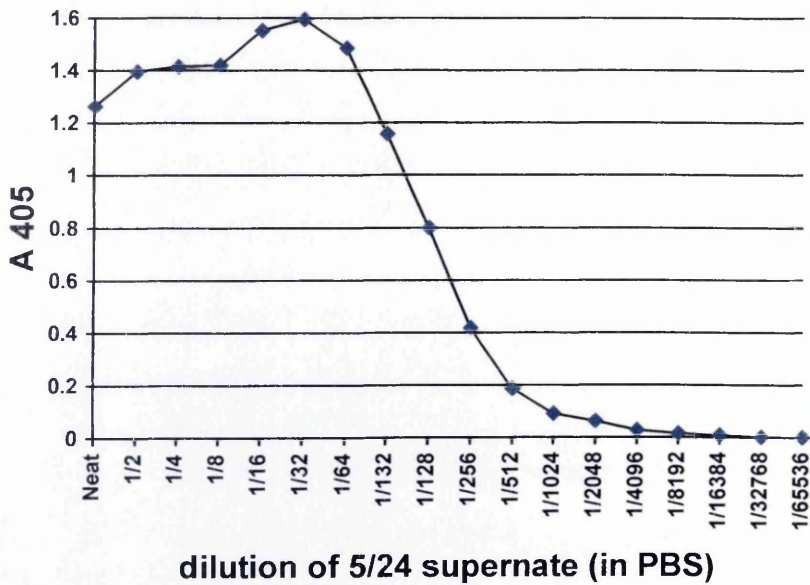


Figure 3.16: This figure shows the A_{405} values obtained from testing a series of dilutions of both the purified [panel (i)] and supernatant [panel (ii)] 5/24 antibody, against 50ng of CAT protein. From panel (i) it is evident that the dilution of purified antibody which gave the highest absorbance reading was 1:8. However, panel (ii) shows that the supernatant antibody can be diluted to 1:32 to give a similar optimal absorbance value.

Methods, Section 2.12) and supernatant fractions. The purified antibody was sequentially diluted ten-fold from 1:10 to 1:100 000. The supernatant antibody was also diluted two-fold from neat to 1:32. The diluted antibodies were tested against the various dilutions of protein.

A large bank of data was obtained from these experiments and many graphs were plotted to determine the optimum CAT protein concentration required to coat the microtitre wells. However, only the relevant graphs are shown in figure 3.15. From the data obtained in these experiments, it was determined that a 1:8 dilution of supernatant 5/24 and a 1:10 dilution of purified 5/24 reacted well, giving good response curves to a range of CAT protein dilutions, see panel (i).

There was a significant antibody-protein interaction detected when the CAT protein was used at 50-500ng/well. It was decided that 50ng/well would be designated as the standard concentration of protein to be used in the reactions as the increased value at 500ng did not warrant 10x more protein being used per reaction.

5.2.2 Optimisation of 5/24 Antibody to 50ng of CAT Protein

The initial bank of experiments (described above) did not allow the optimal antibody dilutions to be determined from the range tested. Panels (ii) and (iii) of figure 3.15 show the activities of various dilutions of purified and supernatant antibody to 50ng of CAT protein. The experiment was extended to encompass a greater range of test antibody dilutions.

Both supernatant and purified forms of 5/24 were re-tested in an ELISA against 50ng of CAT protein. The antibodies were diluted 2-fold in PBS from neat to 1:32768. The results of the assays are shown in figure 3.16.

When comparing panel (i) and (ii), it is evident that the supernatant antibody is more reactive against the CAT protein as it has the greatest absorbance at the lowest dilution. The supernatant was most active at 1:32 dilution, whereas the maximum activity

Figure 3.17: For the SPOTscan Procedure; PC Generated Oligopeptide List and Pipetting Schedule for the CAT Sequence

(i) CAT Amino Acid Sequence

Sequence length: 219
 Oligopeptide Length: 9
 Offset: 1
 Total number of oligopeptides: 211

oligopeptide 3	
oligopeptide 2	
oligopeptide 1	

1: MEKKITGYTT VDISQWHRKE HFEAFQSVAQ CTYNQTVQLD
 41: ITAFLKTVKK NKHKFYPAFI HILARLMNAH PEFMRMAMKDG
 81: ELVIWDSVHP CYTVFHEQTE TFSSLWSEYH DDFRQFLHIY
 121: SQDVACYGEN LAYFPKGFIE NMFFVSANPW VSFTSFDLNV
 161: ANMDNFFAPV FTMGKYITQG DKVLMPLAIQ VHHAVCDGFH
 201: VGRMLNELQQ YCDEWQGGGA

(ii) Excerpt from PC Generated Oligopeptide List

SPOT / Oligopeptide No.	Mr	Sequence
1	1070	MEKKITGYT
2	1040	EKKITGYTT
3	1010	KKITGYTTV
4	997	KITGYTTVD....
208	1212	LQQYCDEWQ
209	1156	QQYCDEWQG
210	1084	QYCDEWQGG
211	1027	YCDEWQGGGA

(iii) Excerpt from PC Generated Pipetting Schedule

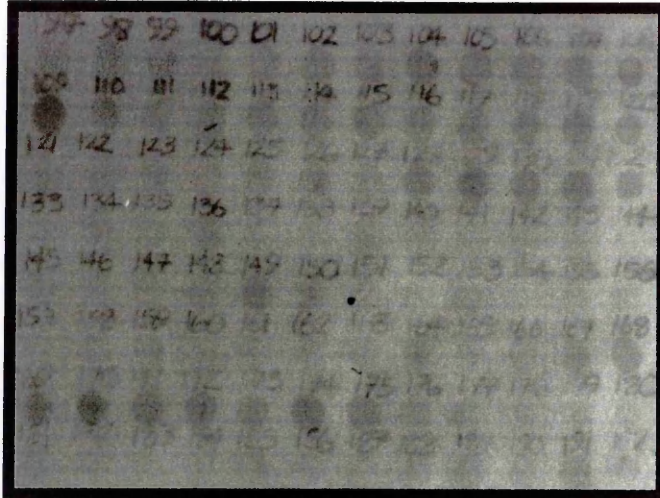
Cycle 1

Amino Acid	SPOT Number
A	16 21 35 50 56 61 68 117 124 139 153 180 186 211
C	23 83 11 81 88 204
D	4 32 71 78 103 104 115 149 156 173 189 205
E	12 15 64 73 89 92 100 121 132 199 206
F	14 17 36 47 51 65 87 94 105 108 126 130 135 136 145 148 158 159 163 191
W	8 77 98 142 207
Y	25 48 84 101 112 119 125 168 169 203

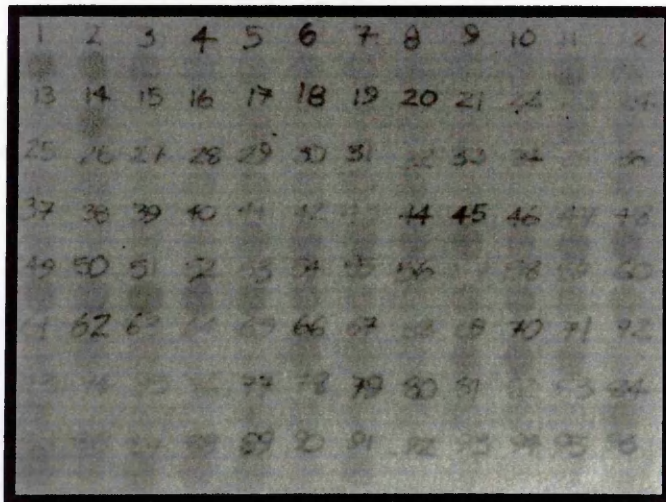
Figure 3.17: This figure details the information fed into the SPOTs programme and the data generated from the SPOTscan programme. Panel (i) shows the data generated from feeding the CAT amino acid sequence into the programme, together with the desired offset of each oligopeptide. Panel (ii) shows an excerpt from the list, generated by the programme, detailing the molecular weight and amino acid sequence for each SPOT or oligopeptide. Panel (iii) shows an excerpt of the pipetting schedule which was followed during Cycle 1, ie addition of the initial amino acid in the chain. This schedule details which amino acid should be added to which SPOT, to generate the correct oligopeptide sequence.

Figure 3.18: SPOTs Membranes

(i)



(ii)



(iii)

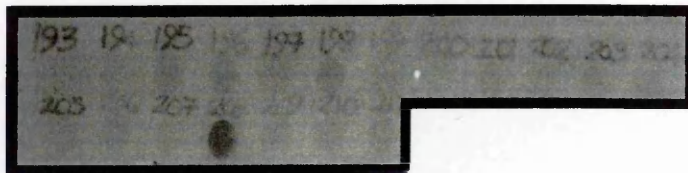


Figure 3.18: Three nitrocellulose membranes containing the nonopeptides, 1 to 211, [panels (i), (ii) and (ii)] were probed with the primary antibody 5/24 (1:32) and visualised with the secondary antibody GAM-HRP (1:100). SPOT numbered 208 [panel (iii)] was significantly darker than the others, indicating a positive SPOT-antibody interaction. This SPOT was designated CAT208.

observed for the purified antibody was at a 1:8 dilution [this was a reduction in activity from the previous experiment, see figure 3.15, panel (ii)].

Some more supernatant was subsequently purified by ammonium sulphate precipitation, but again a similar pattern of activity was observed (results not shown). It was also reported by J Leslie (personal communication) that the purified anti-CAT antibody was extremely unstable and lost considerable activity upon storage. This also appears to be the case here. It was therefore decided to use the supernatant antibody, at 1:32 dilution, for immunological analysis of the oligopeptides on the SPOTs membrane.

5.3 Generation of Oligopeptides by SPOTscan Methodology

The CAT protein sequence is 219 amino acids in length [see figure 3.16, panel (i)] and was entered into the SPOTs programme on the PC to generate a list [figure 3.17, panel (ii)] and a pipetting schedule [figure 3.17, panel (iii)], for the synthesis of 211 oligopeptides, each containing 9 amino acids, which spanned the entire sequence of CAT and overlapped by a single amino acid residue.

The oligopeptides were generated on the membrane by adding each amino acid to the appropriate SPOT in a duplicate cycle, to double couple the reaction. Between each cycle the membranes were washed, protected and deprotected (see Methods, Section 2.11).

5.4 Antibody Assay of SPOTs Oligopeptides

Once the nonapeptides had been synthesised, the membrane was washed and the supernatant antibody, at 1:32 dilution, was added, allowed to react for 4h and washed. The secondary GAM-HRP antibody was added for 2h, washed and the reaction developed with the kit signal developer. After a 2h development period, SPOT 208 was significantly darker than the others (see figure 3.18) indicating that a positive oligopeptide-antibody reaction was occurring.

The membrane was stripped and the antibodies reacted as before and again the SPOT 208 was clearly darker (data not shown), confirming that this oligopeptide, CAT208,

Figure 3.19: Position of CAT208 within the Amino Acid Sequence

1: MEKKITGYTT VDISQWHRKE HFEAFQSVAQ CTYNQTVQLD
41: ITAFLKTVKK NKHKFYPAFI HILARLMNAH PEFRMAMKDG
81: ELVIWDSVHP CYTVFHEQTE TFSSLWSEYH DDFRQFLHIY
121: SQDVACYGEN LAYFPKGFIE NMFFVSANPW VSFTSFDLNV
161: ANMDNFEAPV FTMGKYYTQG DKVLMPLAIQ VHHAVCDGFH
201: VGRMLNELQQ YCDEWQGGGA

↓
CAT208

Figure 3.19: The position of oligopeptide 208, termed CAT208 within the complete CAT sequence is highlighted. This sequence reacted with the 5/24 anti-CAT antibody and is shown in the rectangle, between amino acids 207 and 216, near the C-terminus.

Table 3.1: Summary of 1013 Oligopeptide Sequences

Name	Sequence	Length (amino acids)
1013a	LQQYCDEWQ	9
1013b	LQQYCDEWQGGGA	12
1013c	LQQYCDEWQGGAG	13
1013d	LNELQQYCDEWQGGGA	15

Table 3.2: Summary of 1013 Oligopeptide Analysis

Name	Cleavage Conditions	Predicted Yield (mg)	Actual Yield (mg)	Solubility	Purity (%)
1013a	Reagent K	18.91	6.80	dH ₂ O	62
1013b	Reagent K	21.80	6.54	dH ₂ O + ammonia	-
1013c	Reagent K	22.69	5.78	dH ₂ O + ammonia	46
1013d	Reagent K	27.36	7.72	dH ₂ O + ammonia	52
1013c.2	Trp Mixture	22.69	8.26	dH ₂ O + ammonia	89

was interacting with the antibody and so probably constituted the epitope site, or at least part of it.

From the sequence data CAT208 corresponded to the sequence LQQYCDEWQ, present near the carboxy-terminus of the protein between amino acid 208 and 216 (figure 3.19).

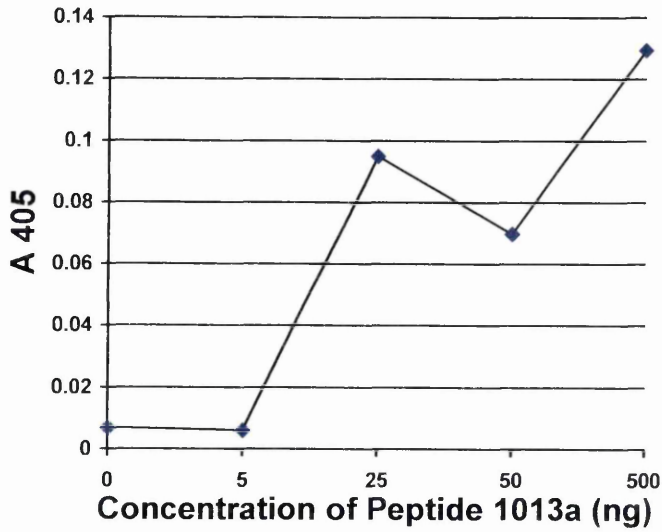
5.5 Oligopeptide Synthesis of CAT208

The positive nonapeptide CAT208 was synthesised on the PSSM-8 synthesiser on 4-branched TGA resin. This resin was selected as it produces multiple antigenic peptides (MAP). The multimeric oligopeptides are more immunogenic, and so produce better antibodies, than the simple monomeric sequence alone. Three other oligopeptides were synthesised in parallel, which incorporated additional amino acid sequences on either side of the proposed epitope (see Table 3.1). Oligopeptide 1013a constituted the 9 amino acids only, oligopeptide 1013b had 3 additional amino acids at the C-terminus, oligopeptide 1013c had an additional 4 amino acids at the C-terminus and oligopeptide 1013d had 3 additional amino acids at both the N- and C-terminus. These sequences were incorporated as it was possible that the epitope extended further than the nine core amino acids but, had not been picked up by the antibody assay of the SPOTs membrane, as the reaction was too weak.

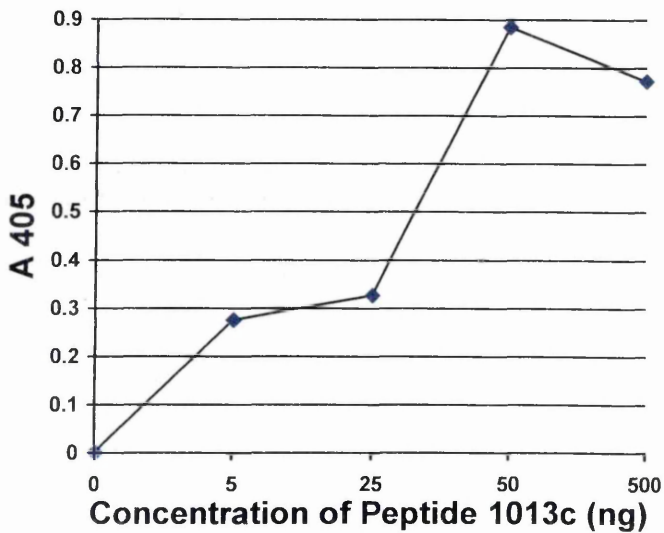
These oligopeptides were cleaved in reagent K (as described in Methods, Section 2.4.2). Oligopeptide 1013a was the only oligopeptide which dissolved well in dH₂O. 1013b, 1013c and 1013d were negatively charged overall and dissolved in dH₂O when ammonia was bubbled through them. The oligopeptides were dried down and their Mr analysed by mass spectrometry. All the oligopeptides were reasonably pure except 1013b (see table 3.2) which, after several separate analyses, produced only random or nonsense readings, indicating that it was very impure. Several re-syntheses of the oligopeptide gave similar results (data not shown), indicating that this oligopeptide may be very unstable. It was therefore decided to proceed with the analysis of the oligopeptides, using only 1013a, 1013c and 1013d.

3.20: Reactivity of Oligopeptides 1013 with 5/24 Antibody Supernatant

(i): Reactivity of Oligopeptide 1013a with 5/24 Supernatant (1:32)



(ii): Reactivity of Oligopeptide 1013c with 5/24 Supernatant (1:32)



(iii): Reactivity of Oligopeptide 1013d with 5/24 Supernatant (1:32)

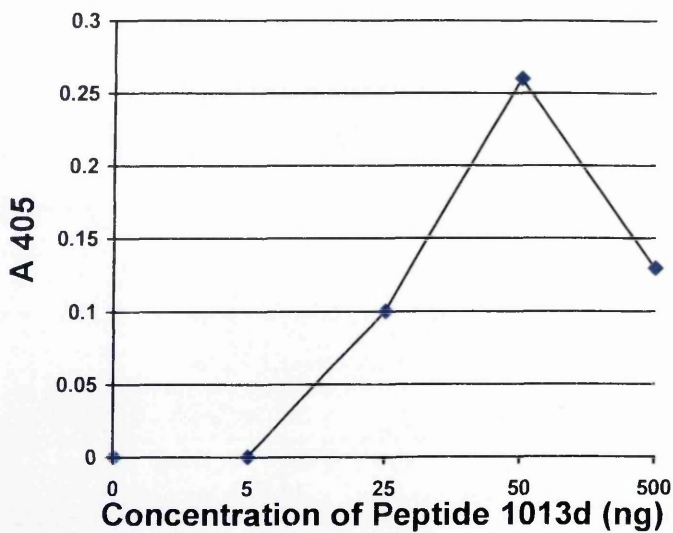
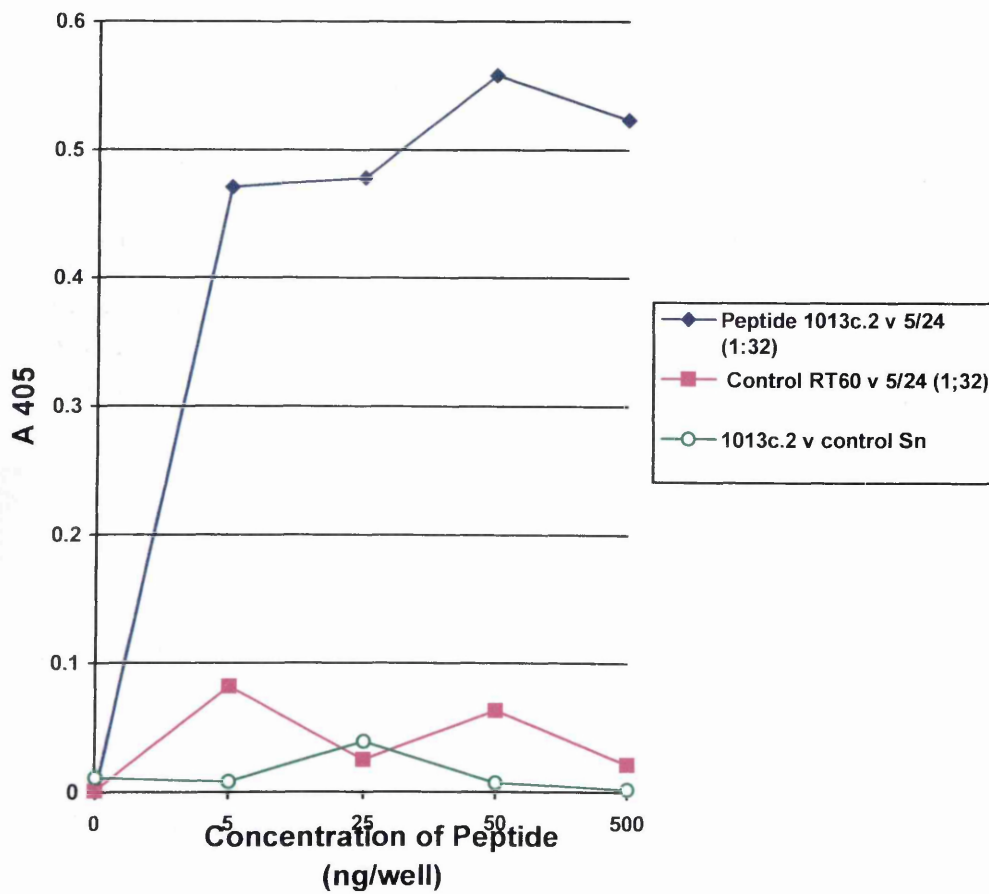


Figure 3.20: The A_{405} values of oligopeptides 1013a, 1013c and 1013d, panels (i) (ii) and (iii) respectively, to the 5/24 antibody supernatant at a 1:32 dilution. Note the differing scales on the y-axis.

Figure 3.21: Reactivity of Oligopeptide 1013c.2 with 5/24 Antibody Supernatant (1:32) Compared to Controls



Results

Reactive dot and negative dot
1013c.2 and Sn

3.3 Assaying of 5/24 Antibody

Antibody Specificity

Antibody 5/24

1013c.2 and RT60

Antibody Sn

1013c.2 and Sn

Figure 3.21: This figure shows the level of Absorbance (A_{405}) detected when oligopeptide 1013c.2 and antibody 5/24 were reacted together and with a series of controls. The blue line shows the A_{405} when 5/24 antibody supernatant, at 1:32 dilution, was reacted with oligopeptide 1013c.2. The pink line shows the level of A_{405} detected when the 5/24 antibody was reacted with an unrelated control oligopeptide, RT60. The green line shows the A_{405} values obtained when oligopeptide 1013c.2 was reacted with an unrelated antibody, Sn.

therefore decided to proceed with the analysis of the oligopeptides, using only 1013a, 1013c and 1013d.

5.6 Reactivity of CAT208 Oligopeptides (1013a, 1013c, 1013d) with 5/24 Antibody Supernatant

To confirm that the sequence mapped from the SPOTscan procedure was indeed the epitope of the 5/24 antibody, a series of ELISA reactions were performed with the 5/24 antibody supernatant, at 1:32 dilution, and the oligopeptides 1013a, 1013c and 1013d. The results are detailed in figure 3.20, panels (i) to (iii).

Oligopeptide 1013a [panel (i)] did not react well with the antibody and the absorbance values were very low. This may be because the oligopeptide is so short and therefore not entirely exposed from the resin core. Similarly 1013d [panel (iii)] did not react well with the antibody, with the maximum absorbance value being only marginally higher. On the other hand, oligopeptide 1013c [panel (iii)] reacted efficiently with 5/24. The additional amino acid residues at the C-terminus of this oligopeptide, compared to 1013a, may be pushing the oligopeptide further out from the core so that it is more exposed and able to interact with the antibody successfully.

5.6.1 Confirmatory Analysis of Oligopeptide 1013c

As the initial synthesis had produced a lower than expected yield and purity of oligopeptide 1013c, it was re-synthesised to generate oligopeptide 1013c.2 (see table 3.2). As the sequence of 1013c.2 contained a tryptophane it was decided that an alternative cleavage mixture from Reagent K, specific to oligopeptides containing this amino acid, would be used to try and increase the yield (see Methods, Section 2.4.2). This time the oligopeptide was found to be 89% pure by mass spectrometry analysis. The activity of oligopeptide 1013c.2 was confirmed in a series of ELISA's. The oligopeptide activity was compared against two unrelated controls, a control oligopeptide (RT60 - supplied by K McCauley) and a control mouse monoclonal antibody (Sn - supplied by S Graham). The results are shown in figure 3.21, where it is clearly evident that the control oligopeptide is not cross-reacting with the 5/24 antibody and similarly the control antibody is not cross-reacting with CAT208 oligopeptide

Table 3.3: Inoculation Schedule for the Production of Rabbit Polyclonals to oligopeptide 1013c.2

Inoculation	Time (days)
Oligopeptide 1013c.2 + Freund's complete adjuvant	0
Oligopeptide 1013c.2 + Freund's incomplete adjuvant	15
Oligopeptide 1013c.2 + Freund's incomplete adjuvant	31
Oligopeptide 1013c.2 + Freund's incomplete adjuvant	78
Oligopeptide 1013c.2 + Freund's incomplete adjuvant	107
bleed rabbits	121

epitope sequence against the mouse monoclonal antibody, 5/24, is contained within the amino acid residues LQQYCDEWQGGAG.

5.7 Production of Rabbit Polyclonal Antibodies to CAT208 Oligopeptide 1013c.2

To try to generate rabbit polyclonal antibodies against the CAT epitope, oligopeptide 1013c.2 was injected intramuscularly into 2 rabbits. All the animal work was performed by Gillian McVey and the inoculation schedule is shown in table 3.3.

The final bleed was taken and the blood allowed to clot. The rabbit blood clots were pelleted and the supernatant fractions tested in a series of ELISA reactions against oligopeptide 1013c.2. No activity was detected at any dilution, from neat to 1:32768 with either rabbit supernatant fractions. A proportion of each antibody supernatant was purified by ammonium sulphate precipitation (Methods, Section 2.12) and again tested in a series of ELISA reactions against oligopeptide 1013.2. Still no activity was evident (data not shown).

pE35T2 (for description see below, Section 5.8) was used in Western blot analysis against both purified and supernatant rabbit antibody fractions. No protein-antibody activity was detected (data not shown). The rabbit supernatants were also tested against a series of CAT tagged proteins (see Section 5.8) by immunofluorescence labelling. No specific labelling was observed, with only a large background of fluorescence picked up.

It can be concluded that no rabbit antibody against CAT208 was produced from either of the two rabbits injected with oligopeptide 1013.2. This suggests that the oligopeptide may be poorly immunogenic.

5.8 Construction of Plasmids Expressing CAT208

Before it was known that attempts to produce a rabbit antibody against the CAT epitope had failed, a series of constructs encoding the tag sequence were made. Due to the nature of the cloning strategy employed for making constructs containing the pp65

Figure 3.22: Constructs encoding the CAT208 epitope tag in pCMV10BglΔEco were constructed using two complementary oligonucleotides XcatE (1) and (2) [panel (i)] encoding the CAT208 tag amino acid sequence, which is marked underneath. These oligonucleotides were used to CAT208 tag the constructs shown in panels (ii) and (iii). The oligonucleotides were inserted following XhoI/EcoRI digestion, to remove the pp65 tag in each case. The presence of the new tag was detected by ScaI digestion.

The figure is not drawn to scale.

Figure 3.23: Construction of pET35CAT

(i) Sequence of Oligonucleotides NhiscatE (1) and NhiscatE (2)

NcoI

CATGGGCAGCAGCCATCATCATCATCATCACAAACGAACTACAACAATACTGTGACGAATGGCAAATGGG
 CCGTCGTCCGTAGTAGTAGTAGTAGTGTGGCTTGATGTTGTTATGACACTGCTTACCGTTACCCTTAA

H H H H H H
L Q Q Y C D E W Q
EcoRI

(ii) pET35CAT

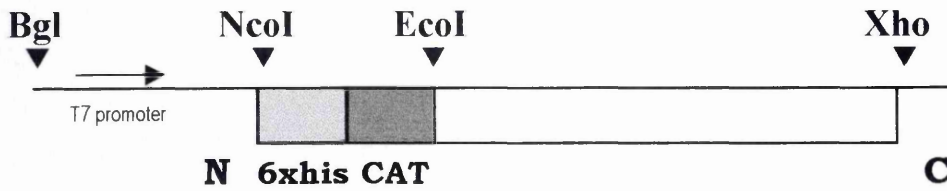


Figure 3.23: Two complementary oligonucleotides, NhiscatE (1) and NhiscatE (2), [panel (i)] were used to incorporate 6xhis (dashed box) and CAT208 (solid box) tags into VP26 in pETmod (see Chapter 4, Section 2.1). The oligonucleotides were inserted following NcoI/EcoRI digestion of pET35pp65 to remove the pp65 tag and generate pET35CAT [panel (ii)].

This figure is not drawn to scale.

epitope tag (Section 2.3), it was relatively simple to manipulate these clones to incorporate the CAT208 sequence LQQYCDEWQ instead. The pp65 epitope had been cloned into the ORF's with unique restriction enzyme sites, XhoI and EcoRI, flanking it. This allowed digestion and removal of the pp65 tag and insertion of oligonucleotides encoding CAT208, with overhanging ends which were compatible with the XhoI and EcoRI sites. A restriction enzyme site, ScaI, was also included in the oligonucleotide sequence to allow diagnostic digests to be performed to confirm the presence of the new oligonucleotide sequence. Two oligonucleotides, XcatE (1) and XcatE (2), were made [figure 3.22, panel (i)] and ligated into XhoI/EcoRI digested and gel purified pSJM1965 and pE35T1. This generated a two constructs in pCMV10BglΔEco (see Section 2.3.2) containing the CAT208 epitope tag [see figure 3.22, panels (ii) and (iii)]:

- pSJM19CAT - encodes the complete UL19 ORF with the CAT208 epitope in the same site as that occupied by the pp65 epitope in pSJM19pp65 (see Section 2.3.2.3).
- pE35T2 - encodes the UL35 ORF with the CAT208 epitope in the same site as that occupied by the pp65 epitope in pE35T1 (see Section 2.3.2.4).

In addition, the CAT epitope was cloned into a bacterial expression vector pETmod (Chapter 4, Section 2). In this instance, oligonucleotides NhiscatE (1) and NhiscatE (2) [figure 3.23, panel (i)] were used to remove and replace the pp65 epitope in pET35pp65, encoding VP26 (see Chapter 4, Section 2.1), by NcoI/EcoRI digestion and ligation. The resulting construct was designated pET35CAT and encoded the 6xhis and CAT tags linked in frame to VP26 [figure 3.23, panel (ii)]. pET35CAT expressed protein to similar levels as pET35pp65 when treated in the same manner (Chapter 4, table 4.4). However, upon solubilisation and purification the VP26CAT protein was recovered at very low concentrations.

Figure 3.24: Western Blot of VP26CAT

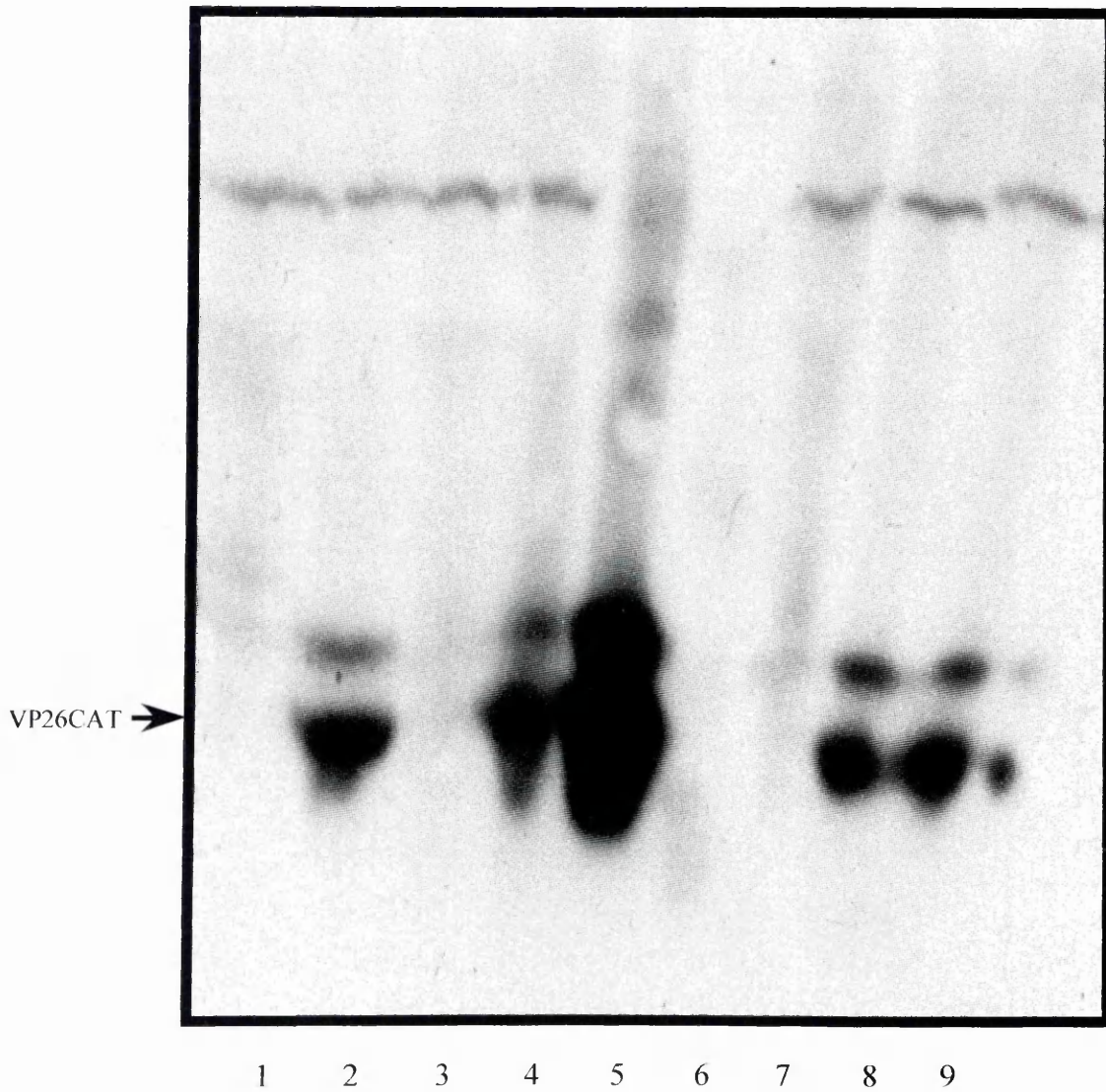


Figure 3.24: Nine clones of pET35CAT were induced at 37°C for 2h with 1mM IPTG. Expression of VP26CAT protein was confirmed by Western blot analysis. The primary antibody, 5/24 (1:32), was detected with GAM-HRP (1:100) and visualised with the ECL developing reagents (see Methods, Section 2.17). The position of VP26CAT is marked by the arrow. This was determined by lining up the blot with the rainbow markers on the original polyacrylamide gel (not shown).

VP26CAT was detected in lanes 2, 4, 5, 8 and 9.

**Figure 3.25: Intracellular distribution of
VP5CAT and VP26CAT**

(i)



(ii)

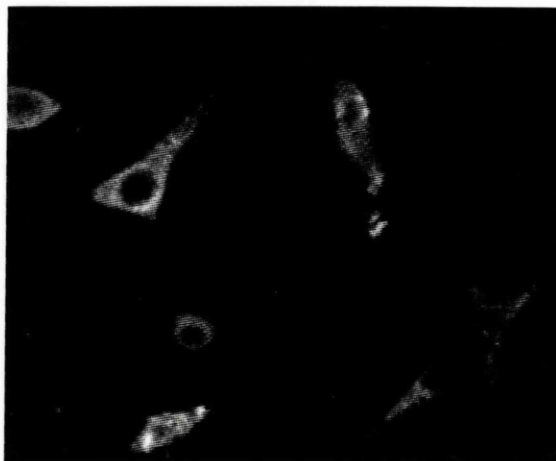


Figure 3.25: Cells were transfected with plasmid pSJM19CAT (VP5CAT) [panel (i)] or, pE35T2 (VP26CAT) [panel (ii)]. The distribution of the CAT constructs was detected with the primary antibody, 5/24 (1:32) and visualised with FITC-GAM. In both instances, the proteins were found throughout the cell but, VP26CAT was predominately localised in the cytoplasm.

Magnification = x200

5.9 Analysis of CAT208 Constructs

5.9.1 Restriction Enzyme Digests

A series of restriction enzyme digests were performed on all the CAT208 constructs detailed in Section 5.8. The digestion profiles were examined on 1% agarose gels to confirm the presence the oligonucleotide insertions (data not shown). Profiles of pSJM19CAT, pE35T2 and pET35CAT showed evidence that the CAT208 epitope tag was present.

5.9.2 Western Blot Analysis

Nine clonal *E coli* isolates of pET35CAT were induced with 1mM IPTG and tested against supernatant 5/24 mouse monoclonal antibody (1:32) by Western blot. From the profiles (figure 3.24) it is clear that many of the clones expressed the CAT tag, with the VP26 protein detected at approximately 14700 Da. Clones numbered 2, 4, 5, 8 and 9 reacted with the anti-CAT antibody supernatant. This confirms that these constructs contain the CAT208 epitope.

5.9.3 Immunofluorescence Labelling

Immunofluorescence was performed by singly transfecting BHK C13 cells with pSJM19CAT (VP5) and pE35T2 (VP26). 5/24 antibody supernatant was used at 1/32 dilution and produced good fluorescence with both the VP5 and VP26 construct. In each case the protein was observed in the expected pattern of distribution and mirrored the results obtained earlier with the pp65 epitope constructs. VP5CAT and VP26CAT were both evident throughout the cell, with VP26CAT predominately in the cytoplasm [see figure 3.25, panels (i) and (ii)]. This confirms the presence of the CAT208 epitope and the ability of the 5/24 mouse monoclonal antibody to work effectively in fluorescence studies.

6. Discussion of Mapping CAT208

Using the SPOTscan technique, it was possible to map the epitope site which interacted with the 5/24 anti-CAT antibody. Oligopeptide 208 encoded the sequence LQQYCDEWQ, which interacted with the antibody and was termed CAT208.

The CAT208 sequence was incorporated into the ORF of UL19 and UL35 by insertion of two overlapping oligonucleotides. The presence of the CAT208 sequence was confirmed by restriction enzyme digestion, Western blot analysis and immunofluorescence studies.

When the CAT208 sequence was synthesised on the PSSM-8 oligopeptide synthesiser, it was found that an oligopeptide, 1013c (or re-synthesised 1013c.2), with 4 additional amino acids at the C-terminus, reacted more efficiently with the 5/24 antibody, than the 9 amino acids mapped. This may be because the protein epitope sequence contained additional amino acids to those detected by the SPOTs technique.

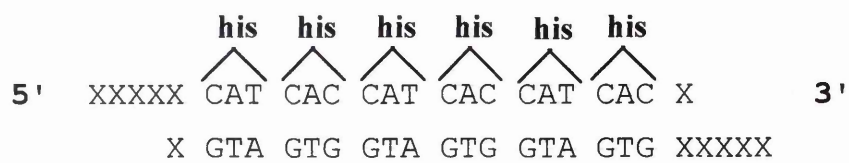
Two rabbits were inoculated with oligopeptide 1013c.2. However, extensive analysis showed no evidence of any anti-1013c.2 antibody being produced by either rabbit. It can only be concluded that since 1013c.2 was synthesised as a MAP on a 4-branched resin and inoculated in the presence of an adjuvant, that it must have very low immunogenicity.

Although it was not possible to produce rabbit antibodies, this work has successfully produced a new epitope tag, CAT208, which reacts with the 5/24 mouse monoclonal antibody. This tag can be used as a tool to label proteins which have no, or only poor, antibodies against them and was used in this context to label VP5 and VP26. CAT tagged VP5 and VP26 constructs were used in immunofluorescence studies and a bacterially expressed, epitope labelled VP26, was also used in Western blot analysis.

CHAPTER 4

PURIFICATION OF VP26 AND VP5

Figure 4.1: Example of a 6xhis Tag Sequence



1. Introduction

VP25 had been shown to be a...

VP25 and VP30 are the major...

Figure 4.1: The two combinations of base pair sequences (ie CAT and CAC) encoding the amino acid histidine (his) are grouped. Six consecutive histidines represent a 6xhis tag and a possible combination of residues is shown in this figure.

VP25 and VP30 are the major...

1. Introduction

VP26 had been demonstrated to interact with VP5 by immunofluorescence (Rixon *et al*, 1996) and in recombinant baculoviruses (Tatman *et al*, 1994; Thomsen *et al*, 1994). However, to study the interaction of VP26 with VP5 at a molecular level, it was felt that it would be useful to express the VP26 protein in a bacterial expression vector. This is a powerful technique for cloning and expressing recombinant proteins and has several advantages:

- large quantities of protein are produced from a relatively small culture.
- the process is rapid.
- mutant versions of VP26 were easily constructed and expressed.

The UL35 ORF was therefore cloned into a pET expression plasmid (supplied by Novagen). This plasmid contained a 6xhis tag (see figure 4.1) which could be utilised to purify the recombinant protein through a Ni²⁺ agarose column. The expression vector was modified to include a novel EcoRI site (designated pETmod), in the correct reading frame for subcloning the UL35 ORF. The UL35 ORF was isolated from pE35T1 (see Chapter 3, Section 2.3.3) and cloned into pETmod, placing the VP26 sequences downstream from the 6xhis tag. Finally, the N-terminal sequences were removed and replaced with an oligonucleotide encoding the pp65 and 6xhis tags.

As described in Section 3, a VP5 protein, also encoding a 6xhis tag, was generated in a baculovirus expression vector. The pp65 epitope tag had been cloned into pSJM1965 (see Chapter 3, Section 2.3.2) with unique restriction enzyme sites flanking it, therefore the pp65 tag could be easily removed and replaced with an oligonucleotide encoding the 6xhis tag. The UL19 ORF, encoding the 6xhis tag was then subcloned into a baculovirus expression vector, pAcCl29.1.

Expression of 6xhis tagged versions of VP5 and VP26 allowed both proteins to be isolated and purified rapidly. It was important to have pure and soluble proteins available

Figure 4.2: Construction of pET35pp65

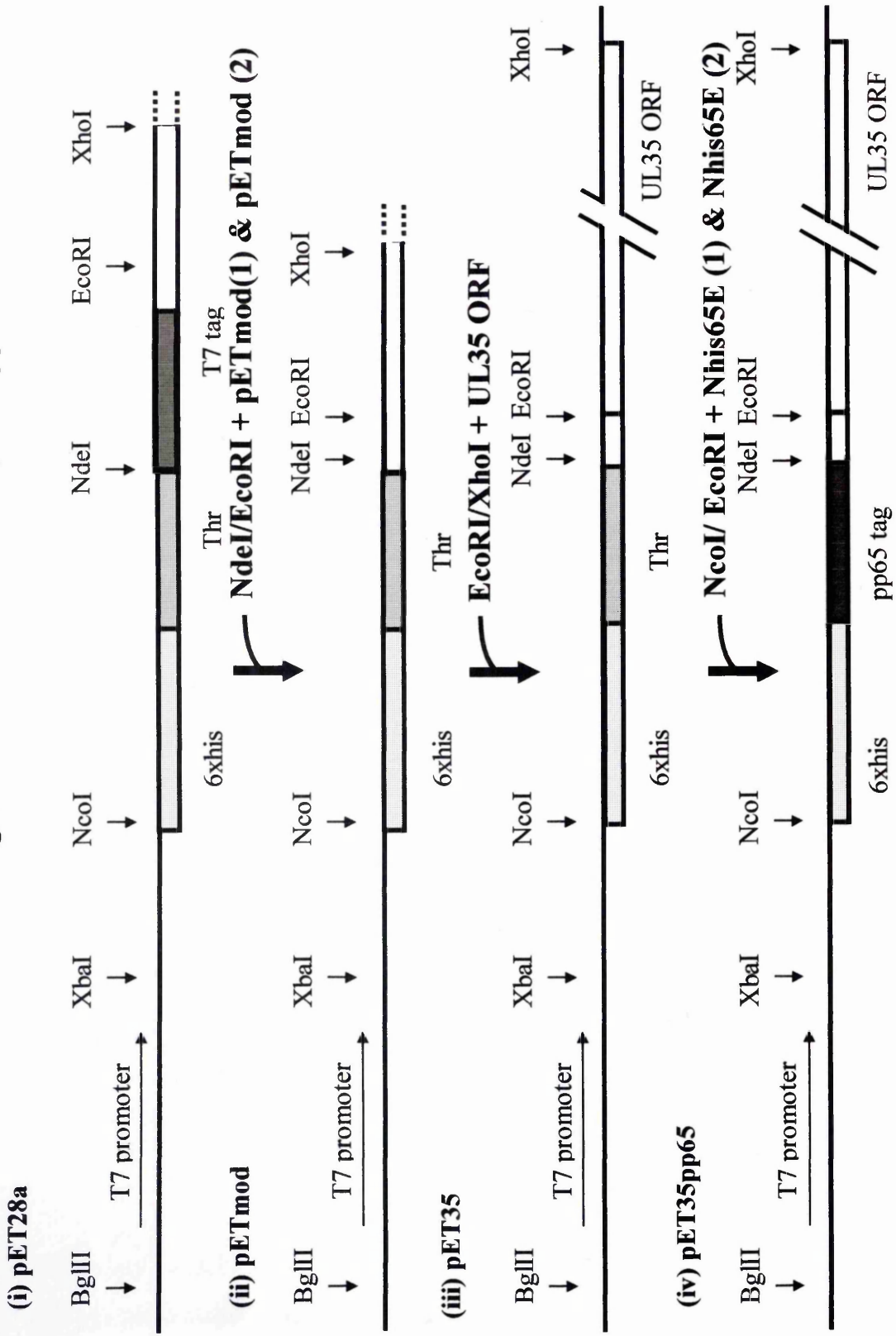


Figure 4.2: The pET28a vector [panel (i)] was EcoRI/NdeI digested to inset oligonucleotides, pETmod (1) & pETmod (2) [see figure 4.3, panel (i)], which genetically modified the restriction enzyme sites for the cloning strategy and give pET28amod [panel (ii)]. This had a novel EcoRI site in the correct reading frame context for subcloning the UL35 ORF and also removed the T7 epitope tag sequence from the vector. The UL35 ORF was isolated as an EcoRI/XhoI fragment from pE35T1 (see Chapter 3, Section 2.3.2.4) and ligated into EcoRI/XhoI digested pET28amod. This placed the gene downstream of the 6xhis and the thrombin cleavage site (Thr) to generate pET35 [panel (iii)]. For expression of an epitope tagged version of VP26, the N-terminal sequences were removed and replaced with two complementary oligonucleotides [Nhis65 (1) and Nhis65 (2), see figure 4.3, panel (ii)]. These were made and inserted into NcoI/EcoRI digested pET35 to generate pET35pp65 [panel (iv)]. This construct encodes a 6-histidine tag and the pp65 epitope tag linked in-frame at the N-terminus of the VP26 protein.

This figure is not drawn to scale.

Figure 4.3: Oligonucleotides Required for Cloning the VP26 Coding Sequence into a Bacterial Expression Vector

(i) pETmod

(1) NdeI EcoRI
TATGGGAATTCCGGATCCACTAGTAC
(2) ACCCTTAAGGCCTAGGTGATCATGTTAA
ΔEcoRI

(ii) Nhis65E

(1) NcoI pp65
CATGGGCAGCACCCATCATCATCATCACGCCGAGCGCAAGACGC
(2) CCGTCGTGGGTAGTAGTAGTAGTAGTACGGCTCGCGTTCTGCG
6xhis

(1)
CCCGCGTCACCGGCGGAATGGG
(2) GGGCGCAGTGGCCGCCTTACCTAA
EcoRI

Figure 4.3: The sequence of the oligonucleotides used in creating pET28amod [panel (i)] and pET35pp65 [panel (ii)], see figure 4.2. pETmod (1) and (2) were inserted into NdeI/EcoRI digested pET28a, to generate pETmod. This insertion destroyed the original EcoRI site (ie ΔEcoRI) and generated a new one.

Nhis65E (1) and (2) inserted the 6xhis and pp65 tag sequences into NcoI/EcoRI digested pET35 to generate pET35pp65, which encoded VP26 with the 6xhis and pp65 tags linked in-frame at the N-terminus.

which could be used in a series of interaction and structural studies (see Chapter 5). If the proteins were not in this form, it would be difficult to obtain accurate data about their properties. For example, in an interaction assay system, if contaminating proteins were present, they may participate in non-specific binding interaction, creating false positive results. Similarly if the proteins were in a soluble but denatured form, the secondary structure of the protein would be affected making interaction and structural analyses unsuccessful. So, to ensure that accurate data was produced from future studies, it was important at the outset to spend time and effort producing pure and soluble VP26 and VP5 proteins.

2. VP26

2.1 Construction of Expression Plasmid

2.1.1 pET28mod

The pET28a(+) [figure 4.2, panel (i)], supplied by Novagen, was modified for subsequent cloning procedures by the insertion of synthetic oligonucleotides [figure 4.3, panel (i)] to generate pET28mod [figure 4.2, panel (ii)]. The pET28a(+) vector was NdeI/EcoRI digested and ligated with two complementary oligonucleotides pETmod (1) and pETmod (2). This placed a novel EcoRI site in the correct reading frame context for sub-cloning the UL35 ORF, from pE35T1, and simultaneously removed a T7 epitope tag sequence from the vector.

2.1.2 pET35pp65

The UL35 ORF was isolated as an EcoRI/XhoI fragment from pE35T1 (see Chapter 3, Section 2.3.3) and sub-cloned into EcoRI/XhoI digested pET28mod. This placed the VP26 sequences downstream of the 6xhis tag and thrombin cleavage site, generating pET35 [figure 4.2, panel (iii)]. For expression of an epitope tagged version, two complementary oligonucleotides [Nhis65E (1) and Nhis65E (2)] [figure 4.3, panel (ii)] were made and inserted into NcoI/EcoRI digested pET35 to give pET35pp65 [figure 4.2, panel (iv)]. This construct encodes a 6xhis tag and the HCMV pp65 epitope tag linked in-frame at the N-terminus of the VP26 protein, under the control of the strong bacteriophage T7 transcription promoter.

**Figure 4.4: Comparison of the Amino Acid Sequences of
VP26 and VP26pp65**

VP26 MAVPQFHRPSTVTTDSVR
VP26.pp65 MGSSHHHHHAERKTPRVTGGMGIQAVPQFHRPSTVTTDSVR

ALGMRGLVLATNNSQFIMDNNHPHPQGTQGAVREFLRGQAAALTDLGLAHANNT
ALGMRGLVLATNNSQFIMDNNHPHPQGTQGAVREFLRGQAAALTDLGLAHANNT

FTPQPMFAGDAPAAWLRPAFGLRRTYSPFVVREPSTPGTP*
FTPQPMFAGDAPAAWLRPAFGLRRTYSPFVVREPSTPGTP*

Figure 4.4: Due to the presence of additional sequences contributed by the pp65 epitope (double underline) and the 6xhis (single underline) tags, VP26pp65 has 24 amino acids at the N-terminus which are not present in wild-type VP26.

Figure 4.5: Expression of pET35pp65

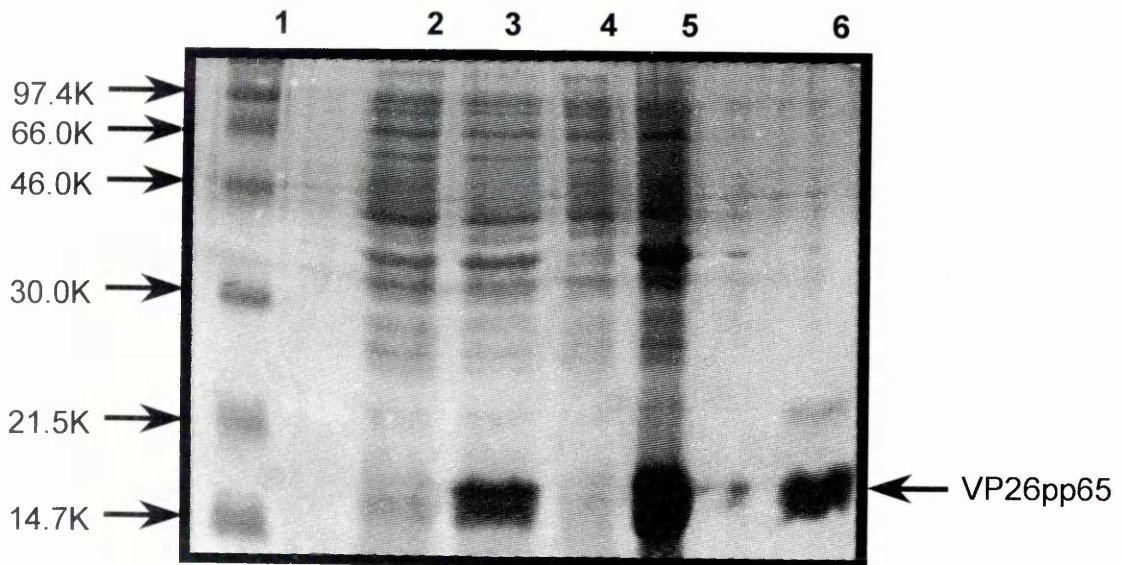


Figure 4.5: Coomassie brilliant blue stained gel showing size markers (lane 1), uninduced pET35pp65 culture (lane 2) and 1mM IPTG (37°C, 2h) induced pET35pp65 culture (lane 3), supernatant (lane 4) and pellet (lane 5) fractions. Ni-NTA purified VP26pp65 is shown in lane 6 and the position of VP26pp65 is marked with an arrow.

As there are extra amino acid residues contributed by the pp65 epitope and the 6xhis tags, VP26pp65 is larger than wild type VP26. There are 24 amino acid residues at the N-terminus of the tagged protein, which are not present in wild type protein (see figure 4.4). This means that the Mr of VP26 is 12096 Da compared to a Mr of 14733 Da for VP26pp65.

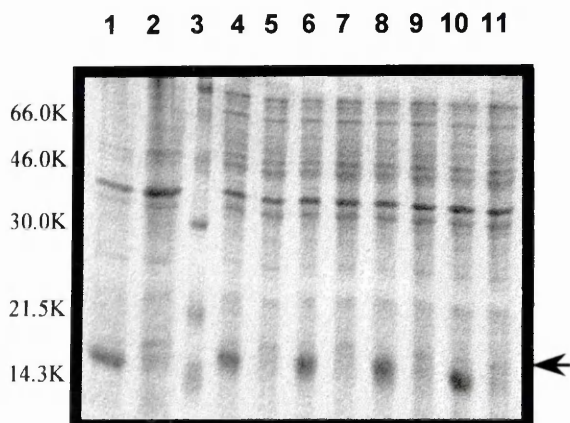
2.2 Expression of VP26pp65

Since preparations of proteins in cells grown from glycerol stocks were often unstable (a common feature of the pET vector) better and more reproducible expression was obtained by transfecting pET35pp65 DNA into fresh bacteria each time. A single colony was then sub-cultured into 100ml growth medium in a 1l glass flask. This provided abundant aeration, important for good expression and induction. The bacteria were grown at 37°C, with agitation, until the $A_{600}=0.5$. 500µl of 'uninduced' (U) bacteria were then removed and pelleted. These bacteria contain a chromosomal copy of the T7 RNA polymerase gene under the control of lacUV5. The addition of IPTG induced expression of the T7 polymerase which transcribed the target gene. IPTG was added to the batch culture, to a final concentration of 1mM and incubation continued for 2-3h, after which another 500µl of 'induced' (I) sample was removed and pelleted. The U and I samples were resuspended in 1x dissociation mix and analysed by SDS-PAGE (see figure 4.5, lanes 2 and 3). The remaining culture was harvested at 3000 rpm for 15 min in 225ml falcon tubes. The pellet was stored at -20°C until required.

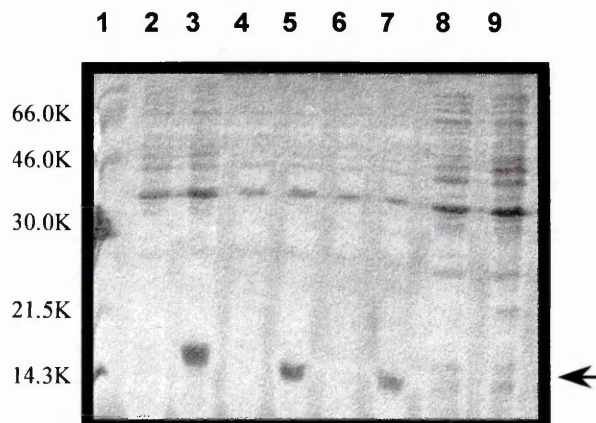
It is clear from the gel (figure 4.5) that the expression levels of VP26pp65 protein were extremely high. When comparing the U and I tracks (lanes 2 and 3 respectively), VP26pp65 was the most abundant protein produced after induction with IPTG. It should be noted that this expression level was not consistently achieved if a glycerol stock was used to inoculate the culture, or a 100ml culture was grown up in a reaction vessel of less than a 1l capacity. If these less favourable conditions were used the protein would either fail to induce, or the expression levels were severely inhibited.

Figure 4.6: Attempts to Solubilise VP26pp65

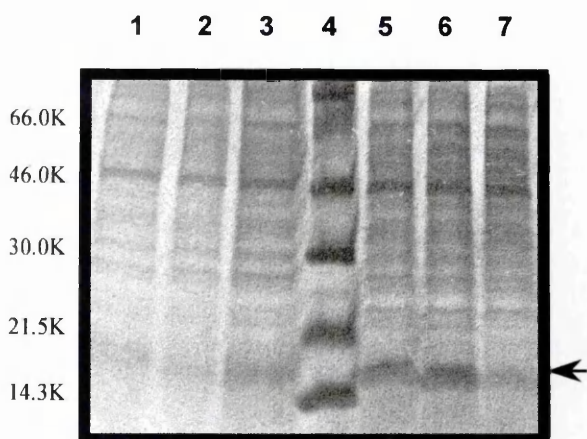
(i) Induction Time at 37°C



(ii) Bacterial Density at Induction



(iii) Concentration of IPTG at Induction



(iv) Sonication Buffer

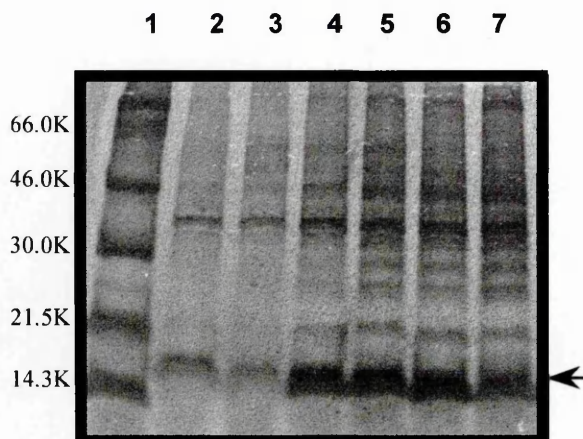


Figure 4.6: Panels (i) to (iv) are coomassie brilliant blue stained gels with 20 μ l of each sample run per well. The arrow in each panel marks the expected position of VP26pp65.

Panel (i) lane 1 shows a typical example of the level of induction, at 37°C with 1mM IPTG for 2h, as compared to the uninduced sample (lane 2). Lane 3 shows the size markers while lanes 4 to 11 represent alternate pellet and supernatant fractions after 2h (lane 4 & 5), 4h (lane 6 & 7), 6h (lane 8 & 9) and o/n (lane 10 & 11) induction with 1mM IPTG. In each case VP26pp65 was detected in the pellet fraction.

Panel (ii) lane 1 shows the size markers. Lanes 2 to 9 represent alternate supernatant and pellet fractions, after induction with 1mM IPTG for 2h at 37°C, when the A_{600} equaled, 0.5 (lanes 2 & 3), 0.4 (lanes 4 & 5), 0.3 (lanes 5 & 6) and 0.2 (lanes 8 & 9). In each case VP26pp65 was detected in the pellet fraction.

Panel (iii) lane 4 shows the size markers, while lanes 1, 2, 3 and 5 represent induced samples after 2h at 37°C with, 0.1mM IPTG (lane 1), 0.2mM IPTG (lane 2), 0.5mM IPTG (lane 3) and 1mM IPTG (lane 5). Lanes 6 and 7 represent the pellet fraction of the 1.0mM and the 0.5mM, respectively, induced samples.

Panel (iv) lane 1 shows the size markers. Lanes 2 to 7 represent the pellet fractions after sonication in the presence of the various 'Good buffers' (see table 4.1).

2.3 Solubility of VP26pp65

The induced bacterial pellet, containing VP26pp65, was resuspended in Sonication Buffer [20mM tris-HCl (pH8.0), 10% glycerol, 0.1% NP40 (as recommended by the QIAexpressionist protocol, Qiagen)] by probe sonication for 5x 10 sec. The solution was spun at 10000 rpm in SM24 tubes to pellet the debris. However, the protein failed to solubilise and upon analysis by SDS-PAGE, VP26pp65 was consistently found in the insoluble pellet fraction and never in the soluble supernatant fraction (figure 4.5, lanes 5 and 4 respectively).

As VP26pp65 was insoluble, extensive investigative measures were undertaken at each stage of the expression procedure, to try and reduce aggregation of the protein and therefore solubilise it. The ultimate aim was to produce pure and soluble VP26pp65 which had native secondary structure and could be used in interaction and structural studies. Unfortunately, this task proved to be extremely difficult. Considerable time and effort was spent varying procedures under non-denaturing and eventually, denaturing conditions to produce suitable VP26pp65 protein. Some of the variations attempted are detailed in the following sections.

2.3.1 Temperature and Time of Induction

It had been reported (QIAexpressionist protocol, Qiagen) that varying the time and temperature of induction could result in the production of soluble protein.

A series of 10ml cultures were set up and induced at 15°C, 20°C and 37°C. For each temperature, the culture were harvested after induction for 2h, 4h, 6h or o/n. The cells were resuspended in sonication buffer and spun as before. Supernatant and pellet fractions were compared on a minigel (15°C and 20°C fractions are not shown).

At each temperature and time point, the protein was detected in the pellet fraction alone [see figure 4.6, panel (i) as a representative example] showing that there had been no effect on the solubility of the protein. At both 15°C and 20°C, there was a slightly

reduced yield of protein, as compared to 37°C (not shown). Induction for 2-4h at 37°C appeared to be a sufficient induction time for producing large amounts of protein.

2.3.2 Bacterial Density

The 'QIAexpressionist' protocol (Qiagen, also suggested that reducing the density of the bacterial culture at the time of induction could help prevent protein aggregation. Therefore, the A_{600} at induction was varied from 0.2, increasing at 0.1 intervals, to 0.5. The induced samples were resuspended in sonication buffer by sonication, centrifuged and the resulting supernatant and pellet fractions analysed by SDS-PAGE [figure 4.6, panel (iii)]. Although the total amount of VP26pp65 induced, increased in line with the increasing cell density, there was no effect on protein solubility. In all cases VP26pp65 was exclusively found in the pellet fractions.

2.3.3 Concentration of IPTG at Induction

The effects of varying the concentration of IPTG, during induction, was also tested [figure 4.6, panel (iii)]. IPTG was added at 0.1mM, 0.2mM, 0.5mM and 1mM, for 2h at 37°C. The VP26pp65 protein did not induce significantly at levels below 0.5mM. Greatest induction was consistently observed at concentrations of 1mM. The bacterial cells were harvested and resuspended in sonication buffer. After analysis of supernatant and pellet fractions, it was clear that there was no effect on the solubility of any of the induced proteins, which remained entirely in the pellet fraction (figure 4.6, lanes 6 and 7).

2.3.4 Time, Temperature and Concentration of IPTG at Induction

The time, temperature and concentration of IPTG at induction were varied in multiple combinations however, the solubility of the VP26pp65 protein remained constant and was found exclusively in the pellet fractions (not shown).

2.3.5 Treatment with Various Buffers and pH Conditions

As it did not seem possible to produce soluble protein by varying conditions at the expression level, it was decided to try and solubilise the protein from the bacterial pellet. A 100ml culture was grown to $A_{600}=0.5$ and induced, at 37°C for 2h, with IPTG. The suspension was aliquoted and harvested at 3000 rpm for 10 min in 15ml Falcon tubes. Attempts were then made to solubilise the VP26pp65 protein from the pellet fractions.

Table 4.1: 'Good Buffers' to Solubilise VP26pp65

'GOOD BUFFER' (20mM)	BUFFER pH	Corresponding lane in figure 4.6, panel (iv)
MES	6.0	2
BIS TRIS	6.5	3
PIPES	7.0	4
HEPES	7.5	5
TRIS	8.0	(figure 4.5, lane 5)
CHES	9.0	6
CAPS	10.0	7

Results

The bacterial pellicles were grown and harvested continuously in different media as described in the figure. Using the same amount of the same cells, the results had been the same. The results showed that the growth of the cells was not affected by the presence of the different buffers. The results also showed that the growth of the cells was not affected by the presence of the different buffers. The results also showed that the growth of the cells was not affected by the presence of the different buffers.

Table 4.1: All the 'Good Buffers' (supplied by Sigma) were prepared at 20mM, in a solution containing 10% glycerol and 0.1% NP40. The pH of the buffer was altered using HCl or NaOH as required. All the fractions were run on gels [see figures 4.5. lane 5 and 4.6, panel (iv)].

The bacterial pellet was probe sonicated, using a Branson soniprobe, in various detergent containing buffers with different pH values (see table 4.1). All the buffers used were described in the Sigma catalogue under 'Good Buffers'. The solutions were prepared with 20mM of the appropriate Good Buffer, 10% glycerol and 0.1% NP40. After the pellet had been thoroughly disrupted, the solution was centrifuged at 10000 rpm for 10 min in SM24 tubes and the supernatant and pellet fractions analysed by SDS-PAGE.

None of the buffers solubilised the VP26pp65 protein as the protein was always exclusively present in the pellet fractions [figure 4.6, panel (iv)] and was not found in any of the supernatant fractions. However, many contaminating bacterial proteins were differentially solubilised by the buffers, helping to clean up the VP26pp65 preparation. The results obtained with 20mM tris (pH 8.0) were as good as those with any other of the buffers tested. Therefore, it was decided that the original buffer used for sonication steps previously, 20mM tris (pH 8.0), 10% glycerol and 0.1% NP40, would be used to wash the bacterial pellet in all subsequent experiments. This will hence forth be referred to as the Sonication Buffer.

2.3.6 Treatment with Denaturant

Even trace amounts of soluble VP26pp65 had not been detected in any of the supernatant fractions analysed in the previous sections. A large range of non-denaturing conditions, some recommended by Qiagen and others standard approaches to solubilising proteins during expression, had been extensively tested and failed. The time, temperature and conditions of induction had been varied in multiple combinations. Several different buffers and pH conditions had been used to try and solubilise the protein from the bacterial pellet.

Until soluble protein was produced, it was impossible to proceed and purify the protein through Ni²⁺ agarose. The only avenue left open appeared to be to try and denature the protein and at some subsequent stage refold it. The QIAexpressionist protocol reported that denatured proteins could still be effectively purified through Ni²⁺ as the 6xhis tag was not affected. Therefore, the washed pellet of an induced culture was resuspended in the presence of a denaturant, 6M GuHCl. The pellet was resuspended, by probe sonication with a Branson soniprobe in Buffer A [6M GuHCl, 100mM NaH₂PO₄, 10mM tris

**Figure 4.7: Treatment of VP26pp65 with
6M GuHCl**

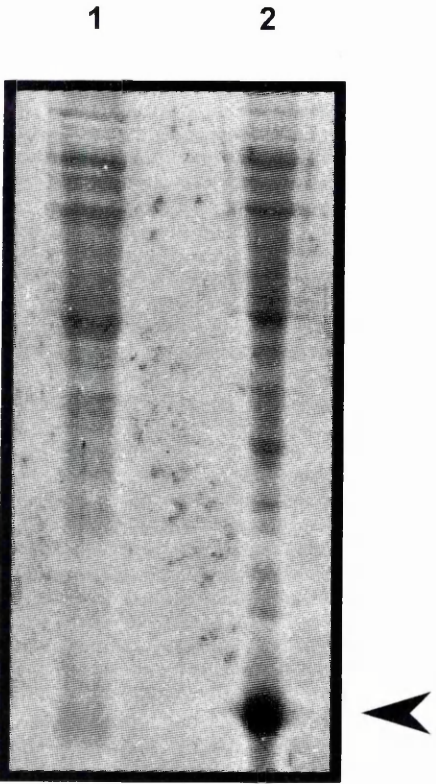


Figure 4.7: Coomassie brilliant blue stained gel showing pellet (lane 1) and supernatant (lane 2) fractions of a culture induced with 1mM IPTG (2h, 37°C), washed in Sonication Buffer, resuspended in Buffer A [6M GuHCl, 100mM NaH₂PO₄, 10mM tris (pH8.0)] and spun to separate the two fractions.

An arrow marks the position of VP26pp65. Markers not shown.

Figure 4.8: Schematic Representation of the Interaction of 6xhis Tagged Proteins with the Ni-NTA Resin

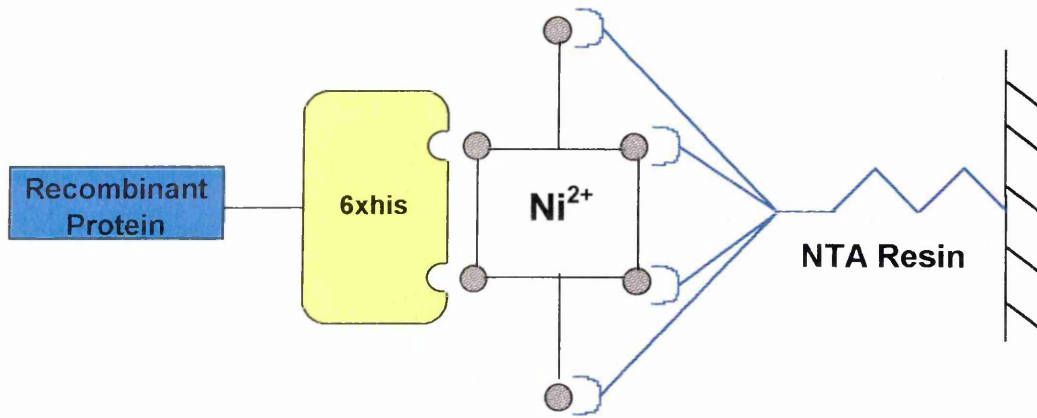
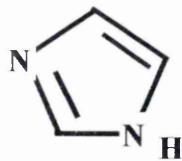


Figure 4.9: Comparison of the Structures of Imidazole and Histidine

(i) Imidazole



(ii) Histidine

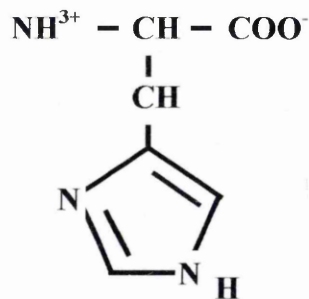


Figure 4.8: Recombinant proteins encoding a 6xhis tag (yellow) bind to the 2 free ligand sites (grey circles) of Ni^{2+} , which are not occupied by the NTA resin (blue). This immobilises the recombinant proteins on the Ni-NTA resin.

Figure 4.9: The structure of imidazole [panel (i)] and the side arm of histidine [panel (ii)] are very similar.

(pH8.0)]. The suspension was mixed end-over-end at rt for 1-2h and spun at 10000 rpm for 10 min in SM24 tubes. The pellet and supernatant fractions were TCA precipitated and analysed by SDS-PAGE. This time, most of the protein was detected in the supernatant fraction (figure 4.7). This means that the greatest percentage of VP26pp65 had been solubilised and could now be purified.

2.4 Purification of VP26pp65

2.4.1 Binding of VP26pp65 to Ni-NTA Agarose

The presence of the 6xhis tag in the pET vector, allowed soluble VP26pp65 protein to be purified through a Ni²⁺ column, by affinity chromatography against the Ni²⁺ agarose. Qiagen supplied a Ni-NTA agarose which consisted of NTA (nitrilo-tri-acetic acid), a stable high capacity resin, with Ni²⁺ tightly complexed to it. Ni²⁺ has 6 ligand binding sites and the NTA occupies 4 of these. This leaves 2 free sites to interact with the 6xhis tag (see figure 4.8). Binding of 6xhis tagged proteins to the charged agarose did not require functional protein structure and so the presence of the 6M GuHCl in the buffer did not interfere with binding.

Soluble 6xhis protein in Buffer A was typically mixed at rt for 1h with 500µl of Ni-NTA which had been pre-equilibrated in Buffer A and resuspended as a 50% slurry (Ni-NTA has a binding capacity of 10mg of 6xhis tagged protein per ml of resin). The mixture was loaded onto a 0.8 x 4.0 cm poly-prep column (Bio-Rad) and allowed to settle. Unbound proteins were allowed to drain through the column by gravity. A series of washing and elution steps followed.

Imidazole was used to elute the protein from the agarose. Imidazole has a similar structure to the side chain of histidine (see figure 4.9) and so competes with and displaces the tagged proteins from the resin.

2.4.2 Denaturing Elution Conditions

As the previous work had shown VP26pp65 to be extremely insoluble, the protein was initially eluted from the column in the presence of denaturant. It was felt that this

Figure 4.10: Elution of VP26pp65 with Imidazole and 8M Urea

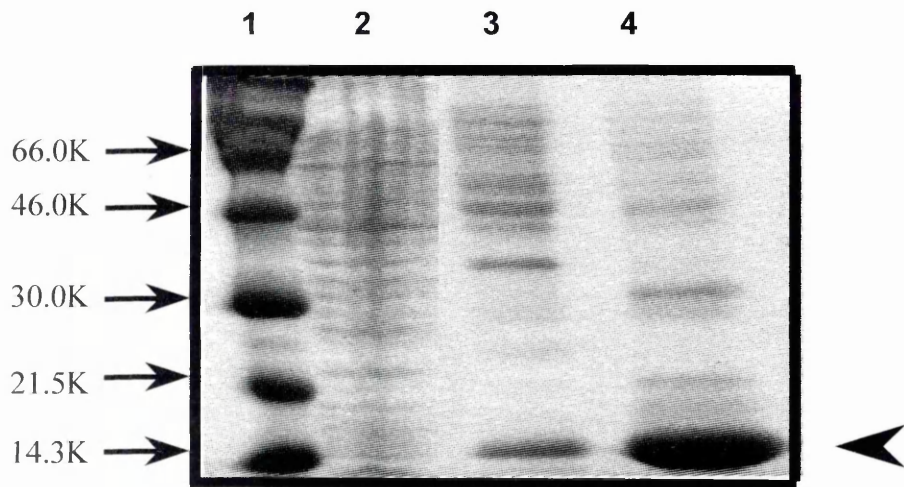


Figure 4.10: Coomassie brilliant blue stained gels. Panel (i) lane 1 shows the size markers while panels 2, 3 and 4 represent the elutions through Ni-NTA, with VP26pp65 bound. Buffer C (lane 2), Buffer D (lane 3) and Buffer E (lane 4), contained 8M urea and 20mM, 60mM or 200mM concentration of imidazole respectively. VP26pp65 was mainly eluted in Buffer E.

The position of VP26pp65 is marked with an arrow.

approach had more chance of succeeding and at this stage it was important to test whether the Ni-NTA purification system would work.

8M urea was added to a phosphate buffer, Buffer B (8M urea, 100mM NaH₂PO₄, 10mM tris HCL (pH8.0), suggested by Qiagen) and this was used to wash the resin. Urea was used, as oppose to 6M GuHCl, for two reasons. Firstly, it is a milder denaturant and secondly, it allowed fractions to be analysed directly on gels without the requirement for removing the GuHCl, which precipitates in loading buffer. A range of concentrations of imidazole were used to see if any eluted the protein from the column. Imidazole at either 20mM, 60mM or 200mM was mixed with Buffer B. The phosphate buffers containing imidazole and 8M urea were designated Buffers C-E (Materials, Section 1.11).

Buffer C, containing 20mM imidazole, removed many of the contaminating proteins (figure 4.10, lane 2). Background contamination can occur from proteins that contain neighbouring his residues and therefore have a low affinity for the Ni-NTA resin. Other proteins may be linked to 6xhis tagged proteins non-specifically or bind the resin non-specifically.

Buffer D, containing 60mM imidazole, removed a little VP26pp65 protein and most of the contaminating proteins which may have been more tightly bound (figure 4.10, lane 3).

Buffer E contained 200mM imidazole. This removed relatively clean VP26pp65 protein from the resin (see figure 4.10, lane 4). The contaminating proteins could be removed by more extensive washing of the resin. Examination of these fractions on a 15% minigel revealed that only a single band, of the expected Mr for VP26pp65, was present (see figure 5.5, panel (iii), lane 5). This shows that the protein has been successfully eluted from the resin, in the absence of any contaminating proteins. If a 70-100ml culture was induced, typically 1-3ml of 5mg/ml (by Bradford assay) of VP26pp65 protein would be produced.

It was now clear that it was possible to produce soluble VP26pp65 bacterially expressed protein, which could be purified successfully through Ni²⁺ agarose. However, denaturant (8M urea) was present at all stages of the purification process. It was essential to remove the 8M urea from the solution, whilst still keeping VP26pp65 soluble, for all subsequent analysis procedures.

2.4.3 Non-denaturing Elution Conditions

As a general rule, protein re-folding should take place slowly to avoid the formation of insoluble aggregates. A few approaches were therefore tried under non-denaturing conditions, to try and produce soluble, pure and non-denatured protein.

Trying to refold the protein on the column was potentially a valuable method, as it is known that immobilising one end of a protein can prevent the formation of mis-folded aggregates, while the denaturant is removed. In this case, the N-terminus of VP26pp65 protein was attached to the Ni-NTA through the 6xhis tag. Many elution buffers were tested to try and remove non-denatured VP26pp65.

(i) Vary Imidazole Concentrations

Qiagen suggested the use of a phosphate buffer [100mM NaH₂PO₄, 10mM tris (pH 8.0)] containing imidazole for elution under non-denaturing conditions. Increasing concentrations of imidazole at 20mM intervals, from 20mM to 200mM, were added in the phosphate buffer to try and elute the protein from the resin.

However, the VP26pp65 protein was not eluted from the resin at any imidazole concentration when the denaturant was absent. Even 200mM concentrations of imidazole failed to remove any VP26pp65 from the column. As it was known that 200mM imidazole was sufficient to remove VP26pp65 from the resin under denaturing conditions, it was clear that the imidazole concentration was sufficiently stringent. It seemed clear that the protein had precipitated on the column and may have formed insoluble aggregates or multimers.

(ii) Reduce Denaturing Conditions Slowly

Attempts were made to reduce the concentration of denaturant over subsequent washing and elution steps. This meant that 8M urea was present in the initial wash with phosphate buffer alone. This was reduced to 4M urea in the wash containing 20mM imidazole and 2M urea, in the wash containing 60mM imidazole. No urea was present in the 200mM imidazole elution buffer.

This approach was used in the belief that re-folding should take place slowly. Unfortunately this proposal was also unsuccessful and failed to elute VP26pp65 from the column. The protein was assumed to have precipitated out again.

(iii) Vary pH and Imidazole Concentrations

It is known that reducing the pH causes histidine residues to become protonated and so dissociate from the Ni^{2+} . The pH of the phosphate buffer was therefore varied with HCl and used at pH 8.0, pH 6.3, pH 5.9 and pH 4.5 (recommended by Qiagen). These buffers were designated Buffers 1-4 respectively.

However, no VP26pp65 protein was eluted at any of the pH values tested (data not shown). This re-reinforces the point that this protein is extremely insoluble and highly resistant to attempts at solubilisation

A final attempt was made to combine the approaches taken in (i) and (iii) and elute the protein from the column in the absence of denaturant. Imidazole at 20mM, 60mM and 200mM was dissolved in the phosphate buffers 1-4, with varying pH values (pH 8.0, 6.3, 5.9, and 4.5 respectively). This meant that 12 different elution buffers were used in a series of experiments.

After carefully analysing all the wash and elution fractions on a 15% minigel, it was concluded that no VP26pp65 protein had been eluted from the Ni-NTA with any of the buffers tested (data not shown).

It was decided to revert back to the successful washing and elution conditions, outlined in Section 2.4.2, which were carried out in the presence of the denaturant, 8M urea, at all stages.

2.5 Re-naturation of VP26pp65

It had been possible thus far, to consistently produce bacterially expressed VP26pp65, in a very pure and soluble form from a 70-100ml culture. The only drawback was that the protein was in the presence of denaturant, therefore attempts were made to remove the 8M urea by dialysis. Protein was dialysed against NTE. NTE was a suitable solution for the protein to be in, as it could be used in this form in ELISA reactions, capsid experiments, sizing and characterisation studies.

Initially a straight dialysis of VP26pp65 was tried. 500µl of protein, in buffer E, was dialysed against 1.5l of NTE at 4°C. The protein came out of solution within 10 min and a visible white precipitate was observed in the dialysis sack. Nevertheless, the dialysis was continued o/n and the solution spun at 80000 rpm for 10 min, in a Beckman TL100 ultra centrifuge, to pellet the precipitated protein. The supernatant fraction was carefully removed and examined by SDS-PAGE analysis. No soluble VP26pp65 was detected in the dialysed supernatant fraction indicating that all of the protein had precipitated out of solution.

Rapid dilution followed by slowly dialysis of the denaturant, has been reported to allow re-naturation of a protein to its native secondary structure. The conditions and extent of dilution vary for individual proteins.

1ml of VP26pp65 protein in Buffer E was diluted in NTE, 20-fold, 10-fold and 2-fold (ie added to 19ml, 9ml and 1ml of NTE respectively). The diluted proteins were dialysed at 4°C o/n against 1.5l of NTE. After incubation the dialysis sacks were visually inspected. No protein precipitate was evident in the 1:10 or 1:20 dilution sacks. At 1:2 dilution a large amount of precipitate was visible.

As before, all the dilutions were spun at 80000 rpm for 10 min, in a Beckman TL100 ultra centrifuge, to ensure any precipitated protein was pelleted. The supernatant fractions were

Figure 4.11: Rapid Dilution and Dialysis of VP26pp65

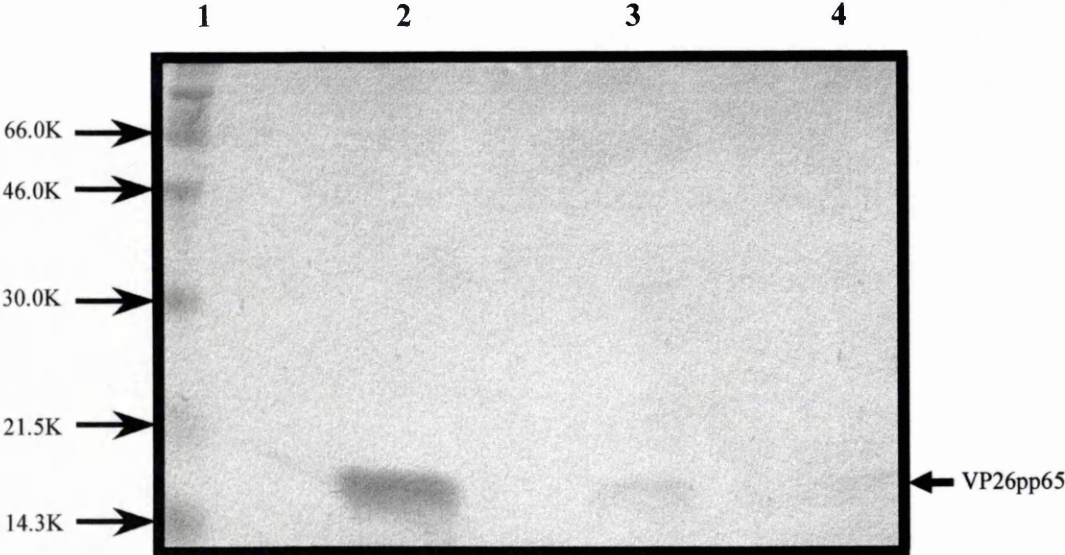


Figure 4.11: Coomassie brilliant blue stained gel showing VP26pp65 supernatant fractions. Lane 1 shows the size markers while lanes 2, 3 and 4 represent the Ni²⁺ purified VP26pp65, rapidly diluted, 1:2 (lane 2), 1:10 (lane 3) and 1:20 (lane 4) in NTE (ie added 1ml of purified VP26pp65 to 1ml, 9ml and 19ml of NTE respectively), dialysed o/n at 4°C and spun at 80000 rpm for 10 min.

removed and analysed by SDS-PAGE (figure 4.11). No protein was evident from the 1:20 dilution (lane 4) and only a very faint band was detected for the 1:10 dilution (lane 3). This may purely reflect a quantitative problem, in that the protein was so dilute that it was unable to be detected, rather than it had precipitated out. A band was observed at the 1:2 dilution (lane 2). However, a Bradford assay detected protein concentrations between only 0.5-1mg/ml. This meant that only 20-40% of the total protein inserted into the dialysis sack had remained in solution.

As there appeared to be less problem with precipitation at the 1:10 and 1:20 dilutions attempts were made to concentrate VP26pp65 by reducing the volume after dialysis. Two approaches were used in parallel:

- (i) Some of the solution was spun through Centricon-10 spin tubes (Amicon). These tubes had a molecular weight cut-off of 10000 Da. This meant that anything above this weight, ie VP26pp65 at approximately 14700 Da, would be retained by the filter. The tubes were spun at 10000 rpm in an SM24 rotor, until 5ml of solution had been concentrated to 1ml.
- (ii) Some of the solution was concentrated using Ultra-thimbles (Scliecher & Shuell). The thimbles also had a molecular weight cut-off of 10000 Da and so were able to retain VP26pp65 (14700 Da). In this case, the solution was concentrated by extracting liquid through the thimble walls, by means of a vacuum pump. Again, 5ml was concentrated down to 1ml.

Both of these attempts were unsuccessful and the concentration of protein was not increased as the volume was decreased. It can only be assumed that the protein was precipitating out of solution. In the case of the centricon tubes, the protein may have stuck to the filter and with the Ultra-thimbles, it may have stuck to the thimble walls.

Since diluting the VP26pp65 protein 2-fold in NTE, and slowly dialysing it at 4°C o/n, had resulted in a usable yield of protein, this approach was used for all future analyses (Chapter 5).

Figure 4.12: Construction of pAcCl19his (191A)

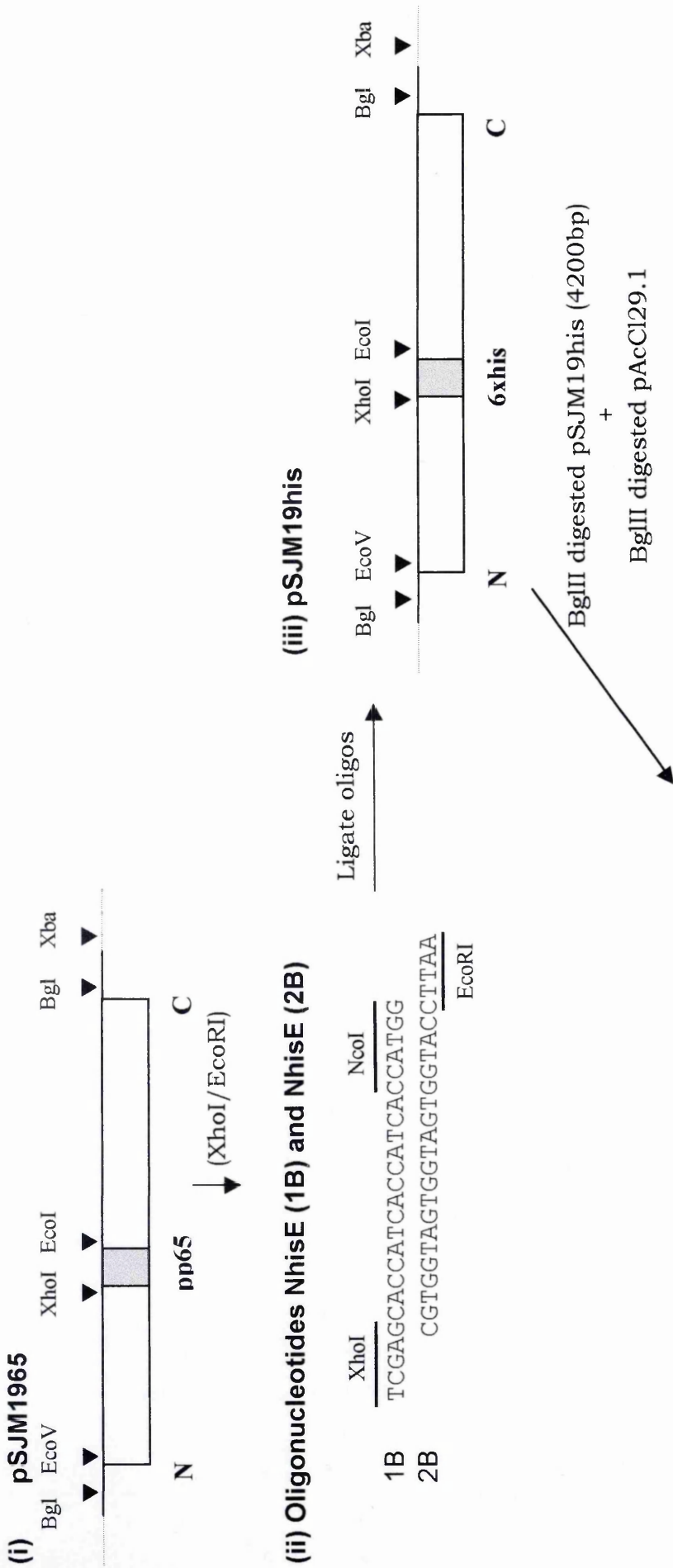


Figure 4.12: pSJM1965 [panel (i)], described in figure 3.3, was XhoI/EcoRI digested, to remove the pp65 tag, and ligated with oligonucleotides NhisE (1B) and NhisE (2B) [panel (ii)] to generate pSJM19his [panel (iii)]. This construct was BglII digested, to release the 4200 bp UL19 fragment, and ligated with BglII digested pAcCl29.1. This generated pAcCl19his, which was designated 191A after plaque purification.

Not drawn to scale.

3. VP5

3.1 Construction of Expressing Baculovirus

To produce a 6xhis tagged version of VP5 in a baculovirus expression vector, a series of cloning steps were performed. pSJM1965 (described in Chapter 3, Section 2.3.2) was EcoRI/XhoI digested to remove the pp65 tag sequences, which were replaced with two complementary oligonucleotides, NhisE (1B) and NhisE (2B), to generate pSJM19his (see figure 4.12). The oligonucleotides encoded a 6xhis tag and an NcoI site for ease of detection. Once the insertion had been confirmed, by restriction enzyme digestion (not shown), the UL19 ORF was isolated as a BglII fragment and sub-cloned into a BglII digested baculovirus expression vector, pAcCl29.1 (Livingston & Jones, 1989). This generated pAcCl19his [see figure 4.12, panel (iv)]. Again, the correct construct was confirmed by a series of restriction enzyme digests.

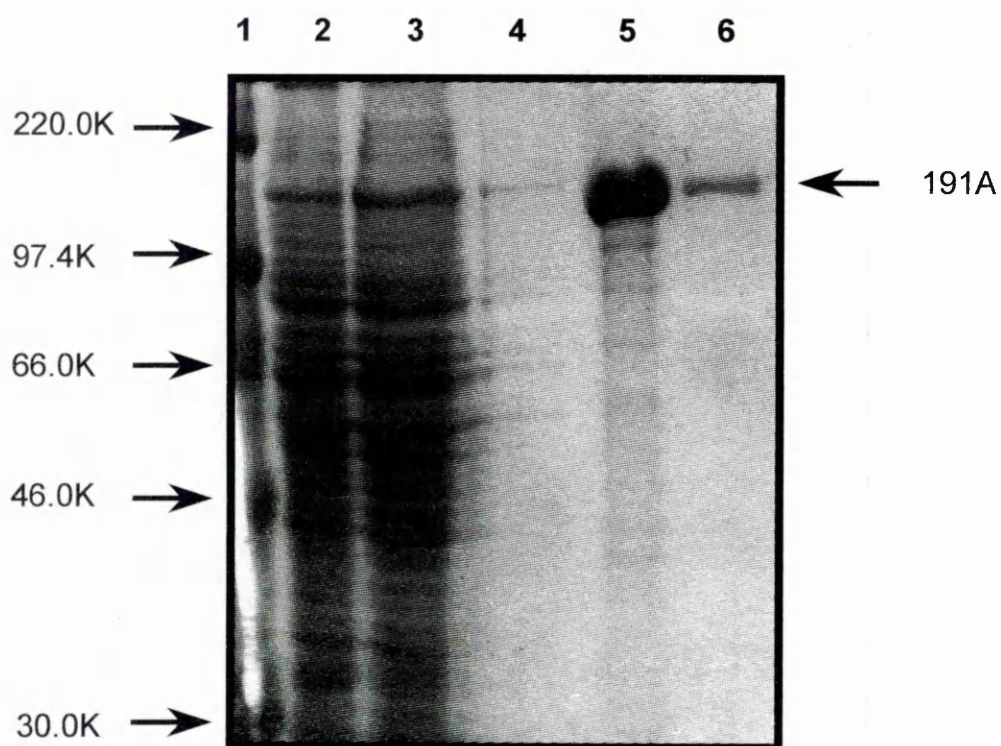
3.2 Production of a Recombinant Baculovirus Expressing VP5his (ie 191A)

A large scale plasmid preparation of pAcCL19his was made (see Methods, Section 2.5.11) and the DNA used to transfect Sf21 cells with viral DNA using CELLECTIN reagents (Methods, Section 2.3.7). The resulting recombinant virus was plaque purified through several rounds of plate harvests (as described in Methods, section 2.3.7.4). It was important at this stage to clearly label each plaque and a simple numbering system was employed. The final positive viral plaque, which was used as the inoculum to produce titred virus stock, was designated 19 (for UL19), from initial plaque 1 and final plaque A, ie the recombinant plaque purified baculovirus was termed 191A.

3.3 Expression of 191A

191A was inoculated into 300ml of Sf 21 cells (2×10^5 /ml) at 0.1 pfu/ml. The cells were incubated at 28°C for 4-5 days and harvested at 3000 rpm for 10 min. The pellet was resuspended in 2.5ml of PBS complete. Soluble protein was released by 3 rounds of freeze thawing followed by a brief sonication in a Kerry ultrasonic bath. The solution was spun at 13000 rpm for 5 min and the supernatant, containing the 191A protein, was stored at -20°C until required.

Figure 4.13: Purification of 191A Through Ni-NTA



3.4 Purification of 191A

3.4.1 Binding to Ni-NTA resin

The 191A supernatant was loaded onto Ni-NTA resin and washed with 4x5ml PBS (lanes 2, shows a sample of the 1st PBS wash) and 5x1ml PBS + 5mM imidazole (lanes 3 and 4, show the 1st and last PBS + 5mM imidazole washes respectively).

3.4.2 Elution of 191A

The 191A protein was eluted in 3x1ml volumes of PBS + 30mM imidazole (lanes 5 and 6 show the 1st and final elutions respectively).

Figure 4.13: Coomassie brilliant blue stained gel with the size markers represented in lane 1. Freeze thawed baculovirus supernatant, in PBS, expressing 191A, was loaded onto Ni-NTA resin, washed in 4x5ml PBS (lanes 2, shows a sample of the 1st PBS wash) and 5x1ml PBS + 5mM imidazole (lanes 3 and 4, show the 1st and last PBS + 5mM imidazole washes respectively). The protein was eluted in 3x1ml volumes of PBS + 30mM imidazole (lanes 5 and 6 show the 1st and final elutions respectively).

3.4 Purification of 191A

3.4.1 Binding and Elution of 191A from Ni-NTA Agarose

The 191A supernatant was mixed with 500 μ l of Ni-NTA, pre-equilibrated in PBS, as described in Section 2.4.1.

The 191A protein bound to the Ni-NTA resin was loaded onto a 0.8x4.0cm poly-prep column (Bio-Rad). The mixture was left to settle and the unbound protein allowed to drain through the column by gravity. The resin was then washed with 20ml (ie 4x5ml volumes) of PBS complete. 1x5ml volumes of PBS complete containing 5mM imidazole removed any non-specifically or weakly bound proteins. The 191A protein was eluted from the column in 3x1ml volumes of PBS complete, containing 30mM imidazole. The protein was eluted in a soluble and relatively pure form, in the absence of denaturant and required no further purification (figure 4.13).

4. Discussion

The properties of the Ni-NTA purified VP5 (191A) and VP26 (VP26pp65) proteins contrasted significantly. The VP5 protein was expressed in a baculovirus system and was soluble in PBS. On the other hand, the VP26 protein was expressed in a bacterial expression system and was extremely insoluble under standard non-denaturing conditions. It is difficult to ascertain exactly why this protein was so insoluble. There are, for example, no Cys residues which could cross-link and cause aggregation. It should be noted however, that the contrast in solubilities between VP5 and VP26 cannot be attributed to the different expression systems used. VP26 has been expressed in the baculovirus system. Both Tatman *et al*, 1994, and Thomsen *et al*, 1994, found that VP26 was relatively insoluble in this system and often difficult to express. It may be that the VP26 protein has a complex secondary structure which is difficult to fold, or it may be that the structure is very unstable when it is not present in its native confirmation within the capsid structure.

It is important to realise that the epitope tags included in these constructs should not be altering or interfering with the properties of VP5 or VP26. Immunofluorescence studies (detailed in Chapter 3) showed that the tagged proteins behaved in an identical manner to

**Table 4.2: Summary of the Conditions Tested to Solubilise
VP26pp65**

CONDITION VARIED	PROTEIN SOLUBILITY
Temperature of induction eg 15°C, 20°C, 37°C	✘
+/- Time of induction eg 2 hrs → o/n	✘
Concentration of IPTG at induction eg 0.1mM → 2mM	✘
Temperature, time, concentration of IPTG at induction ie multiple combinations	✘
A ₆₀₀ at induction eg 0.2 → 0.5	✘
Buffers in sonication eg MES, CAPS etc	✘
pH of elution buffers eg pH 4.5 → pH 8.0	✘
Use denaturant to solubilise and purify ie 6M GuHCl / 8M Urea	✓

**Table 4.3: Summary of the Purification Protocol for VP26pp65
(pET35pp65)**

Step	Procedure
1	from a single colony of BL21 cells transfected with pET35pp65, grow a 100ml culture, in a 1l flask, to $A_{600}=0.5$, at 37°C shaking
2	induce culture: 1mM IPTG, 2-4h, 37°C shaking
3	harvest: 3000 rpm, 10 min
4	resuspend pellet in 10ml of Sonication Buffer by probe sonication
5	spin: 10000 rpm, 10 min
6	resuspend pellet in 10ml of Buffer A by sonication, mix 1h, rt
7	spin: 10000 rpm, 10 min
8	mix supernatant with 500 μ l of pre-equilibrated Ni-NTA, 1h, rt
9	load onto column, wash: Buffer B (20ml) Buffer C (10ml) Buffer D (10ml)
10	elute VP26pp65 protein: Buffer E (3ml)
11	dilute protein 2-fold in NTE
12	dialyse protein against NTE
13	spin: 80000rpm, 10 min
14	remove supernatant fraction: SOLUBLE VP26pp65 IN NTE (0.5-1.0mg/ml)

wild type proteins in several different transfection experiments. This strongly supports the idea that the presence of extra amino acid sequences at these points of the respective genes, does not alter normal protein functioning (see Chapter 5 for clarification of this point for VP26pp65).

One wish had been to purify VP26pp65 at concentrations high enough for structural analysis, especially NMR. For this purpose concentrations greater than 10mg/ml were needed. To solubilise the VP26pp65 protein a large range of approaches were tried and these are summarised in table 4.2. Although a variety of solubilisation and purification conditions were tested, it was only possible to produce soluble and non-denatured VP26pp65 protein at concentrations of 0.5-1.0mg/ml. A complete summary of the expression and purification protocol is detailed in table 4.3. Although the quantities of soluble protein produced were not high enough for NMR analysis, they were good enough to utilise in interaction assay systems (see Chapter 5). The time and effort were well spent.

It is interesting to speculate as to why VP26 is so insoluble, compared to the larger VP5 molecule. When examining the 3D image reconstructions of capsids, it is evident that the VP5 molecules exist within the capsomeres as finger-like structures which appear to have limited contact with each other (Zhou *et al*, 1998b). This is in stark contrast to VP26 which lies on top of the hexon and when looking down appears to cover the upper surface of the hexon. These observations could indicate that VP5 has only a small proportion of its mass involved in binding, whereas a large proportion of VP26 may be involved in binding. It is therefore likely that VP26 has many hydrophobic domains covering a large percentage of its surface area and in the absence of VP5, to guide correct assembly, it forms aggregates in solution.

1. Introduction

There are several...
right labeled...

...of the...
...the...

...the...
...the...

CHAPTER 5

CHARACTERISATION OF VP26pp65 AND MAPPING THE POINTS OF INTERACTION BETWEEN VP26 AND VP5

...the...
...the...

1. Introduction

There were several approaches taken to study the interaction of VP26 with VP5 and these shall be discussed in this chapter.

VP26 had been shown to be located at the tips of the hexons and not pentons (Booy *et al*, 1994; Trus *et al*, 1995; Zhou *et al*, 1994, 1995). However, since VP5 makes up both the hexons and pentons, the mechanism which excludes VP26 from the pentons is not clear. Several suggestions have been made to address this dilemma; Trus *et al* (1995) have proposed that there may be conformational differences between VP5 hexons and VP5 pentons, which only allow VP26 to attach to the hexons; Zhou *et al* (1995) suggested that VP26 may form hexamers in solution, which will then geometrically only fit onto the hexon tips and not the penton tips.

To investigate the properties of VP26 and the interaction with VP5 in more detail, the bacterially expressed protein VP26pp65 (described in Chapter 4) was utilised in a series of assay systems. The initial study undertook to validate that the soluble and purified VP26pp65 protein was structurally and functionally correct and could attach to VP26-capsids. This was followed by a series of experiments to examine the structure, oligomeric status and binding properties of VP26pp65 with VP5. Together with cryo-EM analyses, a clearer picture of the molecular mechanism of VP26-VP5 interaction was revealed.

2. Functional Validity of VP26pp65

2.1 Reattachment of VP26pp65 to VP26 Minus (VP26-) Capsids

From immunofluorescence studies (Chapter 3) it was clear that the presence of extra sequences at the N-terminus, contributed by the pp65 epitope tag, did not interfere with the binding of VP26 to VP5. SDS-PAGE analysis of the purified VP26pp65 (Chapter 4), had confirmed that the bacterially expressed protein was in a very pure form, as only a single band was evident, running at the correct Mr (14733 Da). Throughout the purification process, VP26pp65 was in the presence of denaturant which would have

disrupted the structure. It was hoped that following dialysis to remove the denaturant, the protein would re-fold correctly. To determine if this was the case and whether the VP26pp65 protein was functional, capsids lacking VP26 (VP26- capsids) were made and the VP26pp65 protein mixed with these to see if it would bind at the correct location.

2.1.1 Preparation of Capsids

Capsids lacking VP26 (VP26- capsids) were prepared in two ways:

(i) GuHCl Stripped HSV-1 Capsids

Normal wild type capsids were made in BHK C13 cells (Methods, Section 2.25). The VP26 protein was then stripped from these capsids by treatment with 2M GuHCl, or 4M urea, as described by Newcomb and Brown, 1991. They had shown that greater than 95% of VP26 and VP22a could be removed by this treatment with only limited loss of other capsid proteins. It should be noted that the pentons were also removed during this treatment but, the hexons remained intact. Subsequently, cryo-EM analysis (Booy *et al*, 1994) revealed that these capsids were structurally intact and their icosahedral symmetry was not affected. They went on to demonstrate that VP26, removed in this manner, could be re-attached to the stripped capsids at the correct location.

It was assumed that if re-natured VP26pp65 had the correct secondary structure and was functional, it would reattach to unoccupied binding sites of native VP26, in both the VP26- recombinant capsids and the GuHCl stripped capsids. Initially GuHCl stripped capsids were used in the VP26 re-attachment experiments as these were easier to produce in large quantities and at high concentrations, than the recombinant capsids. Wild type capsids were therefore diluted to 1.0-1.5 mg/ml in NTE containing 2M GuHCl and mixed for 30 min at 4°C. The capsids were pelleted through 1ml of a 40% (w/v) sucrose cushion at 50000 rpm for 15 min, in Beckman 11x34mm tubes. This pelleted capsids and left the stripped proteins above the sucrose cushion [see figure 5.5, Panel (i)]. The pellet was washed, resuspended in NTE and stored at -70°C until required for re-attachment experiments.

Figure 5.1: pAcAB3 Baculovirus Transfer Vector

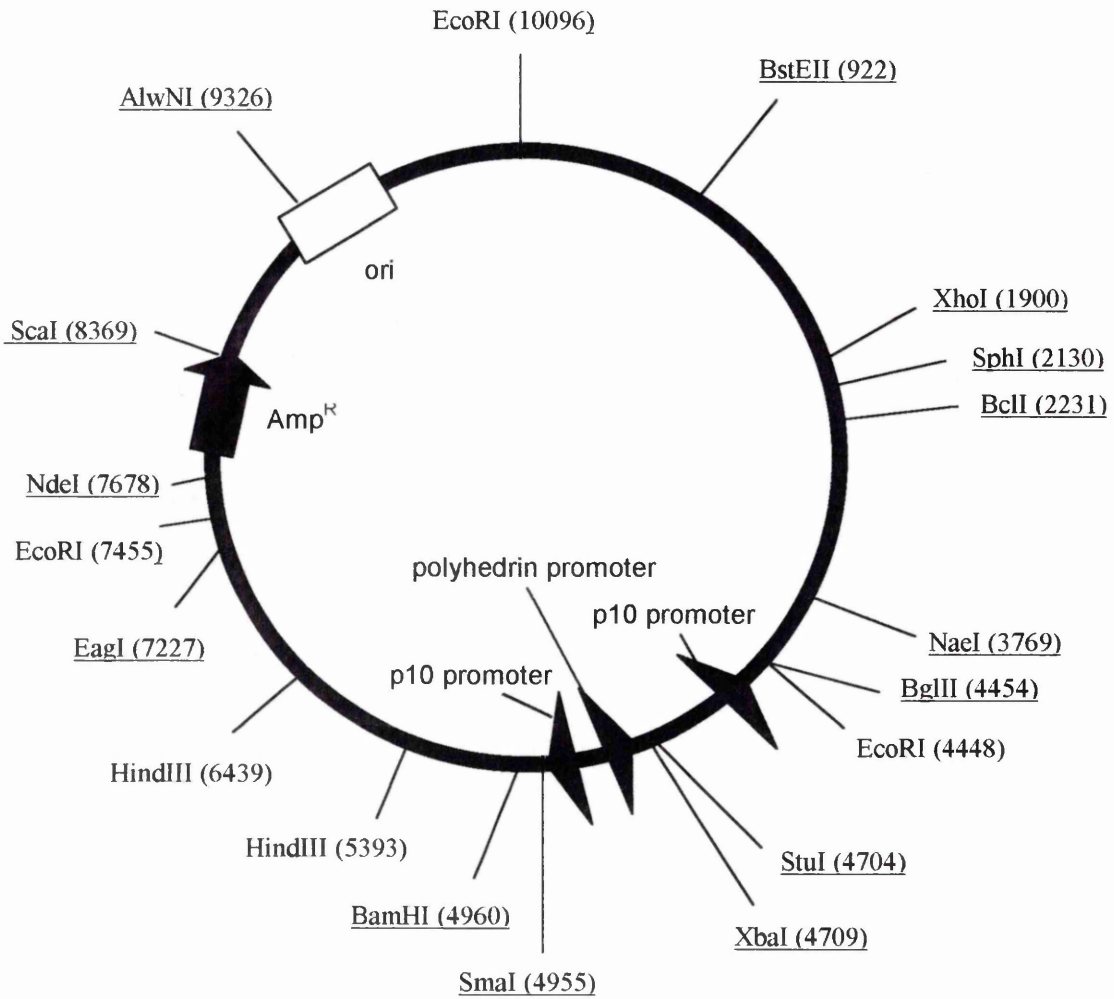


Figure 5.1: This shows pAcAB3, a baculovirus transfer vector, which consists of 10096 base pairs. There are 3 promoters (represented by the triangles), a single origin of replication (rectangle) and an ampicillin resistance (Amp^R) gene (large arrow). The restriction enzyme sites and their location are marked around the plasmid, with the unique sites underlined.

This figure is not drawn to scale.

Figure 5.2: Cloning Strategy to Generate pAcAB3.1

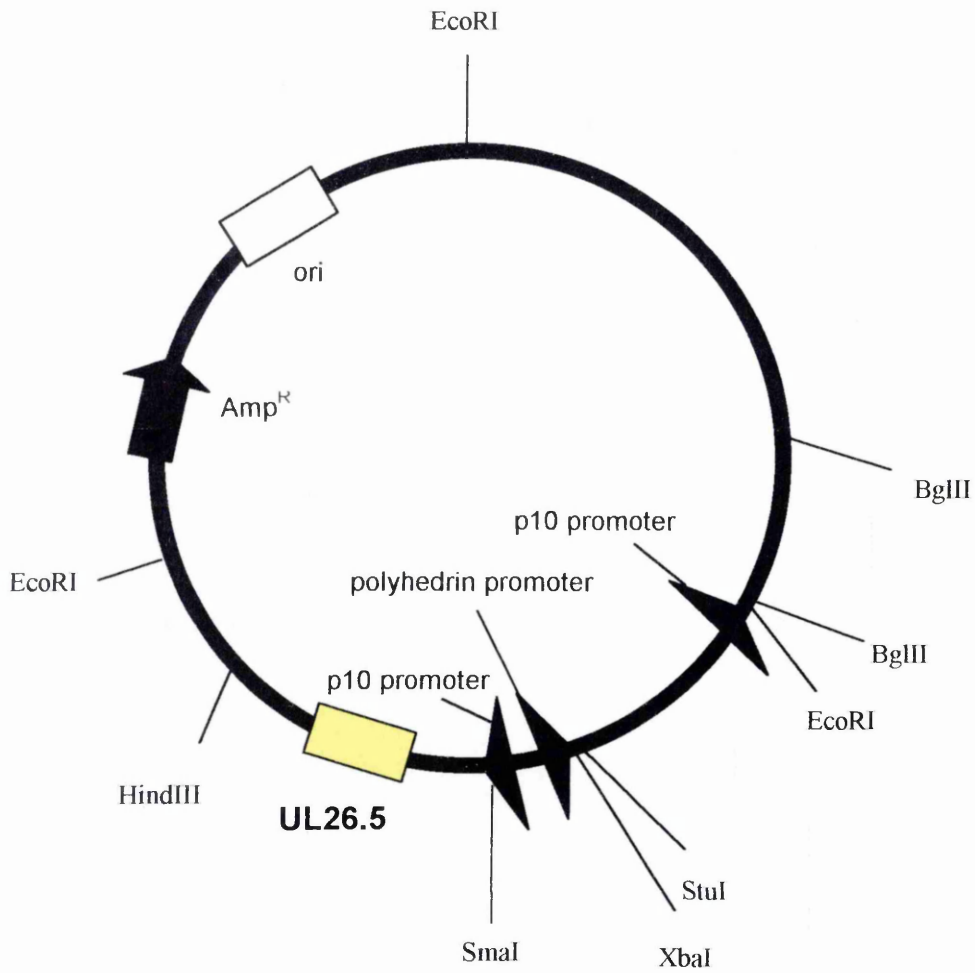
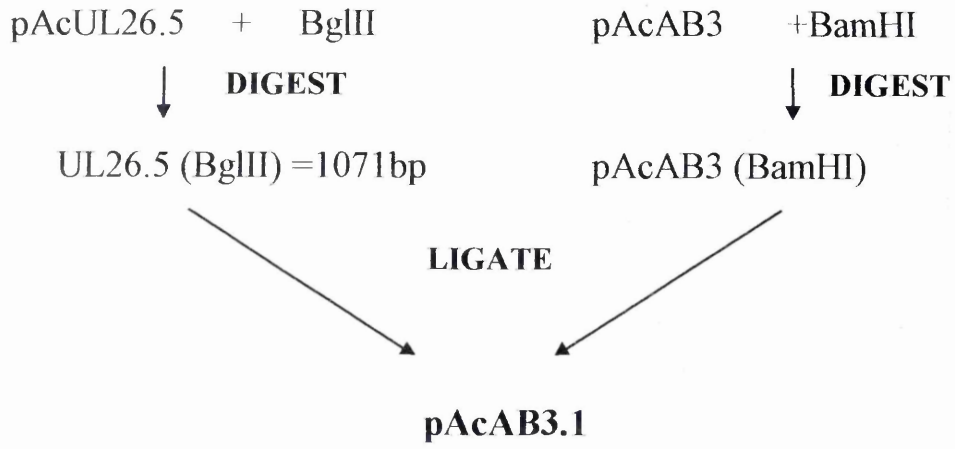


Figure 5.2: This shows the cloning strategy used to insert BglII digested UL26.5 (1071 base pairs), from pAcUL26.5 (J Tatman, 1996), into BamHI digested pAcAB3. This ligation resulted in the loss of the BglII site and generated a vector encoding UL26.5 (yellow box) which was designated pAcAB3.1.

This figure is not drawn to scale.

(ii) Recombinant Capsids

J Tatman (Tatman *et al*, 1994) had cloned all the capsid genes into the baculovirus transfer vector, pACNPV, and created recombinant baculoviruses each expressing a single capsid gene. She had also shown that capsids lacking VP26 could be made and purified using this system. However, it was very time consuming to grow and titre virus stock for each capsid protein. Belyaev & Roy (1993) had reported that more than one foreign gene could be cloned into the baculovirus expression vector, with the successful expression of target proteins. It was felt that producing a baculovirus construct which encoded more than one capsid protein was an attractive prospect and would be extremely useful. The task of growing and titering many viruses individually would be reduced. A triple construct was therefore made which expressed VP5 (UL19), preVP22a (UL26.5) and VP19c (UL38).

The cloning procedure was performed using the strategies described in Methods. Basically, the ORF of UL26.5, UL38 and UL19 were removed from a series of constructs, by digestion and ligated into a version of the baculovirus expression vector pAcAB3 (Pharmingen). The expression vector is shown in figure 5.1. It is 10096 base pairs and contains several unique restriction enzyme sites for cloning the desired genes. These are located downstream from three strong promoters, two p10 promoters and one polyhedrin promoter. Each of these were used to clone a single capsid protein ORF under their control, therefore ensuring high expression levels of each protein.

Initially pAcUL26.5 (Tatman *et al*, 1994) was BglII digested, to release a 1071 base pair fragment containing the UL26.5 ORF. This was cloned into BamHI digested pAcAB3 (see figure 5.2). When BglII and BamHI overhanging ends are ligated, the resulting sequence is not recognised by either enzyme. The BamHI site was therefore lost from the plasmid, designated pAcAB3.1. A series of diagnostic restriction enzyme digests were performed to confirm the correct orientation of UL26.5 ie should be read from right to left, under the control of a p10 promoter.

Figure 5.3: This shows the cloning strategy used to insert XbaI/HincIII digested UL38 (1482 base pairs), from pBJ382 (Nicholson *et al*, 1994), into XbaI/StuI digested pAcAB3.1. This ligation resulted in the loss of the StuI site and generated a double vector encoding UL26.5 (yellow box) and UL18 (blue box) which was designated pAcAB3.4.

This figure is not drawn to scale.

Figure 5.4: This shows the cloning strategy used to insert BglII digested UL19 (4185 base pairs), from pBJ196 (Nicholson *et al.*, 1994), into BglII digested pAcAB3.4. This ligation was the final step in creating a triple construct expressing UL26.5 (yellow box), UL18 (blue box) and UL19 (red box) which was designated pAcAB3.6.

This figure is not drawn to scale.

XbaI/HincII digestion of UL38, from pBJ382 (Nicholson *et al*, 1994), released a 1482 base pair fragment containing the UL38 ORF. Ligation of this fragment into XbaI/StuI digested pAcAB3.1, resulted in the rebuilding of the XbaI site, but the loss of the StuI site from the plasmid (see figure 5.3), termed pAcAB3.4. Consequently, the UL38 gene was placed under the control of the polyhedrin promoter and orientated from left to right.

Finally, pAcAB3.4 was BglII digested and ligated with BglII digested UL19 to generate pAcAB3.6 (see figure 5.4). The UL19 ORF was isolated from pBJ196 (Nicholson *et al*, 1994) as a 4185 base pair fragment. The correct orientation, ie encoded from left to right under the control of a p10 promoter, was confirmed by a series of restriction enzyme digests.

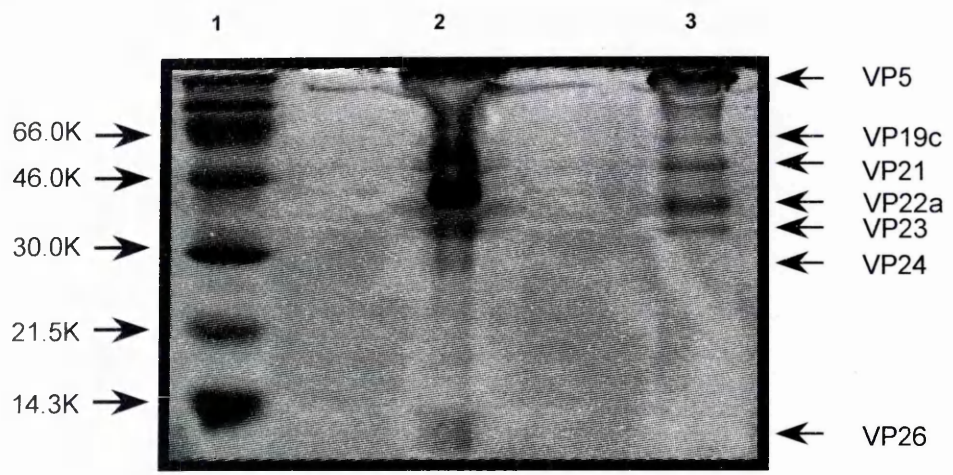
The pAcAB3.6 plasmid DNA, together with Bsu 361 digested pAK6 baculovirus DNA, was transfected on Sf21 cells with CELLECTIN reagent (see Methods, Section 2.3.7). Recombinant virus was isolated through 3 rounds of plaque purification to produce low titre pAcAB3.6 virus stock (see Methods, Section 2.3.2). The expression of all three capsid proteins was confirmed on an analytical protein gel and high titre stocks were subsequently grown (Methods, Section 2.3.3).

To produce VP26- capsids, 300ml of Sf21 cells were infected with 5pfu/cell (as described in Methods, Section 2.3.8) of the recombinant baculoviruses pACUL18, pAcUL26 and pAcAB3.6 and harvested 48-65h post infection. Upon purification through a sucrose gradient, a distinct single B capsid band was observed. This showed that pAcAB3.6 could be successfully used in the production of recombinant capsids.

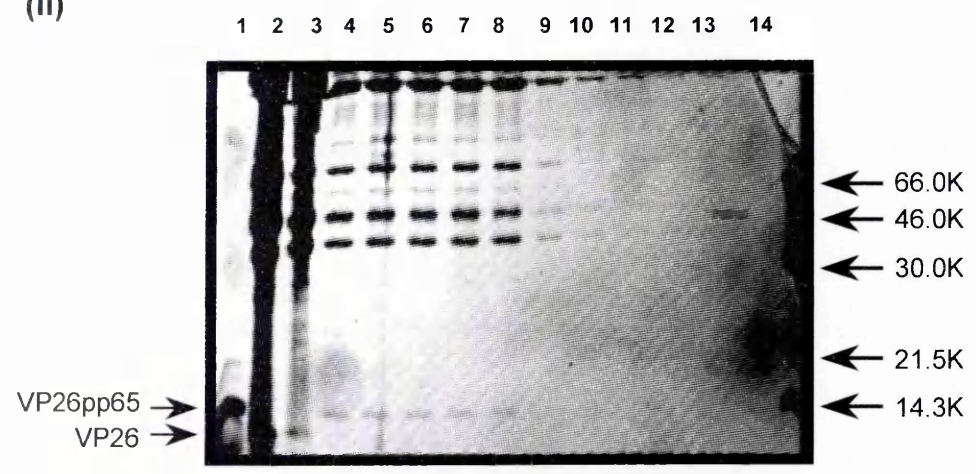
To serve as control samples, capsids containing VP26 (VP26+ capsids) were also made in two ways:

Figure 5.5: Attachment of VP26pp65 to VP26- Capsids

(i)



(ii)



(iii)

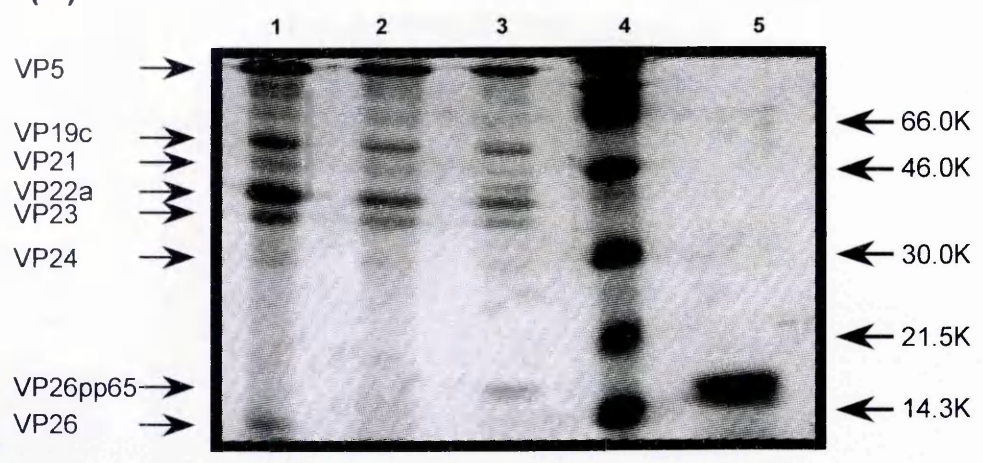


Figure 5.5: Silver stained gels. Panel (i) shows wild type B capsids (lane 2) and capsids which have been stripped of their VP26 protein (ie VP26- capsids) by treatment with GuHCl (lane 3).

Panels (ii) and (iii) show attachment of VP26pp65 to GuHCl stripped VP26-capsids, to generate VP26pp65+ capsids:

In panel (ii), lane 1 represents purified VP26pp65 protein, lanes 2 and 3 show the profile of wild type B capsids and lanes 4-13 show the gradient fractions (collected from the bottom to the top, respectively) following reattachment of VP26pp65 to capsids (ie VP26pp65+ capsids).

In panel (iii) the capsids were not banded on a gradient but pelleted through a 40% (w/v) sucrose cushion. Lane 1 shows wild type B capsids, lane 2 VP26-capsids and lane 3 the pelleted VP26pp65+ capsids. Lane 5 shows purified VP26pp65 for comparison purposes.

(iii) Wild Type HSV-1 capsids; made by infecting BHK C13 cells with HSV-1 virus (see Methods, Section 2.2.5).

(iv) Fully Recombinant Capsids; made by infecting Sf21 cells with recombinant baculoviruses expressing all the capsid proteins (see Methods, Section 2.3.8).

2.1.2 Attachment of VP26pp65 to VP26- Capsids

Since 6 copies of VP26 are present on the tips of each hexon, 900 copies of this protein are present in each capsid. VP26 therefore constitutes approximately 6.7% of the total capsid mass. Based on these calculations, VP26pp65 was mixed with VP26- capsids (ie either pAcUL35 minus recombinant capsids or GuHCl stripped capsids) in slight excess, at concentrations equivalent to 9% of the total capsid mass, to ensure that the vacant hexon binding sites would be saturated.

VP26pp65 in NTE was mixed with capsids, in a volume of approximately 200 μ l, and rotated end-over-end at rt for 2h. To determine if VP26pp65 had attached to the capsids samples were purified on 10-40% sucrose gradients. An extremely faint capsid band was evident. This was attributable to the small quantity of capsids used on a 13ml gradient. Therefore 0.5ml fractions were collected across the gradient by puncturing the bottom of the tube. The samples were spun at 13000 rpm for 10 min in a microfuge, to pellet the capsids, resuspended in 1x loading buffer and analysed on a 15% PAGE minigel. Gradient fractions were run in parallel with wild-type B capsids, purified VP26pp65 and molecular weight markers. Proteins were visualised by silver staining (Methods, Section 2.1.5) as shown in figure 5.5, panel (ii).

It is clear from the gel that the VP26pp65 protein has attached to the VP26- capsids, generating VP26pp65+ capsids. A protein of the expected Mr (14700Da) was evident. There was no doubt that the VP26, attached to the VP26- capsids, represented VP26pp65 for two reasons. The presence of the bacterially expressed protein was confirmed by its greater molecular weight, due to the extra tag sequences at the N-

terminus, compared to wild-type VP26 (see figure 4.4) and a Western blot was performed which detected the pp65 tag of VP26pp65 (not shown).

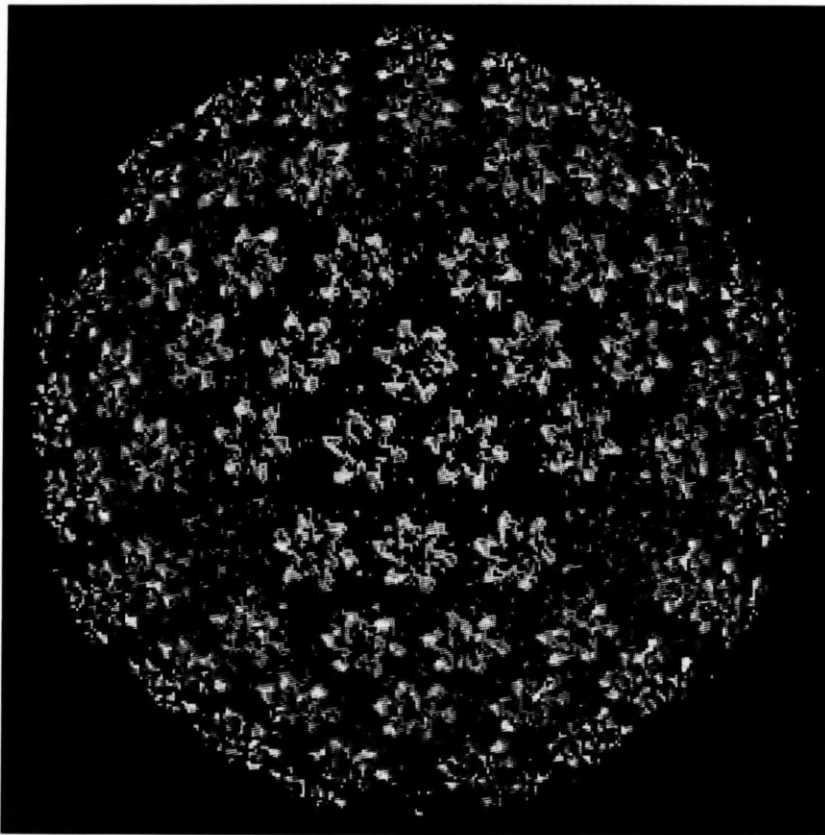
Analysing fractions on gradients takes large amounts of sample and much analysis. Now that it had confirmed that the VP26pp65 protein was attaching to capsids, an alternative purification procedure was developed. The VP26pp65+ capsids were pelleted through 200µl of a 40% (w/v) sucrose cushion, at 50000 rpm for 15 min in a Beckman ultracentrifuge (rotor TLS 55). The pellet was washed in NTE and re-concentrated by spinning at 50000 rpm as above. This time the pellet was resuspended in 1x loading buffer and run on the minigel in parallel with wild-type capsids, VP26- capsids, purified VP26pp65 and the appropriate molecular weight marker. The protein bands were visualised by Coomassie brilliant blue staining (Methods, Section 2.1.4). Again the presence of VP26pp65 was confirmed attached to the capsids, displaying the desired molecular weight, which was greater than wild-type VP26 [figure 5.5, panel (iii)]. In addition, when visually examining both the gradient and pellet fraction of VP26pp65+ capsids on the respective gels [ie figure 5.5, panels (ii) and (iii)], it seemed that the VP26pp65 protein was present at a similar molar ratio as VP26 in wild-type capsids. As previously mentioned, the VP26 protein constitutes approximately 6% of the total capsid mass and so it should be present as a fairly minor band in a capsid protein profile. This was indeed the case for the VP26pp65+ capsids purified by both methods. Although the various capsid protein concentrations were not quantified, the VP26pp65 was not present in great excess, which would be indicative of non-specific binding.

As purifying the capsids by gradient fractions and simple pelleting produced similar results, pelleting became the method of choice for purifying VP26pp65+ capsids as the samples tended to be more concentrated and easier to analyse.

2.1.3 Cryo-EM Analysis of VP26pp65+ Capsids

It was clear from the minigel analysis of VP26pp65+ capsids that VP26pp65 had attached to VP26- capsids. To confirm that the VP26pp65 protein had attached to capsids at the correct location and was not non-specifically bound, it was necessary to

Figure 5.6: Location of VP26pp65 on the Capsid



verify the structure of VP26- and VP26pp65- capsids and to identify the location of VP26pp65 in the recombinant capsid. The difference map was calculated by subtracting the mass density of the 3D reconstruction of VP26- capsids from that of capsids containing VP26pp65 (ie VP26pp65+ capsids). The residual star shaped masses represent 6 copies of VP26pp65 and confirms their location at the tips of the hexons.

Figure 5.6: This image shows the difference map observed when the mass density of the 3D reconstruction of VP26- capsids was mathematically subtracted from that of capsids containing VP26pp65 (ie VP26pp65+ capsids). The residual star shaped masses represent 6 copies of VP26pp65 and confirms their location at the tips of the hexons.

visualise the structure. Dr Wah Chiu and Dr Hong Zhou performed cryo-EM analysis and 3D computer reconstructions on a series of recombinant capsid samples. VP26+ recombinant capsids, VP26pp65+ recombinant capsids and VP26- recombinant capsids were all sent to them for analysis.

They had previously visualised the location of wild-type VP26 on capsids (Zhou *et al*, 1995) by mass difference analysis of capsids lacking VP26 and wild-type capsids. This showed VP26 on the tips of the VP5 hexons, but absent from the pentons. Six copies of VP26 were present on each hexon and formed a star shaped arrangement.

If VP26pp65 had attached to the capsids at the correct location, then an identical star-shaped difference pattern would be expected. This was indeed the case when VP26pp65+ capsids were examined. Figure 5.6, panel (ii), shows the difference map observed when the mass density of the 3D reconstructions of VP26- capsids was mathematically subtracted from that of VP26pp65+ capsids. It is evident that the residual star shaped masses closely resembles those seen by Zhou *et al*, 1995, and confirms the location of VP26pp65 proteins on the tips of the hexons.

This confirms that the bacterially expressed VP26pp65 protein has reacted correctly with the capsids. It shows indubitably that purified VP26pp65 in NTE has the ability to adapt the correct secondary structure and therefore is functionally and structurally valid.

3. Identification of the N-terminus of VP26pp65

As previously described (Chapter 4, Section 2.1.2) VP26pp65 has 24 amino acids present at the N-terminus of the protein, which are not present in the wild-type protein. These additional sequences increase the mass of VP26pp65 by approximately 20%. They clearly do not interfere with secondary structure or prevent correct attachment of this protein to the capsid. If the additional mass was present in an ordered conformation, it should be possible to detect it in the capsid structure by cryo-EM analysis and 3D image reconstruction. A study was therefore undertaken to try and visualise this extra mass and thus identify the N-terminal region of VP26.

Figure 5.7: Comparison of 3D Image Reconstructions of VP26-, VP26+ and VP26pp65+ Capsids

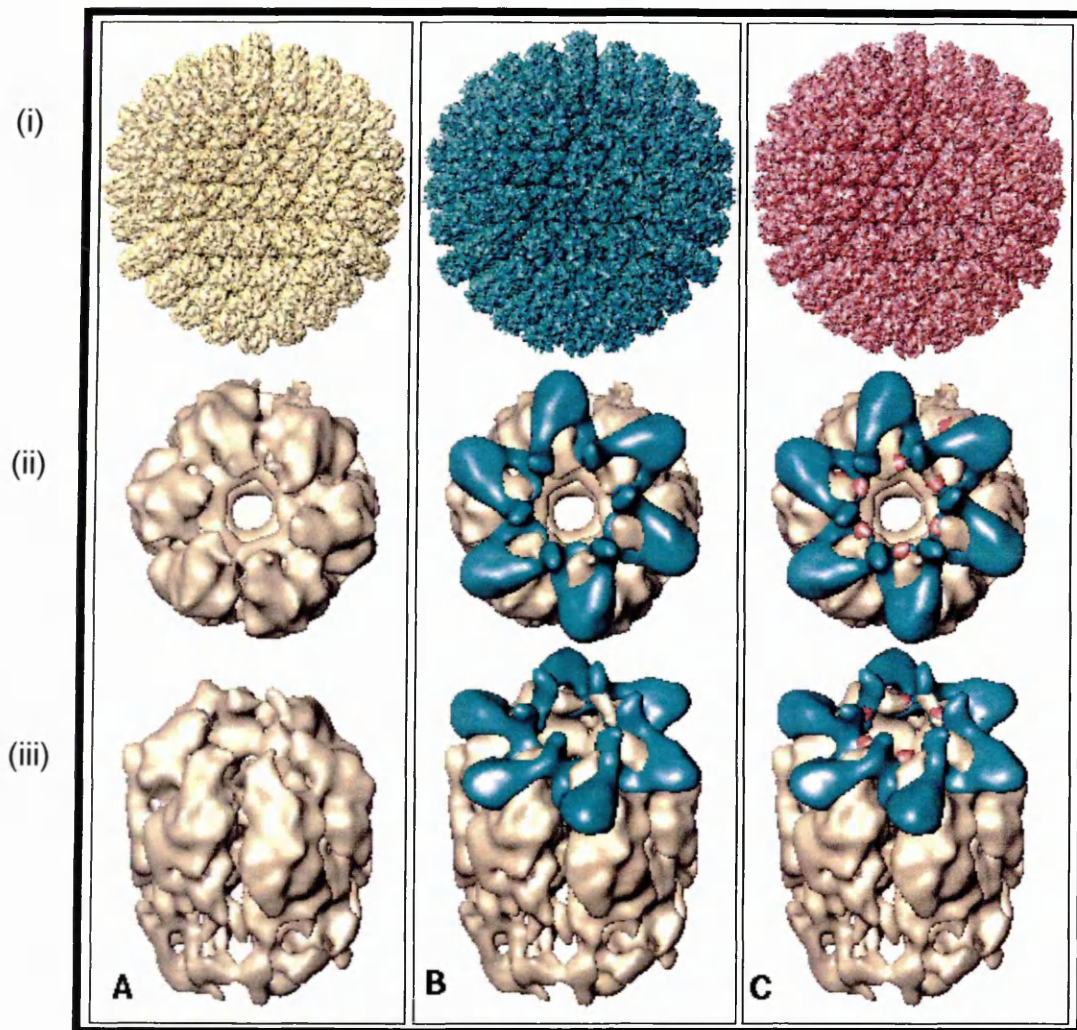
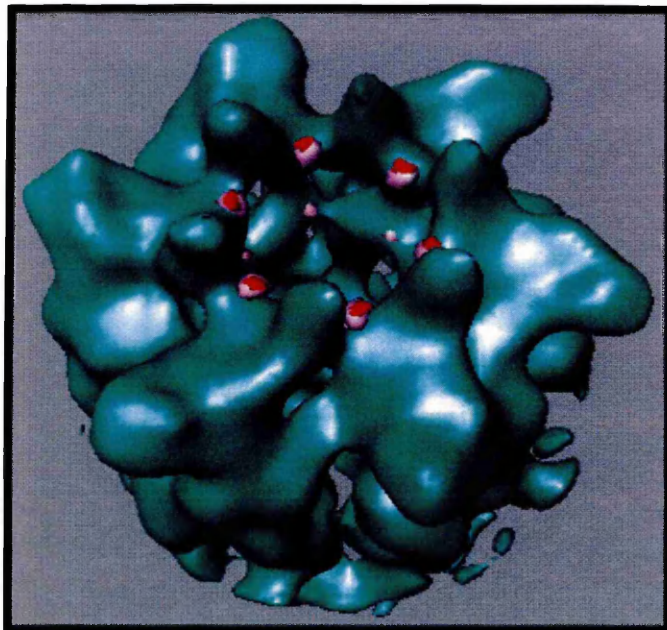


Figure 5.7: Panels (i), (ii) and (iii) show images generated from VP26-recombinant capsids (column A), VP26⁺ recombinant capsids (column B) and VP26pp65⁺ recombinant capsids (column C). To look for the presence of additional masses, hexons were computationally isolated for each capsid type (Panel (ii) shows the top view and panel (iii) shows the side view), and difference maps between them generated. The location of VP26 was revealed by the difference map between VP26⁺ and VP26⁻ hexons (shown in green, column B). The same procedure was used to produce a difference map between VP26pp65⁺ and VP26⁻ hexons (shown in green, column C). Each VP26 difference map was then rendered symmetric by 6-fold averaging and the VP26pp65⁺ hexon and VP26⁺ hexon compared. This revealed an area of extra mass in the VP26pp65⁺ hexons (shown in pink, column C).

Figure 5.8: Location of an Extra Mass in Averaged Hexons of VP26pp65+ Capsids

(i) Side View



(ii) Top View

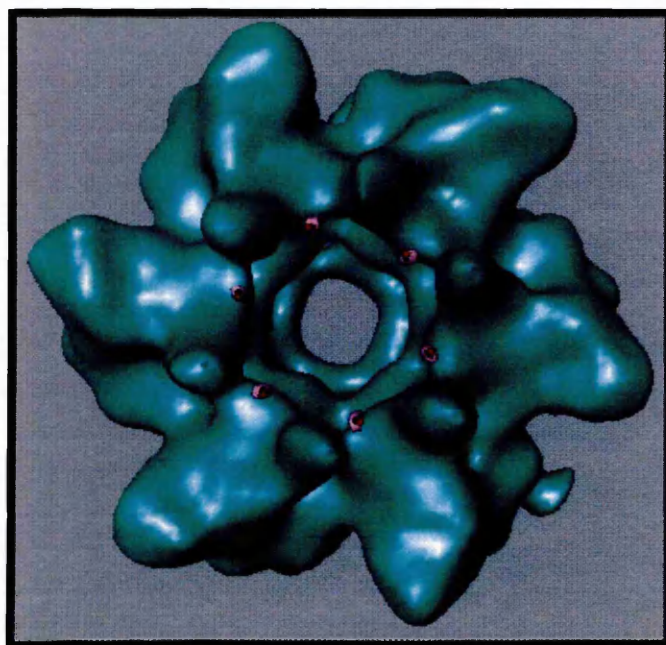


Figure 5.8: The areas of extra mass detected by the difference image of VP26pp65+ capsids and firstly, wild type B capsids (area shown in pink) and secondly, fully recombinant capsids (area shown in purple), was present at the same location on the hexon. Panel (i) shows the top view and panel (ii) the side view, of the VP26pp65+ hexon.

To look for the presence of additional mass in VP26pp65, hexons were computationally isolated and averaged from each capsid type. Difference maps were then generated (see figure 5.7). These were rendered symmetric by a six-fold averaging procedure and the structures examined for the presence of consistent differences.

Figure 5.7, column A represents VP26⁻ capsids, column B represents VP26⁺ (or wild type) capsids and column C represents VP26pp65⁺ capsids. The difference map between VP26⁻ capsids and wild type capsids, is represented in green, panels (ii) and (iii), column B. Here the expected star-shaped arrangement of VP26 is evident. Similarly, when the difference map between VP26pp65⁺ capsids and VP26⁻ capsids was generated, a star-shaped arrangement was also seen (panels (ii) and (iii), column C).

When the VP26pp65⁺ capsid reconstruction (column C) was compared with the wild-type reconstruction (column B), a difference map was produced which pin-pointed an area of extra mass present only in the capsids containing the VP26pp65 protein (column C, area shown in pink). The VP26pp65⁺ capsid reconstruction was then compared with the fully recombinant reconstruction and the difference map again highlighted an area of extra mass in the VP26pp65⁺ capsids (figure 5.8, area shown in purple). The areas of extra mass detected from both difference maps were superimposable (figure 5.8) and present in the part of the hexon known to be formed by VP26. Since no other consistent differences were observed between VP26⁺ capsids and VP26pp65⁺ capsids, this strongly suggests that the area of extra mass detected, correlates directly with the location of the N-terminus, where the tag sequences were inserted into VP26pp65.

4. Characterisation of VP26pp65

As it was now evident that my purified bacterially expressed VP26pp65 protein was a suitable model for native VP26, I wanted to study the properties of the protein further. Nothing was known about the oligomeric status of the protein or content of the secondary structure.

Figure 5.9: Elution Profile of VP26pp65 from the Superdex 75 Column

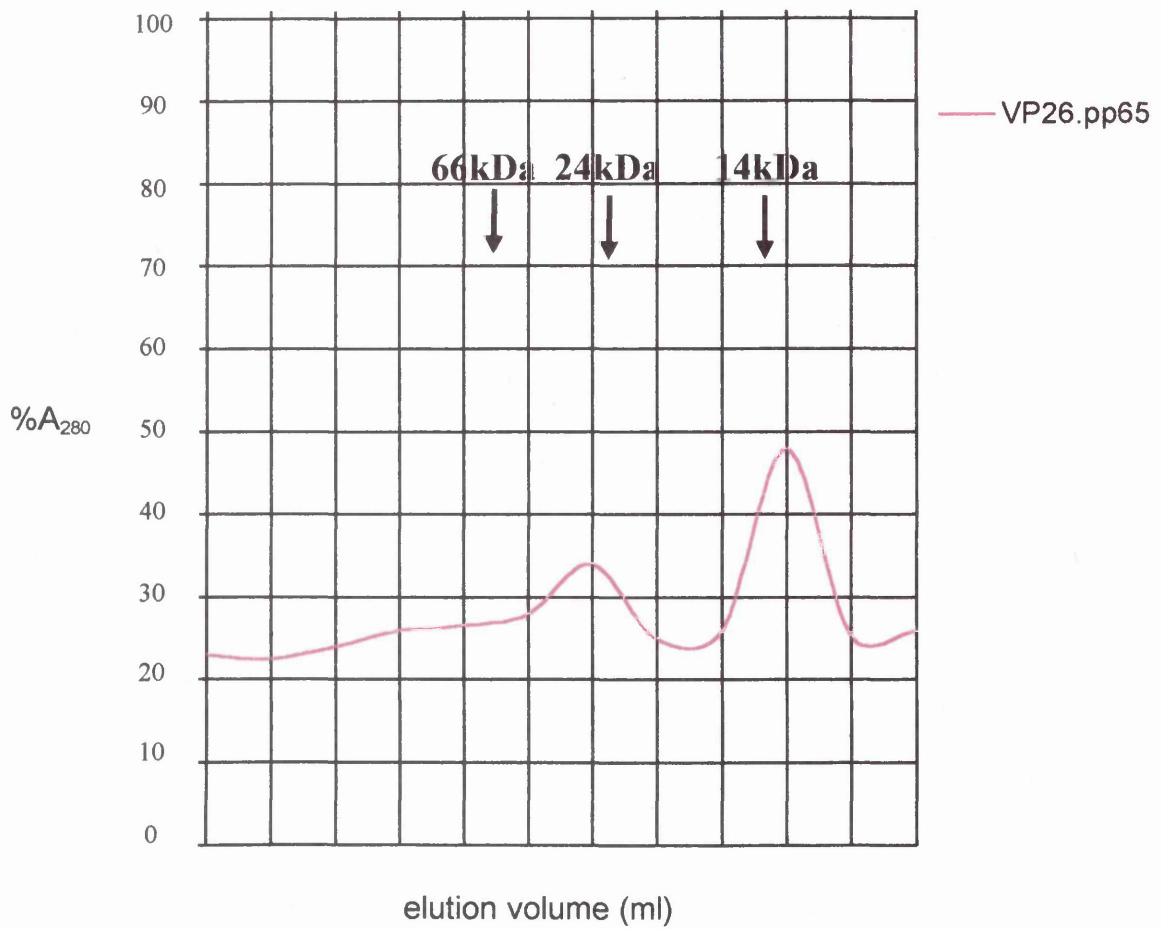


Figure 5.9: This shows the profile detected when VP26pp65 was analysed by FPLC using a Superdex 75 column. The VP26pp65 was added at 0.2mg/ml in NTE. The elution positions of the 14kDa lysozyme, 24kDa trypsin and 66kDa BSA markers are shown at the top of the profile.

Each box on the x-axis (elution volume) represents approximately 2ml.

4.1.1 Oligomeric Status of VP26pp65

As mentioned previously, the mechanism by which VP26 attaches to the VP5 hexons and not pentons is not clear. One theory (Zhou *et al*, 1995) suggested that VP26 spontaneously forms hexamers in solution which will only fit onto the hexons. To test this theory, the VP26pp65 protein was sized by FPLC through a Superdex 75 column (see Methods, Section 2.9) to determine its oligomeric status in solution. The column was equilibrated o/n in equilibration buffer (20mM tris-HCl pH 8.0, 500mM NaCl, 5% glycerol, 1mM DTT) and samples were passed through the column at 1ml/min with protein detected at 280nm.

Known protein standards were diluted to 0.2mg/ml and run through the column. Their traces were plotted and used to calibrate the system. Lysozyme has a Mr of 14 kDa and the peak was detected 9.4cm from the starting point. Trypsin has a Mr of 24 kDa and produced a peak 8.0cm from the starting point. BSA has Mr of 66 kDa and produced a peak 6.6cm from the starting point.

The purified and soluble VP26pp65 protein was diluted to 0.2mg/ml in 200µl, as for protein standards, and loaded onto the column. Unfortunately, the signal for VP26pp65 was much lower than expected, probably due to its insoluble nature, causing the protein to precipitate out on the column. However, two peaks were detected which were confirmed to be attributable to VP26pp65 by Western blot analysis, with the anti-pp65 antibody, of the eluted column fractions.

Although the signal produced by VP26pp65 was weak, the pattern of peaks gave an indication of the oligomeric status of the protein (see figure 5.9). The first peak was seen 7.6cm from the start and the second peak 9.5cm from the start. No other prominent peaks were detected. Measuring the points (in cm) from the VP26pp65 protein trace and extrapolating them against the known standards, the approximate Mr of the protein could be estimated. The first peak eluted at a slightly higher Mr than trypsin, suggesting a Mr of approximately 30 kDa. The second peak was eluted very close to the lysozyme, indicative of a Mr of approximately 14 kDa. VP26pp65 has a Mr of 14733 Da and so

Figure 5.10: Sequence Relatedness of VP26 Proteins

(i) Alphaherpesviruses

```

.....1.....2.....3.....4.....5.....6.....7.....8.....9.....
HSV-1      MAVPQFHRPSTVTTDSVRALGMRGLVLAINNSQFIMDNNHPHPQGTQGAVREFLRGQAAALTDLGLAHANNTFTPQPMFAGDAP
EHV-1      MAADKQQQAPVAFNPADPPNIKAANFKDHLPVVDVITILNQNIDELDTYKYTEDEISEGLKQLFMGTARTMVSLSRQRHLKSLVRRSDMFAQND
VZV        MTQPASSRVVFDPSNPTTFSVEAIAAYTPVALIRLLNASGPLQGHRV  DIADARSIYTVGAAAASAARARAHNANTDRRTAMFAETDP
CON        P           N           G A           H           MFA
,.....10.....11.....12
HSV-1      AAWLRPAFGLRRRTYSPFVREPTPGIP*
EHV-1      STWARPNIGLKRTFPPRFMQPISED*
VZV        MTWLRPTVGLKRTFNPRIIRPQPPNPSMSLGI + 100 aas >>>
CON        W RP  GL RT  P

```

(ii) Betaherpesviruses

```

.....1.....2.....3.....4.....5.....6.....7.....8.....9.....
HCMV      MSNTAPGPTVANKRDEKMRHRVVNVVLELPTETISEATHPVLATMLSKYTRMSSLEFNDKCAFKLDLLRMVAVSRTRR*
HHV-6     MTTIRSDDLLSNQITQISG SSKKEEEKKKQQLTGVLGLQPNM  ASHPVLGVFLPKYAKQNGNVVDKTAFRLLDIRMLALHRLNKTGSD*
HHV-7     MAATRGEITAIQINQISGNSKKKEEKKKQMQMFTNILGLHSSM  GSHPVGTGTFLAKYAKQNTGNIKAAFRLLDFLRMLALHRLNSKVSESS*
CON        G           K           L L           L KY           L KY           K AF LD  RM A  R

```

Figure 5.10: Alignments of the amino acid sequences of three alphaherpesvirus [panel(i)] and three betaherpesvirus [panel (ii)] VP26 counterparts, generated by the GCG programme Pileup. VZV has 100 additional amino acids (100 aas) at the C-terminus, which are unrepresented in the other proteins. The consensus prediction (con) is shown in bold underneath each of the alignments.

this suggested that the protein is forming monomers (expected M_r =approx 14700 Da) and dimers (expected M_r =29400 Da). There was a stronger trace picked up for the monomer peak than the dimer peak which may be indicative of a mainly monomeric population. It is difficult to draw accurate conclusions about the proportion of monomers to dimers in the solution but the ratio appears to be approximately 3:1 (monomer:dimer). There was no evidence of any hexameric structures in the solution.

4.1.2 Secondary Structure of VP26pp65

The secondary structure of VP26 is unknown for HSV-1 or any of the other VP26 homologues in alpha and beta herpesviruses. To try and gain an insight into the properties of HSV-1 VP26, the sequences of 3 alpha herpesvirus (HSV-1, EHV-1 and VZV) VP26 counterparts were fed into the GCG programme, Pileup, to generate an alignment and consensus [see figure 5.10, panel (i)]. The same approach was taken to generate an alignment for 3 beta herpesvirus (HCMV, HHV-6 and HHV-7) VP26 counterparts [figure 5.10, panel (ii)]. The proteins within each family are not highly conserved in sequence or in length, indeed VZV has an additional 100 amino acids at the C-terminus, which are not represented in the other proteins. The HCMV protein shown here has recently been identified as the small capsid protein and the gene encoding it is a positional homologue of the HSV-1 gene, UL35 (Gibson *et al*, 1996). This suggests that this protein has a similar role in the HCMV capsid. Apart from the extra sequence of VZV, the poorest area of conservation occurs at the N-terminus for both the alpha and beta herpesviruses.

Upon examination of the sequence comparisons, it is notable that there is no detectable sequence homology between the alpha herpesviruses [panel (i)] and the beta herpesvirus counterparts [panel (ii)].

The secondary structure of VP26 was initially predicted by feeding the sequence into the neural network based protein predict program, EMBL, Heidelberg (Rost & Sander, 1994). This program scores the likelihood of amino acid sequences to form α -helix (H), β -sheet (E) or random loop (L) using multiple alignments of related but non-identical

Figure 5.11: Consensus Protein Predictions of Alpha and Beta Herpesviruses

```

(i)
      . . . . .1 . . . . .2 . . . . .3 . . . . .4 . . . . .5 . . . . .6 . . . . .7
ALPHA      HHHHHH      EEEEE      HHHHHHHHHHHHHHHHH
BETA      HHHHHHHHHHEEE EEEE      EEEEEHHHHHHH      HHHH

      . . . . .8 . . . . .9 . . . . .10 . . . . .11 . . . . .12
ALPHA      HHHHHHHH      EE      EE
BETA      HHHHHHHHHHHHHHHHH

(ii)
      . . . . .1 . . . . .2 . . . . .3 . . . . .4 . . . . .5 . . . . .6 . . . . .7
ALPHA      LLLLLLLL . . . LLLLLL . . . HHHHHH . LLL . EEEEE . LLLLLLLLLLLLLL HHHHHHHHHHHHHHH
BETA      LLL . LLL . . . . . LLLLLL . . . . . LLLLLLLL . . . . . HH . HH . . L . . HHHH

      . . . . .8 . . . . .9 . . . . .10 . . . . .11 . . . . .12
ALPHA      HHHHHHHH . LL . . . . . LLLL . . . . . LLL . . . . . LLLL
BETA      HHHHHHHHHHH . . . LLLLLL
  
```

Figure 5.11: Consensus protein predictions (EMBL, Heidelberg) for the alpha (HSV-1, EHV-1, VZV) and beta (HCMV, HHV-6, HHV-7) VP26 homologues, beginning with the first methionine in each sequence. H represents predicted α -helix, E, β -sheet and L, loop. Panel (i) shows the predictions for lower, and panel (ii) for higher stringency assignments of secondary structure.

solved structures. This generates a consensus prediction of their secondary structure. The program assigns a score to each amino acid prediction with a 9 equal to a high probability prediction and 1 equal to a poor probability prediction. The programme can also assign different stringency levels for the secondary structure predictions produced. The alignment or consensus for the 3 alpha and 3 beta herpes viruses (mentioned above) was sent for analysis by this programme. The predictions are shown in figure 5.11. What is surprising about these predictions is that although the amino acid sequences for each protein varied significantly, the predicted secondary structure for each protein follows a very similar pattern. For example, the consensus prediction for the alphaherpesviruses follows a pattern of α -helix, followed by an area of β -sheet, then α -helix again etc. This is exactly the same pattern predicted for the consensus of the betaherpesviruses. The consensus of the structural predictions of the alpha and beta herpesviruses is shown in figure 5.11, starting with the first methionine in each pileup. Panel (i) shows the predictions for lower stringency and panel (ii) shows the predictions for higher stringency of the secondary structure. The pattern of predicted structure is extremely similar between the alpha and beta herpesviruses and generates a picture of the proteins with extensive loop at both the N- and C-termini with alpha helix in the middle.

Unfortunately this predicted model appears to be wrong, from subsequent CD analysis, performed after this work was completed (see Discussion, Section 6). However, it did prove useful in interpreting the inhibition and mutation studies described below.

5. Mapping of the Points of Interaction Between VP26 and VP5

5.1 Development of an ELISA Assay Using VP26 Inhibitory Oligopeptides

I felt that it would be interesting to develop an ELISA system to study the interaction of VP26 with VP5. This had several advantages over the capsid attachment experiments. Firstly, several different interaction conditions could be tested simultaneously, in one experiment on a single microtitre plate and so this was a rapid assay system. Secondly, the quantities of protein required for each interaction study were reduced as the assays are generally extremely sensitive, this was a considerable advantage due to the difficulty of producing soluble VP26pp65 protein. Thirdly, oligopeptide blocking and mutagenesis

Figure 5.12: Microtitre Plate Plan for ELISA of VP26- Capsids and VP26pp65

	1	2	3	4	5	6	7	8	9	10	11	12
A												
B												
C												
D												
E												
F												
G												
H	BLANK	1:8	1:16	1:32	1:64	1:128	1:256	1:512	1:8 VP26- capsids alone	VP26 pp65 alone	PBS alone	

Conc VP26- capsids

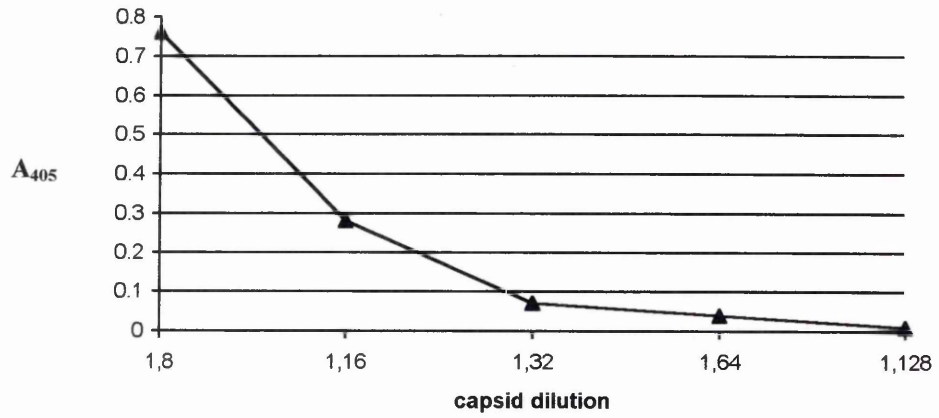
Conc VP26pp65

0.50
μg
0.25
μg
0.10
μg

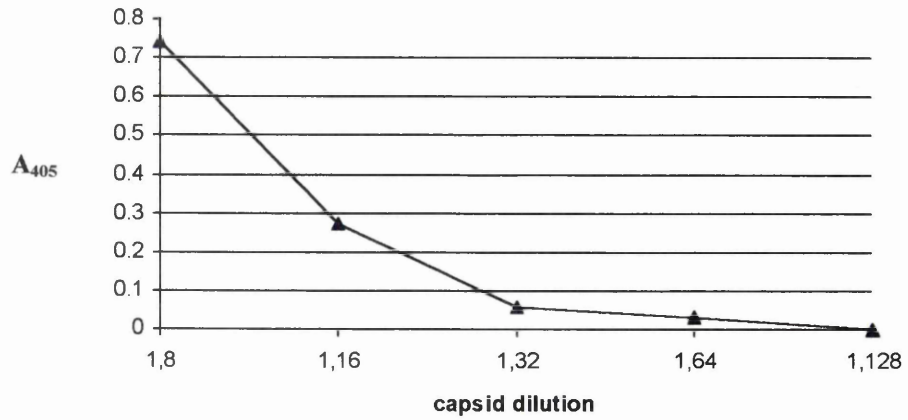
Figure 5.12: This is a schematic representation of a microtitre plate showing details the contents of each well. Column A was blank and used to calibrate the readings against the developing reagent alone. The shaded area was coated with VP26- capsids, o/n at 37°C, at the concentrations shown (NB, initial concentration of VP26- capsids was approximately 2mg/ml) and reacted, in duplicate with the 3 amounts (0.50µg, 0.25µg, 0.10µg) of VP26pp65. Control wells were also included. These contained VP26-capsids, PBS and VP26pp65 which were added to the wells o/n at 37°C. These had no VP26pp65 added to them at subsequent stages.

Figure 5.13: Optimisation of ELISA Conditions for the Interaction of VP26pp65 with VP26- Capsids

(i) 0.5 μ g



(ii) 0.25 μ g



(iii) 0.1 μ g

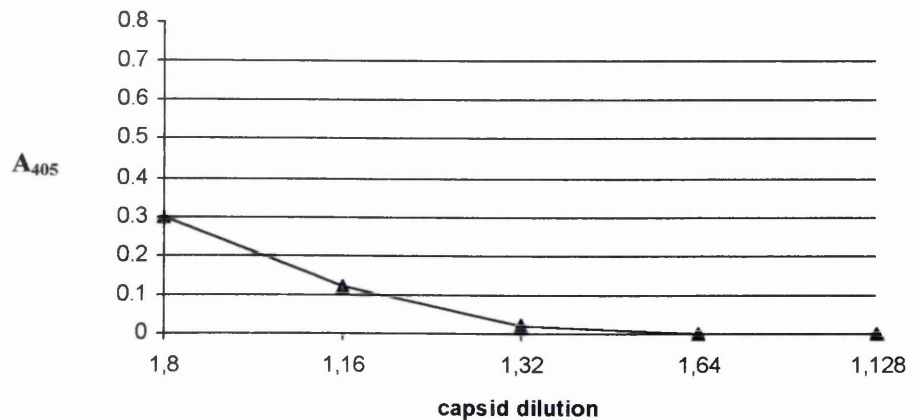


Figure 5.13: 0.5 μ g [panel (i)], 0.25 μ g [panel (ii)] and 0.1 μ g [panel (iii)] of VP26pp65 protein was reacted against VP26- stripped capsids, diluted from 1:8- 2-fold- to 1:128, in an ELISA type assay.

(NB Initial concentration of VP26- capsids was approximately 2mg/ml)

assays could be developed to map the points of interaction. Lastly, the assays were initially set up using VP26- capsids to ensure that the ELISA system worked. However, once this had been established, a system was developed which utilised VP5 (191A) and VP26pp65 and had no requirement for capsids. This reduced the effort required to produce VP26- capsids.

5.1.1 Optimising ELISA Conditions; VP26- Stripped Capsids + VP26pp65

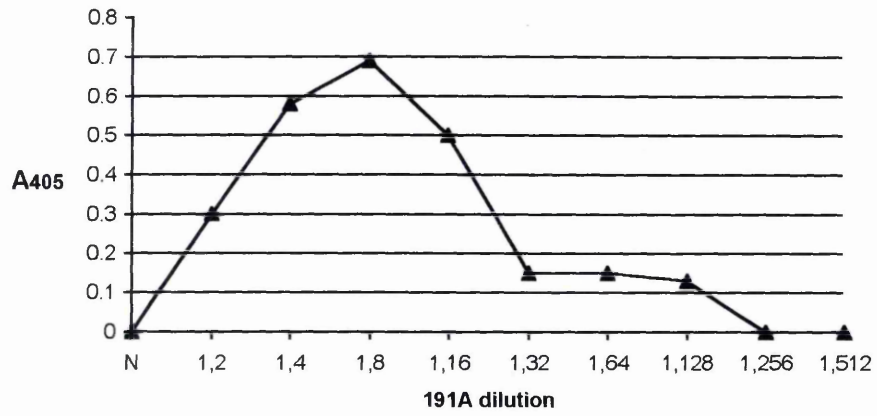
The ELISA protocol detailed in Methods, Section 2.10 was followed. Stripped VP26-capsids, at 2mg/ml, were diluted 2-fold in NTE from 1:8 to 1:512. The diluted capsids were used to coat the microtitre wells o/n at 37°C. NTE alone was used to coat control wells. After blocking non-specific binding sites with BSA, VP26pp65, at an initial concentration of 1mg/ml, was diluted and added to the wells at 0.50µg, 0.25µg and 0.10µg per well, for 1h at 37°C (see microtitre plan, figure 5.12). Unbound VP26pp65 was washed off with PBS containing 0.1% Tween 20 and the primary antibody, pp65, added at 1:800 dilution. Binding was detected with the secondary antibody, GAM-peroxidase conjugate (1:800), and the signal developer (supplied by Kindergaard & Perry Laboratories) The activity was detected at A_{405} on a Multiskan plate reader (Titrttek; ICN Biomedicals).

Figure 5.13 shows the results obtained from a series of experiments. Panel (i), (ii) and (iii) show the absorbance values obtained when 0.50µg, 0.25µg and 0.10µg respectively, of VP26pp65 protein was tested against the various dilutions of stripped capsids. From these graphs it is evident that in each case, 1:8 gave the highest A_{405} values. It is clear that either 0.50µg or 0.25µg of VP26pp65 protein per well, produced a high absorbance value, at 0.77 and 0.74 respectively. Since the signal with less VP26pp65 protein was as strong, 0.25µg was chosen as the optimal VP26pp65 concentration for this assay. Note, an A_{405} of <0.05 was detected for the control wells containing no VP26- capsids.

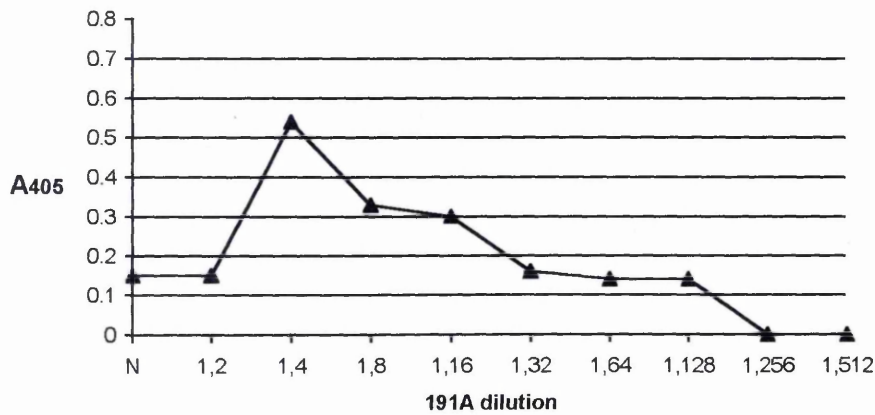
This series of experiments showed that it was possible to develop an ELISA based system to study the interaction between VP26 and capsids. However, a large amount of

Figure 5.14: Optimisation of ELISA Conditions for the Interaction of VP26pp65 with VP5 (191A)

(i) 0.50 μ g



(ii) 0.25 μ g



(iii) 0.10 μ g

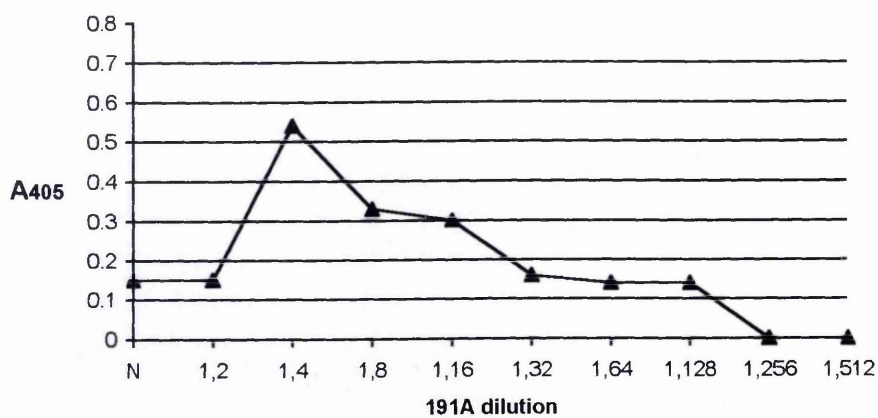


Figure 5.14: 0.5 μ g [panel (i)], 0.25 μ g [panel (ii)] and 0.1 μ g [panel (iii)] of VP26pp65 protein was reacted against 191A, used neat (N) and diluted from 1:2, 2-fold, to 1:512, in an ELISA type assay.

(NB The initial concentration of 191A was approximately 1mg/ml).

effort was required to produce VP26- capsids for this system since either wild type GuHCl stripped capsids, or VP26- recombinant capsids had to be made. The task of making capsids involved labour intensive procedures to grow and titrate virus stocks, passage and maintain cell lines and harvest and purify capsids. It was decided that a working ELISA system which could utilise VP5 alone, with VP26pp65 would be extremely useful.

5.1.2 Optimising ELISA Conditions; Purified VP5 (191A) + VP26pp65

As described in Chapter 4, Section 3, UL19 had been cloned, with a 6xhis tag, into a baculovirus expression vector. VP5 (191A) was expressed to high levels in the Sf21 cells. The protein was readily solubilised and purified through Ni-NTA in low concentration of imidazole in PBS. 191A was therefore an ideal protein to use in the development of a new VP26-VP5 interaction ELISA system.

Purified 191A, at 1mg/ml, was used neat and diluted 2-fold in PBS, from 1:2 to 1:512, and used to coat the microtitre wells, o/n at 37°C. Wells containing PBS alone were included as controls. VP26pp65 was again used at 0.50µg, 0.25µg and 0.10µg per well and reacted with the primary pp65 antibody. Absorbance values were detected by addition of the secondary antibody and signal developer.

Figure 5.14, illustrates the results obtained from a series of experiments. Firstly, the most important point to note is that this approach has been successful and an interaction has been detected between 191A and VP26pp65. Panels (i), (ii) and (iii) show the Absorbance values obtained when 0.50µg, 0.25µg and 0.10µg respectively, of VP26pp65 protein were tested against the various dilutions of 191A. From this figure, it is clear that either 0.50µg or 0.25µg of VP26pp65 per well, produces a good interaction with VP5 (191A). The optimal conditions were set by the lowest dilutions of 191A and VP26pp65 which gave the highest Absorbency values. Panel (i) shows that 191A, diluted to 1:4, with VP26pp65, at 0.50µg, gave the overall highest reading of $A_{405}=0.74$. However, this was not significantly higher than the value obtained when less 191A (1:8 dilution) was reacted with less VP26pp65 (0.25µg/well). In this instance the $A_{405}= 0.69$

Figure 5.15: UL35 Oligopeptide Sequences

(i)

MAVPQFHRPSTVTTDSVRALGMRGLVLA
 TNSQFIMDNNHHPHQGTQGAVREFLRGQAAALTDLGLAHANNTFTPPQPMFAGDAPAAWLRPAFGLRRTYSPFVVREPSTPGTP

MAVPQFHRPSTVTTDSVRAL
 TVTTDSVRALGMRGLVLA
 TNSQFIMDNNHHPHQGTQGAV
 REFVRGQAAALTDLGLAHAN
 NTFTPPQPMFAGDAPAAWLRP
 AFGLRRTYSPFVVREPSTPGTP

(ii)

Sequence	Length	Name
MAVPQFHRPSTVTTDSVRAL	(20)	35/1
TVTTDSVRALGMRGLVLA TNSQFIMDNNHHPHQGTQGAV	(20)	35/2
GMRGLVLA TNSQFIMDNNHHPHQGTQGAV	(20)	35/3
NSQFIMDNNHHPHQGTQGAV	(20)	35/4
PHPQGTQGAVREFLRGQAA	(19)	35/5
REFLRGQAAALTDLGLAHAN	(20)	35/6
LTDLGLAHANNTFTPPQPMFA	(20)	35/7
NTFTPPQPMFAGDAPAAWLRP	(20)	35/8
GDAPAAWLRPAFGLRRTYSP	(20)	35/9
AFGLRRTYSPFVVREPSTPGTP	(22)	35/10

Figure 5.15: Panel (i) shows the UL35 amino acid sequence with the 10 overlapping oligopeptides displayed below. Panel (ii) details the specific length and name for each oligopeptide sequence.

Table 5.1: Summary of 35/1-35/10 Oligopeptide Analysis

Name	Predicted Yield (mg)	Actual Yield (mg)	Purity (%)
35/1	44.25	36.10	70.00
35/2	41.49	34.87	88.22
35/3	44.63	40.29	74.70
35/4	42.47	31.00	80.24
35/5	43.91	29.14	91.94
35/6	40.38	36.90	98.8
35/7	43.17	36.94	84.58
35/8	43.75	30.40	74.40
35/9	44.03	32.90	94.86
35/10	60.89	34.80	90.77

[see panel (ii)]. The optimal conditions for this ELISA reaction were therefore designated as:

- 191A = 1:8 of 1mg/ml
- VP26pp65 = 0.25ug/well

This system shows that intact capsids are not required for VP26 to interact with VP5 and it was possible to set-up an interaction study in their absence.

5.1.3 Blocking the Interaction of VP5 -VP26 With UL35 Oligopeptides

As VP26 is a relatively short protein, consisting of only 112 amino acids, it was possible to produce short oligopeptides which spanned the entire sequence of UL35. It was proposed that these oligopeptides could be used in the VP5-VP26 ELISA system to try and block the interaction between the two proteins. By disrupting the binding site, it would be possible to map the parts of VP26 important in its interaction with VP5.

5.1.3.1 Synthesis of UL35 Oligopeptides

A series of 10 oligopeptides were made which spanned the entire sequence of UL35. The oligopeptides overlapped by 10 amino acids [see figure 5.15, panel (i)] and were all 20-mers except 35/5 and 35/10 [see figure 5.15, panel (ii)]. 35/5 was only 19 amino acids in length as its C-terminus contained 3 alanines in succession. It was felt that it might be difficult to correctly couple 3 identical and sequential amino acid residues at a terminal end. The oligopeptide was therefore shortened to 19 amino acids to remove 1 of the alanines. The final oligopeptide, 35/10, was 22 amino acids in length to ensure that entire sequence of UL35 was represented. All the oligopeptides were synthesised on the PSSM-8 synthesizer (see Methods, Section 1.3) as amines, except 35/10, which was synthesised as an acid as it constituted the C-terminal end. The oligopeptides were all cleaved for 5h in Reagent K (Methods, Section 2.4.2) and dissolved in dH₂O. A good yield and purity was obtained for each (see table 5.1).

5.1.3.2 Blocking ELISA; Disruption of VP5-VP26 Interaction

For ELISA reactions, a 1mM stock of each oligopeptide was prepared in 1ml of dH₂O. Before blocking assays were set-up, all 10 oligopeptides were tested in duplicate against

Figure 5.16: Oligopeptide (35/1 - 35/10) Interaction with pp65 Antibody

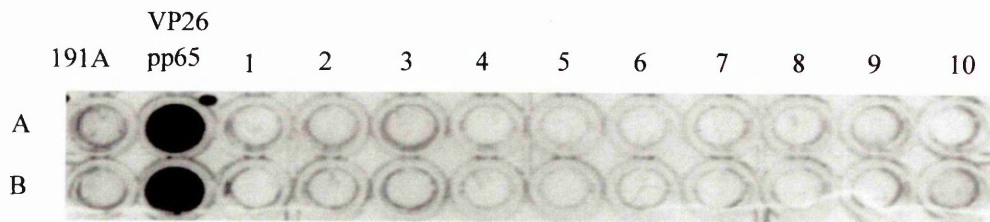
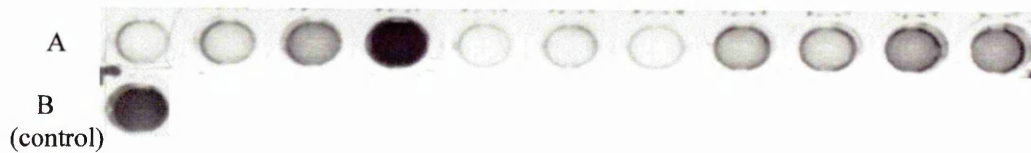


Figure 5.17: Oligopeptide (35/1 - 35/10) Inhibition of the VP26 - VP5 Interaction

(i) ELISA Wells



(ii) A₄₀₅ Values



Figure 5.16: To confirm that oligopeptides 35/1 to 35/10 did not cross react with the pp65 antibody, a microtitre plate was coated with each oligopeptide in duplicate (see wells 1-10, rows A and B respectively). These were reacted with the pp65 antibody in an ELISA type assay. No reaction was detected and absorbance values were comparable with the negative control (see rows A and B, 191A). A positive control, containing the VP26pp65 protein was included to validate the assay (see rows A and B, VP26pp65)

Figure 5.17: Panel (i) shows the results of an ELISA assay when all the oligopeptides were tested together (row A, first well) and individually, ie oligopeptides 35/1 to 35/10 are found in row A, wells 2 to 11, from left to right respectively. The oligopeptides were used to inhibit the binding between VP26pp65 and VP5. An example of a control well, with no oligopeptide present is shown in row B.

Panel (ii) shows the A_{405} values obtained for the assay. The control well produced a consistent A_{405} of approximately 1.2 over several repeats (represented by the dashed line). However, the presence of the oligopeptides caused a variation in absorbance (refer to text, section 5.1.3.2).

the anti-pp65 antibody, to ensure that they did not cross-react with it. The microtitre wells were coated with 50 μ moles of each oligopeptide, o/n at 37°C. VP26pp65 (1:8) and 191A (1:8) were included as positive and negative controls. The pp65 antibody was reacted at 1:800 and detected with the GAM-conjugate and the signal developer.

It is clear from figure 5.16 that the only positive signal with the pp65 antibody, was when VP26pp65 was used to coat the wells. In this instance, the $A_{405}=0.7$. In all other wells no reactivity was seen and the $A_{405} < 0.05$.

To set up the blocking ELISAs, microtitre wells were coated o/n at 37°C with 191A, as previously described. The VP26pp65 protein was added to each well at 0.25 μ g in parallel with either a single peptide, or all 10 oligopeptides together, each at 50 μ moles per well. This set up a competition assay where VP26pp65 and the oligopeptide would compete for the binding site on 191A. As the protein and oligopeptide were added in parallel, each had an equal chance of binding to 191A. VP26pp65 and the appropriate oligopeptide were reacted with 191A for 1h at 37°C. A control row, containing VP5 and VP26pp65 alone, with no oligopeptide, was also included for comparison purposes. The reaction was developed with GAM-conjugate and the signal developer.

Figure 5.17 (panel (i), row B) shows that there was no inhibition in binding between VP5 and VP26 when no oligopeptide was present. In this case the $A_{405} > 1.0$. However, it can be seen that 3 overlapping oligopeptides, 35/4, 35/5 and 35/6, were causing the greatest reduction in binding, with the A_{405} less than half the control value at < 0.5 [panel (ii)]. Oligopeptide 35/1 was also causing a consistent reduction in Absorbance, comparable with the levels observed for oligopeptides 35/4-35/6. When the 3 successive wells and 35/1 were compared visually with the control well (VP26pp65 + 191A alone) it is obvious that there was a significant reduction in the colour development.

An apparent increase in binding activity was observed in the well containing 35/3. The Absorbance values recorded exceeded that of the positive control wells. This was a consistent feature which cannot be explained as none of the oligopeptides cross-reacted

Figure 5.18: The solid line in panels (i) and (iii) represents the position of the oligopeptides, 35/4 to 35/6, which caused an inhibition in the binding of VP26pp65 to VP5.

Panel (i) represents the UL35 ORF. The * in panel (ii) represents the amino acid sequences which are conserved between the alpha herpesviruses and panel (iii) shows the protein predict (Heidelberg) for the alphaherpesviruses.

Figure 5.19: The amino acid sequence of VP26pp65 is shown with the positions corresponding to unique restriction enzyme sites used in the mutagenesis studies, marked by the arrows. The extra sequences in pET35pp65, contributed by the 6xhis (double underline) and pp65 (single underline) tags, are also shown.

Figure 5.20: Construction of pET35pp65 N-Terminal Deletion Mutants

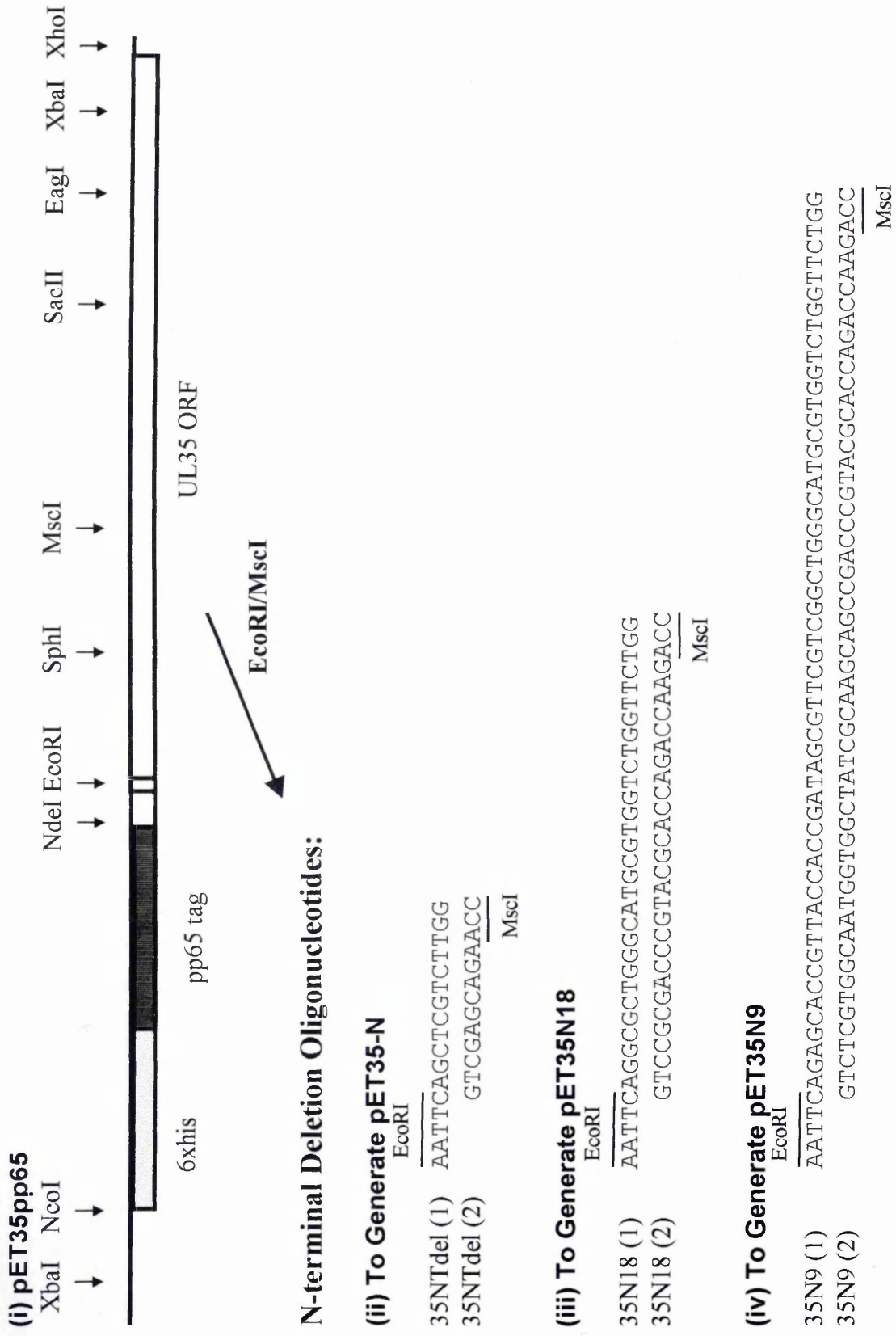


Figure 5.20: pET35pp65 [panel (i)] was EcoRI/MscI digested and ligated with the complementary oligonucleotides in either panel (ii), (iii) or (iv). This generated 3 N terminal deletion mutants respectively. PET35-N has the N terminal 24 amino acids deleted. PET35N18 has 18 amino acids deleted at the N terminus. PET35N9 has 9 amino acids deleted at the N terminus.

with the pp65 antibody. Apparently, this is a phenomenon which has been previously reported to occur using oligopeptides in this type of blocking ELISA reaction (Howard Marsden; personal communication).

The well containing all the oligopeptides together showed a significant decrease in binding activity, comparable with the levels observed for oligopeptides 35/4-35/6. It seems probable that this reduction in binding would be attributable to the additive effect of having multiple inhibitory oligopeptides present.

The fact that 3 consecutive overlapping oligopeptides produced a decrease in binding of VP26pp65 to VP5 (191A) strongly suggests that this area is important for the binding of VP26 to VP5. The amino acid sequence encoded by these oligopeptides is located between positions 31-70 (see figure 5.18). This is an area with very poor amino acid sequence conservation between the alpha herpesviruses [panel (ii)]. However it, includes a region of predicted alpha helix (EMBL, Heidelberg) for all 3 alpha herpesviruses [panel (iii)]. Furthermore, all the alpha and beta herpesviruses have a similar predicted secondary structure, yet poor amino acid sequence homology.

5.2 Attachment of VP26 Mutants to VP26- Capsids

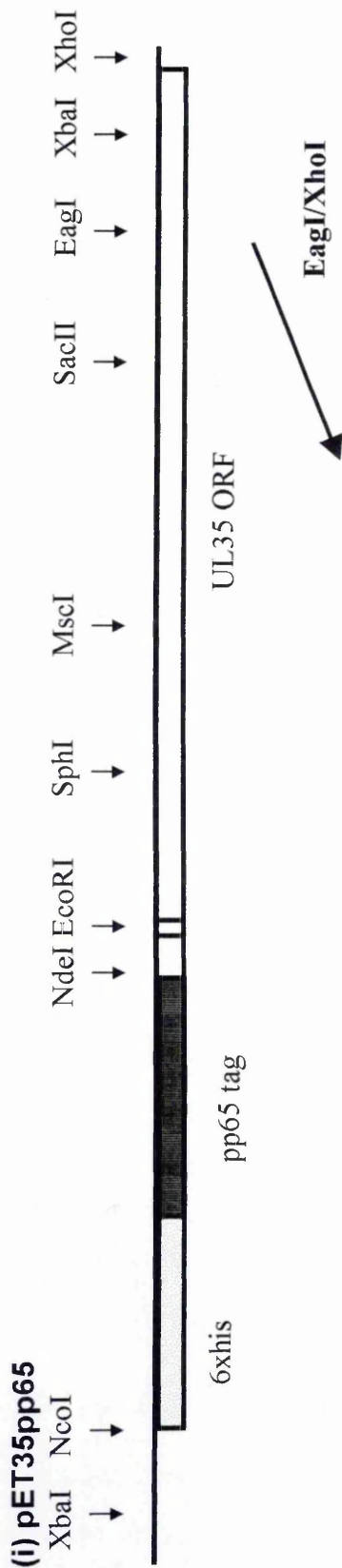
In order to confirm that the region of VP26 contained within oligopeptides 35/4-35/6 was required for the interaction with VP5 and to further define the sequences important for the binding of VP26 to capsids, a series of mutants was constructed. Both insertion and deletion mutants of pET35pp65 were made to produce mutated VP26pp65 protein for use in an interaction assay system.

5.2.1 Construction of Deletion Mutants

UL35 had several restriction enzyme sites, well spaced and positioned throughout the gene (see figure 5.19). These were used to digest and remove portions of the UL35 ORF thus creating a series of deletion mutants.

Firstly, deletions of the N-terminal portion of the protein were constructed (see figure 5.20). An EcoRI/MscI digest, followed by the insertion of two small complementary

Figure 5.21: Construction of pET35pp65 C-Terminal Deletion Mutants



C-terminal Deletion Oligonucleotides:

(ii) To Generate pET35-C

EagI
GGCCGGCCTGACTGCAGC
 35CTdel (1)
 XhoI
CGGACTGACGTCGAGCT
 35CTdel (2)

(iii) To Generate pET35C18

EagI
GGCCGGCTTGGCTGCGTCCGGCGTTCGGCCTGTGAAC
 35N18 (1)
 XhoI
CGAACCGACGCAGGCCCGCAAGCCGGACGCGTGGATGAGAGGCAACAACTTGAGCT
 35N18 (2)

(iv) To Generate pET35C9

EagI
GGCCGGCTTGGCTGCGTCCGGCCGTTCCGGCCTGCGTCCGTTCCGTTGTTGAAC
 35N9 (1)
 XhoI
CGAACCGACGCAGGCCCGCAAGCCGGACGCGTGGATGAGAGGCAACAACTTGAGCT
 35N9 (2)

Figure 5.21: pET35pp65 [panel (i)] was EagI/XhoI digested and ligated with the complementary oligonucleotides in either panel (ii), (iii) or (iv). This generated 3 C terminal deletion mutants respectively. PET35-C has the C terminal 26 amino acids deleted. PET35C18 has 18 amino acids deleted at the C terminus. PET35C9 has 9 amino acids deleted at the C terminus.

oligonucleotides, 35NTdel (1) and 35NTdel (2), created pET35-N [see panel (ii)]. This removed 24 amino acids from the N-terminus. An identical approach was used to generate two other N-terminal deletions. This time after the EcoRI/MscI digest, larger oligonucleotides were used to re-build defined portions of the UL35 native sequence. pET35N18 was generated by inserting two complementary oligonucleotides, 35N18 (1) and 35N18 (2) [panel (iii)], which rebuilt all of the native UL35 amino acid sequence between the restriction enzyme sites, except for 18 of the N-terminal residues. Similarly, pET35N9 was created by inserting the complementary oligonucleotides 35N9 (1) and 35N9 (2) [panel (iv)], which regenerated all the appropriate native amino acid residues except 9, at the N-terminal end.

Secondly, a series of C-terminal deletions were made using an identical strategy to that described above (see figure 5.21). An EagI/XhoI digest, followed by the insertion of two very small complementary oligonucleotides, 35CTdel (1) and 35CTdel (2), created pET35-C [see panel (ii)]. This removed 26 amino acids from the C-terminus. An identical approach was used to generate 2 other C-terminal deletions. This time, after the EagI/XhoI digest larger oligonucleotides were used to re-build defined portions of the UL35 native sequence. pET35C18 was generated by inserting two complementary oligonucleotides, 35C18 (1) and 35C18 (2) [panel (ii)], which rebuilt all of the native UL35 amino acid sequence between the restriction enzyme sites, except for 18 of the most C-terminal residues. Similarly, pET35C9 was created by inserting the complementary oligonucleotides 35C9 (1) and 35C9 (2) [panel (iv)], which regenerated all the appropriate native amino acid residues except 9, at the C-terminal end.

5.2.2 Expression and Purification

Unfortunately, all of the deletion mutant proteins were very difficult to induce and their expression levels were highly variable. Even when glycerol stocks were not used, for fear of plasmid instability, but DNA was transfected each time to produce fresh colonies for starter cultures, the expression levels were still poor and any protein which was expressed was extremely insoluble. It was thought that the high expression levels of pET35pp65 been a factor which had contributed to the protein's insolubility but this explanation could not be used for the deletion mutants. The same denaturing and

solubilisation protocol used for VP26pp65 was followed and the protein was purified through Ni-NTA resin (as Chapter 4, table 4.4). However, there was an extremely poor purification yield in all cases. Virtually no protein, even in Buffer E, containing 200mM imidazole and 8M urea, was eluted. This suggested the deletion mutants were even more insoluble than the full length VP26pp65 protein or, that they were not sufficiently concentrated to be detected.

As so much time had already been spent developing the solubilisation procedure for VP26pp65, it was decided to concentrate on the development of insertion mutants, in the hope that these would prove more successful and could be utilised in an assay system.

5.3 Construction of Insertion Mutants

Insertional mutants of VP26pp65 were constructed using the modified Kunkel method of site directed mutagenesis (Kunkel, 1985) (see Methods, Section 2.5.13). This was a rapid and efficient site-specific approach which allowed the insertion of specific bases into the UL35pp65 ORF. The approach involved manipulating single stranded viral DNA, from M13 phage, grown in an *E coli dut⁻ ung⁻* strain. The deficiency of the *dut* gene, which encodes dUTPase, resulted in an increase of dUTP. UTP competed with TTP for incorporation into the DNA. Due to the absence of the *ung* gene, which encodes uracil glycosylase, incorporated uracil was not removed. The M13 phage template ssDNA therefore contained a significant amount of uracil residues, ie 20-30 per genome. Primers containing the modified sequences were then annealed to the ssDNA and the elongation reaction performed with TTP and no dUTP. The resulting dsDNA phage contained one strand of the native sequence, with uracil residues, and one strand with the mutant insertion, and no uracils. This phage was grown in *E coli dut⁻ ung⁺*. The presence of uracil glycosylase removed the uracil bases from the template strand, creating lethal abasic sites. This favoured selection of the mutant strand containing the extra inserted sequences.

Figure 5.22: Sequence and Location of 3x Glycine (3xG) Insertion Primers

(i) pET35pp65.1: rightward 5' to 3', position 28 to 66 (bp)

ATCGGTGGTAACGGTaccgccaccGCTGGGGCGTGAAA

(ii) pET35pp65.2: rightward 5' to 3', position 58 to 96 (bp)

CATGCCAAGCGCCCGgccgccaccGACGCTATCGGTGGT

(iii) pET35pp65.3: rightward 5' to 3', position 63 to 138 (bp)

CTGAGAGTTATTGGTaccgccaccGGCCAAGACGAGCCC

(iv) pET35pp65.4: rightward 5' to 3', position 142 to 180 (bp)

CTGGGGGTGCGGGTGgccggtaccGTTGTTATCCATGAT

(v) pET35pp65.5: rightward 5' to 3', position 193 to 231 (bp)

GCGGAGAAACTCCCGgccgccaccCACGGCCCTTGGGT

(vi) pET35pp65.6: rightward 5' to 3', position 232 to 270 (bp)

ACCAAGGTCCGTCAGgccaccgccgGCCGCCGCCTGACC

(vii) pET35pp65.7: rightward 5' to 3', position 274 to 312 (bp)

CTGCGGGGTAAAGGTaccgccaccGTTGTTTCGCGTGGGC

(viii) pET35pp65.8: rightward 5' to 3', position 322 to 358 (bp)

CCGCAACCAGGCGGCgccaccgccCGGGGCGTCGCCCCG

(ix) pET35pp65.9: rightward 5' to 3', position 367 to 405 (bp)

AAACGGTGAATAGGTaccgccaccGCGCCGCAGGCCAAA

(x) pET35pp65.10: rightward 5' to 3', position 418 to 456 (bp)

CGGGCCTCACGGGGTaccgccaccCCCGGGCGTCGAAGG

Figure 5.22: The sequence of the oligonucleotides are shown in panels (i)-(x). The native UL35 sequence is shown in capital letters, while the 3xG coding insert is represented in lower case letters. The position of the insertions (1-10) within the UL35 ORF sequence genome is detailed in panels (i) to (x) and their approximate location in pET35pp65 marked with an arrow in panel (xi). The restriction enzyme sites which are generated as a result of these insertions are shown.

Panel (xi) also shows the extra sequences in pET35pp65, contributed by the 6xhis (single underline) and pp65 (double underline) tags, the location of the sequence mapped by the inhibitory oligopeptides, 35/4-35/6, (represented by the dashed line) and the protein predict (PP) generated by EMBL, Heidelberg (with L representing loop, H, α -helix and E, β -sheet).

Figure 5.23: Sequence Data for pET35pp65.1

5'

1 CATTGTGGAGCGGATAACAATTCCCCTCTAGAAAATAATTTTGTTTAACTTTAAGAATGAGA
59 TACCANGGGTTNNCAGCCCATCATCATCATCACNCCGAGCGCAAGACGCCCCGCCTACC
117 GCGGAATGGAATTCAGGCCNTCCCGCAATTTACCAGCCCCACCGGTGGCGGTACC GTTACC
233 ACCGATAGCGTCCGGGCGCTTGGCATGCNCGGGCTCNTCTTGGNCACCNATAACTCTCAGTT
291 TATCNTGGATAACAACCNCCCGCACCCCNNGGGNACCCNANGGGNCGTGNNGGAATTTCTCC
349 CTCGGTCNNGGGGGGGGGCCTNANAGAACNTTTNTTTTTNTNCACNCNAACANNCNTTTTTTA
407 CCCCCACCNTNTTTTTTTTCGGGGCGANACCCGCCCCCTTGGTTNTNTGGCCCCCTTTTT
465 GGCTTNCNGGGGGCNCNNNTCNCCCNCTTTGTTCTTTCNAAAAACCTTTTAACCCCCGGG
523 AACCCCNNTAAGNCCCNGGGGAATTCNCTCNTGGGGTGTTCCTNTAAATCTAANAACCT
581 TNTNGGGCGCACTCCNAAANCCACCACCCACACCAACTNAAATTTNCGGGTGCCTAACANAA
639 NCCCCAAAAAGGAAAACTNNAATTTGGCTTNTTNCCCCCNCTGAAACAACCTCAACCAACAA
697 TNAACCCCTTTGGGGCCTNTTANAACCGGTCCTTGAAAGGGTTTTTTTTGGTTTTCANACG
755 GAAGGAAATTATTTTCCCGAATTNNGCAANCNGGAACCCCCCTNTTCCCNGGGGCCCTT
TANACCCGNNCGGGTNTTNGTTGGTTTACTCCCCCAACGTTNACCNTN

3'

871



Figure 5.23: Sequence data for pET35pp65.1. The position of the 6x his tag is shown by the solid line and the position of the 3x glycine insert is confirmed by the dashed line. A, T, C and G represent the four DNA bases and N represents a base undefinable during the sequence analysis.

This approach was used to construct 10 mutants in pET35pp65 namely, pET35pp65.1-pET35pp65.10 (see figure 5.22). All had extra sequences which, when inserted, allowed the creation of a restriction enzyme site. This constituted insertion of 3 glycine residues (3xG) at all the points indicated in the figure, except for pET35pp65.4 which had a GTG insertion, ie glycine, threonine, glycine (to allow the creation of a restriction enzyme site). However, for simplicity all the mutants will be referred to as containing a 3xG insert.

The 3xG residues were inserted at points throughout the UL35 ORF, based on the protein prediction (EMBL, Heidelberg) because at this stage the CD data, which gave a different interpretation of the structure (see Discussion and Wingfield *et al*, 1997), was not available. 3xGs were chosen as they would disrupt a predicted alpha-helical secondary structure.

An attempt was made to insert at least one 3xG insert within each predicted motif of the sequence [see figure 5.22, panel (xi)]. So, for example, pET35pp65.1 had an insert in the N-terminal loop region, pET35pp65.2 had an insert in the N-terminal β -sheet region and pET35pp65.3 had an insert in the N-terminal α -helix region etc. The presence of the inserts was confirmed firstly by restriction enzyme digestion (data not shown) and then sequence analysis (see figure 5.23 as a representative example). It was hoped that this approach would disrupt the structure of the binding site(s) and allow the points of interaction between VP26 and VP5 to be definitively mapped. It should be noted that the inhibitory peptide sequences of 35/4-35/6, spanned the amino acids where insertion points numbered 4, 5 and 6 occurred, ie pET35pp65.4-pET35pp65.6.

5.3.1 Expression and Purification

Unlike the deletion mutants, the 3xG mutants were expressed to high levels when induced with 1mM IPTG (the VP26 mutant proteins shall henceforth be designated VP26pp65.1 – VP26pp65.10). The mutant proteins were all insoluble and so were denatured and purified through Ni-NTA in the manner described for pET35pp65 (see Chapter 4, Section 2.4). Good yields, typically 5-10mg/ml, were obtained from the initial

Figure 5.24: Elution of VP26pp65 3xG Mutants in 200mM Imidazole

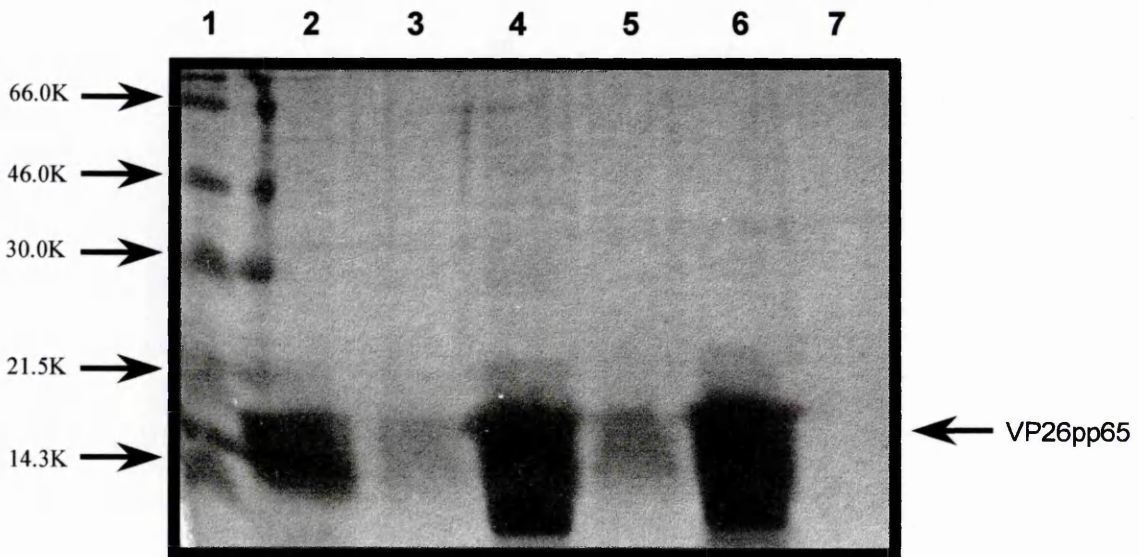


Figure 5.25: Generation of VP26- Capsids by Treatment with 4M Urea

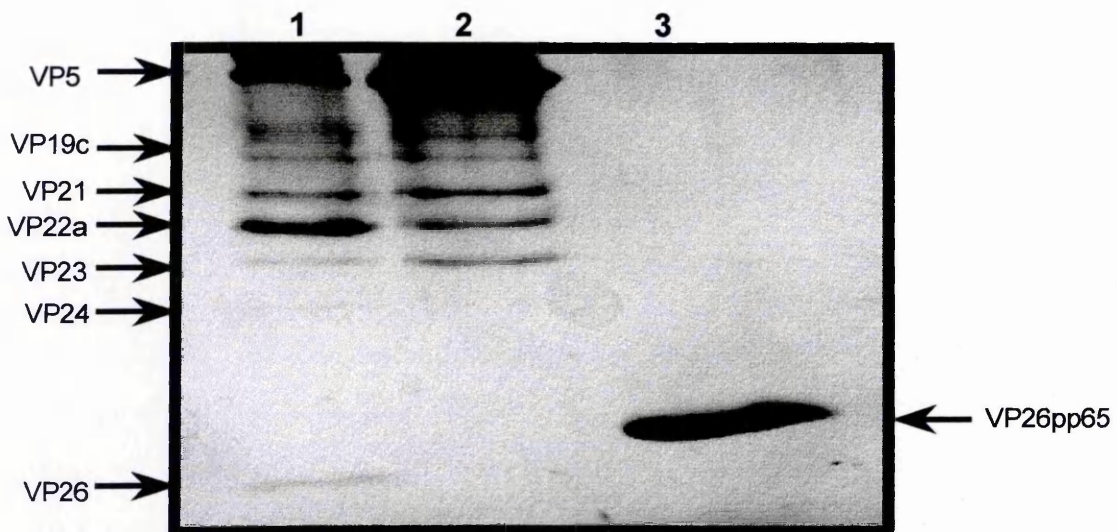


Figure 5.24: Coomassie brilliant blue stained gel with the size marker in lane 1. Lanes 2 to 7 represent Ni-NTA purified, 200mM imidazole (Buffer E), fractions (elution 1 and 2 respectively) of the VP26pp65 protein carrying a 3xG insert (ie VP26pp65.1 [lanes 2 and 3], VP26pp65.2 [lanes 4 and 5] and VP26pp65.3 [lanes 6 and 7]).

Figure 5.25: Coomassie brilliant blue stained gel. Lane 1 shows wild type B capsids and lane 2 shows VP26- capsids, which have been stripped of their VP26 through treatment with 4M urea. Lane 3 shows soluble VP26pp65 protein.

elution in Buffer E (figure 5.24). However, unlike the VP26pp65 protein, none of the mutants remained substantially soluble when dialysed against NTE.

5.4 Development of an Interaction Assay System for 3xG Mutants and VP26- Capsids

It was decided not to use the ELISA system, developed in Section 5.1, to study the interaction of the 3xG mutants with either VP5 or VP26- capsids as none of the mutant proteins were soluble in NTE with no urea present. As the ELISA had been optimised in the absence of urea, it would have been necessary to find conditions for removing the 8M urea from each of the 10 mutant proteins. Time constraints did not allow this avenue to be considered.

It had been reported (Newcomb *et al*, 1993) that extraction of B capsids with 4M urea removed VP26, some penton (approximately 10%) and scaffold, leaving otherwise structurally intact capsids. As the 3xG mutant proteins were soluble in urea, it was felt that it might be easier to generate VP26- capsids using this method (Section 2.1), and bind the mutant proteins in the presence of urea. M Kikitadze (University of Edinburgh) had reported (personal communication) that VP26 had a largely stable secondary structure, by CD analysis, in concentrations up to 2M urea.

5.4.1 Production of VP26- capsids by Treatment with 4M Urea

B capsids in NTE, at approximately 10mg/ml, were diluted to 1-2mg in 4M urea, with 0.05M DTT present. The solution was mixed end-over-end at rt for 1h. The capsids were then pelleted through 25% (w/w) sucrose at 28000 rpm for 1h. The sucrose layer was carefully removed and the pellet washed and resuspended in 100µl of NTE by sonication in a Kerry sonibath. 5µl was run on a minigel to confirm that the VP26 protein had been removed (figure 5.25) and VP26- capsids had been generated. These were stored at -20°C until required.

5.4.2 Attachment of 3xG Proteins (VP26pp65.1 – VP26pp65.10) to VP26- Capsids

As the quantities of B capsids available were small and the task of making more was time consuming, an assay system was developed which utilised very small quantities of capsids.

Figure 5.26: Mini Gradients and Western Blots of VP26pp65+ Capsids and VP26- Capsids Mixed with 3xG VP26pp65 Constructs

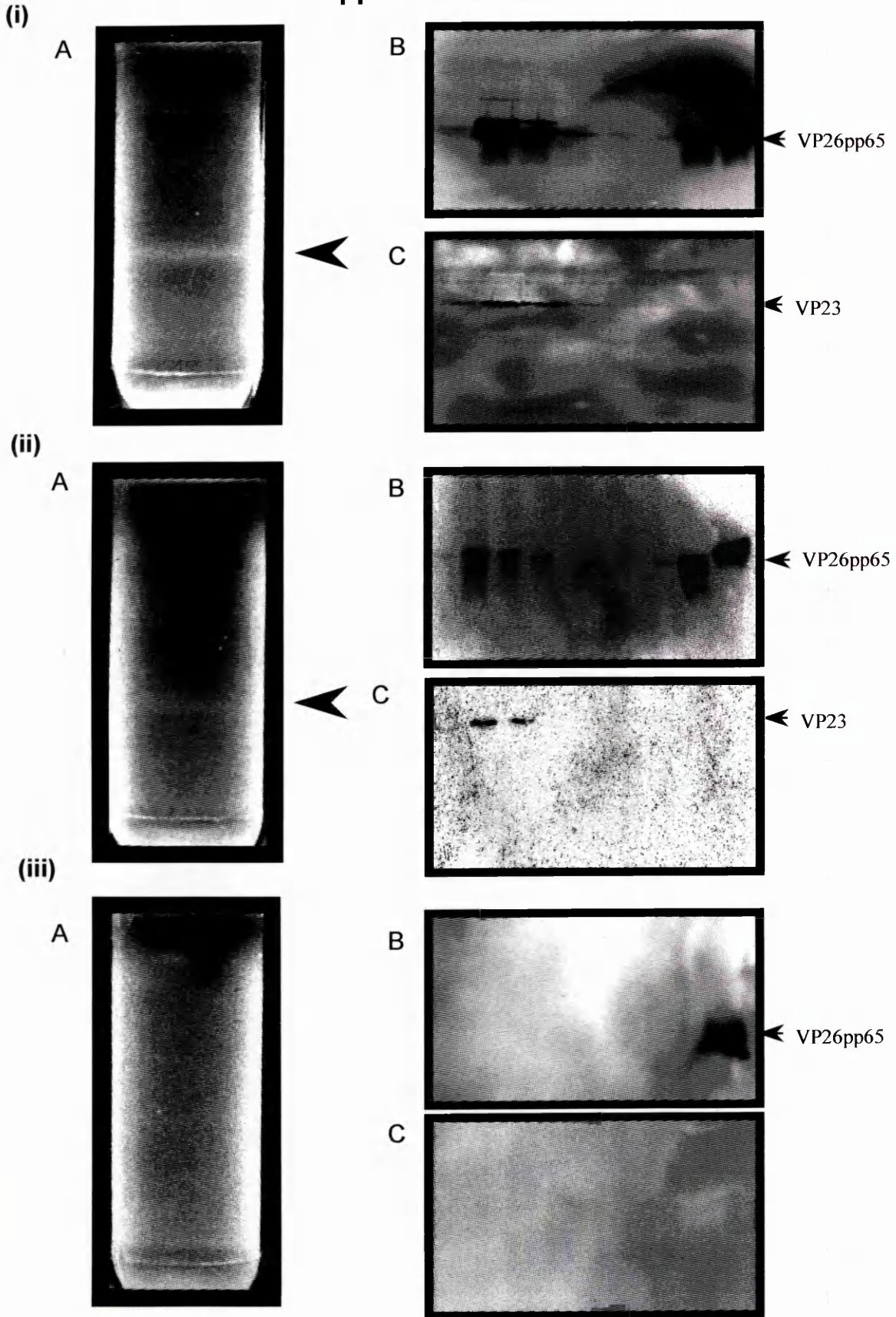


Figure 5.26: Mini gradients were viewed under fibre optic light (A panels) and 200µl fractions collected from the bottom to the top of the tube. The fractions were run sequentially on an SDS gel from left (bottom of the gradient) to right (top of the gradient). The blots were probed with pp65 antibody (B panels) and anti-VP23 antibody (C panels).

Panel (i) shows the results obtained for VP26pp65⁺ capsids.

Panel (ii) shows a representative example (ieVP26pp65.3) of the results obtained when the 3xG mutant proteins VP26pp65.3, VP26pp65.4 and VP26pp65.7 to VP26pp65.10 were mixed with VP26- capsids.

Panel (iii) shows a representative example (ieVP26pp65.1) of the results obtained when the 3xG mutant proteins VP26pp65.1, VP26pp65.2, VP26pp65.5 and VP26pp65.6 were mixed with VP26- capsids.

(i) Production of 'Mini gradients'

The initial step in the development procedure was to produce very small sucrose gradients. Previously 13ml, 10-40%, sucrose gradients had been used, which made it difficult to distinguish small amounts of capsid (see Section 2.1.2). The process was scaled down and 2ml 'mini gradients' were prepared by layering 1ml of 40% (w/w) sucrose and 1ml of 10% (w/w) sucrose in a Beckman 11x34 mm tube and mixing at 18000 rpm for 1 min at an angle of 80°, on a Gradient Master 106 (Biocomp Instruments Inc).

(ii) Attachment of 3xG Mutant Proteins to VP26- Capsids

Preparations were made by adding 2ul of 8M urea, and 10ul of the appropriate 3xG mutant protein (or VP26pp65 control), in 8M urea (Elution buffer E) to 70ul of NTE. 14ul of the VP26- capsids, in 4M urea, were added last to generate a final urea concentration of 1M. The solution was mixed, end-over-end, at rt for 1h.

(iii) Purification of Capsids Containing 3xG mutant Proteins

The 100µl preparations [stage (ii)] were each overlaid on to a mini gradient and spun at 20000 rpm for 1h, at 4°C, in the Beckman TL400 ultracentrifuge, to band the capsids. The gradients were viewed under a fibre optic light in a darkened room.

5.4.3 Attachment of VP26pp65.1 to VP26pp65.10 to VP26- Capsids

The control protein VP26pp65, in a final concentration of 1M urea, attached successfully to the VP26- capsids. A visible band was evident on the mini gradient [see figure 5.26, panel (i) A]. 200µl fractions were dripped across it and analysed by Western blot. VP26pp65 was detected in several fractions [figure 5.26, panel (i) B]. To confirm that the protein was attached to the capsids, the fractions were also probed with an anti-VP23 antibody (186, from D McClelland). VP23 was detected in comparable fractions to that which had contained VP26pp65 [figure 5.26, panel (i) C], confirming that the VP26pp65 protein was attached to the capsids. These result showed that the assay system was successful and capsids could be banded on the mini gradients. In addition

VP26pp65 alone was detected at the top of the gradient (panel (i) B, right hand side), indicative of residual protein which had not attached to the capsids.

The pattern of interaction for the 10, 3xG mutant proteins varied. Visible bands, comparable with the control sample, were clearly evident for preparations containing VP26pp65.3, VP26pp65.4 and VP26pp65.7 to VP26pp65.10 [see figure 5.26, panel (ii) A, as a representative example]. 200µl gradient fractions were collected and analysed by Western blot [see figure 5.26, panel (ii) B, as a representative example]. The 3xG VP26pp65 proteins was detected in fractions which coincided with the detection of VP23 (using 186 antibody) [see figure 5.26, panel (ii) B], confirming that the mutant proteins were attached to the capsids. Again, unattached VP26pp65 mutant protein was detected at the top of the gradient (panel (ii) B, right hand side). However, no capsid bands were evident on the gradient when VP26pp65.5 and VP26pp65.6 were present and only extremely faint bands, or in some experiments no band at all, were evident for VP26pp65.1 or VP26pp65.2 (see figure 5.26, panel (iii) A, as a representative example). 200µl fractions were also collected across these gradients and analysed by Western blot. The VP26pp65 protein was only detected at the very top of the gradient [see figure 5.26, panel (iii) B], indicating that it had not bound to the capsids. When the fractions were probed with anti-VP23 antibody (186), no capsids were detected in any of the fractions.

The experiment was repeated using VP26- capsids mixed with either VP26pp65 (control), VP26pp65.3 (which had banded on the gradient) or VP26p65.5 (which had not banded on the gradient). This time, all the fractions were not banded but were spun through a 25% (w/v) sucrose cushion (28 000rpm, 1h) and analysed by western blot, gel electrophoresis and negative staining.

Each blot was probed with anti-VP23 antibody (186) and then the anti-pp65 antibody (pp65). As expected VP26 was found to be attached to capsid in the samples which had been mixed with VP26pp65 and VP26pp65.3 [not shown, similar pattern to figure 5.26, panels (i) and (ii)]. However, unlike the gradient banding experiment, VP26pp65.5 was

Figure 5.27: Confirmation of Attachment of VP26pp65.5 (3xG mutant) to VP26- Capsids

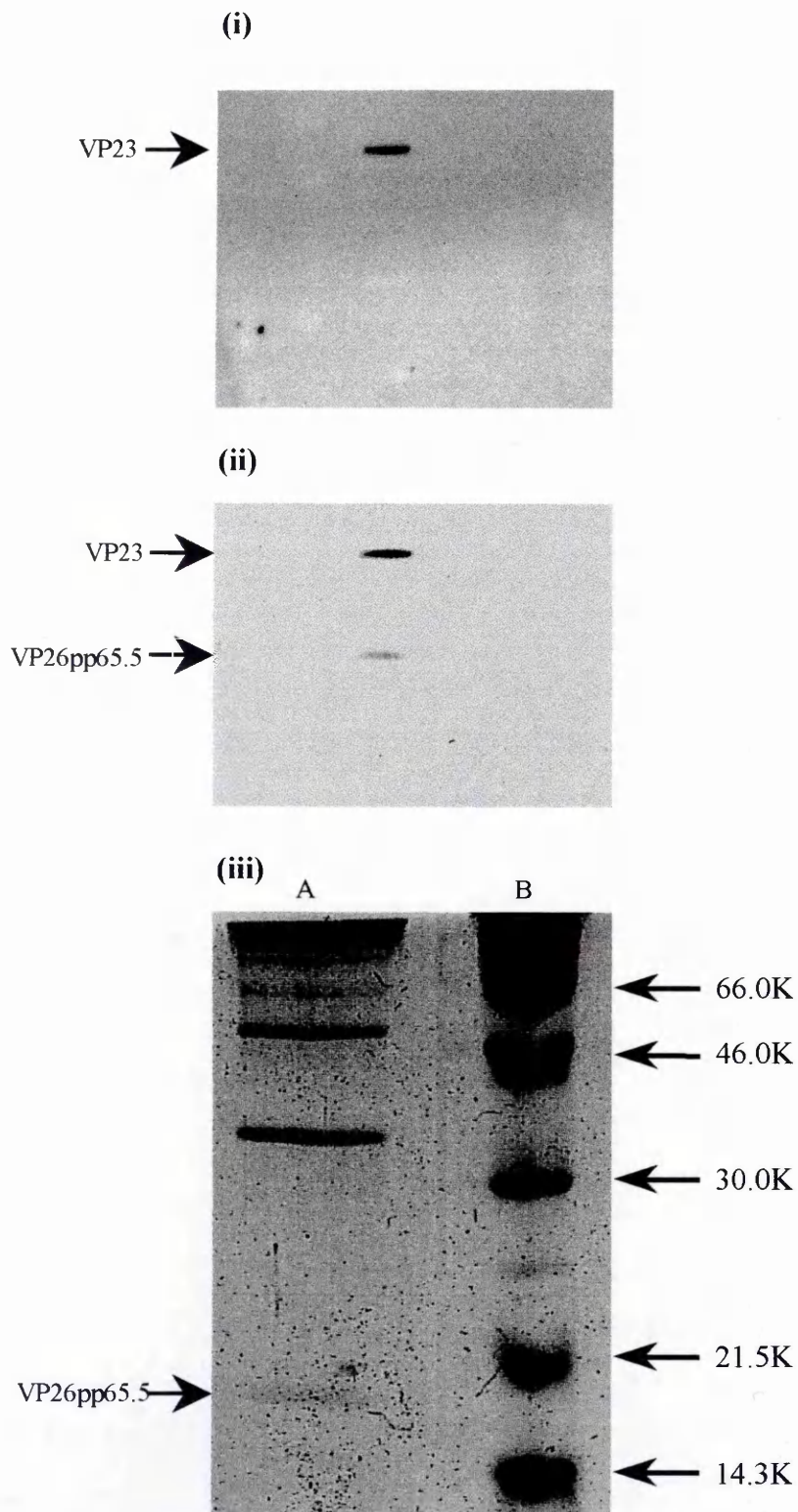
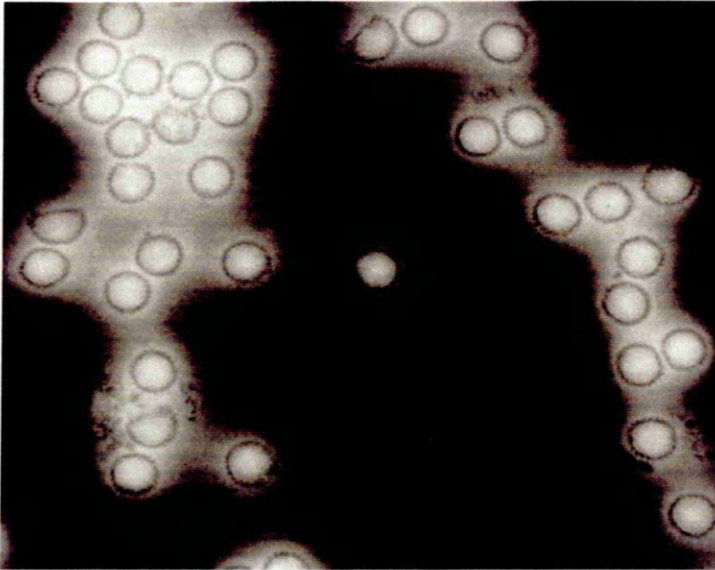


Figure 5.27: VP26pp65.5+ capsids were analysed by western blot. The presence of capsids was confirmed with anti-VP23 antibody (186) [see panel (i)]. The blot was then probed with anti-pp65 antibody. The VP26pp65.5 protein was detected in the same lane as VP23 [see panel (ii)] confirming that VP26pp65.5 had attached to VP26-capsids.

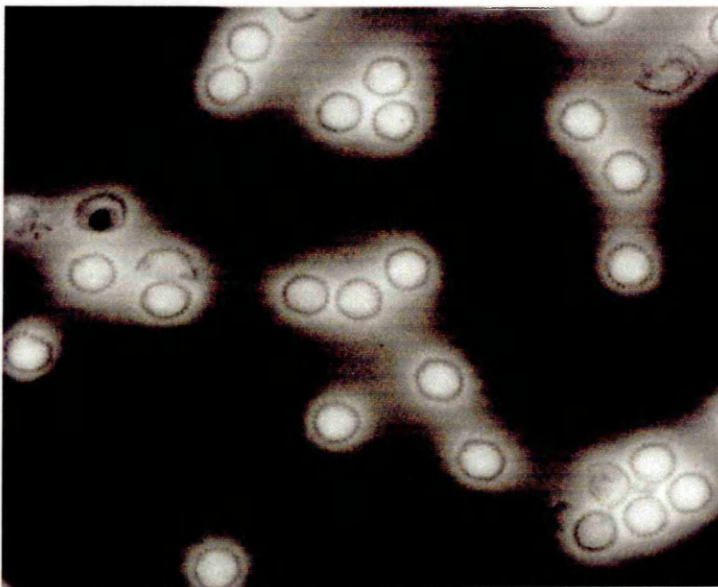
The protein profile of the VP26pp65.5+ capsids is shown in the coomassie brilliant blue stained gel (panel (iii), lane A) and the position of VP26pp65.5 is marked with an arrow. [The marker is shown in panel (iii), lane B].

Figure 5.28: Electron Micrographs of VP26pp65+ Capsids and VP26pp65.5+ Capsids

(i) VP26pp65+ Capsids



(ii) VP26pp65.5+ Capsids



It is not attached to the

part of the

Figure 5.28: VP26pp65+ capsids [panel (i)] and VP26pp65.5+ capsids [panel (ii)] were viewed by negative staining.

part of the

found to be attached to the capsids and VP23 and VP26 were detected in the same lane. [see figure 5.27, panels (i) and (ii)]. Analysis of these fractions by SDS-PAGE confirmed that the VP26pp65 proteins had attached to the capsids in each case (see figure 5.27, panel (iii), as a representative example).

Examination of all fractions by negative staining (see figure 5.28) revealed that, even although samples containing VP26pp65.5 had not banded on gradients, they were formed and intact in all cases. VP26- capsids which had been mixed with VP26pp65 [panel (i)], VP26pp65.3 [not shown] or VP26pp65.5 [panel (ii)] did not differ in appearance from wild type capsids, at this resolution.

6. Discussion

6.1 Function validity of VP26pp65

It was possible to confirm that the soluble bacterially expressed protein, VP26pp65, in NTE (described in Chapter 4) was structurally and functionally valid. The protein bound correctly to VP26- capsids at the tips of the VP5 hexons and not pentons. Even though VP26pp65 was added in slight excess, the penton sites remained unoccupied. This mimicked the pattern of wild-type and fully recombinant capsids (Trus *et al*, 1995; Zhou *et al*, 1995). Therefore the extra 25 amino acid residues at the N-terminus of VP26, attributed by the 6xhis and pp65 tags, do not interfere with the binding of VP26pp65 to capsids. This shows that this region of the protein can have additional sequences added without the binding to capsids being affected. This is highly indicative that the specific amino acid sequence at the N-terminus, are not important for the correct binding of VP26 to the capsid. Recent data (Desai & Person, 1998) has shown that the 270 amino acid green fluorescent protein (GFP) can be attached to the N-terminus of VP26 and not disrupt the binding of the protein to capsids. This further confirms that this area of the protein is not important for binding.

6.2 Possible Location of the N-terminus of VP26

The presence of the extra mass, contributed by the 6xhis and pp65 tags, proved to be an asset to the analysis. This region was mapped by comparing VP26pp65 containing hexons with wild type VP26 containing hexons. Cryo-EM and computational data

analysis revealed an area of extra mass, present only in VP26pp65 hexons. It is important to realise that the extra mass detected is not large enough to constitute all 24 of the extra amino acids present in the tags. It may be that this region is the only visible part of the additional sequences. The rest of the sequence may be in the form of a flexible loop or some other unresolved structure or, it may be that some amino acids are folded inside the protein and so are not visible on the surface.

This technique is a potentially useful way for orientating proteins within a complex structure. It is not known how 6 copies of VP26 on the hexon interact with each other. Attempts at crystallisation and NMR have proved unsuccessful (personal communication; M Kirkitadze, University of Edinburgh) due to the insoluble nature of the protein and the problems involved in producing high concentrations. This means that the structure of a single molecule of VP26 is unknown and it is not clear when looking at the star shaped ring of 6x VP26, where one molecule starts and another one stops. Zhou *et al* (1995) suggested that the protein has a large and small domain contained within each monomer. The type of approach taken in this study, may pin-point the location of the N-terminus of VP26 and helps us to begin building a picture of how the VP26 proteins are interacting with the capsids and each other.

6.3 Oligomeric Status and Secondary Structure of VP26

Examination of the oligomeric status of VP26pp65, suggested that the protein consisted of monomers and dimers in solution. No evidence of any hexamerisation was detected which would have supported the model of Zhou *et al*, 1995, where a VP26 hexamer can only fit onto a VP5 hexamer and not pentamer. Instead it would seem that although all capsomeres are primarily composed of the same protein, VP5 in hexons must be conformationally different from the VP5 in pentons and the difference must define a VP26 binding site. Evidence for a difference between hexons and pentons is supported by data which shows that distinct monoclonal antibodies label either the hexons or pentons and do not cross-react with either structure (Trus *et al*, 1992). However, this does not fully explain how the VP26-VP5 ELISA reaction worked. VP5 (191A) has not been accurately sized in solution and so it is not known whether this protein spontaneously forms hexons and/or pentons. It is possible that VP26pp65 was only

interacting with VP5 which had hexamerised. Alternatively, a monomer or dimer of VP5 might bind to VP26 but, upon undergoing conformational changes involved in forming hexon and penton capsomeric subunits, the penton arrangement could lose its ability to interact with VP26. Recent results produced by sizing VP5 by its light scattering properties, have suggested that the protein spontaneously forms multimers (B Barnes; personal communication) but, it was not possible to distinguish between 5-mer and 6-mer arrangements. This data supports the theory that VP26 is binding to preformed VP5 hexons. However, Newcomb *et al* (1999) have published conflicting data which suggests that purified VP5, from the baculovirus expression system, forms monomers in solution. Therefore the stage at which VP26 binds to VP5 is not clear.

Fluorescence data presented in this thesis (Chapter 3) has shown that VP26 is only found to be nuclear when VP5 is also nuclear, ie in the presence of preVP22a or VP19c. This shows that VP26 itself does not carry a nuclear localisation signal and is in fact mainly in the cytoplasm when transfected alone. It is possible that VP26-VP5 + either preVP22a or VP19c, is transported as a complex to the nucleus, or, the complex may assemble within the nucleus and be held there. The precise order of events is unclear.

Again the oligomeric status of VP5 in the nucleus of infected cells during fluorescence studies is not known. Single VP5 molecules may be present in the nucleus with and without VP26 attached. Those VP5's without VP26 could form the pentamers at the vertices and those containing VP26 would form the hexamers. However, it is known that VP26 is not required to form a structurally intact capsid shell (Tatman *et al*, 1994; Thomsen *et al*, 1994) and so it is not VP26 which is directly governing the formation of hexamers of VP5. Alternatively, VP26 may be attached to all the VP5 molecules and released when the pentomeric conformation is formed. Or, the VP26 may only attach to pre-formed hexamers of VP5. VP26 is small enough to be transported in and out of the nucleus by diffusion through the nuclear pores (ie it is <90kDa). The protein may move at random until it encounters VP5 in a hexameric form, at which time it binds.

Newcomb *et al*, 1994, have developed a cell free assembly system in which they were able to detect capsid intermediates. They have proposed a model whereby partial capsids, containing VP5, scaffold and triplex, from segments which grow into spherical procapsids. This undergoes a spontaneous structural transformation and angularises to form polyhedral capsids, closely resembling B capsids (Newcomb *et al*, 1996). Unfortunately VP26 was not incorporated in the cell free assembly system and so it does not help us determine at which stage the protein binds. The authors suggest that the protein may be binding to sedimentable material in cell free extracts and so was not available. With knowledge of how insoluble the protein is, it may simply be precipitating out of the PBS reaction mixture. The findings in this thesis suggest a model where VP5 does not require to be present in an angularised capsid for VP26 to interact. VP26 does not form a spontaneous hexameric ring but appears to react in monomers or dimers. The oligomeric status of the VP5 which it is reacting with must be defined in future studies to help pin-point the stage at which VP26 is binding.

After this work had been completed, a paper was published by Wingfield *et al* (1997), which suggested a different secondary structure to the predicted one. This group had attempted and failed to express VP26 directly in *E coli*. Instead, they expressed it fused to the C-terminus of GST. When isolated from the fusion protein, they found VP26 reacted very like VP26pp65. It was extremely insoluble, had to be extracted in GuHCl and re-folded by dialysis in the presence of CHAPS detergent. They took a similar approach to that described here and confirmed that their protein was functional by attachment to VP26- recombinant capsids. Cryo-EM and 3D image reconstructions revealed 'six horns of density around the rim of each hexon' indicative of correctly bound VP26.

Using CD analysis of purified VP26 they found that the protein formed a reversible monomer-dimer interaction. The spectrum estimated the secondary structure of the protein to be 80% β -sheet and 13-15% α -helix. This closely matched the finding of D

McClelland (this Institute) & M Kirkitadze (University of Edinburgh) who had produced a spectrum using a concentrated sample of VP26 from pET35 (Chapter 4, table 4.4). Their measurements suggested 70% β -sheet and 20% α -helix. These patterns were in stark contrast to the protein prediction which suggested only 20% β -sheet and 45% α -helix. This prediction held true for all the VP26 homologues of the α - and β -herpesviruses, even though their native amino acid sequences varied considerably. It was not clear from the published data exactly which proteins constituted the bank at Heidelberg, against which structures were calculated. It is probable that it consists largely of readily soluble and non-structural proteins. These would not be the best model to use for determining the structure of VP26pp65, a highly insoluble protein which interacts within a large complex molecule. Also, there were no homologues of VP26 in the database, apart from other herpesvirus VP26's. It is not possible to confirm if the protein predict was inaccurate for the other VP26 homologues, as no data had been published to the contrary. However, as the programme predicted all 3 α - and all 3 β -herpesviruses to have an almost identical structure, despite different amino acid sequences, the suggestion is that these proteins may have a similar charge and spacing distribution which produced this protein prediction in the first place. Obviously different amino acid residues can fold to form a similar structure. It is not difficult to imagine that the area which constitutes the binding site on VP26, to the capsids, involves not just a specific amino acid sequence but, a defined secondary structure. It must be considered that when VP26 is choosing to bind selectively to the VP5 hexons, there must be a binding site on these capsomers which is not present on the VP5 pentons. The hexons themselves must also vary in conformation due to their quasiequivalent environment. VP26 therefore must adjust slightly to fit onto P, C and E hexons and it is here that its basic secondary structure may play an important role in helping amino acid residues to bind.

6.4 Mutations of VP26pp65

It is interesting to speculate as to why the deletion mutants were so insoluble and induced so poorly. Deleting amino acids at the terminal ends of VP26pp65 made it even more insoluble than the wild-type VP26pp65 protein. This may indicate that it is the central portion of the protein, which this work has suggested is the possible binding site

with capsids, which is the contributing to its insolubility. So, when the N- or C-terminal 'soluble' portions are deleted, the protein is left with the insoluble residues and so precipitates. If the central portion of the protein does indeed constitute the binding site with capsids, it is not unreasonable to speculate that this area may have a more defined and 'rigid' secondary structure to allow it to function correctly and interact specifically. On the other hand, recent data (Kirkitaдзе *et al*, 1998) has suggested that VP23 may be in a molten globule state. This means that the protein has a poorly defined structure initially to allow it to be flexible while the capsid assembles. Once all the major components are in place, the protein becomes more stable and the structure more defined. In this instance the VP26 binding site would be quite flexible and in the absence of the N and C terminus to stabilise the structure, the protein aggregates to a greater extent.

For insertional mutagenesis, glycines were chosen as the inserts before it became clear that the protein prediction was wrong. If it had been known that the protein consisted of mainly β -sheet and not α -helix, a different insertion may have been chosen. For example alanines were not chosen as they have a tendency to form α -helix and so they would not have caused such disruption in an α -helical protein. The use of glycines did not prevent further experimentation and it was possible to purify the mutant proteins in 8M urea (see table 4.4, Chapter 4) use them in the assay systems.

6.5 Amino Acid Residues Important for Binding VP26 to VP5

To try and map the amino acid sequences involved in the interaction of VP26 with VP5, two approaches were taken. Inhibitory ELISA reactions, involving short oligopeptides which spanned the UL35 ORF, were developed and a series of reattachment experiments, involving insertional mutants, were used. These preliminary results mapped an area which appeared to be important for binding.

The oligopeptides 35/4 to 35/6, spanning amino acids 31 to 70, significantly blocked the interaction of VP26 with VP5 in a series of ELISA assays. Oligopeptide 35/1, spanning amino acids 1 to 20, also caused a less pronounced inhibition in binding. Similarly, the mutant proteins VP26pp65.5 and VP26pp65.6, with inserts at amino acid 50 and 60

respectively, totally disrupted capsids banding on a mini gradient. Mutants VP26pp65.1 and VP26pp65.2, with inserts disrupting at amino acid 10 and amino acid 20 respectively, disrupted capsid banding to a lesser extent, with faint bands generally visible.

Failure to see capsid bands on a gradient was an interesting and unexpected result. The presence of the mutant protein obviously interferes with the sedimentation pattern of the capsids. It is difficult to speculate on what has happened to the capsids. At first it was thought that the mutant proteins may have disrupted the capsids and caused them to fragment. It is hard to envisage how this would occur in view of the extreme external location of the VP26 protein and the fact that VP26- capsids are known to be stable (Zhou *et al*, 1995; Newcomb *et al*, 1995). EM examination of pelleted capsids proved this theory to be incorrect as normal looking capsids were identified from samples which had not banded on the gradient. Another possibility is that the mutant proteins have caused the capsids to aggregate. As the predicted binding site has been disrupted within these VP26 proteins, perhaps they are partially binding to capsids and non-specifically cross-linking them, causing them to aggregate and thus pellet to the bottom of the gradient.

These results strongly support the idea that the area between amino acid residues between 31 and 70, and possibly more specifically 40 and 60, on VP26, are important for the proteins binding to VP5. Exactly which amino acids interact with which part of VP5 remains to be determined. It must also be considered that amino acid residues between 1 and 20, on VP26, may play a less significant role in the binding of VP26 to VP5. Since in both experimental approaches taken, this area was highlighted. It is unlikely that the extreme N-terminal 5 residues are involved in any binding as these were disrupted by insertion of the pp65 and 6xhis tags. It has been shown that insertion of a tag into this area does not alter the capacity of VP26 to bind to capsids normally (Section 2). Perhaps a very short sequence of residues at the N-terminus is important. This warrants further study. The 50 amino acids at the C-terminus do not seem to play a role in the binding of VP26 to VP5. Neither the oligopeptides spanning this region, nor

the 3xG insertions, which disrupted this area, caused any effect on the binding of VP26 to VP5.

The main area of importance for binding of VP26 to capsids appears to fall within amino acids 40 to 60. This area falls within a region of poor sequence homology between the α - and β - herpesviruses yet one which was strongly predicted to be alpha-helical in all. Although it now seems unlikely that this region is in fact alpha-helical, it is interesting to speculate that some common feature in the secondary structure of this region may play a significant role in the binding of VP26 to VP5.

1. Introduction

Complete formation of HSV 1 capsids requires the presence of a scaffold protein. However, the method of capsid assembly and the site of action of the scaffold protein are poorly understood. This chapter describes the use of freeze-etching and cryo-EM and 3D image processing techniques to determine the site of interaction between the scaffold and the capsid. The results of these studies are presented in this chapter. The results of these studies are presented in this chapter. The results of these studies are presented in this chapter. (see Zhou et al., 1994)

Three types of capsid exist, A, B, and C.

DNA is packaged into the capsid.

indicated that B capsids are the

CHAPTER 6

IDENTIFICATION OF THE SITES OF INTERACTION BETWEEN THE SCAFFOLD AND THE OUTER SHELL IN HSV 1 CAPSIDS

Protein structure of the capsid

ATPase is located on the surface

of the capsid. The capsid is

made of 162 subunits.

The capsid is composed of

protein subunits.

The capsid is composed of

The scaffold protein is

its C-terminal 25 amino acids

et al., 1996). (Zhou et al., 1994)

This is an essential protein

and B-capsids are heavily

1. Introduction

Complete formation of HSV-1 capsids requires the presence of intact scaffold. However, the method of capsid assembly and the mode of action of the scaffold is poorly understood. This chapter describes an approach taken, using high resolution cryo-EM and 3D image processing, which has allowed identification of the points of contact between the scaffold and outer capsid shell (Zhou *et al*, 1998a). The results in this chapter were attained through a collaboration between myself, Dr F J Rixon (Institute of Virology) and scientists in Houston, principally Dr W Chiu and Dr H Zhou (see Zhou *et al*, 1998a).

Three types of capsid exist, A (empty), B (containing scaffold) and C (containing viral DNA). Pulse-chase experiments performed with cells infected with EHV-1 have indicated that B capsids are the progenitors of A and C capsids (Perdue *et al*, 1976), with A capsids the result of unsuccessful packaging of DNA. However, recent investigations have suggested that the process may not be as simple as this. Newcomb *et al*, 1994, have isolated procapsid intermediates in the assembly process (see Chapter 7, Conclusion for further details).

Formation and processing of B capsid scaffold involves 3 proteins, VP21, VP24 and VP22a, which are encoded by 2 overlapping genes (see Chapter 1, Introduction, section 4.4.1.5). Based on the phenotypical appearance of this scaffold, B type capsids can be sub-divided into 2 distinct types:

- Large cored capsids, which contain VP22a which has not been cleaved by the protease and is termed preVP22a
- Small cored capsids, which contain VP22a in the cleaved form.

The scaffold protein, preVP22a, interacts with the major capsid protein, VP5, through its C-terminal 25 amino acids (Kennard *et al*, 1995; Matusick-Kumar *et al*, 1995; Hong *et al*, 1996). Cleavage by the viral protease of these 25 amino acids generates VP22a. This is an essential step which breaks the link between the scaffold and shell. Large cored B-capsids are hence converted to small cored B-capsids. However, if the protease

is inactivated or absent, the large cored phenotype remains and DNA cannot be packaged.

To investigate these B-capsid variants in more detail, small and large cored B-capsids were generated and analysed.

2. Preparation of Capsids

Large and small cored B-capsids were required for this analysis and were prepared in two different ways:

2.1 Small cored B capsids

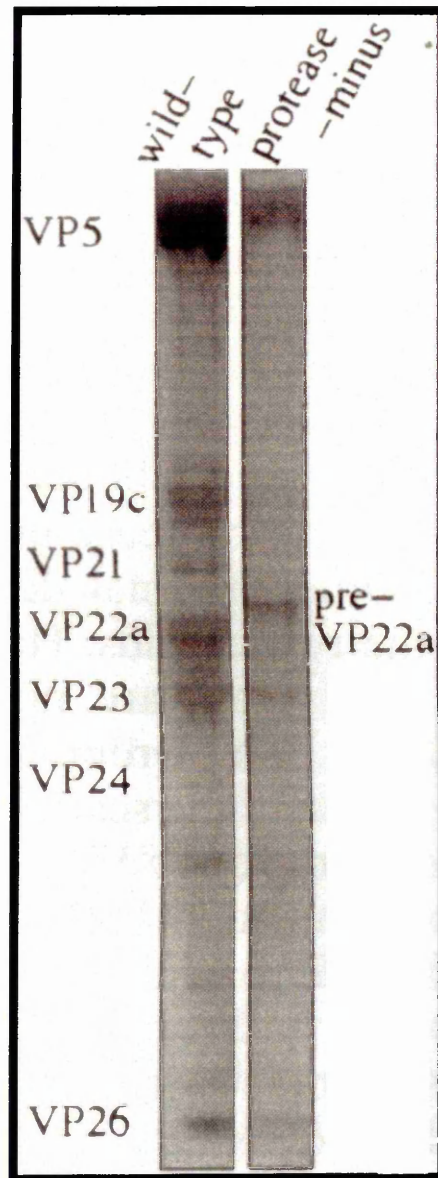
Small cored B capsids are the form which predominate in a wild type HSV-1 infection. BHK C13 cells were therefore virally infected, at 5pfu/cell for 16h at 37°C, and capsids purified on a 10-40% sucrose gradient (see Methods, Section 2.2.5). It has previously been found that baculovirus generated small cored B capsids and wild type B capsids have identical structures (H Zhou; personal communication).

2.2 Large Cored B-capsids

To produce capsids with uncleaved VP22a, ie preVP22a, it was necessary to generate capsids in the absence of active protease. The baculovirus system was therefore used (see Methods, Section 2.3.8). Sf21 cells were co-infected, at 5 pfu/cell for 48-65h, with baculoviruses AcUL19(VP5), AcUL18(VP23), AcUL26.5(preVP22a), AcUL35(VP26) and AcUL38(VP19c) (Tatman *et al*, 1994). The absence of the protease, encoded by UL26, resulted in only large cored capsids being produced. These were designated protease minus capsids.

Separate batches of large cored capsids were purified in 2 ways. One batch was purified through a sucrose gradient in exactly the same manner as that described in Methods, Section 2.2.5.2. A second batch was also purified in this manner, except that NP40 was not included at any stage of the purification procedure. This is because it had been

Figure 6.1: Comparison of Wild type and Protease Minus Capsids' Protein Profiles



reported that the interaction between the capsid and the protease is essential for the assembly of the virus (Flores et al., 1994).

2.3 SDS-PAGE Analysis of Synthetic and Recombinant Capsids

Both mutant and wild type capsids were purified from the supernatant of the infected cells. The wild type capsids were purified from the supernatant of the infected cells, while the mutant capsids were purified from the supernatant of the infected cells. The wild type capsids were purified from the supernatant of the infected cells, while the mutant capsids were purified from the supernatant of the infected cells. The wild type capsids were purified from the supernatant of the infected cells, while the mutant capsids were purified from the supernatant of the infected cells.

3. Analysis of Wild Type and Recombinant Capsids

The wild type and recombinant capsids were analyzed by SDS-PAGE. The wild type capsids were purified from the supernatant of the infected cells, while the recombinant capsids were purified from the supernatant of the infected cells.

Figure 6.1: SDS gel of purified wild type capsids (left) and recombinant baculovirus expressed protease minus capsids (right). In the absence of an active protease, the major scaffolding protein is present in the unprocessed form, preVP22a, and the 2 autoproteolytic products of the protease, VP21 and VP24 are absent.

reported that the interactions between VP5 and preVP22a were detergent sensitive (Hong *et al.*, 1996).

2.3 SDS-PAGE Analysis of Small and Large Cored Capsids

Both small and large cored capsids were analysed by SDS-PAGE on a 15% gel. It is clear from figure 6.1 [panel (i)] that the expected protein profiles were detected for each capsid type. The wild type capsids (lane 1) were composed of the 7 capsid proteins, whereas the protease minus capsids (lane 2) expressed the scaffold protein in the uncleaved form as preVP22a. Also VP21 and VP24 were absent from these capsids as no protease was present.

3. Analysis of Wild Type and Protease Minus Capsids

To determine the difference between wild type and protease minus capsids, cryo-EM analysis was undertaken by our collaborators at Baylor College of Medicine, Houston, Texas. Dr W Chiu and Dr H Zhou performed all the cryo-EM and produced the 3D image reconstructions. It was hoped that at a high resolution, the points of contact which were occurring between preVP22a and VP5, and not evident in the wild type capsids, would be detected and identified.

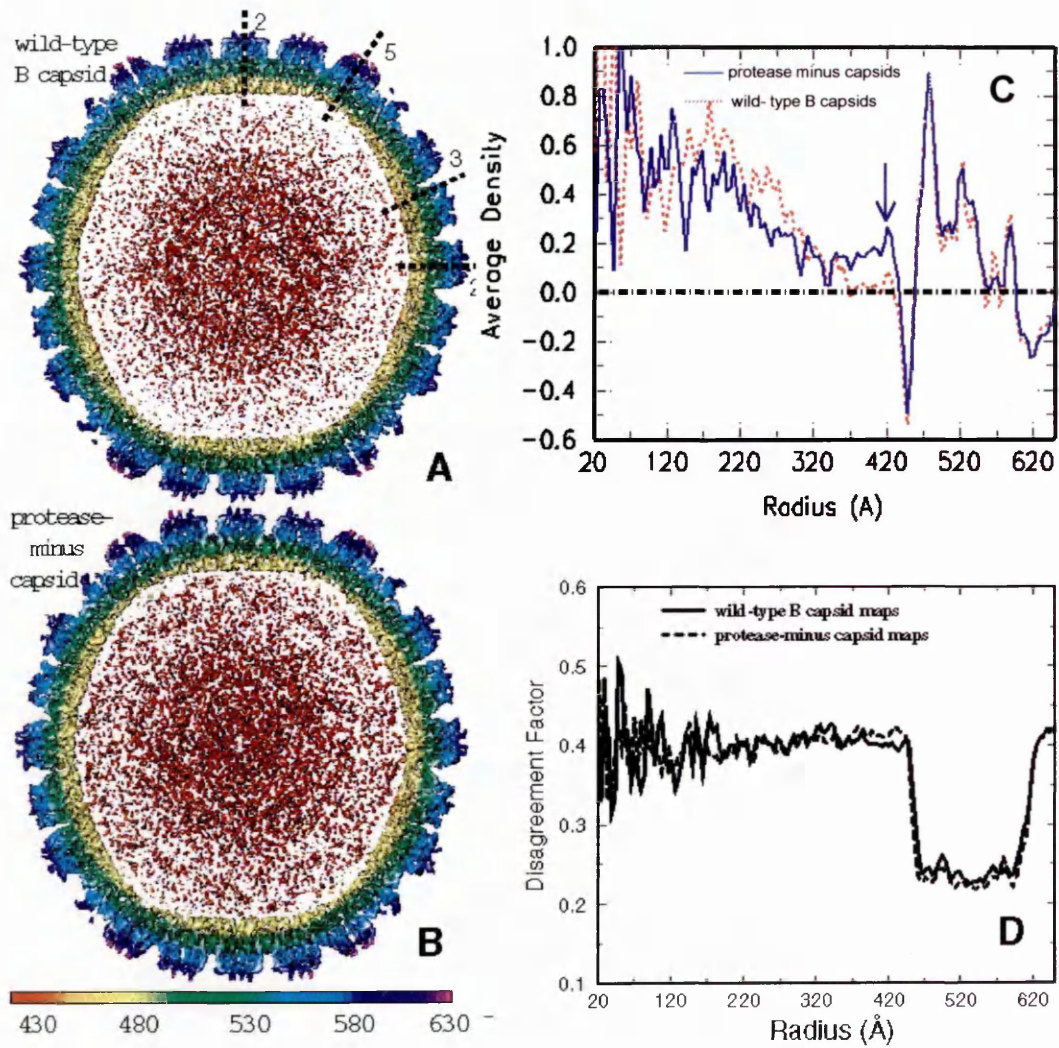
It should be noted at this point, that no differences were observed between capsids purified in the presence or absence of NP40 and the results presented in the subsequent section apply equally to both batches of capsids.

3.1 Symmetry of Wild Type and Protease Minus Capsids

3.1.1 Comparison of Capsid Shells

Both wild type and protease minus capsids were analysed by electron microscopy (not shown). They appeared very similar at this resolution, with an electron dense internal core, representative of the scaffold. Indeed, when the 3D structure was generated by cryo-EM analysis, the external structures appeared to be virtually identical with pentons at the vertices, p, e and c hexons and each of the 6 types of triplex (not shown, images were identical to figure 1.6, Chapter 1). This indicated that the state of the internal scaffold (ie cleaved or uncleaved) did not affect the ability of the capsid to form an icosahedral shell.

Figure 6.2: Comparison of the Outer Shells and Internal Cores of Wild Type and Protease Minus Capsid Reconstructions



3.1.2 Comparison of Capsid Types

One central 4.67 Å thick section of wild type

capsids were figured in the middle of

capsid types are shown in the middle of

capsid cover sheet. The middle of

revealed that the average of the

width of the capsid is 4.67 Å.

whereas the average of the

capsid thickness is 4.67 Å.

the average of the

of the capsid is 4.67 Å.

the average of the

Figure 6.2: Panel A and panel B show one central 4.67 Å thick section of wild type and protease minus capsids respectively. The numbers 2, 3 and 5 indicate the symmetry at these points. The densities at the same radius were averaged to show the density distribution plots (panel C) for each capsid type (blue line represents protease minus capsids and the red line represents wild type B capsids). The arrow indicates an additional density peak, close to the capsid shell of protease minus capsids. The disagreement factor was calculated and plotted (panel D) for 2 independent reconstructions of each capsid type (solid line represents wild type B capsids and the dashed line represents protease minus capsids).

3.1.2 Comparison of Capsid Mass Distributions

One central 4.67Å thick section was isolated for the wild-type and protease minus capsids [see figure 6.2, panels A and B, respectively]. The core structures for the two capsid types are clearly different. In order to examine the mass distributions within the capsid cores further, radial density plots were produced (figure 6.2, panel C). This revealed that the distribution of density between 70-330Å radii, ie the core region, was lower in the protease minus capsids than the wild-type. This was indicative of a substantial radial translocation of protein mass as a result of proteolytic cleavage of the capsid and confirmed the appearance of the large and small cored phenotypes. An area of extra mass, at 340-450Å, was present in the protease minus capsids and completely absent from the wild-type capsids. This area corresponded to a location just underneath the capsid shell. In contrast, the distribution patterns for the capsid shell area (460-625Å) was remarkably similar and matched the observation from the 3D image reconstructions, which showed that protease minus capsids had virtually identical shells to wild type capsids. This confirms that the shell areas of the protease minus and wild-type capsids do not undergo any radial density dislocation upon proteolysis of the scaffold.

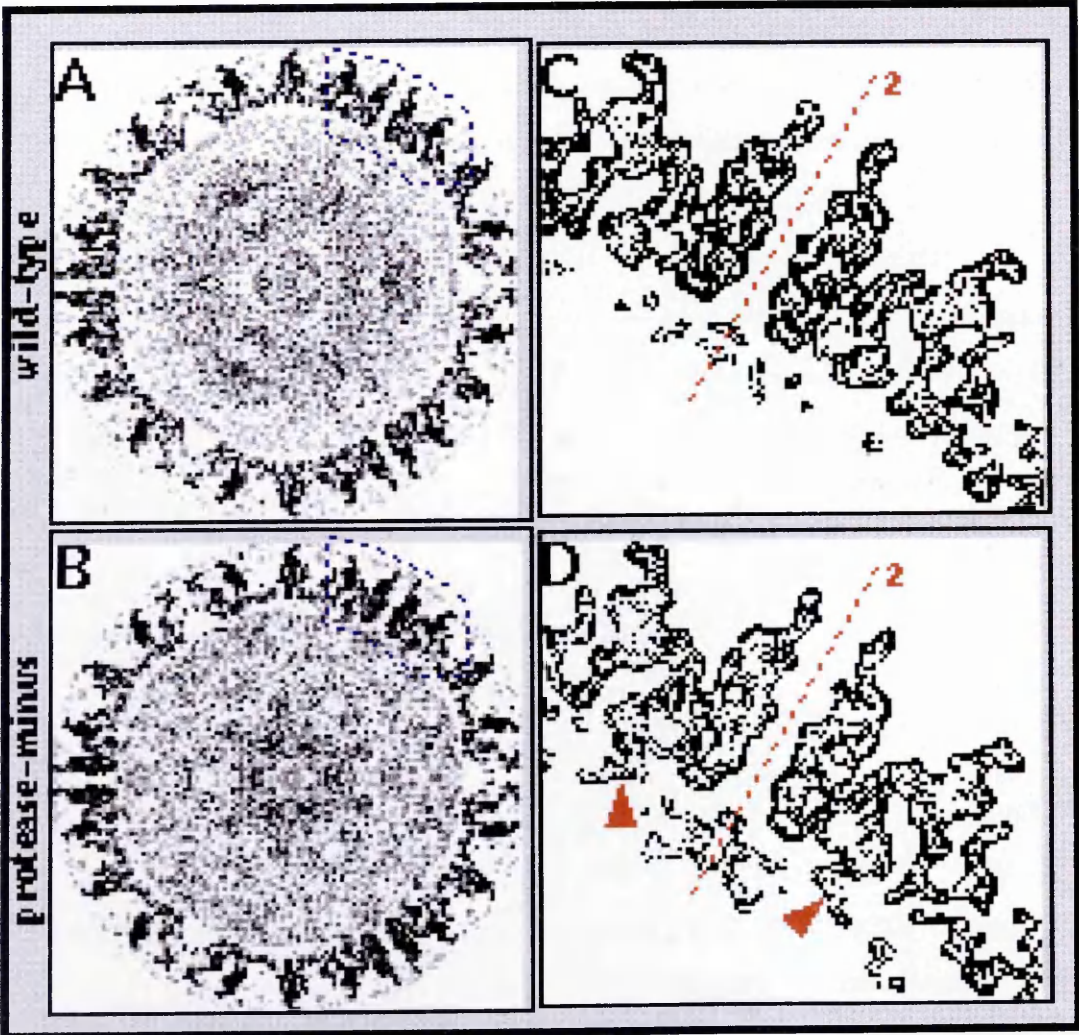
Two independent reconstructions of each capsid type produced almost identical profiles and so confirmed that the data was statistically significant and that the detection of extra mass in the protease minus capsids real.

3.1.3 Structural Disagreement Factor

Based on the fact that the 3D reconstructions have icosahedral symmetry, it was expected that there would be close agreement between 2 independent reconstructions of wild-type capsids and 2 independent reconstructions of protease minus capsids, in the regions of icosahedral symmetry. Therefore the structural disagreement factor between the 2 reconstructions of each capsid type was plotted and is shown in figure 6.2, panel D.

The region of capsid shell (440Å-620Å) had extremely good agreement between like capsid types and supported the data of the density plots and 3D image reconstructions,

Figure 6.3: Identification of Additional Attached Mass in Protease Minus Capsids



which deemed these areas to have good icosahedral symmetry and no variation in structure. On the other hand, there is a high disagreement factor below 440Å, showing that there is no icosahedral symmetry in this area for either the wild-type or the protease minus capsids. This showed that the scaffold itself does not possess icosahedral symmetry either in its cleaved or uncleaved form. The formation of an icosahedral capsid shell is therefore not dependent on assembly around an icosahedral scaffold.

3.2 Identification of the Points of Contact Between Scaffold and Shell

3.2.1 Visual Inspection

Upon visual inspection, it is evident from the micrograph sections of the wild-type and protease minus capsids (figure 6.3, panels A and B respectively), that there are sharp drops in mass just under the inner capsid shells. The absence of matter in this area is confirmed by the low readings obtained in the density plots (figure 6.2, panel C).

This suggests that there is very little contact between the scaffold and shell. However, it is known that there is an absolute requirement for the interaction of VP5 with preVP22a for the production of sealed capsids (Kennard *et al*, 1995; Matusick-Kumar *et al*, 1995). To try and locate the positions of these vital interaction points within the capsid, a portion of the inner and outer shell was computationally isolated, from each capsid type, between radii 430Å-630Å (figure 6.3, panels A and B) and enlarged (figure 6.3, panels C and D). Examination of these 2 shells revealed firstly that the outer shell areas were very similar, as expected. Secondly, additional masses, which appeared to be attached to VP5, were present in the protease minus capsids. These rods extended inwards towards the capsid core for approximately 40Å before the resolution was lost. No similar densities were observed in the wild-type capsids indicating that these represented the points of contact between preVP22a and VP5.

Other differences were noted in the internal densities between the capsid types however, these did not represent points of contact with the capsid floor and appeared to have a more random nature. Unlike the attached densities, the other masses were not

Figure 6.4: Visualisation of Additional Densities Attached to the Floor of Protease Minus Capsids

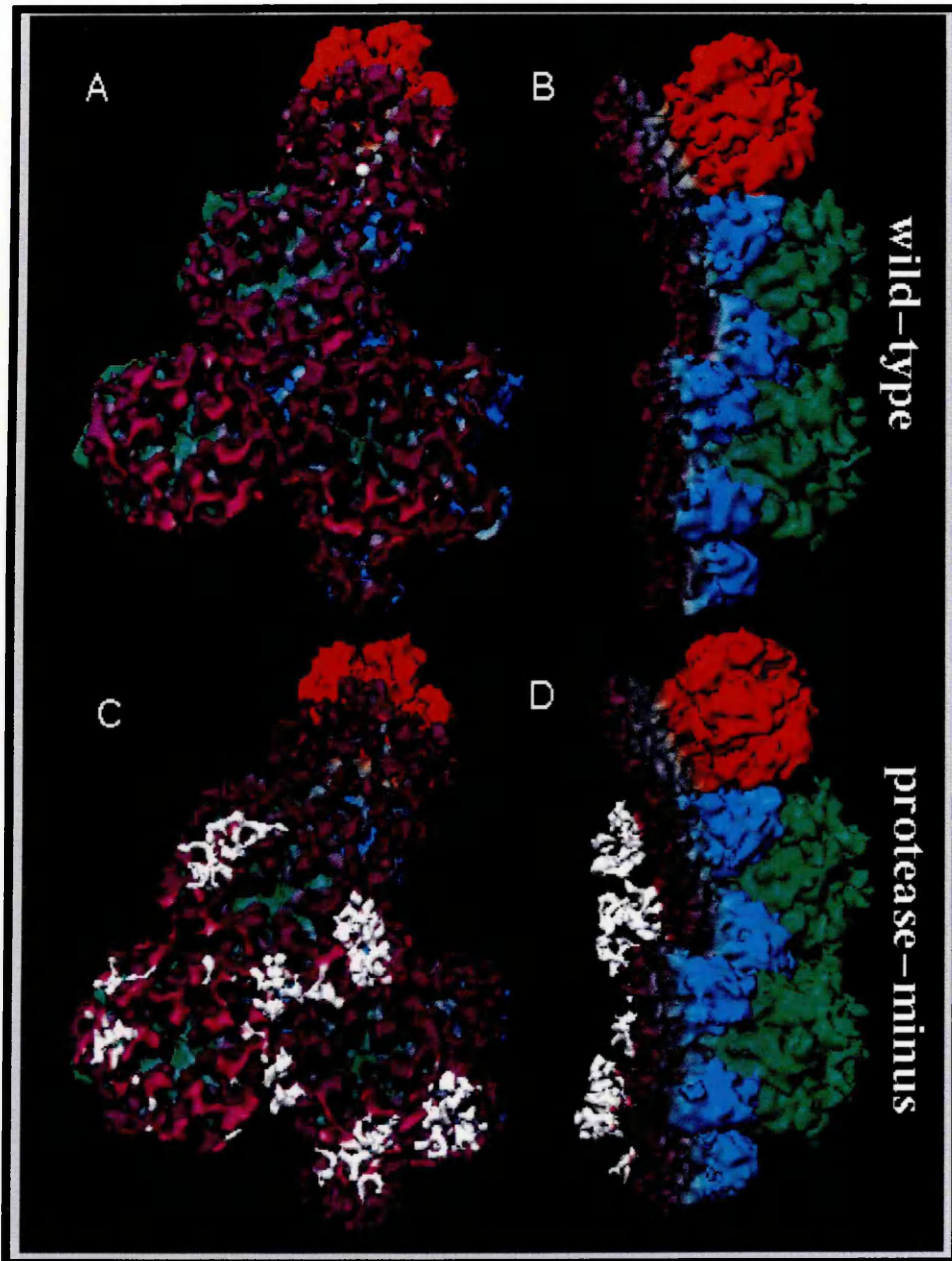


Figure 6.4: A region consisting of one penton, one c, e and p hexon and each of the six triplexes was computationally isolated from wild type (panels A and B) and protease minus (panels C and D) capsid reconstructions. The sections were viewed inside the capsid shell (panels A and C) and from one side (panels B and D). The additional masses present in the protease minus capsids are shown in white. For clarity, any densities which do not make contact with the capsid floor have been removed.

Figure 6.5: Contact Points of Scaffolding Proteins on the Capsid Floor

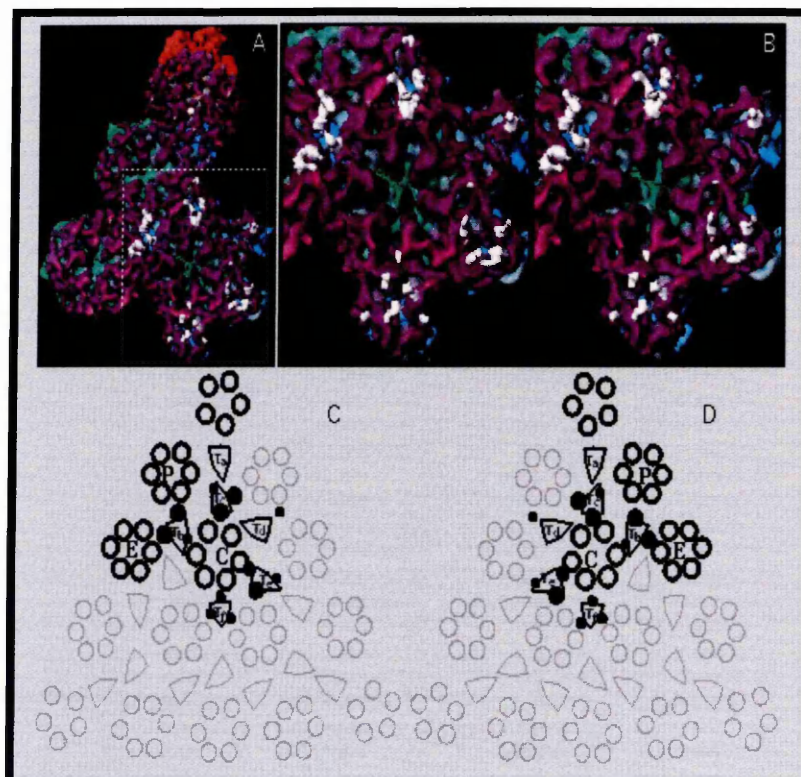
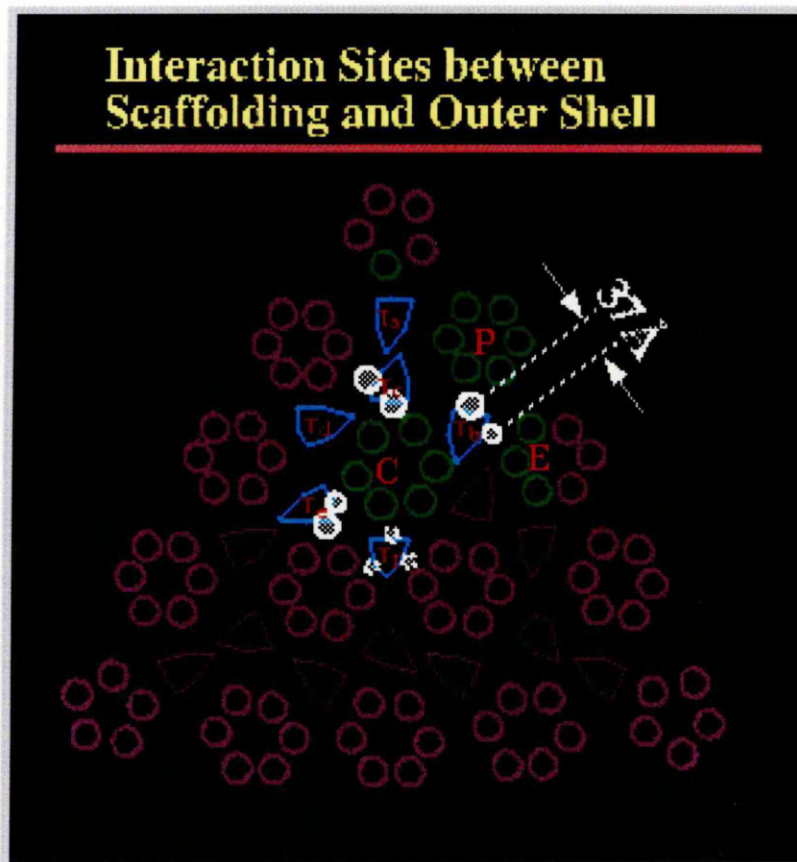


Figure 6.5: The additional densities from the protease minus capsids were superimposed on the inner surface of the shell of wild type B capsids (panels A and B, areas shown in white). For clarity, only those densities that were within a radial distance of 10Å from the shell are shown. Panel B shows a stereo pair of an enlarged region surrounding the c hexon (indicated by the dotted rectangle in panel A).

Panels C and D are schematic representations of one triangular face of the capsid floor, as viewed from inside (panel C) and outside (panel D) of the capsid. The dark filled circles designate the points of contact of the scaffold protein and shell. The larger circles are indicative of extensive contacts, whereas the smaller ones represent less extensive ones.

Figure 6.6:



consistently observed at the same location and appeared to have a more random or disordered pattern. These will not be discussed further.

3.2.2 Analysis of Asymmetric Units

To give a better indication of how the extra masses, in the protease minus capsids, were distributed, all unattached densities were removed, leaving only the material which was icosahedrally ordered and in close contact with the capsid shell. A region was computationally isolated for each capsid type (see figure 6.4) which consisted of a penton (red), one of each of the p, e and c hexons (green) and one of each of the 6 types of triplexes (aquamarine). This area was enlarged and rotated so that the internal (panels A and C) and side views (panels B and D) could be seen. The capsid floor is shown in purple and the extra masses, present in only the protease minus capsids are shown in white.

To increase clarity of the points of contact further, the additional masses were trimmed back to approximately 10Å from the floor and superimposed onto wild-type B-capsids (figure 6.5, panel A). This indicated that the most prominent attached masses were located beneath four of the triplexes, which surround the c hexon. The enlarged view of this area (figure 6.5, panel B) showed that all the contact points occurred at junctions between the floor domains of adjacent hexons, with both extensive and smaller contacts evident.

Figure 6.5 (panels C and D) show a schematic representation of an icosahedral face from the outside and inside respectively. The position of the extensive contacts are shown underneath triplexes Tb, Tc and Te (large circles), and the smaller points of contact were evident at the third quasi-equivalent position under these triplexes (small circles). Triplex Tf, has a different pattern of small contacts and Td has only a single small density. No extra densities were detected underneath the pentonal triplex Ta. The separation between each major point of contact on a triplex was estimated to be 37 Å (figure 6.6).

4. Discussion

These results have allowed the probable points of contact between the preVP22a and VP5 to be identified. Difference analysis studies between protease minus and wild-type capsids, has identified 40Å rod-like structures. These densities are present only in the protease minus capsids, which have large cores and contain uncleaved preVP22a. They extend inwards towards the capsid core and appear to be present mainly underneath the triplexes surrounding the c hexon. In the wild-type small cored capsids, preVP22a has been cleaved by the protease, losing its C-terminal 25 amino acids and breaking the interaction between scaffold and shell. In these capsids no extra densities were seen attached to the capsid floor.

The group in Texas also analysed large cored capsids prepared from ts1201. Ts1201 has a lesion in the protease gene which results in an inactive protease at the non-permissive temperature (Preston *et al*, 1983). This prevents cleavage of the scaffold and blocks DNA packaging. As a result, large cored B capsids accumulate. However, this step is reversible. A downshift in temperature in the presence of inhibitors of protein synthesis, results in the conversion of large cored B capsids to a mixture of A, small core B capsids and C capsids. This pattern is concurrent with the pattern observed for wild-type infections and shows that large cored B capsids are competent for packaging.

When these large cored ts1201 B capsids were compared to the wild type and protease minus recombinant capsids. It was found that extra densities were present in similar positions in the large cored ts1201 mutants and the protease minus capsids. However, due to difficulties in purifying large cored ts1201 capsids, the resolution of the reconstructions was much lower.

No differences were observed in any of the data between capsids prepared in the presence or absence of NP40. The VP5-preVP22a interaction *in vitro* had been shown to be detergent sensitive (Hong *et al*, 1996). This indicates that the VP5-preVP22a interaction, within the context of the capsid, is more stable. Either the proteins form a

slightly different confirmation within the capsid *in vivo*, or, the interaction may be 'hidden' or embedded in a hydrophobic pocket which is not accessible to the detergent.

All of the data presented in this Chapter (see also Zhou *et al*, 1998) suggests that preVP22a does not form extensive contacts with the capsid floor, which is almost entirely composed of VP5. This is not surprising in view of the fact that the interaction is occurring through only 25 amino acids at the C-terminus of preVP22a. As the 25 amino acids do not appear to be retained after proteolysis (A Davison; personal communication) this is highly suggestive that the ordered rod-like domains, present in only the protease minus capsids, correspond to the points of contact in the uncleaved scaffold and represent the C-terminus of preVP22a.

The extra densities detected extend for approximately 40Å towards the capsid core. This converts to an amino acid length of 25-30 amino acids in an alpha-helical conformation. However, the mass of each density accounts for more than the 25 amino acids known to be required for the VP5-preVP22a interaction. This means that either, the scaffold domain which, interacts with VP5, is larger than previously thought, or, that more than one preVP22a molecule is participating in the interaction. Data has been published which supports the latter conclusion and suggests that the 25 amino acids of preVP22a bind more efficiently to VP5 as a parallel homo-dimer (Pelletier *et al*, 1997). Using an assumption that each point of contact represents 2 molecules of preVP22a, the number of copies of scaffold protein was calculated from the data presented in this chapter.

Three pairs of well defined rod-like densities were observed for each asymmetric unit and these were assumed to be the C-terminal 25 amino acids of a preVP22a dimer. Therefore 12 molecules of preVP22a were present for each asymmetric unit. As 60 units constitute a capsid, this leads to an estimation of 720 scaffold molecules attached to the capsid. However, 3-fold averaging at Tf may have obscured the position of contacts but, if a dimer is also proposed to occur at this location, this gives a figure of 800 scaffolding proteins. This number falls short of the biochemical prediction of 1200 copies of preVP22a in B capsids (Newcomb *et al*, 1993). However, it has been reported that

functional scaffolds can be made using mixtures of preVP22a and VP22a (Oien *et al*, 1997). VP22a cannot interact with VP5 and would not be accounted for in the above calculation. It would therefore appear that incorporation of scaffold into capsids is not dependant on binding to VP5 and the scaffold binding to itself may be important for determining the overall dimensions of the structure which are necessary for correct capsid assembly. Certainly, work presented in this chapter has illustrated that formation of an icosahedral scaffold is not a prerequisite for the formation of an icosahedral shell.

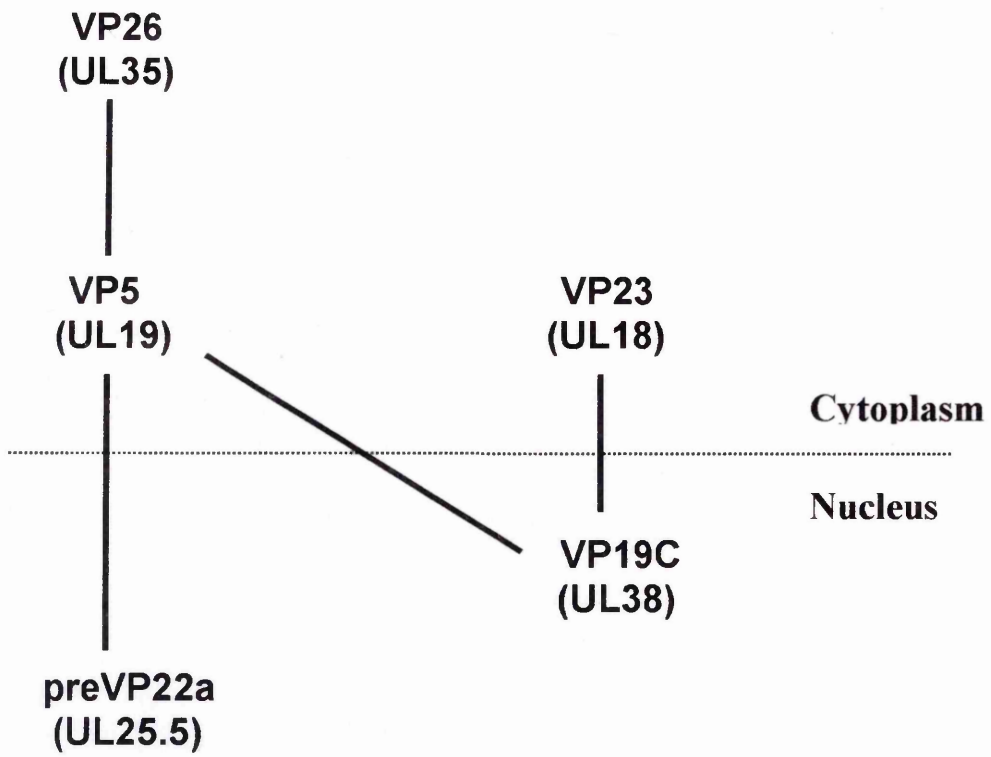
Another interesting point, which was highlighted by this study, is the fact that the separation distance between each pair of extensive extra mass connections, is 37Å (figure 5.6). Shieh *et al* (1996) and Tong *et al* (1996) have suggested that the crystal structure of the HCMV protease domain exists as a dimer, with 2 catalytic domains spaced 36.5Å apart. This obviously correlates closely with the spacing observed in HSV-1 preVP22a connections. This data is highly provocative and one may speculate that the extra mass may represent the protease domain in HSV-1.

In conclusion, the stage at which the scaffold is cleaved and DNA is packaged as yet remains unclear but, this study has allowed the probable points of preVP22a-VP5 interaction to be mapped and visualised within the capsid. Using cryo-EM and 3D image reconstruction techniques to visualise and pin-point such small interactions within a complex particle had not previously been possible at this low a resolution (13-15Å). This approach therefore takes another step towards solving the nature of the protein-protein interactions within the HSV-1 capsid.

CHAPTER 7

CONCLUSION

Figure 7.1: Pattern of Capsid Protein-Protein Interactions



Drawing on all the information available, it is possible to conclude that the proteins shown in Figure 7.1 may be interacting in the nucleus.

1 The Pattern of capsid protein interactions

The immunofluorescence studies (this thesis; Rixon *et al*, 1996; Nicholson *et al*, 1994) and electron microscope analysis (Rixon *et al*, 1996; Tatman *et al*, 1994; Thomsen *et al*, 1994; Kennard *et al*, 1995) are shown by the solid lines. The dashed line separates those proteins which have an intrinsic capacity to localise to the nucleus and those which do not.

Figure 7.1: The capsid protein-protein interactions suggested by the immunofluorescence studies (this thesis; Rixon *et al*, 1996; Nicholson *et al*, 1994) and electron microscope analysis (Rixon *et al*, 1996; Tatman *et al*, 1994; Thomsen *et al*, 1994; Kennard *et al*, 1995) are shown by the solid lines. The dashed line separates those proteins which have an intrinsic capacity to localise to the nucleus and those which do not.

Drawing on all the results within this thesis, together with published literature, it is possible to comment on the inherent roles of the respective capsid proteins and how they may be interacting with and influencing each other.

1 The Pattern of the Capsid Protein-Protein Interactions

Immunofluorescence data has given an indication of the nature of the interactions which are occurring between capsid proteins and their inherent distribution patterns within an infected cell (summarised in figure 7.1). Two capsid proteins, preVP22a (the scaffold protein) and VP19c (a component of the triplex), carry an inherent NLS, while VP5, VP23 and VP26 do not. A series of complex protein-protein interactions therefore occur which allow capsid assembly to occur in the nucleus. Not surprisingly, VP5 is central to this scheme as it interacts with 3 different capsid proteins, enabling it to fulfill its role as the MCP. These results allow a model for the interaction patterns within the capsid to be drawn (figure 7.1).

Although the pattern of protein interactions, determined from immunofluorescence studies, appears to be correct [cryo-EM (Zhou *et al*, 1994), baculovirus (Tatman *et al*, 1994; Thomsen *et al*, 1994) and yeast 2-hybrid studies (Desai & Person, 1996)] support this pattern of interaction) it cannot tell us anything about the interaction patterns of the proteins within the context of the capsid shell. Here, the capsid environment enforces symmetry and influences positioning. Also, the oligomeric status and assembly pathway cannot be determined by this line of experimentation.

2 A Study of the Interaction of VP26 with VP5

To look at capsid protein interactions in more detail, the smallest capsid protein, VP26, and its interaction with VP5 was targeted as interesting to study and map. The method, by which VP26 attached to hexons, but not pentons, was not understood and as the VP26 protein was small, it could be readily manipulated. Also, the external location of VP26 on capsids, allowed it to be removed and replaced for development of assay systems.

It was not foreseen that this small protein would be extremely insoluble, making experimentation approaches lengthy and difficult. However, full-length VP26 protein was produced in a bacterial expression system and purified through a Ni-NTA column.

Determinations of the secondary structure of purified VP26, by CD analysis, showed it to be approximately 70% β -sheet and 20% α -helix (D McClelland & M Kirkitadze; personal communication; Wingfield *et al*, 1997). This contrasted strongly with the predicted secondary structure (Protein Predict, Heidelberg).

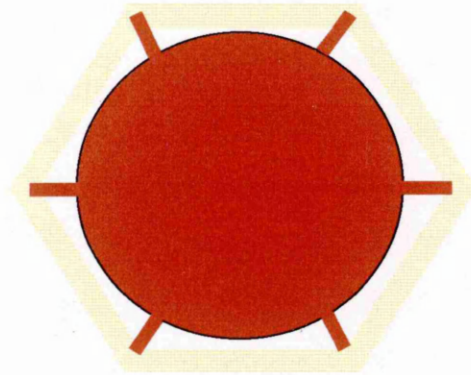
The oligomeric status of VP26 appeared to be monomeric or dimeric in solution. This allowed speculation that, VP26 spontaneously formed hexamers and so only attached to VP5 hexons, to be dispelled. Instead it would seem that it is the conformation of the VP5 molecule which governs the specificity of VP26's location. This project used purified VP5 and VP26- capsids as tools to study VP26. Much work remains to be done to determine the nature and status of VP5. This would help to determine if VP26 can only interact with pre-formed hexons or, if it interacts with all VP5 molecules, becoming detached when the penton arrangement forms. Very recent data has shown that although the location of VP26 on the tips of the hexons exposes it to the tegument layer, it does not interact with it (Zhou *et al*, 1999). 3D image reconstructions of virions have revealed that the interaction between the capsid and tegument is confined to the pentonal vertices (Zhou *et al*, 1999). The occupation of the hexons with VP26 may make it inaccessible for tegument binding.

VP26 appears to interact most strongly with VP5 through an area between amino acids 31 and 70. This area has very poor homology among the alphaherpesviruses. However, this area does have a strongly conserved predicted secondary structure. While this prediction is inaccurate, it may be indicative of an important role for the secondary structure of the binding site.

Amino acids 1-20 may also play a role in the binding of VP26 to VP5. Cryo-EM reconstructions show that a large portion of VP26 is in contact with VP5. The VP26 protein is a flattened molecule that appears to have a large surface area in contact with

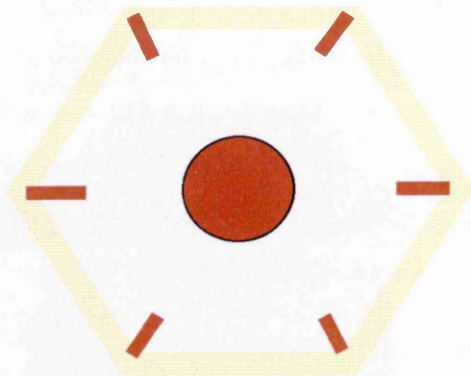
Figure 7.2: Transition from Large Cored to Small Cored Capsids

(i) Large Cored B Capsids



proteolytic
cleavage

(ii) Small Cored B Capsids



VP5 This type of capsid is found in many other viruses including the hepatitis B virus (Wingfield et al., 1997). The capsid is composed of 240 subunits, each of which has a high hydrophobic content. The capsid is highly stable and is resistant to proteolytic cleavage. The prediction (Chen et al., 1997) is that the capsid is highly stable and is resistant to proteolytic cleavage.

The proteolytic cleavage of the capsid is a key step in the maturation of the virus. The cleavage of the capsid is mediated by the action of the protease, which is encoded by the virus genome. The cleavage of the capsid results in the formation of small cored B capsids, which are the infectious form of the virus.

3. A Study of Capsids

Figure 7.2: Large cored B capsids, which have not undergone proteolytic cleavage are schematically represented in panel (i). The capsid shell is shown in yellow and the internal scaffold is shown in red. The red lines, which connect the scaffold to the shell, represent the 25 amino acids of preVP22a. After proteolytic cleavage [panel (ii)], the contact between the scaffold and shell is broken and small cored B capsids are formed. It is probable that the 25 amino acid contacts are lost at this stage (A Davison; personal communication) however, these have been included as it is not clear exactly when they are lost.

4. Interactions

Protein-protein interactions are essential for the assembly and function of the virus. The interactions between the capsid and the genome are particularly important for the formation of the infectious virus particle.

VP5. This type of structure is indicative of the β -sheet formation, suggested by Wingfield *et al* (1997), and not the α -helical one suggested by the protein predict. The high hydrophobic content of the protein is probably responsible for the computer prediction. Cryo-EM analysis of capsids containing mutant VP26 proteins will shortly be underway. These will help to clarify the interaction pattern in more detail.

The points of interaction between adjacent VP26 molecules was not studied and this is also a future aspect to be considered. However, the probable location of the N-terminus was visualised by cryo-EM analysis. This approach opens an experimental pathway to study how the VP26 molecule is orientated within the capsid by visualising the location of extra amino acid sequences which have been inserted into the UL35 gene.

3 A Study of the Interaction of Scaffold with VP5

The scaffold is only attached to VP5 in the uncleaved form (preVP22a) when it is present in capsids as a large core. When the protein is cleaved by the protease (VP22a) the C-terminal 25 amino acids appear to be lost and the connection is broken, producing small cored capsids (figure 7.2).

As both large and small cored capsids can be purified, it was possible to examine and compare both types by cryo-EM and 3D image reconstructions. Difference maps revealed several areas of extra mass in the protease minus capsids, attached to VP5 underneath the triplexes surrounding the c hexon. These probably represent the contact points between scaffold and shell, with 2 copies of preVP22a predicted to be present at each major interaction point.

There was no evidence to suggest that an icosahedral scaffold was required to form an icosahedral capsid shell. To understand how an apparently disordered scaffold may be influencing a highly ordered shell, it is first necessary to understand how individual proteins influence each other.

4 Inherent Properties of VP5, VP19c, VP23 and Scaffold

Baculovirus studies, using single, and combinations, of capsid proteins, and immunofluorescence data have provided clues as to the inherent properties of particular

proteins and the way in which they influence each other. This aspect is summarised in the following section.

4.1 VP5 and VP19c

When the shell proteins VP5 and VP19c are co-expressed, they form densely staining spherical 90nm particles (Rixon *et al*, 1997). Very recent cryo-EM reconstructions have shown that these particles do have a defined structure and appear to be 880Å in diameter (Saad *et al*, 1999). Distinct capsomeric subunits are evident in the form of distorted hexons and pentons. The structure has T=7 icosahedral symmetry, which contrasts with the T=16 symmetry associated with mature capsids. The bacteriophage, P22, forms similar small particles when the scaffold has been mutated (Lenk *et al*, 1975; Earnshaw & King, 1978).

It would appear that these shell proteins have an inherent ability to self assemble into an icosahedral structure however, accessory proteins are required to mediate the correct curvature of the capsid shell. In this respect, VP23 and the scaffold are involved in forcing the shell proteins into a different confirmation.

4.2 VP23

The exact function of the triplex protein VP23 remains unclear but, fluorescence data (Chapter 3 and Nicholson *et al*, 1994) and yeast 2-hybrid studies (Desai & Person, 1996) have indicated that it does not interact directly with VP5. Thomsen *et al* (1994) claimed that VP22a did not interact with VP5 in the absence of VP23 and suggested that VP23 was required for this interaction. Fluorescence studies have shown that this is clearly not the case. Also as protease was present in the Thomsen study, it is likely that the 25 amino acids essential for the interaction of preVP22a with VP5 (Preston *et al*, 1994) had been cleaved.

So, what is the function of VP23? When the shell proteins VP5, VP19c and VP23 are co-expressed, partial or incomplete shell structures are formed and no 90nm particles formed by VP5 and VP19c are observed. This shows that the triplex protein is altering the curvature of the shell but cannot guide the formation of an icosahedral capsid. [Scaffold proteins are required to form the correctly assembled capsid (Tatman *et al*,

1994; Thomsen *et al*, 1994)]. Nevertheless, VP23 is influencing the interaction of VP5-VP19c and the publication of the reconstruction of the 880Å particles (Saad *et al*, 1999) has suggested that VP23 appears to connect the body of the triplex to the capsid floor. Since the capsid floor is composed of predominately VP5, this strongly suggests that VP23 is interacting directly with VP5. Although no such interaction has been detected by previous studies (see above) it may be that this interaction is only formed in mature capsids, when the VP5 floor is adopts a different conformation to that found in procapsids. VP23, in the triplex, could therefore act to fix and stabilise this region of the capsid floor.

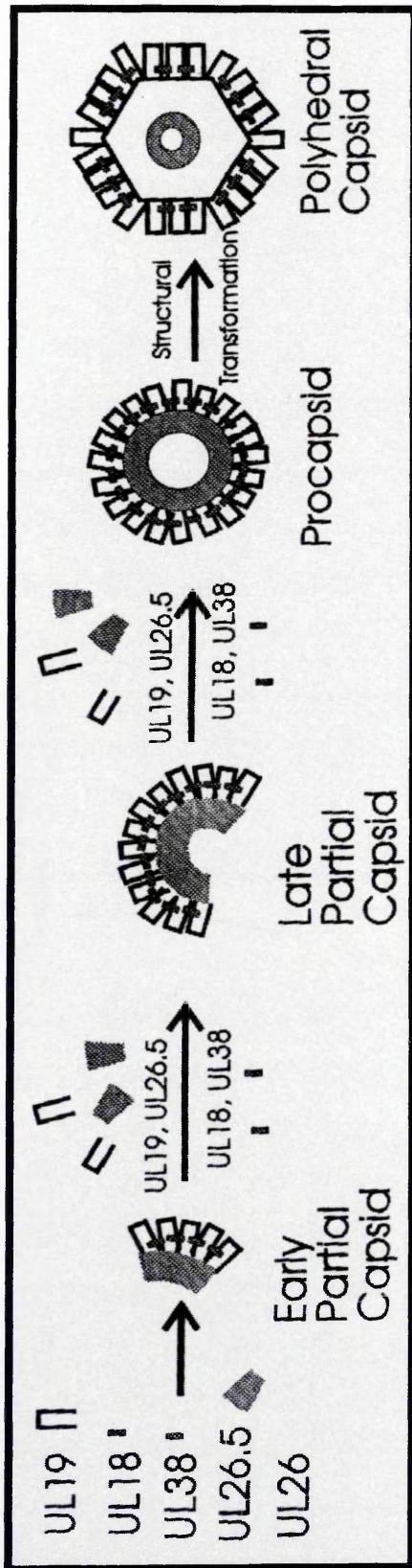
4.3 Scaffold

Preston *et al* (1994) have shown that when the scaffold encoding genes, UL26 and UL26.5, are co-expressed, circular scaffold-like structures, similar to capsid cores, (40-60nm in diameter) are formed. Similar structures have been widely reported in both HSV-1 and HSV-2 infections (Atkinson *et al*, 1978; Miyamoto 1971; Roizman 1969; Nii *et al*, 1968a, 1968b) and were reported as occasionally occurring in cells infected with all 6 recombinant baculoviruses (Tatman, 1996). Scaffold-like 60nm spheres have also been prepared from VP22a extracted in 2M GuHCl from B capsids (Newcomb & Brown, 1991).

Kennard *et al*, 1995 found that when preVP22a was expressed alone, few scaffold-like structures were observed. Instead, fibrillar structures, which aggregated together, were evident. However, when preVP22a was co-infected with VP5 indistinct structures, different from scaffolds, were observed. No fibrillar aggregates were visible suggesting that the interaction with VP5 was preventing aggregation of the scaffold and allowing a more defined or precise structure to form.

The above observations indicate that the proteins expressed by UL26 and UL26.5 have an inherent capacity to form scaffold-like structures. However, as it is known that VP22a does not participate in capsid assembly, these structures are not intermediates of the capsid assembly pathway. Although preVP22a alone cannot form scaffold like structures, more defined structures are evident when VP5 is present. It is possible that UL26 has a role in limiting the number of copies of protease which can be incorporated

Figure 7.3: Procapsid Assembly Model



into the scaffold, resulting in a complex of structures, as proposed in aggregates, while VPS is thought to be a component of the nucleocapsid (Section 5). Therefore, the relative concentrations of these proteins and the order in which they assemble will determine the final structure.

So, to summarise the assembly pathway, it is thought that the early partial capsid (that VPS and VPI are thought to be associated with) is an important intermediate in the assembly of the mature polyherdral capsid. The availability of these proteins and the order in which they assemble will determine the final structure of the procapsid.

5 HSV-1 Procapsid Assembly Pathway

Figure 7.3: This is a suggested pathway for *in vitro* assembly of HSV 1 capsids. Assembly is thought to begin with an early partial capsid, which expands into a late partial capsid and finally a spherical procapsid. The procapsid angularises to form the mature polyherdral capsid.

Reproduced from Newcomb *et al* (1996).

into the scaffold, resulting in the formation of scaffold-like structures, as opposed to aggregates, while VP5 is influencing the morphology and curvature of the scaffold (see Section 6). Therefore the constraint on the size of the scaffold may act as the factor which determines the size of the capsid.

So, to summarise the data cited to explain the formation of the capsid, it would appear that VP5 and VP19c have the inherent capacity to form an icosahedral shell. VP23 is important for defining the correct curvature of the shell and scaffold is required to guide assembly of the shell proteins and ultimate size of the capsid. But, how is the scaffold fulfilling its role? The answer to this question may be contained in the recently proposed procapsid assembly model.

5 HSV-1 Procapsid Assembly Model and Analogies with Bacteriophage

Newcomb *et al* (1994; 1996) have developed a cell free assembly system which has allowed intermediates to be isolated during capsid assembly. They have proposed a model, (summarised in figure 7.3) whereby arc-like structures, containing preVP22a, VP19c, VP5 and VP23, form after a short incubation time. Such structures may correspond to the partial capsids which had been previously observed in electron micrographs of HSV-1 infected cells (Nii *et al*, 1968a, 1968b). Upon further incubation, these partial capsids become spherical structures, which have been designated procapsids. Even although the protease was present, the scaffold at this stage was not cleaved and the procapsids contained a large cored scaffold. The *in vitro* system has recently been used to show that VP5 and the scaffolding proteins form a complex during assembly (Newcomb *et al*, 1999). These may act as building blocks of the procapsids.

3D cryo-EM has shown that these procapsids have distorted hexons and a very open structure. They differ from wild-type capsids, which have narrow axial channels and hexagonal hexons (Zhou *et al*, 1994). The procapsids are also relatively unstable, being sensitive to reductions in temperature, ie they fall apart at 2°C. Upon incubation at rt these procapsids spontaneously angularise into the familiar polyhedral type capsids.

As the procapsids are extremely unstable and thermolabile it is interesting to speculate as to why the virus forms such an intermediate and how it spontaneously reconfirms. The formation of procapsids, is not unique to HSV-1. Indeed, it is a well characterised assembly pathway for many dsDNA bacteriophages. For example, capsid assembly of P22 initiates from a portal protein (gp1), which sits at a vertex. The 47kDa coat protein (gp5) and the 34kDa scaffold protein (gp8) copolymerise, in association with other minor proteins, to form a spherical procapsid. The scaffold protein then exits from the procapsid while the DNA enters through the portal vertex. How the scaffold exits is not known however, holes or channels at the centre of the hexamers and pentamers were detected in the initial 3D image reconstructions of the procapsids (Prasad *et al*, 1993). These are not in the mature capsid. It is speculated that these channels are the exit points for gp8 (Greene & King, 1994). A 19Å structure of procapsids, containing scaffold, confirmed the presence of these channels (Thuman-Commike *et al*, 1996) and gave further support to the hypothesis that these are important for scaffold exit.

Exit of the scaffold and entry of DNA is coupled with shell expansion and formation of the expected T=7 icosahedral capsid (Prevelige & King, 1993). If scaffold is absent, limited assembly of apparently normal capsid shells will occur, at a greatly reduced rate, but aberrant spiral and small capsids with T=4 symmetry are also formed (Thuman-Commike *et al*, 1996). Recent electron cryomicroscopy images of scaffold containing and scaffold lacking procapsids (Thuman-Commike *et al*, 1999) have suggested that specific interactions form between coat proteins and scaffold proteins. Together these provide overlapping sets of binding interactions, which drive the formation of the procapsid.

The main difference between the assembly of P22 procapsids and HSV-1 procapsids is that the HSV-1 procapsids have a similar diameter (120nm) to the icosahedral capsid (125nm) and so do not undergo an expansion. Three main proposals have been put forward to explain why the bacteriophage capsids expand during DNA packaging:

- Steven *et al* (1991,1992) proposed that there are subunit to subunit motions which are required for packaging and so the structure requires to be flexible. After DNA has been successfully packaged, the proteins 'lock' into position and stabilise the structure
- Earnshaw & Casjens (1980) suggested the capsid forms around a scaffold to prevent random cytoplasmic proteins being incorporated into the growing structure, which would disrupt it. The initial stage of the procapsid is therefore very compact while the shell proteins assemble. Once the proteins are in place the virus specific scaffold is removed and the structure expanded to allow DNA packaging.
- King & Chiu (1997) proposed that the scaffold exit, shell expansion and DNA packaging were directly coupled. They suggested that because the DNA in phage is injected into cells upon infection, leaving the capsid intact, the DNA must be free to leave the capsid and not tightly associated with the inner capsid shell. However, initial entry and organisation of the DNA within the shell may require binding to the capsid subunits. Any such binding sites would require to be exposed for entry but then either lost, inactivated, or removed at a subsequent stage. They therefore suggest that the coat proteins in the procapsid contain these binding sites and when they swivel and the structure expands as the icosahedron is formed, the binding sites are lost

So why does HSV-1 not undergo expansion? This is a difficult problem to address however, it is important to realise that although analogies do exist between P22 and HSV-1, they are two distinct viruses whose capsids require to exist in distinct environments.

HSV-1 capsids are assembled in the nucleus of infected cells and surrounded by tegument and envelope before exiting the host cell. In contrast, P22 capsids constitute the external shell of the bacteriophage and are left intact when DNA is injected into the host cell. Even different phage vary in their mechanism for losing scaffold from the capsid. P22 scaffold leaves uncleaved and is recycled, whereas T4 and λ scaffold is proteolysed into small fragments and lost well in advance of DNA packaging (Ontorato & Showe, 1975; Ray & Murialdo, 1975). No potential 'exit' holes are visible in these phage (Dokland & Murialdo, 1993). Since the assembly and packaging pathway can vary between different bacteriophage, it is not surprising that the model for P22 does

not fit exactly to HSV-1. The reason that HSV-1 does not undergo head expansion is because it does not require to do so to fulfil its function. Therefore, expansion is not fundamental to DNA packaging but is specific to some aspects of phage assembly.

Newcomb *et al* (1996) suggest that the procapsid is the precursor for all capsid types. However, as the cell free assembly system is an *in vitro* model, whether the procapsids can package DNA cannot be determined, using this approach. Trus *et al* (1996) found that only preVP22a was present in polyhedral capsids which had matured from procapsids. If procapsids mature into polyhedral capsids without the cleavage of preVP22a, what does this tell us about the procapsid as the starting point for capsid maturation? All evidence suggests that DNA cannot be packaged in the absence of preVP22a cleavage. It may be the case therefore, that the conversion of procapsid to polyhedral capsid *in vitro* is not mimicking the situation *in vivo*. The best model available for studying scaffold *in vivo* is by using the ts1201 HSV-1 mutant (Preston *et al*, 1983). As previously described (Chapter 6, Discussion), ts1201 has a lesion in the protease gene which inactivates the protease at the non-permissive temperature causing large cored capsids to accumulate. However, this step is reversible with a downshift in temperature resulting in the conversion of large cored B capsids to a mixture of A, small core B capsids and C capsids. All experiments to date, have shown that the capsids isolated from ts1201, have been icosahedral. However this did not rule out the possibility that procapsids were being lost during the purification procedure. Very recent investigations have shown that the great majority of assembly products of ts1201 infection are thermolabile and unstable, indicative of a procapsid form (Rixon & McNab, 1999). It seems likely therefore, that procapsids are in fact an intermediate in HSV-1 assembly. This model can be used to fit the data obtained in this thesis. However, until an *in vitro* packaging model has been developed the exact mechanism of capsid assembly cannot be determined.

6 Proposed Model for Capsid Assembly

Obviously the pathway of capsid assembly, scaffold cleavage and DNA packaging is very complex. Newcomb *et al* (1996) have shown that the capsid proteins spontaneously interact to form partial shells which come together to form procapsid. As previously mentioned, icosahedral 880Å particles are formed in the absence of scaffold.

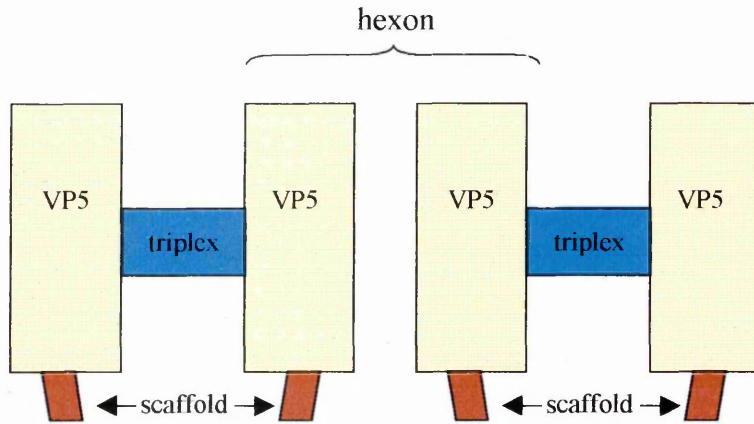
The scaffold therefore appears to be involved in defining the curvature and ultimate size of the capsid. It is interesting that the work presented in this chapter has mapped the points scaffold and shell interact to beneath the triplexes. High resolution cryo-EM of the capsid, to 13Å, has shown that there is an extensive network of triplexes forming 4 types of interaction with VP5 (Zhou *et al*, 1998). Interactions of different types designated strong, weak, tail and arm interactions were all observed. The major points of scaffold contact appear underneath one strong and one very weak, or arm, triplex interaction in each case. It is thought that the triplex proteins play an important role in ordering the capsomeres and VP23 is thought to mediate the curvature of the capsid shell (Saad *et al*, 1999). In the procapsid the triplexes and capsomeres are loosely bound and the capsid floor is not well formed (Newcomb *et al*, 1996) making the structure very unstable and fragile. This is in stark contrast to the robust nature of the icosahedral capsid. The transformation must require structural rearrangement into a more stable form. Some of the proteins in the procapsid may therefore require to be inherently flexible and able to move to achieve the icosahedral shape.

Recent data has suggested that VP23 is in a molten globule, or, partially folded state (Kirkitadze *et al*, 1998). This would allow the protein to be flexible in the procapsid intermediate, before it was locked into its final form by an undefined trigger. It is known that VP23 and VP19c (the triplex proteins) can form complexes in the absence of any other capsid proteins (Spencer *et al*, 1998). It is therefore possible, that it is VP19c which induces the structural rearrangement of VP23. The presence of a molten globule in viral structures is not unique to HSV-1. Two proteins of P22 have been described as having a molten globule state (Tescke & King, 1993).

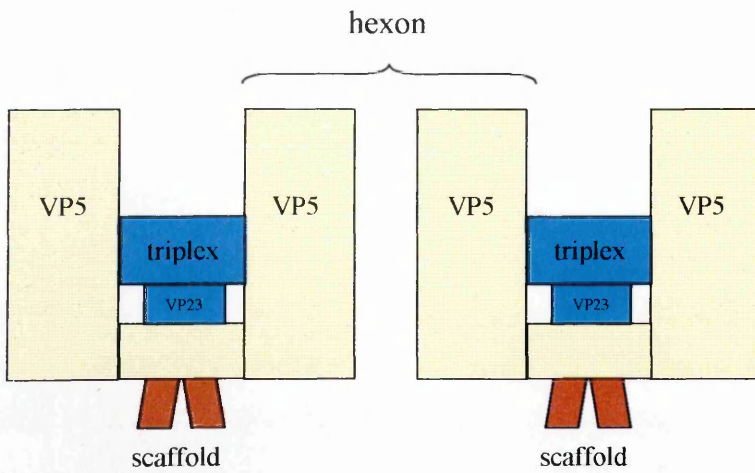
The scaffold protein itself could therefore be playing the important role of stabilising the structure. This situation is analogous to the spokes of a bicycle wheel where the spokes are helping to define the curvature. The scaffold may not adopt a precise structure but provide the overall dimensions and tension necessary to ensure correct shell formation. The subsequent intermediate steps of conversion from large cored procapsids to icosahedral type capsids are unclear. It can be envisaged that coming together of 2 copies of preVP22a pulls the VP5 capsomeres together and thus the

Figure 7.4: Possible Mechanism of preVP22a in the Procapsid to Capsid Transition

(i) Procapsid



(ii) Capsid



Conclusion

capid floor is expanded (see figure 7.4). The procapsid is a much more open structure than the mature capsid. The scaffold protein (preVP22a), shown in red, may act to stabilise the structure, with 2 copies coming together and helping the VP5 capsid floor to form. The triplexes, shown in turquoise, help to bind the VP5 molecules together and appear to be located above the points of contacts between scaffold and shell in the mature capsid.

Figure 7.4: The procapsid has a much more open structure [panel (i)] than the mature capsid [panel (ii)] and neighbouring hexons, shown in yellow, are not tightly bound. The scaffold protein (preVP22a), shown in red, may act to stabilise the structure, with 2 copies coming together and helping the VP5 capsid floor to form. The triplexes, shown in turquoise, help to bind the VP5 molecules together and appear to be located above the points of contacts between scaffold and shell in the mature capsid.

This figure is not drawn to scale.

capsid floor is expanded (see figure 7.4). This action results in the transformation of procapsid to capsid. Certainly if the scaffold's role is to stabilise the structure, without forming extensive contacts, it would seem reasonable to assume that it may be interacting with the shell proteins at the weakest links on the capsid floor. The nature of the contact points is such that a single scaffold protein is not interacting with a single hexon. Instead it seems likely that the scaffold may be forming contacts at areas in the capsid floor where several VP5 molecules come together. The scaffold would therefore be acting as an extra securing point, reinforcing and stabilising the contact points. The UL26 product in turn will be limiting the size of the scaffold and thus capsid. Once the scaffold has helped the capsid floor to form, the VP23 molecule will act as extra cement, helping to stabilise and guide correct conformation. This model is speculative and this type of detail remains to be resolved.

The stage at which VP26 binds to capsids is not clear. When VP26 was included in the cell free assembly model, it did not form part of either the procapsid or capsid. However, this may have been attributable to its highly insoluble nature under these experimental conditions, as oppose to a reflection of its binding pattern. There is no reason, based on available data, to assume that VP26 would not bind to VP5 hexons during the assembly stages *in vivo*. The exact function of VP26 is unknown however, its external location on the capsid might suggest that it is important for interacting with the surrounding tegument. However, recent visualisation, by cryomicroscopy, of the capsid tegument interaction in intact virions has shown that tegument binding is confined to the vicinity of the pentonal vertices (Zhou *et al*, 1999). It seems that the occupation of VP26 at the hexonal tips results in this site being unavailable for tegument binding. If the protein is shown not to be present *in vivo* on procapsids, therefore only attaching to angularised capsids, it may have a role in locking the polyhedral capsid in place. As yet, the role of VP26 remains to be resolved

To conclude, clearly the process of capsid assembly is extremely complex, with many proteins interacting and influencing each other simultaneously. However, this thesis has provided an insight into some of the properties of these proteins. VP26 has been purified and its oligomeric status determined. Probable points of contact with VP5, both

purified and within the context of the capsid, have also been mapped together with the location of the N-terminus. The points of contact of between scaffold and shell have been visualised, which has allowed further clarification of the capsid structure. The probable location of many capsid proteins within transfected cells has been determined, in parallel with the pattern of interaction which is occurring. During the course of all this work, many useful assay systems have been developed which can be adapted to further study the capsid protein interactions and draw a clearer and more precise pattern of events in the process of capsid assembly.

REFERENCES

- Ablashi, D., Balanchandran, N., Josephs, S., Hung, C., Krueger, G., Kramarsky, B., Salahuddin, S., and Gallo, R. (1991): Genetic polymorphism, growth properties, and immunologic variants in humanherpesvirus-6 isolates. *Virology* **184**, 545-552.
- Ace, C., Dalrymple, M., Ramsay, F., Preston, V., and Preston, C. (1988): Mutational analysis of the herpes simplex virus type 1 trans-inducing factor Vmw65. *Journal of General Virology* **69**, 2595-2605.
- Ace, C., McKee, T., Ryan, J., Cameron, J., and Preston, C. (1989): Construction and characterisation of a herpes simplex type 1 mutant unable to transinduce immediate-early gene-expression. *Journal of Virology* **63**, 2260-2269.
- Addison, C., Rixon, F. J., Palfreyman, J. W., O'Hara, M., and Preston, V. G. (1984): Characterization of a herpes simplex virus type-1 mutant which has a temperature-sensitive defect in penetration of cells and assembly of capsids. *Virology* **138**, 246-259.
- Ali, M., Farhany, B., and Cantin, E. (1996): Characterisation of an essential HSV-1 protein encoded by the UL25 gene reported to be involved in virus penetration and capsid assembly. *Virology* **216**, 278-283.
- Almedia, J., Lang, D., and Talbot, P. (1978): Herpesvirus morphology: Visualisation of a structural subunit. *Intervirology* **10**, 318-320.
- Asher, Y., Heller, M., and Becker, Y. (1969): Incorporation of lipids into herpes simplex virus particles. *Journal of General Virology* **4**, 65-76.
- Atkinson, M., Barr, S., and Timbury, M. (1978): The fine structure of cells infected with temperature sensitive mutants of herpes simplex virus type 2. *Journal of General Virology* **40**, 103-119.
- Avitable, E., Di Gaeta, S., Torrisi, M., Ward, P., Roizman, B., and Campadelli-Fiume, G. (1995): Redistribution of microtubules and golgi apparatus in herpes simplex virus infected cells and their role in viral exocytosis. *Journal of Virology* **69**, 7472-7482.
- Baines, J., and Roizman, B. (1992): The cDNA of UL15, a highly conserved herpes simplex virus 1 gene, effectively replaces the two exons of the wild-type virus. *Journal of Virology* **66**, 5621-5626.
- Baines, J., Poon, A., Rovnak, J., and Roizman, B. (1994): The herpes simplex virus 1 UL15 gene encodes two proteins and is required for cleavage of genomic viral DNA. *Journal of Virology* **68**, 8118-8124.
- Baker, T. S., Newcomb, W. W., Booy, F. P., Brown, J. C., and Steven, A. C. (1990): Three-dimensional structures of maturable and abortive capsids of equine herpesvirus 1 from cryoelectron microscopy. *Journal of Virology* **64**, 563-573.
- Balachandran, N., Harnish, D., Killington, R., Bacchetti, S., and Rawls, W. (1981): Monoclonal antibodies to 2 glycoproteins of herpes simplex virus type 2. *Journal of Virology* **39**, 438-446.
- Batchelor, A., and O'Hare, P. (1992): Localisation of cis-acting sequence requirements in the promoter of the latency associated transcripts of herpes simplex virus type 1 required for cell type specific activity. *Journal of Virology* **66**, 3563-3582.

- Batterson, W., and Roizman, B. (1983): Characterisation of the herpes simplex virion associated factor responsible for the induction of alpha genes. *Journal of Virology* **46**, 371-377.
- Batterson, W., Furlong, B., and Roizman, B. (1983): Molecular genetics of HSV. VIII. Further characterisation of a temperature sensitive mutant defective in release of viral DNA and in other stages of viral reproductive cycle. *Journal of Virology* **45**, 397-407.
- Belyaev, A., and Roy, P. (1993): Development of baculovirus triple and quadruple expression vectors- coexpression of 3 or 4 bluetongue virus proteins and the synthesis of bluetongue virus-like particles in insect cells. *Nucleic Acids Research* **21**, 1219-1223.
- Ben-Porat, T., and Kaplan, A. (1971): Phospholipid metabolism of herpesvirus infected and uninfected rabbit kidney cells. *Virology* **45**, 252-264.
- Beswick, T. (1962): The origin and use of the word herpes. *Medical History* **6**, 214-300.
- Black, B., and Center, M. (1979): DNA binding properties of the major core protein of adenovirus 2. *Nucleic Acid Research* **6**, 2339-2353.
- Booy, F. P., Newcomb, W. W., Trus, B. L., Brown, J. C., Baker, T. S., and Steven, A. C. (1991a): Liquid-crystalline, phage-like packing of encapsidated DNA in herpes simplex virus. *Cell* **64**, 1007-1015.
- Booy, F. P., Newcomb, W. W., Trus, B. L., Brown, J. C., Baker, T. S., and Steven, A. C. (1991b): The DNA in herpes simplex virus capsids is arranged in parallel bundles with an inter-duplex spacing of 2.6 nm. *Biophys. J.* **59**, 193a.
- Booy, F. P., Trus, B. L., Newcomb, W. W., Brown, J. C., Conway, J. F., and Steven, A. C. (1994): Finding a needle in a haystack: detection of a small protein (the 12-kDa VP26) in a large complex (the 200-MDa capsid of herpes simplex virus). *Proceedings of the National Academy of Sciences of the U.S.A.* **91**, 5652-5656.
- Booy, F., Trus, B., Davison, A., and Steven, A. (1996): The capsid architecture of channel catfish virus, an evolutionarily distant herpesvirus, is largely conserved in the absence of discernible sequence homology with herpes simplex virus. *Virology* **215**, 134-141.
- Braun, D., Roizman, B., and Pereira, L. (1984): Characterisation of post-translational products of herpes simplex virus gene 35 proteins binding to the surfaces of full capsids but not empty capsids. *Journal of Virology* **49**, 142-153.
- Brenner, S., and Horne, R. W. (1959): A negative staining technique for high resolution electron microscopy of viruses. *Biochimica et Biophysica Acta* **34**, 103-110.
- Britt, W. (1996a): Human cytomegalovirus overview: the virus and its pathogenicity. *Baillieres Clinical Infectious Diseases* **3**, 307-325.
- Britt, W. (1996b): Human cytomegalovirus infection during pregnancy. *Baillieres Clinical Infectious Diseases* **3**, 327-343.
- Bronstein, J. C., Weller, S. K., and Weber, P. C. (1997): The product of the UL12.5 gene of herpes simplex virus type 1 is a capsid-associated nuclease. *Journal of Virology* **71**, 3039-3047.

- Brooks, L., Wilson, A., and Crooks, T. (1997): Kaposi's sarcoma-associated herpesvirus (KSHV) / human herpesvirus 8 (HHV8)- A new human tumor virus. *Journal of Pathology* **182**, 262-265.
- Brown, M., and Faulkner, P. (1977): A plaque assay for nuclear polyhedrosis viruses using a solid overlay. *Journal of General Virology* **36**, 361-364.
- Brown, S., Ritchie, D., and Subak-Sharpe, J. (1973): Genetic studies with herpes simplex virus type 1. The isolation of temperature sensitive mutants, their arrangement into complementation groups and recombination analysis leading to a linkage map. *Journal of General Virology* **18**, 329-346.
- Browne, H., Bell, S., Minson, T., and Wilson, D. W. (1996): An endoplasmic reticulum-retained herpes simplex virus glycoprotein H is absent from secreted virions: evidence for reenvelopment during egress. *Journal of Virology* **70**, 4311-4316.
- Bruckner, R., Crute, J., Dodson, M., and Lehman, I. (1991): The herpes simplex virus 1 origin binding protein: A DNA helicase. *Journal of Biological Chemistry* **266**, 2669-2674.
- Buckmaster, A., Scott, S., Sanderson, M., Boursnell, M., Ross, N., and Binns, M. (1988): Gene sequence and mapping data from Marek's disease virus and herpesvirus of turkeys- Implications for herpesvirus classification. *Journal of General Virology* **69**, 2033-2042.
- Bush, M., Yager, D., Gao, M., Weissbart, K., Marcy, A., Coen, D., and Knipe, D. (1991): Correct intranuclear localisation of herpes simplex virus DNA polymerase requires the viral ICP8 DNA binding protein. *Journal of Virology* **65**, 1082-1089.
- Cai, W., Person, S., Warner, S., Zhou, J., and DeLuca, N. (1987): Linker-insertion nonsense and restriction site mutations of the gB glycoprotein gene of herpes simplex type 1. *Journal of Virology* **61**, 714-721.
- Cai, W., Gu, B., and Person, S. (1988): Role of glycoprotein B of herpes simplex virus type 1 in viral entry and cell fusion. *Journal of Virology* **62**, 2596-2604.
- Calder, J., and Stow, N. (1990): Herpes simplex virus helicase-primase: The UL8 protein is not required for DNA-dependant ATPase and DNA helicase activities. *Nucleic Acids Research* **18**, 3573-3578.
- Calder, J., Stow, E., and Stow, N. (1992): On the cellular localisation of the components of the herpes simplex virus type 1 helicase-primase complex and the viral origin-binding protein. *Journal of General Virology* **73**, 531-538.
- Campadelli-Fiume, G., Arsenakis, M., Farabegoli, F., and Roizman, B. (1988): Entry of herpes simplex virus 1 in BJ cells that constitutively express viral glycoprotein D is by endocytosis and results in the degradation of the virus. *Journal of Virology* **62**, 159-167.
- Campadelli-Fiume, G., Farabeoli, F., Di Gaeta, S., and Roizman, B. (1991): Origin of unenveloped capsids in the cytoplasm of cells infected with herpes simplex type 1. *Journal of Virology* **65**, 1589-1595.
- Campbell, M., Palfreyman, J., and Preston, C. (1984): Identification of herpes simplex virus DNA which encode a trans-acting polypeptide responsible for stimulation of immediate early transcription. *Journal of Molecular Biology* **180**, 1-19.
- Challberg, M. (1986): A method for identifying the viral genes required for herpes DNA replication. *Proceedings of the National Academy of Sciences of the U.S.A.* **83**, 9094-9098.

- Challberg, M. (1991): Herpes simplex virus DNA replication. *Seminars in Virology* **2**, 247-256.
- Chang, Y., Cesarean, E., Pessin, M., Lee, F., Culpepper, J., Knowles, D., and Moore, P. (1994): Identification of herpesvirus-like DNA sequences in AIDS-associated Kaposi's sarcoma. *Science* **266**, 1865-1869.
- Chase, C., Lohff, C., and Letchworth, G. (1993): Resistance and susceptibility of bovine cells expressing herpesviral glycoprotein D homologs to herpesviral infections. *Virology* **194**, 365-369.
- Cheng, P., Banfield, B., and Tufaro, F. (1991): Brefeldin A arrests the maturation and egress of herpes simplex virus particles during infection. *Journal of Virology* **65**, 1893-1904.
- Clements, J., Watson, R., and Wilkie, N. (1977): Temporal regulation of herpes simplex virus 1 transcription: Location of transcripts on the viral genome. *Cell* **12**, 275-285.
- Cohen, G. H., Ponce de Leon, M., Diggelmann, H., Lawrence, W. C., Vernon, S. k., and Eisenberg, R. J. (1980): Structural analysis of the capsid polypeptides of herpes simplex virus types 1 and 2. *Journal of Virology* **34**, 521-531.
- Colby, W. W., and Shenk, T. (1981): Adenovirus type 5 virions can be assembled in vivo in the absence of detectable polypeptide IX. *J. Virol.* **39**, 977-980.
- Conley, A., Knipe, D., Jones, P., and Roizman, B. (1981): Molecular genetics of herpes simplex virus. VII. Characterisation of a temperature sensitive mutant produced by in vitro mutagenesis and defective in DNA synthesis and accumulation of gamma polypeptides. *Journal of Virology* **37**, 191-206.
- Cook, M., and Stevens, J. (1973): Pathogenesis of herpes simplex neuritis and ganglionitis in mice. Evidence of axonal transport of infection. *Infection and Immunity* **7**, 272-276.
- Costa, R., Draper, K., Banks, L., Powell, K., Cohen, G., Eisenberg, R., and Wagner, E. (1983): High resolution characterisation of herpes simplex type 1 transcripts encoding alkaline exonuclease and a 50000 dalton protein tentatively identified as a capsid protein. *Journal of Virology* **48**, 591-603.
- Costa, R., Cohen, G., Eisenberg, R., Long, D., and Wagner, E. (1984): Direct demonstration that the abundant 6-kilobase herpes simplex virus type 1 mRNA mapping between 0.23 and 0.27 map units encodes the major capsid protein VP5. *Journal of Virology* **49**, 287-292.
- Costanzo, F., Campadelli-Fiume, G., Foa-Tomasi, L., and Cassai, E. (1977): Evidence that herpes simplex virus DNA is transcribed by cellular RNA polymerase B. *Journal of Virology* **21**, 996-1001.
- Coulter, L., Moss, H., Lang, J., and McGeoch, D. (1993): A mutant of herpes simplex virus type 1 in which the UL13 protein kinase gene is disrupted. *Journal of General Virology* **74**, 387-395.
- Crute, J., Mocarski, E., and Lehman, I. (1988): A DNA helicase induced by herpes simplex virus type 1. *Nucleic Acids Research* **16**, 6585-6596.
- Crute, J., and Lehman, I. (1989): Herpes simplex virus-1 DNA polymerase. Identification of an intrinsic 5'-3' exonuclease with ribonuclease H activity. *Journal of Biological Chemistry* **264**, 19266-19270.

- Crute, J., Tsurumi, T., Zhu, L., Weller, S., Olivio, P., Challberg, M., Mocarski, E., and Lehman, I. (1989): Herpes simplex virus 1 helicase-primase: A complex of three herpes-encoded gene products. *Proceedings of the National Academy of Sciences of the U.S.A.* **86**, 2186-2189.
- Crute, J., and Lehman, I. (1991): Herpes simplex virus-1 helicase-primase. Physical and catalytic properties. *Journal of Biological Chemistry* **266**, 4484-4488.
- Dargan, D. J. (1986): The structure and assembly of herpesviruses, pp. 359-437. In J. R. Harris, and R. W. Horne (Eds): *Electron microscopy of proteins. 5 viral structure*, Academic Press Inc., London.
- Darlington, R., and Moss, L. (1968): Herpesvirus envelopment. *Journal of Virology* **2**, 48-55.
- Davidson, A., and Taylor, P. (1987): Genetic relations between Varicella zoster virus and Epstein Barr virus. *Journal of General Virology* **68**, 1067-1079.
- Davison, A., and Wilkie, N. (1981): Nucleotide sequences of the joint between the L and S segments of herpes simplex viruses type 1 and 2. *Journal of General Virology* **55**, 315-331.
- Davison, A., and Wilkie, N. (1983): Location and orientation of homologous sequences in the genomes of five herpes viruses. *Journal of General Virology* **64**, 1927-1942.
- Davison, A. (1983): DNA sequence of the Us component of the varicella zoster of the varicella zoster virus genome. *The EMBO Journal* **2**, 2203-2209.
- Davison, A. (1992): Channel catfish virus – A new type of herpesvirus. *Virology* **186**, 9-14.
- Davison, M. D., Rixon, F. J., and Davison, A. J. (1992): Identification of genes encoding 2 capsid proteins (VP24 and VP26) of herpes simplex virus type-1. *Journal of General Virology* **73**, 2709-2713.
- Davison, A., and Davison, M. (1995): Identification of structural proteins of channel catfish virus by mass spectrometry. *Virology* **206**, 1035-1043.
- Davison, A. (1998): The genome of salmonid herpesvirus 1. *Journal of Virology* **72**, 1974-1982.
- Davison, A., Sauerbier, W., Dolan, A., Addison, C., and McKinnell, R. (1999): Genomic studies of the Lucke tumor herpesvirus (RaHV-1). *Journal of Cancer Research and Clinical Oncology* **125**, 232-238.
- Deatly, A., Spivack, J., Lavi, E., and Fraser, N. (1987): Reactivation from an immediate early region of the type 1 herpes simplex virus genome is present in the trigeminal ganglia of latently infected mice. *Proceedings of the National Academy of Sciences of the U.S.A.* **84**, 3204-3208.
- Deiss, L., Chou, J., and Frenkel, N. (1986): Functional domains within the a sequence involved in the cleavage-packaging of herpes simplex virus DNA. *Journal of Virology* **59**, 605-618.
- Delius, H., and Clements, J. (1976): A partial denaturation map of herpes simplex virus type 1 DNA: Evidence for the inversion of the unique DNA regions. *Journal of General Virology* **33**, 125-133.

- Desai, P., Schaffer, P., and Minson, A. (1988): Excretion of non-infectious virus particles lacking glycoprotein H by a temperature sensitive mutant of herpes simplex type 1: evidence that gH is essential for virion infectivity. *Journal of General Virology* **69**, 1147-1156.
- Desai, P., DeLuca, N., Glorioso, J., and Person, S. (1993): Mutations in herpes simplex type 1 genes encoding VP5 and VP23 abrogate capsid formation and cleavage of replicated DNA. *Journal of Virology* **67**, 1357-1364.
- Desai, P., and Person, S. (1996): Molecular interactions between the HSV-1 capsid proteins as measured by the yeast two-hybrid system. *Virology* **220**, 516-521.
- Desai, P., and Person, S. (1998): Incorporation of the green fluorescent protein into the herpes simplex virus type 1 capsid. *Journal of Virology* **72**, 7583-7567.
- Desai, P., DeLuca, N., and Person, S. (1998): Herpes simplex virus type 1 VP26 is not essential for replication in cell culture but influences production of infectious virus in the nervous system of infected mice. *Virology* **247**, 115-124.
- Dilanni, C., Drier, D., Deckman, I., McCann, P., F, L., Roizman, B., Colonno, R., and Cordingley, M. (1993): Identification of the herpes simplex virus-1 protease cleavage sites by direct sequence analysis of autoproteolytic cleavage products. *Journal of Biological Chemistry* **268**, 2048-2051.
- Dingwell, K., Brunetti, C., Hendricks, R., Tang, Q., Tang, M., Rainbow, A., and Johnson, D. (1994): Herpes simplex virus glycoprotein E and glycoprotein I facilitate cell to cell spread in vivo and across junctions of cultured cells. *Journal of Virology* **68**, 834-845.
- Dixon, R., and Schaffer, P. (1980): Fine structure mapping and functional analysis of the temperature sensitive mutants in the gene encoding the herpes simplex virus type 1 immediate early protein VP175. *Journal of Virology* **36**, 189-203.
- Dodson, M., Crute, J., Bruckner, R., and Lehman, I. (1989): Over expression and assembly of the herpes simplex type 1 helicase-primase in insect cells. *Journal of Biological Chemistry* **264**, 20835-20838.
- Dodson, M., and Lehman, I. (1991): Association of DNA helicase primase activities with a subassembly of the herpes simplex virus 1 helicase-primase composed of the UL5 and UL52 gene products. *Proceedings of the National Academy of Sciences of the U.S.A.* **88**, 1105-1109.
- Dokland, T., and Murialdo, H. (1993): Structural transitions during maturation of bacteriophage lambda capsids. *J. Mol. Biol.* **233**, 682-694.
- Dolyniuk, M., Wolff, E., and Kieff, E. (1976): Proteins of Epstein-Barr virus. II. Electrophoretic analysis of the polypeptides of the nucleocapsid and the glucosamine- and polysaccharide-containing components of enveloped virus. *Journal of Virology* **18**, 289-297.
- Earnshaw, W., and King, J. (1978): Structure of phage P22 coat protein aggregates formed in the absence of the scaffolding protein. *J Mol Biol* **126**, 721-747.
- Earnshaw, W. C., and Casjens, S. R. (1980): DNA packaging by the double-stranded DNA bacteriophages. *Cell* **21**, 319-331.

- Eberle, R., and Courtney, R. (1980): gA and gB glycoproteins of herpes simplex virus type 1: two forms of a single polypeptide. *Journal of Virology* **36**, 665-675.
- Efstathiou, S., Kemp, S., Darby, G., and Minson, A. (1989): The role of herpes simplex virus type 1 thymidine kinase in pathogenesis. *Journal of General Virology* **70**, 869-879.
- Eggers, M., Bogner, E., Agricola, B., Kern, H., and Radsak, K. (1992): Inhibition of human cytomegalovirus maturation by brefeldin A. *Journal of General Virology* **73**, 2679-2692.
- Elliott, G., and O'Hare, P. (1997): Intracellular trafficking and protein delivery by a herpesvirus structural protein. *Cell* **88**, 223-233.
- Elliott, G., and O'Hare, P. (1999): Live cell analysis of a green fluorescent protein tagged herpes simplex virus infection. *Journal of Virology* **73**, 4110-4119.
- Everett, R. (1984): Transactivation of transcription by herpesvirus products. Requirement for two HSV-1 immediate early polypeptides for maximum activity. *EMBO* **3**, 3135-3141.
- Everett, R. (1986): The products of herpes simplex virus type 1 (HSV-1) immediate early genes 1, 2 and 3 can activate HSV-1 genes expression in trans. *Journal of General Virology* **67**, 2507-2513.
- Everett, R., O'Hare, P., O'Rourke, D., Barlow, P., and Orr, A. (1995): Point mutations in the herpes simplex virus type 1 Vmw110 ring finger helix affect activation of gene expression, viral growth and interaction with PML containing nuclear structures. *Journal of Virology* **69**, 7339-7344.
- Everett, R., Meredith, M., Orr, A., Cross, A., Kathoria, M., and Parkinson, J. (1997): A novel ubiquitin specific protease is dynamically associated with the PML nuclear domain and binds to a herpesvirus regulatory protein. *EMBO* **16**, 1519-1530.
- Fenwick, M., and Clark, J. (1982): Early and delayed shut-off of host protein synthesis in cells infected with herpes simplex virus. *Journal of General Virology* **61**, 121-125.
- Fenwick, M. (1984): The effects of herpesvirus on cellular macromolecular synthesis. In H. Fraenkel-Conrat, and E. Wagner (Eds): *Virology*, Plenum Publishing Corporation, New York.
- Forrester, A., Farrell, H., Wilkinson, G., Kaye, J., Davis-Poynter, N., and Minson, T. (1992): Construction and properties of a mutant of herpes simplex virus type 1 with glycoprotein H coding sequences deleted. *Journal of Virology* **66**, 341-348.
- Frenkel, N., Schirmer, L., Wyatt, L., Katsafanas, G., Roffman, E., Danovich, R., and June, C. (1976): Anatomy of herpes simplex virus DNA. VI. Defective DNA originates from the S component. *Journal of Virology* **20**, 527-531.
- Frenkel, N., Schirmer, E., Wyatt, L., Katsalanas, G., Roffman, E., Danovich, R., and June, C. (1990): Isolation of a new herpesvirus from CD4+ T cells. *Proceedings of the National Academy of Sciences of the U.S.A.* **87**, 748-752.
- Friedrichs, W., and Grose, C. (1986): Varicella zoster virus p32/p36 complex is present in both the viral capsid and the nuclear matrix of the infected cell. *Journal of Virology* **57**, 155-164.
- Fuller, M., and King, J. (1981): Purification of the coat and scaffolding protein from procapsids of bacteriophages P22. *Virology* **112**, 529-547.

- Furlong, D., Swift, H., and Roizman, B. (1972): Arrangement of herpes virus deoxyribonucleic acid in the core. *Journal of Virology* **10**, 1071-1074.
- Galisteo, M., and King, J. (1993): Conformational transformations in the protein lattice of phage P22 procapsids. *Biophysical Journal* **65**, 227-235.
- Gallo, M., Dorsky, D., Crumpacker, C., and Parris, D. (1989): The essential 65kD DNA-binding protein of herpes simplex virus stimulates the virus encoded DNA polymerase. *Journal of Virology* **63**, 5023-5029.
- Gao, M., Matusick-Kumar, L., Hurlburt, W., DiTusa, S., Newcomb, W., Brown, J., McCann, P., III, Deckman, I., and Colonna, R. (1994): The protease of herpes simplex virus type 1 is essential for functional capsid formation and viral growth. *Journal of Virology* **68**, 3702-3712.
- Gelb, L. (1990): Varicella zoster virus, pp. 2011-2054. In B. Fields, and D. Knipe (Eds): *Virology, 2nd edition*, Raven Press, New York.
- Geraghty, R., Krummenacher, C., Cohen, G., Eisenberg, R., and Spear, P. (1998): Alphaherpesvirus entry mediated by poliovirus receptor related protein 1 and poliovirus receptor. *Science*.
- Gibson, W., and Roizman, B. (1972): Proteins specified by herpes simplex virus.VIII. Characterisation and composition of multiple capsid forms and sub-types of 1 and 2. *Journal of Virology* **10**, 1044-1052.
- Gibson, W., Baxter, M., and Clopper, K. (1996): Cytomegalovirus 'missing' capsid protein identified as heat agreeable product of human cytomegalovirus UL46. *Journal of Virology* **70**, 7454-7461.
- Gibson, W., Clopper, K., Britt, W., and Baxter, M. (1998): Human cytomegalovirus (HCMV) smallest capsid protein identified as a product of a short open reading frame located between UL48 and UL49. *Journal of Virology* **70**, 5680-5663.
- Gottlieb, J., Marcy, A., Coen, D., and Challberg, M. (1990): The herpes simplex virus type 1 UL42 gene product: A sub-unit of DNA polymerase that functions to increase processivity. *Journal of Virology* **64**, 5976-5987.
- Greber, U. R., Willetts, M., Webster, P., and Helenius, A. (1993): Stepwise dismantling of adenovirus 2 during entry into cells. *Cell* **75**, 477-486.
- Greene, B., and King, J. (1994): Binding of scaffold subunits within the P22 procapsid lattice. *Virology* **205**, 188-197.
- Grutter, M., and Franklin, R. (1974): Studies on the molecular weight of the adenovirus type 2 hexon and its subunit. *Journal of Molecular Biology* **89**, 163-178.
- Haar, L., and Skulstad, S. (1994): The herpes simplex virus type 1 particle: Structure and molecular functions. *APMIS* **102**, 321-346.
- Haffey, M., and Spear, P. (1980): Alteration in glycoprotein gB specified by mutants and their partial revertants in herpes simplex virus type I and relationship to other mutant phenotypes. *Journal of Virology* **35**, 114-128.
- Haguenau, F., and Michelson-Fiske, S. (1975): Cytomegalovirus: Nucleocapsid assembly and core structure. *Intervirology* **5**, 293-299.

- Harris-Hamilton, E., and Bachenheimer, S. (1985): Accumulation of herpes simplex virus type 1 RNAs of different kinetic classes in the cytoplasm of infected cells. *Journal of Virology* **53**, 144-151.
- Hayward, S., Jacob, R., Wadsworth, R., and Roizman, B. (1975): Anatomy of herpes simplex virus DNA: Evidence for four populations of molecules that differ in the relative orientations of their long and short components. *Proceedings of the National Academy of Sciences of the U.S.A.* **72**, 4243-4247.
- Hayward, G. (1993): Immediate early gene regulation in herpes simplex virus. *Seminars in Virology* **4**, 15-23.
- Heilman, C., Zweig, M., Stephenson, J., and Hampar, B. (1979): Isolation of a nucleocapsid polypeptide of herpes simplex virus types 1 and 2 possessing immunologically type-specific and cross-reactive determinants. *Journal of Virology* **29**, 34-42.
- Heine, J., Honess, R., Cassai, E., and Roizman, B. (1974): Proteins specified by herpes simplex virus. XII. The virion polypeptides of type 1 strains. *Journal of General Virology* **14**, 640-651.
- Hernandez, T., and Lehman, I. (1990): Functional interaction between the herpes simplex-1 DNA polymerase and UL42 protein. *Journal of Biological Chemistry* **265**, 11227-11232.
- Herold, B., WuDunn, D., Sotcys, N., and Spear, P. (1991): Glycoprotein C of herpes simplex virus type 1 plays a principal role in the adsorption of virus to cells and in infectivity. *Journal of Virology* **65**, 1090-1098.
- Hidaka, Y., Sukuma, S., Kumano, Y., Minagawa, H., and Mori, R. (1990): Characterisation of glycoprotein C-negative mutants of herpes simplex virus type I isolated from patients with keratitis. *Archives of Virology* **113**, 195-207.
- Hill, T. (1985): Herpesvirus latency, pp. 175-240. In B. Roizman (Ed.): *The herpesvirus*, Plenum Publishing Corp, New York.
- Hill, J., Sedarati, F., Javier, R., Wagner, E., and Stevens, J. (1990): Herpes simplex virus latent phase transcription facilities in vivo reactivation. *Virology* **174**, 17-125.
- Hill, A., Jugovic, P., York, I., Russ, G., Bennit, J., Yewdell, J., Ploegh, H., and Johnson, D. (1995): Herpes simplex virus turns off TAP to evade host immunity. *Nature* **375**, 411-415.
- Ho, D., and Mocarski, E. (1989): Herpes simplex virus latent RNA (LAT) is not required for latent infection in the mouse. *Proceedings of the National Academy of Sciences of the U.S.A.* **86**, 7596-7600.
- Hohn, B. (1983): DNA sequences necessary for packaging of bacteriophage 1 DNA. *Proceedings of the National Academy of Sciences of the U.S.A.* **80**, 7456-7460.
- Homa, F. L., and Brown, J. C. (1997): Capsid assembly and DNA packaging in herpes simplex virus. *Medical Virology* **7**, 107-122.
- Honess, R., and Roizman, B. (1974): Regulation of herpesvirus macromolecular synthesis I. Cascade regulation of the synthesis of three groups of viral proteins. *Journal of Virology* **14**, 8-19.

- Hong, Z., Beaudet-Miller, M., Durkin, J., Zhang, R., and Kwong, A. D. (1996): Identification of a minimal hydrophobic domain in the herpes simplex virus type 1 scaffolding protein which is required for interaction with the major capsid protein. *Journal of Virology* **70**, 533-540.
- Horne, R., Brenner, S., Waterson, A., and Wildy, P. (1959): The icosahedral form of an adenovirus. *Journal of Molecular Biology* **1**, 84-86.
- Hosokawa, K., and Sung, M. (1976): Isolation and characterisation of an extremely basic protein from adenovirus type 5. *Journal of Virology* **17**, 924-934.
- Hsu, H., Solovyev, I., Colombero, A., Elliot, R., Kelley, M., and Boyle, W. (1997): ATAR, a novel tumor necrosis factor receptor family member, signals through TRAF2 and TRAF5*. *Journal of Biological Chemistry* **272**, 13471-13474.
- Hutchinson, L., Browne, H., Wargent, V., Davis-Poynter, N., Primorac, S., Goldsmith, K., Minson, A., and Johnson, D. (1992): A novel herpes simplex virus protein, gL, forms a complex with glycoprotein H (gH) and affects normal folding and surface expression of gH. *Journal of Virology* **66**, 2240-2250.
- Irmiere, A., and Gibson, W. (1985): Isolation of human cytomegalovirus intranuclear capsids, characterisation of their protein constituents, and demonstration that the B-capsid assembly protein is also abundant in non-infectious enveloped particles. *Journal of Virology* **56**, 277-283.
- Jacob, R., Morse, L., and Roizman, B. (1979): Anatomy of herpes simplex virus DNA. XII. Accumulation of head-to-tail concatamers in nuclei of infected cells and their role in the generation of the four isomeric arrangements of viral DNA. *Journal of Virology* **29**, 448-457.
- Javier, R., Stevens, J., Dissette, V., and Wagner, E. (1988): A herpes simplex virus transcript abundant in latently infected neurons is dispensable for establishment of the latent state. *Virology* **166**, 254-257.
- Johnson, D., and Ligas, M. (1988): Herpes simplex viruses lacking glycoprotein D are unable to inhibit virus penetration: quantitative evidence for virus specific cell surface receptors. *Journal of Virology* **62**, 4605-4612.
- Johnson, D., Burke, R., and Gregory, T. (1990): Soluble forms of herpes simplex virus glycoprotein D bind to a limited number of cell surface receptors and inhibit virus entry into cells. *Journal of Virology* **62**, 1347-1354.
- Jones, F., and Grose, C. (1988): Role of cytoplasmic vacuoles in varicella-zoster virus glycoprotein trafficking and virion envelopment. *Journal of Virology* **62**, 2701-2711.
- Karger, A., and Mettenleiter, T. (1993): Glycoproteins gIII and gp50 play dominant roles in the biphasic attachment of pseudorabies virus. *Virology* **194**, 654-664.
- Kennard, J., Rixon, F. J., McDougall, I. M., Tatman, J. D., and Preston, V. G. (1995): The 25 amino acid residues at the carboxy terminus of the herpes simplex virus type 1 UL26.5 protein are required for the formation of the capsid shell around the scaffold. *Journal of General Virology* **76**, 1611-1621.
- King, J., and Casjens, S. (1974): Catalytic head assembling protein in virus morphogenesis. *Nature* **251**, 112-119.

- King, J., and Chiu, W. (1997): The procapsid-to-capsid transition in double-stranded DNA bacetriophage, pp. 288-311. In W. Chiu, R. Burnett, and R. Garcea (Eds): *Structural biology of viruses*, Oxford University Press, New York.
- Kirkitadze, M., Barlow, P., Price, N., Kelly, S., Boutell, C., Rixon, F., and McClelland, D. (1998): The herpes simplex virus triplex protein, VP23, exists as a molten globule. *Journal of Virology* **72**, 10066-10072.
- Knopf, K. (1979): Properties of Herpes simplex virus DNA polymerase and characterisation of its associated exonuclease activity. *European Journal of Biochemistry* **62**, 4096-4103.
- Koslowski, K., Shaver, P., Wang, X., Tenney, D., and Pederson, N. (1997): The pseudorabies virus UL28 protein enters the nucleus after coexpression with the herpes simplex virus UL15 protein. *Journal of Virology* **71**, 9118-9123.
- Kristensson, K., Lycke, E., Roytta, M., Svennerholm, B., and Vahlne, A. (1986): Neuritic transport of herpes simplex in rat sensory neurons in vitro. Effects of substances interacting with microtubular function and axonal flow (nocodazole, taxol and erythro-9-3-(2-hydroxynonyl)-adenine). *Journal of General Virology* **67**, 2023-2028.
- Kunkel, T. (1985): Rapid and efficient site-specific mutagenesis without phenotypic selection. *Proceedings of the National Academy of Sciences of the U.S.A* **82**, 488-492.
- Kwon, B., Tan, K., Ni, J., Oh, K., Lee, Z., Kim, K., and al, e. (1997): A newly identified member of the tumor necrosis factor receptor superfamily with a wide tissue distribution and involvement in lymphocyte activation. *Journal of Biological Chemistry* **272**, 14272-14276.
- Kwong, A., Kruper, J., and Frenkel, N. (1988): Herpes simplex virus virion host shut off function. *Journal of Virology* **62**, 912-921.
- Ladin, B., Ihara, S., Hampl, H., and Ben-Porat, T. (1982): Pathway of assembly of herpesvirus capsids: an analysis using DNA temperature sensitive mutants of Pseudorabies virus. *Virology* **116**, 554-561.
- Lee, W., and Fuller, A. (1993): Herpes simplex virus type 1 and pseudorabies virus bind to a common saturable receptor on vero cells that is not heparan sulphate. *Journal of Virology* **67**, 5088-5097.
- Lemaster, S., and Roizman, B. (1980): Herpes simplex virus phosphoproteins. II. Characterisation of the virion protein kinase and of the polypeptides phosphorylated in the virion. *Journal of Virology* **35**, 798-811.
- Lenk, E., Casjens, S., Weeks, J., and King, J. (1975): Intracellular visualisation of precursor capsids in phage P22 mutant infected cells. *Virology* **68**, 182-199.
- Leslie, J., Rixon, F. J., and McLauchlan, J. (1996): Overexpression of the herpes simplex virus type 1 tegument protein VP22 increases its incorporation into virus particles. *Virology* **220**, 60-68.
- Levine, A. (1992): *Viruses*. Scientific American Library. New York.
- Levy, J. (1997): Three new human herpesviruses (HHV6, 7, and 8). *Lancet* **349**, 558-563.

- Ligas, M., and Johnson, D. (1988): A herpes simplex virus mutant in which glycoprotein D sequences are replaced by B-galactosidase sequences binds to but is unable to penetrate into cells. *Journal of Virology* **62**, 1486-1494.
- Lillicrop, K., Estridge, J., and Latchman, D. (1993): The octamer binding protein Oct-2 inhibits transactivation of the herpes simplex virus immediate early genes by the virion protein Vmw65. *Virology* **196**, 888-891.
- Little, S., Jofre, J., Courtney, R., and Schaffer, P. (1981): A virion associated glycoprotein essential for infectivity of herpes simplex virus type I. *Virology* **115**, 149-160.
- Liu, F., and Roizman, B. (1991a): The promoter, transcriptional unit, and the coding sequences of herpes simplex virus 1 family 35 proteins are contained within the UL26 ORF. *Journal of Virology* **65**, 206-212.
- Liu, F., and Roizman, B. (1991b): The herpes simplex virus 1 gene encoding a protease also contains within its coding domain the gene encoding the more abundant substrate. *Journal of Virology* **65**, 5149-5156.
- Liu, F., and Roizman, B. (1992): Differentiation of multiple domains in the herpes simplex virus 1 protease encoded by the UL26 gene. *Proceedings of the National Academy of Sciences of the U.S.A.* **89**, 2076-2080.
- Livingston, C., and Jones, I. (1989): Baculovirus expression vectors with single strand capacity. *Nucleic Acids Research* **17**, 2366-2370.
- Longnecker, R., and Roizman, B. (1986): Generation of an inverting herpes simplex virus 1 mutant lacking the L-S junction a sequences, an origin of DNA synthesis and several genes including those specifying the glycoprotein E and the alpha 47 gene. *Journal of Virology* **58**, 583-591.
- Lycke, E., Hanmark, M., Johansson, M., Krotwil, A., Lycke, J., and Svennerholm, B. (1988): Herpes simplex infection of the human sensory neuron. An electron microscopic study. *Archives of Virology* **101**, 87-104.
- MacLean, C., Dolan, A., Jamieson, F., and McGeoch, D. (1992): The myristylated virion proteins of herpes simplex virus type 1: Investigation of their role in the virus life cycle. *Journal of General Virology* **73**, 539-547.
- MacPherson, I., and Stoker, M. (1962): Polyoma transformation of hamster cell clones: an investigation of genetic factors affecting cell competence. *Virology* **16**, 147-151.
- Maizel, J. V., White, D. O., and Scharff, M. D. (1968): The polypeptides of adenovirus. II. Soluble proteins, cores, top components and the structure of the virion. *Virology* **36**, 126-136.
- Maniatis, T., Fritsch, E., and Sambrooke, J. (1982): *Molecular cloning; A laboratory manual*. Cold Spring Harbour Laboratory. New York.
- Marsden, H., Campbell, M., Haar, L., Frame, M., Parris, D., Murphy, M., Hope, R., Muller, M., and Preston, C. (1987): The 65000-mr DNA-binding and virion trans-inducing proteins of herpes simplex virus type 1. *Journal of Virology* **61**, 2428-2437.

- Marsters, S., Ayres, T., Skubatch, M., Gray, C., Rothe, M., and Ashkenazi, A. (1997): Herpesvirus entry mediator, a member of the tumor necrosis factor receptor (TNFR) family, interacts with members of the TNRF-associated factor family and activates the transcription factors NF-KB and AP-1*. *Journal of Biological Chemistry* **272**, 14029-14032.
- Martinez, R., Sarisky, R. T., Weber, P. C., and Weller, S. K. (1996): Herpes simplex virus type 1 alkaline nuclease is required for efficient processing of viral DNA replication intermediates. *Journal of Virology* **70**, 2075-2085.
- Matsuura, Y., Possee, R., Overton, H., and Bishop, D. (1987): Baculovirus expression vectors: the requirements for high level expression of proteins, including glycoproteins. *Journal of General Virology* **68**, 1233-1250.
- Matthews, D., and Russell, W. (1995): Adenovirus protein-protein interactions: Molecular parameters governing the binding of protein VI to hexon and the activation of the adenovirus 23K protease. *Journal of General Virology* **76**, 1959-1969.
- Matusick-Kumar, L., Newcomb, W. W., Brown, J. C., McCann III, P. J., Hurlburt, W., Weinheimer, S. P., and Gao, M. (1995): The C-terminal 25 amino acids of the protease and its substrate ICP35 of herpes simplex virus type 1 are involved in the formation of sealed capsids. *Journal of Virology* **69**, 4347-4356.
- McGeoch, D. J., Dalrymple, M. A., Davison, A. J., Dolan, A., Frame, M. C., McNab, D., Perry, L. J., Scott, J. E., and Taylor, P. (1988): The complete DNA sequence of the long unique region in the genome of herpes simplex virus type 1. *Journal of General Virology* **69**, 1531-1574.
- McGeoch, D., Cook, S., Dolan, A., Jamieson, F., and Telford, E. (1995): Molecular phylogeny and evolutionary timescale for the family of mammalian herpesviruses. *Journal of Molecular Biology* **247**, 443-458.
- McLauchlan, J., Addison, C., Craigie, M. C., and Rixon, F. J. (1992a): Noninfectious L-particles supply functions which can facilitate infection by HSV-1. *Virology* **190**, 682-688.
- McLauchlan, J., and Rixon, F. J. (1992b): Characterization of enveloped tegument structures (L particles) produced by alphaherpesviruses: integrity of the tegument does not depend on the presence of capsid or envelope. *Journal of General Virology* **73**, 269-276.
- McLauchlan, J., Liefkins, K., and Stow, N. (1994): The herpes simplex virus type 1 UL37 gene product is a component of virus particles. *Journal of General Virology* **75**, 2047-2052.
- McLean, G., Abbotts, A., Parry, M., Marsden, H., and Stow, N. (1994): The herpes simplex virus type 1 origin binding protein interacts specifically with the viral UL8 protein. *Journal of General Virology* **75**, 2699-2706.
- McNab, D., and Courtney, R. (1992): Analysis of the UL36 open reading frame encoding the large tegument protein (ICP1/2) of herpes simplex virus type 1. *Journal of Virology* **66**, 7581-7584.
- McNab, A. R., Desai, P., Person, S., Roof, L. L., Thomsen, D. R., Newcomb, W. W., Brown, J. C., and Homa, F. L. (1998): The product of the herpes simplex virus type 1 UL25 gene is required for encapsidation but not for cleavage of replicated viral DNA. *Journal of Virology* **72**, 1060-1070.

- Mehta, A., Maggioncalda, J., Bagasra, O., Thikkavarapu, S., Saikumari, P., Valyinagy, T., Fraser, N., and Block, T. (1995): In situ DNA PCR and RNA hybridisation detection of herpes simplex sequences in trigeminal ganglia of latently infected mice. *Virology* **206**, 633-640.
- Mellerick, D., and Fraser, N. (1987): Physical state of the latent herpes simplex virus genome in a mouse model system: Evidence suggesting an episomal state. *Virology* **158**, 265-275.
- Meredith, M., Orr, A., Elliott, M., and Everett, R. (1995): Separation of sequence requirements for HSV-1 Vmw110 multimerisation and interaction with a 135kDa cellular protein. *Virology* **209**, 174-187.
- Merrifield, B. (1964): Solid phase peptide synthesis. *Biochemistry* **3**, 1385-1390.
- Merrifield, B. (1986): Solid phase peptide synthesis. *Science* **232**, 341-344.
- Miller, G. (1990): Epstein Barr virus: Biology, pathogenesis and medical aspects, pp. 1843-1887. In B. Fields, D. Knipe, and e. al (Eds): *Virology, 2nd edition*, Raven Press, New York.
- Mitchison, T. (1988): Microtubule dynamic and kinetochome function in mitosis. *Annual Reviews in Cell Biology* **4**, 527-549.
- Miyamoto, K., and Morgan, C. (1971): Structure and development of viruses as observed in the electron microscope. XI. Entry and uncoating of herpes simplex virus. *Journal of Virology* **8**, 910-918.
- Miyamoto, K. (1971): Mechanism of intranuclear crystal formation of herpes simplex virus as revealed by the negative staining of thin sections. *Journal of Virology* **8**, 534-550.
- Mocarski, E., and Roizman, B. (1981): Site-specific inversion sequence of the herpes simplex virus genome: domain and structural features. *Proceedings of the National Academy of Sciences of the U.S.A.* **78**, 7047-7051.
- Mocarski, E., and Roizman, B. (1982): Structure and role of herpes simplex virus DNA termini in inversion, circularisation and generation of virion DNA. *Cell* **31**, 89-97.
- Monini, P., de Lellis, L., Fabris, M., Rigolin, F., and Cassai, E. (1996): Kaposi's sarcoma-associated herpesvirus-like DNA sequences in prostate tissue and human serum. *New England Journal of Medicine* **334**, 1168-1172.
- Monoto, A. (1992): Acute respiratory infections, pp. 125-131. In J. Last, and R. Wallace (Eds): *Maxcy-Rosenau-Last Public Health and Preventative Medicine*, Appleton & Lange, Nowalk.
- Montgomery, R., Warner, M., Lum, B., and Spear, P. (1996): Herpes virus 1 entry into cells mediated by a novel member of the TNF/NGF receptor family. *Cell* **87**, 427-436.
- Morgan, C., Ellison, S., Rose, H., and Moore, D. (1954): Structure and denvelopment of viruses as observed in the electron microscope. I. Herpes simplex virus. *Journal of Experimental Medicine* **100**, 195-202.

- Morgan, C., Rose, H., Holden, M., and Jones, E. (1959): Electron microscopic observations on the development of herpes simplex virus. *Journal of Experimental Medicine* **110**, 643-656.
- Morgan, C., Rose, H., and Mednis, B. (1968): Electron microscopy of herpes simplex virus type 1 entry. *Journal of Virology* **2**, 507-516.
- Nahmais, A., and Dowdle, W. (1968): Antigenic and biological differences in herpesvirus hominis. *Programs in Medical Virology* **10**, 110-115.
- Newcomb, W. W., Brown, J. C., Booy, F. P., and Steven, A. C. (1989): Nucleocapsid mass and capsomer protein stoichiometry in equine herpesvirus 1: scanning transmission electron microscopic study. *Journal of Virology* **63**, 3777-3783.
- Newcomb, W. W., and Brown, J. C. (1991): Structure of the herpes simplex virus capsid: effects of extraction with guanidine hydrochloride and partial reconstitution of extracted capsids. *Journal of Virology* **65**, 613-620.
- Newcomb, W. W., Trus, B. L., Booy, F. P., Steven, A. C., Wall, J. S., and Brown, J. C. (1993): Structure of the herpes simplex virus capsid: molecular composition of the pentons and the triplexes. *Journal of Molecular Biology* **232**, 499-511.
- Newcomb, W. W., Homa, F. L., Thomsen, D. R., Ye, Z., and Brown, J. C. (1994): Cell-free assembly of the herpes simplex virus capsid. *Journal of Virology* **68**, 6059-6063.
- Newcomb, W. W., and Brown, J. C. (1994): Induced extrusion of DNA from the capsid of herpes simplex virus type-1. *Journal of Virology* **68**, 433-440.
- Newcomb, W. W., Homa, F. L., Thomsen, D. R., Booy, F. P., Trus, B. L., Steven, A. C., Spencer, J. V., and Brown, J. C. (1996): Assembly of the herpes simplex virus capsid: characterization of intermediates observed during cell-free capsid formation. *Journal of Molecular Biology* **263**, 432-446.
- Newcomb, W., Homa, F., Thomsen, D., Trus, B., Cheng, N., Steven, A., Booy, F., and Brown, J. (1999): Assembly of the herpes simplex virus procapsid from purified components and identification of small complexes containing the major capsid and scaffolding proteins. *Journal of Virology* **73**, 4239-4250.
- Nicholson, P., Addison, C., Cross, A. M., Kennard, J., Preston, V. G., and Rixon, F. J. (1994): Localization of the herpes simplex virus type 1 major capsid protein VP5 to the cell nucleus requires the abundant scaffolding protein VP22a. *Journal of General Virology* **75**, 1091-1099.
- Nii, S., Morgan, C., and Rose, H. M. (1968a): Electron microscopy of herpes simplex virus. II. Sequence development. *Journal of Virology* **2**, 517-536.
- Nii, S., Morgan, C., and Hsu, K. (1968b): Electron microscopy of herpes simplex virus. IV. Studies with ferritin conjugated antibodies. *Journal of Virology* **2**, 1172-1184.
- Nishioka, Y., and Silverstein, S. (1978): Alterations in the protein synthetic apparatus of friend erythroleukimia cells infected with vesicular stomatitis virus or herpes simplex virus. *Journal of Virology* **25**, 422-426.
- O'Donnell, M., Elias, P., and Lehman, I. (1987): Processive replication of single stranded DNA templates by the herpes virus-induced DNA polymerase. *Journal of Biological Chemistry* **262**, 4252-4259.

- O'Hare, P., and Hayward, G. (1985): Evidence for a direct role for both the 175000- and 110000- molecular weight immediate early proteins of herpes simplex virus in the transactivation of delayed early promoters. *Journal of Virology* **53**, 751-760.
- Oien, N., Thomsen, D., Wathen, N., Newcomb, W., Brown, J., and Homa, F. (1997): Assembly of herpes simplex virus capsids using the human cytomegalovirus scaffold protein: critical role of the C terminus. *Journal of Virology* **71**, 1281-1291.
- Olivio, P., Nelson, N., and Challberg, M. (1988): Herpes simplex virus DNA replication: The UL9 gene encodes an origin binding protein. *Proceedings of the National Academy of Sciences of the U.S.A.* **85**, 5414-5418.
- Onorato, L., and Showe, M. (1975): Gene gp21 protein-dependent proteolysis in vivo of purified gene gp22 product of bacteriophage T4. *Journal of Molecular Biology* **92**, 395-412.
- Palmer, E., Martin, M., and Gary, G. (1975): The ultrastructure of disrupted herpesvirus nucleocapsids. *Virology* **65**, 260-265.
- Patel, A., and MacLean, J. (1995): The product of the UL6 gene of herpes simplex virus type 1 is associated with virus capsids. *Virology* **206**, 465-478.
- Patel, A. H., Rixon, F. J., Cunningham, C., and Davison, A. J. (1996): Isolation and characterization of herpes simplex virus type 1 mutants defective in the UL6 gene. *Virology* **217**, 111-123.
- Pelletier, A., Do, J., Brisebois, L., Lagace, L., and Cordingley, M. (1997): Self-association of herpes simplex virus type 1 ICP35 is via coiled-coil interactions and promotes stable interaction with the major capsid protein. *Journal of Virology* **71**, 5197-5208.
- Penfold, M., Armati, P., and Cunningham, A. (1994): Axonal transport of herpes simplex virions to epidermal cells: evidence for a specialised mode of virus transport and assembly. *Proceedings of the National Academy of Sciences of the U.S.A.* **91**, 6529-6533.
- Perdue, M., Cohen, J., Kemp, M., Randall, C., and O'Callaghan, D. (1975): Characterisation of three species of nucleocapsid of equine herpesvirus type 1 (EHV-1). *Virology* **64**, 187-204.
- Perdue, M., Cohen, J., Randall, C., and O'Callaghan, D. (1976): Biochemical studies on the maturation of herpesvirus nucleocapsid species. *Virology* **74**, 194-208.
- Person, S., and Desai, P. (1998): Capsids are formed in a mutant virus blocked at the maturation site of the UL26 and UL26.5 open reading frames of herpes simplex virus type 1 but are not formed in a null mutant of UL38 (VP19C). *Virology* **242**, 193-203.
- Pertuiset, B., Boccara, M., Cebrain, J., Berthelot, N., Chousterman, S., Puvion-Dutilleul, F., Sisman, J., and Sheldrick, P. (1989): Physical mapping and nucleotide sequence of a herpes simplex virus type 1 gene required for capsid assembly. *Journal of Virology*, 2169-2179.
- Poffenberger, K., and Roizman, B. (1985): A non-reverting genome of a viable herpes simplex virus 1: Presence of head-to-tail linkages in packaged genomes and requirements for circularisation after infection. *Journal of Virology* **53**, 587-595.

- Poffenberger, K., Idowu, A., Frasersmith, E., Raichlen, P., and Herman, R. (1994): A herpes simplex virus type 1 ICP22 deletion mutant is altered for virulence and latency in vivo. *Archives of Virology* **139**, 111-119.
- Pokinghorne, I., and Roy, P. (1995): Transient expression in insect cells using a recombinant baculovirus synthesising bacteriophage T7 RNA polymerase. *Nucleic Acids Research* **23**, 188-191.
- Polvino-Bodnar, M., Orberg, P., and Schaffer, P. (1987): Herpes simplex virus type 1 oriL is not required for virus replication or for establishment and reactivation of latent infection in mice. *Journal of Virology* **61**, 3582-3535.
- Poon, A., and Roizman, B. (1993): Characterisation of a temperature sensitive mutant of the UL15 ORF of herpes simplex virus 1. *Journal of Virology* **67**, 4497-4503.
- Post, L., Mackem, S., and Roizman, B. (1981): Regulation of alpha genes of herpes simplex virus: Expression of chimeric genes produced by fusion of thymidine kinase with alpha gene promoters. *Cell* **24**, 555-565.
- Powell, K., and Watson, D. (1975): Some structural antigens of herpes simplex type 1. *Journal of General Virology* **29**, 167-178.
- Powell, K., and Purifoy, D. (1977): Nonstructural proteins of herpes simplex virus. I. Purification of the induced DNA polymerase. *Journal of Virology* **24**, 618-626.
- Prasad, B. V. V., Prevelige, P. E., Marietta, E., Chen, R. O., Thomas, D., King, J., and Chiu, W. (1993): Three-dimensional transformation of capsids associated with genome packaging in a bacterial virus. *J. Mol. Biol.* **231**, 65-74.
- Preston, C. (1979): Abnormal properties of an immediate early polypeptide in cells infected with the herpes simplex virus type 1 mutant tsK. *Journal of Virology* **32**, 357-369.
- Preston, V. G., Coates, J. A. V., and Rixon, F. J. (1983): Identification and characterization of a herpes simplex virus gene product required for encapsidation of virus DNA. *Journal of Virology* **45**, 1056-1064.
- Preston, C., Frame, M., and Campbell, M. (1988): A complex formed between cell components and an HSV-1 structural polypeptide binds to a viral immediate early regulatory DNA sequence. *Cell* **52**, 425-434.
- Preston, V. G., Rixon, F. J., McDougall, I. M., McGregor, M., and Al-Kobaisi, M. F. (1992): Processing of the herpes simplex virus assembly protein ICP35 near its carboxy terminal end requires the product of the whole of the UL26 reading frame. *Virology* **186**, 87-98.
- Preston, V. G., Al-Kobaisi, M. F., McDougall, I. M., and Rixon, F. J. (1994): The herpes simplex virus gene UL26 proteinase in the presence of the UL26.5 gene product promotes the formation of scaffold-like structures. *Journal of General Virology* **75**, 2355-2366.
- Prevelige, P., and King, J. (1993): Assembly of bacteriophage P22: A model for ds DNA virus assembly. *Programmes of Medical Virology* **40**, 206-221.

- Purves, F., and Roizman, B. (1992): The UL13 gene of herpes simplex virus encodes the functions for post-translational processing associated with phosphorylation of the regulatory protein alpha-22. *Proceedings of the National Academy of Sciences of the U.S.A.* **89**, 7310-7314.
- Puvion-Dutilleul, F., Pichard, E., Laither, M., and Leduc, E. (1987): Effect of hydrating agents on DNA organisation in herpes viruses. *Journal of Histochemistry & Cytochemistry* **35**, 635-645.
- Quinlan, M., Chen, L., and Knipe, D. (1984): The intranuclear location of a herpes simplex virus DNA-binding protein is determined by the status of viral DNA replication. *Cell* **36**, 857-868.
- Quinlan, M., and Knipe, D. (1985): Stimulation of expression of a herpes simplex DNA binding protein by two viral functions. *Molecular and Cellular Biology* **5**, 957-963.
- Quinn, J., and McGeoch, D. (1985): DNA sequence of the region in the genome of herpes simplex virus type 1 containing genes for DNA polymerase and the major DNA binding protein. *Nucleic Acids Research* **13**, 8143-8163.
- Ray, P., and Murialdo, H. (1975): The role of gene Nu3 in bacteriophage lambda head morphogenesis. *Virology* **64**, 247-263.
- Rice, S., and Knipe, D. (1993): Genetic evidence of two distinct transactivation functions of herpes simplex virus alpha protein ICP27. *Journal of Virology* **64**, 1704-1715.
- Rice, S., Long, M., Lam, V., Schaffer, P., and Spencer, C. (1995): Herpes simplex virus immune protein ICP22 is required for viral modification of host mRNA polymerase II and establishment of the normal transcription program. *Journal of Virology* **69**, 5550-5559.
- Rixon, F. J., Atkinson, M. A., and Hay, J. (1983): Intranuclear distribution of herpes simplex virus type-2 DNA synthesis: examination by light and electron microscopy. *Journal of General Virology* **64**, 2087-2092.
- Rixon, F. J., Cross, A. M., Addison, C., and Preston, V. G. (1988): The products of herpes simplex virus type-1 gene UL26 which are involved in DNA packaging are strongly associated with empty but not with full capsids. *Journal of General Virology* **69**, 2879-2891.
- Rixon, F. J., Davison, M. D., and Davison, A. J. (1990): Identification of the genes encoding two capsid proteins of herpes simplex virus type 1 by direct amino acid sequencing. *Journal of General Virology* **71**, 1211-1214.
- Rixon, F. J., Addison, C., and McLauchlan, J. (1992): Assembly of enveloped tegument structures (L particles) can occur independently of virion maturation in herpes simplex virus type 1-infected cells. *Journal of General Virology* **73**, 277-284.
- Rixon, F. J. (1993): Structure and assembly of herpesviruses. *Seminars in Virology* **4**, 135-144.
- Rixon, F. J., Addison, C., McGregor, A., Macnab, S. J., Nicholson, P., Preston, V. G., and Tatman, J. D. (1996): Multiple interactions control the intracellular localization of the herpes simplex virus type 1 capsid proteins. *Journal of General Virology* **77**, 2251-2260.

- Rixon, F., and McNab, D. (1999): Packaging-competent capsids of a herpes simplex virus temperature sensitive mutant have properties similar to those of in vitro assembled procapsids. *Journal of Virology* **73**, 5714-5721.
- Roberts, M., White, J., Grutter, M., and Burnett, R. (1986): Three dimensional structure of the adenovirus major coat protein. *Science* **232**, 1148-1151.
- Roffman, E., Albert, J., Goff, J., and Frenkel, N. (1990): Putative site for the acquisition of human herpesvirus 6 virion tegument. *Journal of Virology* **64**, 6308-6313.
- Roizman, B. (1969): The herpesvirus- A biochemical definition of the group, pp. 1-79. In W. e. a. Arber (Ed.): *Current Topics in Microbiology and Immunology*, Springer Verlag, Berlin.
- Roizman, B., and Furlong, D. (1974): The replication of herpesviruses, pp. 229-403. In H. Fraenkel-Conrat, and R. Wagner (Eds): *Comprehensive Virology*, Plenum Press, New York.
- Roizman, B. (1979): The structure and isomerisation of herpes simplex virus genomes. *Cell* **16**, 481-494.
- Roizman, B., Carmicheal, L., Deinhardt, F., Nahmais, A., Plowright, W., Rapp, F., Sheldrick, P., Takahashi, M., and Wolf, K. (1981): Herpesviridae: Definition, provisional nomenclature and taxonomy. *Intervirology* **16**, 201-217.
- Roizman, B., and Sears, A. (1990): Herpes simplex viruses and their replication, pp. 1795-1841. In B. Fields, and D. Knipe (Eds): *Virology*, Raven Press Ltd, New York.
- Roizman, B., Desrosier, R., Fleckenstein, B., Lopez, C., Minson, A., and Studdert, M. (1992): The family herpesviridae: An update. *Archives of Virology* **123**, 425-449.
- Roizman, B. (1996): The function of herpes simplex virus genes- A primer for genetic engineering of novel vectors. *Proceedings of the National Academy of Sciences of the U.S.A.* **93**, 11307-11312.
- Roizman, B., and Sears, A. (1996): Herpes simplex viruses and their replication, pp. 2231-2295. In B. Fields, D. Knipe, P. Howley, and e. al (Eds): *Fields Virology*, Raven publishers, Philadelphia.
- Rose, J., Buoncore, L., and Whitt, M. (1991): A new cationic liposome reagent mediating nearly quantitative transfection of animal cells. *Biotechniques* **10**, 520-525.
- Rost, B., and Sander, C. (1994): Combining evolutionary information and neural networks to predict protein secondary structure. *Proteins-Structure Function and Genetics* **19**, 55-72.
- Ruigrok, R. W. H., Barge, A., Albiges-Rizo, C., and Dayan, S. (1990): Structure of the adenovirus fibre II. Morphology of single fibres. *J. Mol. Biol.* **215**, 589-596.
- Saad, A., Zhou, Z., Jakana, J., Chui, W., and Rixon, F. (1999): Roles of the triplex and scaffolding proteins in HSV-1 capsid formation suggested by the structures of recombinant particles. *awaiting publication*.
- Salahuddin, S., Ablashi, D., Markham, P., Josephs, S., Sturzenegger, S., Kaplan, M., Halligan, G., Biberfeld, P., Wongstaal, F., Kramarsky, B., and Gallo, R. (1986): Isolation of a new virus, HBLV, in patients with lymphoproliferative disorders. *Science* **234**, 596-601.

- Salmon, B., and Baines, J. (1988): Herpes simplex virus DNA cleavage and packaging: Association of multiple forms of UL15 encoded proteins with B capsids requires at least the UL6, UL17 and UL28 genes. *Journal of Virology* **72**, 3045-3050.
- Salmon, B., Cunningham, C., Davison, A. J., Harris, W. J., and Baines, J. D. (1998): The herpes simplex virus type 1 U_L17 gene encodes virion tegument proteins that are required for cleavage and packaging of viral DNA. *Journal of Virology* **72**, 3779-3788.
- Sarimento, M., Haffey, M., and Spear, P. (1979): Membrane proteins specified by herpes simplex viruses. III. Role of glycoprotein VP7 (B2) in virion infectivity. *Journal of Virology* **29**, 1149-1158.
- Sawtell, N., Poon, D., Tansky, C., and Thompson, R. (1998): The latent herpes simplex virus type 1 genome copy number in individual neurons is virus specific and correlates with reactivation. *Journal of Virology* **72**, 5343-5350.
- Schirmer, E., Wyatt, L., Yamanishi, K., Rodriguez, W., and Frenkel, N. (1991): Differentiation between two distinct classes of virus now classified as human herpesvirus 6. *Proceedings of the National Academy of Sciences of the U.S.A.* **88**, 5922-5926.
- Schrag, J. D., Prasad, B. V. V., Rixon, F. J., and Chiu, W. (1989): Three-dimensional structure of the HSV-1 nucleocapsid. *Cell* **56**, 651-660.
- Schroder, C., Stegmann, B., Lauppe, H., and Kaerner, H. (1975): An unusual defective genotype derived from herpes simplex virus strain AGN. *Intervirology* **6**, 270-284.
- Sevanni, A., Morgan, A., Tovell, D., and Tyrrell, D. (1994): Study of the structure of replicative intermediates of HSV-1 DNA by pulse-field gel electrophoresis. *Virology* **200**, 248-435.
- Severi, B., Landini, M., and Govoni, E. (1988): Human cytomegalovirus morphogenesis: An ultrastructural study of the late cytoplasmic phases. *Archives of Virology* **98**, 51-64.
- Sheldrick, P., and Berthelot, N. (1974): Inverted repetitions in the chromosome of herpes simplex virus. *Cold Spring Harbour Symposium on Quantitative Biology* **9**, 667-678.
- Shenk, T. (1996): Adenoviridae and their replication, pp. 2111-2148. In B. Fields, P. Howley, and D. Knipe (Eds): *Virology*, Raven Press, New York.
- Shieh, H., Kurumbail, R., Stevens, A., Stegeman, R., Sturman, E., Pak, J., Wittwer, A., Palmier, M., Wiegand, R., Holwerda, B., and Stallings, W. (1996): Three-dimensional structure of human cytomegalovirus protease. *Nature* **384**, 288.
- Smibert, C., Popova, B., Xiao, P., Capone, J., and Smiley, J. (1994): Herpes simplex virus VP16 forms a complex with the virion host shut off protein vhs. *Journal of Virology* **68**, 2339-2346.
- Smith, C., Marchetti, M., Edmonson, P., and Schaffer, P. (1989): Herpes simplex virus type 2 mutants with deletions in the intergenic region between ICP4 and ICP22/47: Identification of nonessential cis-acting elements in the context of the viral genome. *Journal of Virology* **63**, 2036-2047.
- Sodeik, B., Ebersold, M., and Helenius, A. (1997): Microtubule mediated transport of incoming herpes simplex virus capsids to the nucleus. *Journal of Cell Biology* **136**, 1007-1021.

- Spear, P., and Roizman, B. (1972): Proteins specified by herpes simplex virus. V. Purification and structural proteins of the herpes virion. *Journal of Virology* **9**, 143-159.
- Spear, P. (1976): Membrane proteins specified by herpes simplex virus I. Identification of four glycoprotein precursors and their products in type 1 infected cells. *Journal of Virology* **17**, 991-1008.
- Spear, P. (1993): Entry of alphaherpesviruses into cells. *Seminars in Virology* **9**, 143-159.
- Spencer, J. V., Newcomb, W. W., Thomsen, D. R., Homa, F. L., and Brown, J. C. (1998): Assembly of the herpes simplex virus capsid: preformed triplexes bind to the nascent capsid. *Journal of Virology* **72**, 3944-3951.
- Spivack, J., and Fraser, N. (1988): Expression of herpes simplex type 1 (HSV-1) latency associated transcripts and transcripts affected by deletion in mutant HFEM: Evidence for a new class of genes. *Journal of Virology* **62**, 3281-3287.
- Stackpole, C. (1969): Herpes type virus of the frog renal adenocarcinoma. I. Virus development in tumor transplants maintained at low temperatures. *Journal of Virology* **4**, 75-93.
- Stannard, L. M., Fuller, A. O., and Spear, P. G. (1987): Herpes simplex virus glycoproteins associated with different morphological entities projecting from the virion envelope. *Journal of General Virology* **68**, 715-725.
- Steiner, I., Spivack, J., O'Boyle, D., Lavi, E., and Fraser, N. (1988): Latent herpesvirus type 1 transcription in the human trigeminal ganglia. *Journal of Virology* **62**, 493-496.
- Steiner, I., Spivack, J., Deshmane, S., Ace, C., Preston, C., and Fraser, N. (1990): A herpes simplex virus type 1 mutant containing a non-transducing Vmw65 protein establishes latent infection in vivo in the absence of viral replication and reactivates efficiently when expanded in trigeminal ganglia. *Journal of Virology* **64**, 1630-1634.
- Steiner, I., and Kennedy, P. (1995): Herpes simplex virus latent infection in the nervous system. *Journal of NeuroVirology* **1**, 19-29.
- Steven, A., Roberts, C., Hay, J., Bisher, M., Pun, T., and Trus, B. (1986): Hexavalent capsomeres of herpes simplex type 2: symmetry, shape, dimensions and oligomeric status. *Journal of Virology* **57**, 578-584.
- Steven, A. C., Bauer, A. C., Bisher, M. E., Robey, F. A., and Black, L. W. (1991): The maturation-dependent conformational change of phage T4 capsid involves the translocation of specific epitopes between the inner and the outer capsid surfaces. *J Struct Biol* **106**, 221-36.
- Steven, A. C., Greenstone, H. L., Booy, F. P., Black, L. W., and Ross, P. D. (1992): Conformational changes of a viral capsid protein. Thermodynamic rationale for proteolytic regulation of bacteriophage T4 capsid expansion, co-operativity, and super-stabilization by soc binding. *J Mol Biol* **228**, 870-84.
- Steven, A. C. (1993): Conformational change: an alternative energy source? Exothermic phase transition in phage capsid maturation. *Biophys J* **65**, 5-6.

- Stevenly, W. (1975): Virus induced proteins in pseudo-rabies infected cells. II. Proteins of the virions and nucleocapsid. *Journal of Virology* **16**, 944-950.
- Stevens, J., Wagner, E., Devi, R., GB, Cook, M., and Feldman, L. (1987): RNA complementary to a herpesvirus alpha gene mRNA is prominent in latently infected neurons. *Science* **235**, 1056-1059.
- Stevens, J., Haarr, L., Porter, D., Cook, M., and Wagner, E. (1988): Prominence of the herpes simplex virus latency associated transcript in trigeminal ganglia of seropositive humans. *Journal of Infectious Disease* **158**, 17-22.
- Stewart, P. L., Fuller, S. D., and Burnett, R. M. (1993): Difference imaging of adenovirus: Bridging the resolution gap between X-ray crystallography and electron microscopy. *EMBO J.* **12**, 2589-2599.
- Stow, N. (1982): Localisation of an origin of DNA replication within the TRS/IRS repeated region of the herpes simplex virus type 1 genome. *EMBO J.* **1**, 863-867.
- Stow, N., and McMonagle, E. (1983): Characterisation of the TRS/IRS origin of DNA replication of herpes simplex virus type 1. *Virology* **130**, 427-438.
- Stow, N., Hammarstein, O., Arbuckle, M., and Elias, P. (1993): Inhibition of herpes simplex virus type 1 DNA replication by mutant forms of the origin binding protein. *Virology* **196**, 413-418.
- Subak-Sharpe, J., and Dargan, D. (1998): HSV molecular biology: General aspects of herpes simplex virus molecular biology. *Virus Genes* **16**, 239-251.
- Swanstrom, R., and Wagner, E. (1974): Regulation of synthesis of herpes simplex type 1 virus mRNA during productive infection. *Virology* **60**, 522-533.
- Sydiskis, R., and Roizman, B. (1967): The disaggregation of host polyribosomes in productive and abortive infection with herpes simplex virus. *Virology* **32**, 678-686.
- Szilagyi, J. F., and Cunningham, C. (1991): Identification and characterization of a novel non-infectious herpes simplex virus-related particle. *Journal of General Virology* **72**, 661-668.
- Tatman, J. D., Preston, V. G., Nicholson, P., Elliott, R. M., and Rixon, F. J. (1994): Assembly of herpes simplex virus type 1 capsids using a panel of recombinant baculoviruses. *Journal of General Virology* **75**, 1101-1113.
- Tatman, J. (1996): An investigation into the structure and assembly of the herpes simplex virus type 1 (HSV-1) capsid using the baculovirus expression system: *MRC Institute of Virology*, University of Glasgow, Glasgow.
- Terry-Allison, T., Montgomery, R., Whitbeck, J., Xu, R., Cohen, G., Eisenberg, R., and Spear, P. (1998): HVEM, a co-receptor for herpes simplex virus entry, also participates in virus induced cell fusion. *Journal of Virology*.
- Teschke, C. M., and King, J. (1993): Folding of the phage P22 coat protein in vitro. *Biochemistry* **32**, 10839-47.

- Thomsen, D. R., Roof, L. L., and Homa, F. L. (1994): Assembly of herpes simplex virus (HSV) intermediate capsids in insect cells infected with recombinant baculoviruses expressing HSV capsid proteins. *Journal of Virology* **68**, 2442-2457.
- Thuman-Commike, P., Greene, B., Jakana, J., Prasad, B., King, J., Prevelige, P., and Chiu, W. (1996): Three-dimensional structure of scaffolding-containing phage P22 procapsids by electron cryo-microscopy. *Journal of Molecular Biology* **260**, 85-98.
- ThumanCommike, P., Greene, B., Malinski, J., Burbea, M., McGough, A., Chiu, W., and Prevelige, P. (1999): Mechanism of scaffolding-directed virus assembly suggested by comparison of scaffolding-containing and scaffolding-lacking P22 procapsids. *Biophysical Journal* **76**, 3267-3277.
- Tong, L., Qian, C., Massariol, M., Bonneau, P., Cordingley, M., and Lagace, L. (1996): A new serine-protease fold revealed by the crystal structure of human cytomegalovirus protease. *Nature* **383**, 272-275.
- Trousdale, M., Steiner, I., Spivack, J., Deshman, S., Brown, S., MacLean, A., Subak-Sharpe, J., and Fraser, N. (1991): In vivo and in vitro reactivation impairment of herpes simplex virus type 1 latency associated variant in a rabbit eye model. *Journal of Virology*, 6989-6993.
- Trus, B. L., Newcomb, W. W., Booy, F. P., Brown, J. C., and Steven, A. C. (1992): Distinct monoclonal antibodies separately label the hexons or the pentons of herpes simplex virus capsid. *Proceedings of the National Academy of Sciences of the U.S.A.* **89**, 11508-11512.
- Trus, B., Homa, F., Booy, F., Newcomb, W., Thomsen, D., Cheng, N., Brown, J., and Steven, A. (1995): Herpes simplex virus capsids assembled in insect cells infected with recombinant baculoviruses: Structural authenticity and localisation of VP26. *Journal of Virology* **69**, 7362-7366.
- Trus, B. L., Booy, F. P., Newcomb, W. W., Brown, J. C., Homa, F. L., Thomsen, D. R., and Steven, A. C. (1996): The herpes simplex virus procapsid: structure, conformational changes upon maturation, and roles of the triplex proteins VP19c and VP23 in assembly. *Journal of Molecular Biology* **263**, 447-462.
- Van Genderan, I., Brandimarti, R., Torrisi, M., Campadelli, G., and Van Meer, G. (1994): The phospholipid composition of extracellular herpes virions differs from that of host cell nuclei. *Virology* **200**, 831-836.
- Van Grunsven, W., Van Heerde, E., De Haard, H., Spaan, W., and Middeldorp, J. (1993): Gene mapping and expression of 2 immunodominant Epstein-Barr virus capsid proteins. *Journal of Virology* **67**, 3908-3916.
- Van Oostrum, J., and Burnett, R. (1985): Molecular composition of the adenovirus type 2 virion. *Journal of Virology* **56**, 439-448.
- Varmuza, S., and Smiley, J. (1985): Signals for site specific cleavage of HSV DNA: Maturation involves two specific cleavage events at sites distal to the recognition sequences. *Cell* **41**, 793-802.
- Vaughn, J., Goodwin, R., Tompkins, G., and McCawley, P. (1977): The establishment of 2 cell lines from the insect *Spodoptera fugiperda* (Lepidoptera: Nucleotidae) in vitro. *Virology* **16**, 147-151.

- Vaughn, P., Banks, L., Purifoy, D., and Powell, K. (1984): Interactions between herpes simplex virus DNA binding proteins. *Journal of General Virology* **65**, 2033-2041.
- Vernon, S., Lawrence, W., and Cohen, G. (1974): Morphological components of herpesvirus 1. Intercapsomeric fibrils and the geometry of the capsid. *Intervirology* **4**, 237-248.
- Vernon, S., Lawrence, W., Long, C., Cohen, G., and Rubin, B. (1978): Herpesvirus vaccine development: studies of virus morphological components. In A. Voller, and H. Friedman (Eds): *New trends and developments in vaccines*, MTP Press, Lancaster.
- Vernon, S., Ponce de Leon, M., and Cohen, G. (1981): Morphological components of herpesvirus. III. Localisation of herpes simplex virus type 1 nucleocapsid polypeptides by immune electron microscopy. *Journal of General Virology* **54**, 39-46.
- Vlazny, D., Kwong, A., and Frenkel, N. (1982): Site-specific cleavage and packaging of herpes simplex virus DNA and the selective maturation of nucleocapsids containing full-length viral DNA. *Proceedings of the National Academy of Sciences of the U.S.A.* **79**, 1423-1427.
- Wadsworth, S., Hayward, G., and Roizman, B. (1976): Anatomy of herpes simplex virus DNA. V. Terminally repetitive sequences. *Journal of Virology* **17**, 503-512.
- Wagner, E., and Roizman, B. (1969): Ribonucleic acid synthesis in cells infected with herpes simplex. *Journal of Virology* **4**, 36-46.
- Warner, M., Geraghty, R., Martinez, W., Montgomery, R., Whitbeck, J., XU, R., Eisenberg, R., Cohen, G., and Spear, P. (1998): A cell surface protein with herpesvirus entry activity (HveB) confers susceptibility to infection by mutants of herpes simplex virus type 1, herpes simplex virus type 2 and pseudorabies virus. *Virology* **246**, 179-189.
- Weber, J. (1976): Genetic analysis of adenovirus type 2. III. Temperature sensitivity of processing of viral proteins. *Journal of Virology* **17**, 462-471.
- Weinheimer, S., Boyd, B., Durham, S., Resnick, J., and O'Boyle, D. (1992): Deletion of the VP16 open reading frame of herpes simplex virus type 1. *Journal of Virology* **66**, 258-269.
- Weinheimer, S., McCann, P., III, O'Boyle, D., II, Stevens, J., Boyd, B., Drier, D., Yamanaka, G., Dilanni, C., Deckman, I., and Cordingley, M. (1993): Autoproteolysis of herpes simplex virus type 1 protease releases an active catalytic domain found in intermediate capsid particles. *Journal of Virology* **67**, 5813-5822.
- Weller, S., Spadaro, A., Scaffer, J., Murray, A., Maxam, A., and Scaffer, P. (1985): Cloning, sequencing, and functional analysis of ori L, a herpes simplex type 1 origin of DNA synthesis. *Molecular and Cellular Biology* **5**, 930-942.
- Weller, S., Carmicheal, E., Aschmann, D., Goldstein, D., and Schaffer, P. (1987): Genetic and phenotypic characterisation of mutants in four essential genes that map to the left half of HSV-1 UL DNA. *Virology* **161**, 198-210.
- Weller, S. (1991): Genetic analysis of HSV genes required for genome replication, pp. 105-135. In E. Wagner (Ed.): *Herpesvirus transcription and its regulation*, CRC Press, Boca Raton.
- Weller, S. (1995): Herpes simplex virus DNA replication and genome maturation, pp. 189-213. In G. Cooper, R. Temin, and B. Sugden (Eds): *The DNA Provirus- Howard Temin's Scientific Legacy*, American Society for Microbiology, Washington DC.

- Whealy, M., Card, J., Meade, R., Robbins, A., and Enquist, L. (1991): Effect of brefeldin A on alphaherpesvirus membrane protein glycosylation and virus egress. *Journal of Virology* **65**, 1066-1081.
- Whitley, R., and Schlitt, M. (1991): Encephalitis caused by herpesviruses, including B virus, pp. 41-69. In W. Scheld, R. Whitley, and D. Durack (Eds): *Infections of the central nervous system*, Raven Press, New York.
- Wildy, P., Russell, W., and Horne, R. (1960): The morphology of herpesvirus. *Virology* **12**, 201-222.
- Wildy, P. (1973): Herpes: History and classification. In A. Kaplan (Ed.): *The herpesvirus*, Academic Press, New York.
- Wilkie, N. (1973): The synthesis and sub-structure of herpesvirus DNA: The disruption of alkali labile single strand interruptions in HSV-1 DNA. *Journal of Virology* **20**, 222-233.
- Wilkie, N. (1976): Physical maps for herpes simplex virus type 1 DNA for restriction endonuclease HindIII, Hpa-1 and Xba. *Journal of Virology* **20**, 222-233.
- Wingfield, P. T., Stahl, S. J., Thomsen, D. R., Homa, F. L., Booy, F. P., Trus, B. L., and Steven, A. C. (1997): Hexon-only binding of VP26 reflects differences between the hexon and penton conformations of VP5, the major capsid protein of herpes simplex virus. *Journal of Virology* **71**, 8955-8961.
- Wolf, K., and Darlington, R. (1971): Channel catfish virus: A new herpesvirus of ictalurid fish. *Journal of Virology* **8**, 525-533.
- Wu, C., Nelson, N., McGeoch, D., and Challberg, M. (1988): Identification of herpes simplex virus type 1 genes required for origin dependent DNA synthesis. *Journal of Virology* **62**, 435-443.
- WuDunn, D., and Spear, P. (1989): Initial interaction of herpes simplex virus with cells is binding to heparin sulphate. *Journal of Virology* **63**, 52-58.
- Yei, S., Chowdhury, S., Bhat, B., Conley, A., Wold, W., and Batterson, W. (1990): Identification and characterisation of the herpes simplex virus type-2 gene encoding the essential capsid proteins ICP32/VP19c. *Journal of Virology* **199**, 1124-1134.
- Yu, D., Sheaffer, A. K., Tenney, D. J., and Weller, S. K. (1997): Characterization of ICP6:lacZ insertion mutants of the UL15 gene of herpes simplex virus type 1 reveals the translation of two proteins. *Journal of Virology* **71**, 2656-2665.
- Yu, D., and Weller, S. (1998): Herpes simplex type 1 cleavage and packaging proteins UL15 and UL28 are associated with B but not C capsids during packaging. *Journal of Virology* **72**, 7428-7439.
- Zezulak, K., and Spear, P. (1984): Mapping of the structural gene for the herpes simplex virus type 2 counterpart of herpes simplex type 1 glycoprotein C and identification of a type 2 mutant which does not express this protein. *Journal of Virology* **49**, 741-747.

- Zhang, X., Efsthathiou, S., and Simmons, A. (1994): Identification of novel herpes simplex virus replicative intermediates by field inversion gel electrophoresis: Implications for viral DNA amplification strategies. *Virology* **202**, 530-539.
- Zhou, Z. H., Prasad, B. V. V., Jakana, J., Rixon, F. J., and Chiu, W. (1994): Protein subunit structures in the herpes simplex virus A-capsid determined from 400 kV spot-scan electron cryomicroscopy. *Journal of Molecular Biology* **242**, 456-469.
- Zhou, Z. H., He, J., Jakana, J., Tatman, J. D., Rixon, F. J., and Wah, C. (1995): Assembly of VP26 in herpes simplex virus-1 inferred from structures of wild-type and recombinant capsids. *Nature Structural Biology* **2**, 1026-1030.
- Zhou, Z. H., Macnab, S. J., Jakana, J., Scott, L. R., Chiu, W., and Rixon, F. J. (1998a): Identification of the sites of interaction between the scaffold and the outer shell in HSV-1 capsids by difference electron imaging. *Proceedings of the National Academy of Sciences of the U.S.A.* **95**, 2778-2783.
- Zhou, Z. H., Chiu, W., Haskell, K., Spears, H. J., Jakana, J., Rixon, F. J., and Scott, L. R. (1998b): Refinement of herpesvirus B-capsid structure on parallel supercomputers. *Biophysical Journal* **74**, 576-588.
- Zhou, Z., Chen, D., Jakana, J., Rixon, F., and Chiu, W. (1999): Visualisation of tegument/capsid interactions and DNA in intact Herpes simplex virus type 1 virions. *Journal of Virology* **73**, 3210-3218.
- Zweerink, H., and Neff, B. (1981): Immune response after exposure to varicella zoster virus: characterisation of virus-specific antibodies and their corresponding antigens. *Infection and Immunity* **31**, 436-444.
- Zweig, M., Heilman, C., and Hampar, B. (1979a): Identification of disulphide-linked complexes in the nucleocapsid of herpes simplex virus type 2. *Virology* **94**, 442-450.
- Zweig, M., Heilman, C., Rabin, H., Hopkins, R., Naubauer, R., and Hampar, B. (1979b): Production of monoclonal antibodies against nucleocapsid proteins of herpes simplex virus types 1 and 2. *Journal of Virology* **32**, 676-678.

